Charles University

Faculty of Science

Department of Physical and Macromolecular Chemistry

Study programme: Macromolecular Chemistry

RNDr. Lenka Loukotová

Novel hybrid polysaccharide-based polymers for biomedicine

Doctoral Thesis

Supervisor: Mgr. Martin Hrubý, DSc.

Institute of Macromolecular Chemistry AS CR

Prague 2018

Univerzita Karlova

Přírodovědecká fakulta

Katedra fyzikální a makromolekulární chemie

Studijní program: Makromolekulární chemie

RNDr. Lenka Loukotová

Nové hybridní polymerní materiály na bázi polysacharidů využitelné v biomedicíně

Disertační práce

Školitel: Mgr. Martin Hrubý, DSc.

Ústav makromolekulární chemie AV ČR, v.v.i.

Praha 2018

Tímto prohlašuji, že jsem tuto disertační práci zpracovala samostatně pod vedením Mgr Martina Hrubého, DSc a že jsem uvedla všechny použité informační zdroje a literaturu. Tato práce ani její podstatná část nebyla předložena k získání jiného nebo stejného akademického titulu.

Hereby I declare that this thesis describes my original work that has been done on my own under the supervision of Mgr. Martin Hrubý, DSc. This work or part of it has not been submitted to obtain any other degree, diploma or qualification. To the best of my knowledge, I have cited all used sources.

Prague, 23.10.2018 Lenka Loukotová

Acknowledgment

First of all, I would like to thank my supervisor Mgr., Martin Hrubý, DSc. for his support during my study, valuable advices, willingness to help and also for his contagious enthusiasm for chemistry, which he basically spreads all around himself.

Many thanks belong to all my colleagues from the department of Supramolecular Polymer Systems for their positive thinking, helpful consultations and valuable comments within my experimental work. A special thanks to my closest colleagues Maria Rabyk, Jiří Trousil, Linda Srbová, Kristýna Kolouchová, Pavel Švec and Tomáš Urbánek for their help any time I needed, valuable discussions, good mood and also for never-ending patience which they had with me.

I would like to thank also all my friends who was continuously and successfully distracting my attention from the study responsibilities. And finally, the greatest thanks belong to my beloved mum, brother and dear grandparents for their support, unconditional love and belief.

Table of contents

List of abbreviations

AFM	atomic force microcopy
ANSAAS	8-anilino-1-naphthalenesulfonic acid ammonium salt
CPT	cloud point temperature
CS	chondroitin sulfate
DC-SIGN	dendritic cell-specific intercellular adhesion molecule-3-grabbing non-integrin receptors
DLS	dynamic light scattering
DNA	deoxyribonucleic acid
DOTA	1,4,7,10-tetraazacyclododecane-1,4,7,10-tetraacetic acid
ELISA	enzyme-linked immunosorbent assay
FTIR	Fourier-transform infrared spectroscopy
HA	hyalauronic acid
HER2	human epidermal growth factor receptor 2
LCST	lower critical solution temperature
LG	leaving group
MALS	multiangle light scattering detectors
N	nucleoside
NDP	nucleoside diphosphate
NMR	nuclear magnetic resonance
NTP	nucleoside triphosphate
PBS	phosphate-buffered saline
PEO	poly(ethylene oxide)
PG	protecting group
PHPMA	poly[*N*-(2-hydroxypropyl)methacrylamide]
PMA	phorbol myristate acetate
PNIPAm	poly(*N*-isopropylacrylamide)
POX	poly(2-isopropyl-2-oxazoline-*co*-2-butyl-2-oxazoline)
PPG	"participating" protecting group
SEC	size-exclusion chromatography
TLR	Toll-like receptor
TNBSA	2,4,6-trinitrobenzene-1-sulfonic acid
TNF-α	tumor necrosis factor α

Abstract

This doctoral thesis is focused on the synthesis and characterization of novel hybrid polysaccharide-based polymers applicable for biomedicine, specifically for a conceptually new bimodal cancer treatment – immunoradiotherapy. For this purpose, polysaccharides β-glucan from *Auricularia auricula-judae* and κ-carrageenan from *Kappaphycus alvarezii*, exhibiting immunostimulatory and anticancer activities, were chosen to be grafted with thermoresponsive poly(2-isopropyl-2-oxazoline-*co*-2-butyl-2-oxazoline)s (POXs) (with different graft lengths and grafting densities) that induced a lower critical solution temperature of the final polymers. The thermoresponsive behavior of resulting polymers was studied with temperature-dependent light scattering methods, fluorescence measurements and also nuclear magnetic spectroscopy to select a polymer material with the most suitable properties for the intended application, aiming at a polymer depot formation after the injection of a polymer solution into the body. The chosen polymer, β-glucan-*graft*-POX with graft length of 2500 Da, was then modified to bear 1,4,7,10-tetraazacyclododecane-1,4,7,10-tetraacetic acid and a fluorescent dye Dyomics-615 at the graft ends and tested first *in vitro* to investigate its immunostimulatory properties and also the cellular uptake. Subsequently, the polymer was radiolabeled with yttrium-90(III) and used in the *in vivo* antitumor efficiency experiment on mice with EL4 lymphoma, demonstrating an extraordinary treatment success (~ 50 % cured mice), which was probably caused by a considerable synergistic effect of using immunoradiotherapy compared to separate use of immunotherapy or radiotherapy.

Furthermore, a special attention was dedicated to the characterization of κ-carrageenan-*graft*-POXs, which showed except for the above mentioned desired biological properties also a sensibility to the presence of potassium cations and an interesting "schizophrenic" thermoresponsive behavior with both lower and upper critical solution temperatures in aqueous environment.

Keywords: β-glucan, κ-carrageenan, poly(2-alkyl-2-oxazoline), multimodal cancer therapy, immunotherapy, radiotherapy.

Abstrakt

Tato disertační práce je zaměřena na syntézu a charakterizaci nových hybridních polymerních materiálů využitelných pro biomedicínální aplikace, konkrétně pro koncepčně novou bimodální léčbu rakoviny – imunoradioterapii. Pro tento účel byly vybrány polysacharidy β-glukan z *Auricularia auricula-judae* a κ-karagenan z *Kappaphycus alvarezii*, vykazující imunostimulační a protirakovinné účinky, přičemž tyto polymery byly následně roubovány termoresponzivním poly(2-izopropyl-2-oxazolin-*co*-2-butyl-2-oxazolin)em (POX) (s různými délkami a hustotami graftů), který způsobuje tzv. dolní kritickou rozpouštěcí teplotu roztoku. Termoresponzivní chování výsledných polymerů bylo následně studováno pomocí teplotně závislých měření rozptylu světla, fluorescence a také nukleární magnetické rezonance, přičemž pro zamýšlenou aplikaci byl vybrán polymer s nejvhodnějšími termoresponzivními vlastnostmi, schopný po intratumorální injekci polymerního roztoku vytvořit v místě vpichu polymerní depo. Vybraný polymer β-glukan-*graft*-POX s délkou graftů 2500 Da byl poté modifikován tak, aby na konci jednotlivých graftů byla skupina 1,4,7,10-tetraazacyklododekan-1,4,7,10-tetraoctová kyselina nebo fluorescenční barvivo Dyomics-615. Imunostimulační vlastnosti a rychlost endocytózy takto modifikovaného polymeru byly testovány *in vitro*. Poté byl vybraný polymer označen radioaktivním ytriem-90(III) a použit v *in vivo* experimentu, zkoumajícím protinádorovou účinnost. Tento experiment demonstroval neobyčejný úspěch léčby pomocí imunoradioterapie – cca 50 % myší, majících původně EL4 lymfom, bylo zcela vyléčeno. Tento vyjímečný úspěch byl pravděpodobně způsoben významným synergickým účinkem imunoradioterapeutické léčby v porovnání s léčbou pouze radioterapeutickou nebo imunoterapeutickou.

Navíc, speciální pozornost v této práci je věnována polymerům κ-karagenan-*graft*-POX, které kromě požadovaných biologických vlastností vykazují také responzivitu na přítomnost draselných kationtů a ještě velmi zajímavé „schizofrenní" termoresponzivní chování ve vodných roztocích, neboť u nich byla pozorovaná dolní i horní kritická rozpouštěcí teplota roztoku.

Klíčová slova: β-glukan, κ-karagenan, poly(2-alkyl-2-oxazolin), multimodální léčba rakoviny, imunoterapie, radioterapie.

List of publications and contributions at conferences

Publications included into this thesis

1. Loukotová, L.; Konefał, R.; Venclíková, K.; Machová, D.; Janoušková, O.; Rabyk, M.; Netopilík, M.; Mázl Chánová, E.; Štěpánek, P.; Hrubý, M. Hybrid thermoresponsive graft constructs of fungal polysaccharide β-glucan: Physico-chemical and immunomodulatory properties, *Eur. Polym. J.* **106**, 117 – 127 (2018). IF = 3.741.

2. Loukotová, L.; Kučka, J.; Rabyk, M.; Höcherl, A.; Venclíková, K.; Janoušková, O.; Páral, P.; Kolářová, V.; Heizer, T.; Šefc, L.; Štěpánek, P.; Hrubý, M. Thermoresponsive β-glucan-based polymers for bimodal immunoradiotherapy – Are they able to promote the immune system? *J. Control. Release* **268**, 78 – 91 (2017). IF = 7.877.

3. Loukotová, L.; Bogomolova, A.; Konefał, R.; Špírková, M.; Štěpánek, P.; Hrubý, M. Hybrid κ-carrageenan-based polymers showing "schizophrenic" lower and upper critical solution temperatures and potassium responsivity, *Carbohydr. Polym.*, submitted article. IF = 5.158.

4. Loukotová, L.; Hrubý, M. Polysacharidy jako stavební bloky hybridních kopolymerů, *Chem. Listy* **112**, 497 – 507 (2018). IF = 0.260.

Publications not included into this thesis

5. Loukotová, L.; Yuan, K.; Doucet, H. Regiocontroled Palladium-Catalysed Direct Arylation at Carbon C2 of Benzofurans using Benzenesulfonyl Chlorides as the Coupling Partners, *ChemCatChem* **6**, 1303 – 1309 (2014). IF = 4.674.

6. Loukotová, L.; Dodda, J. M.; Bělský, P.; Kullová, L.; Kadlec, J.; Podivinská, M.; Vohlídal, J. Structure–stability correlation of copolyimide membranes derived from aliphatic/alicyclic/aromatic diamine and aromatic dianhydrides, *J. Appl. Polym. Sci.* **134**, 45227 (2017). IF = 1.900.

7. Pánek, J.; Loukotová, L.; Hrubý, M.; Štěpánek, P. Distribution of Diffusion Times Determined by Fluorescence (Lifetime) Correlation Spectroscopy, *Macromolecules* **51**, 2796 – 2804 (2018). IF = 5.914.

8. Rabyk, M.; Galisová, A.; Jiratová, M.; Patsula, V.; Srbová, L.; Loukotová, L.; Parnica, J.; Jirák, D.; Štěpánek, P.; Hrubý, M. Mannan-based conjugates as a multimodal imaging platform for lymph nodes, *J. Mater. Chem. B* **17**, 2584 – 2596 (2018). IF = 4.776.

Contributions on international conferences

Oral presentations

1. Loukotová, L.; Kučka, J.; Štěpánek, P.; Hrubý, M. Combined immuno- and brachytherapy using thermoresponsive polymers, World Congress of Smart Materials 2017, Bangkok, Thajsko. Conference Abstract Book. Dalian: BIT Group Global Ltd., 2017. s. 425.
2. Loukotová, L.; Kučka, J.; Rabyk, M.; Venclíková, K.; Machová, D.; Šebestová Janoušková, O.; Kolářová, V.; Páral, P.; Šefc, L.; Štěpánek, P.; Hrubý, M. Bimodal immunoradiotherapy using thermoresponsive polysaccharide-based polymers: are they able to promote immune system?, World Polymer Congress Macro 2018. Cairns, Austrálie. Abstract Book. Cairns: IUPAC, 2018. s. 254

Poster presentations

1. Loukotová, L.; Hrubý, M. Thermoresponsive beta-glucan-based polymers for biomedical applications, Self-assembly in the World of Polymers 2016, Praha. Česká republika. Book of Abstracts and Programme. Prague: Institute of Macromolecular Chemistry AS CR, 2016. s. 138.

2. Loukotová, L.; Kučka, J.; Rabyk, M.; Höcherl, A.; Venclíková, K.; Janoušková, O.; Konefal, R.; Kolářová, V.; Šefc, L.; Štěpánek, P.; Hrubý, M. Polymers for bimodal immunoradiotherapy - are they able to promote immune system?, Zjazd chemikov 2017, Horný Smokovec, Slovenská republika. ChemZi. Roč. 13, č. 1 (2017), s. 192.

1. Introduction

Biopolymers and synthetic polymers have been previously investigated in relatively separated research areas. Such a distinction is justified because these polymer classes differ in many basic aspects. In general, biopolymers have a well-defined structure optimized within the billion years of evolution, involving especially their precise chemical structure, their sequences order, their supramolecular structure and also their exact number of monomer units incorporated in one chain, making many biopolymers molecularly uniform. By contrast, majority of synthetic polymers have much simpler and more random structure but chemically much more diverse. However, several decades ago, these separate research areas partially merged and created a new research sector of hybrid polymers (also known as polymer bioconjugates), composed of both natural and synthetic polymers. These polymers were first extensively studied and used in the field of pharmaceutical chemistry.[1,2] Nevertheless, recent explosion of developments in nano- and biotechnology has contributed to the fact that the use of polymeric bioconjugates far exceeds the pharmaceutical field and involves also many other areas, such as biosensors, artificial enzymes, biometrics, photonics or nanoelectronics.[3,4]

The hybrid polymers combine the advantages of both bio- and synthetic polymers, and thus, the motivation for their preparation can be driven by numerous reasons. The general outlook on the primary motivations, lying behind polymer bioconjugates, is illustrated in **Fig. 1**. The biological systems used for polymer bioconjugate preparation can be conformationally organized in various hierarchical level structures – from oligomers up to the highly organized supramolecular structures. Therefore, oligonucleotides or oligopeptides are conjugated with the synthetic polymers due to their extraordinary tendency for self-organization, allowing to prepare *e.g.,* highly organized hybrid nanomaterials. However, the particles with higher level of complexity (*e.g.,* proteins or enzymes) are exploited mainly because of their biological properties rather than for their self-assembling abilities. Moreover, utilized synthetic polymer plays a crucial role in the final bioconjugate properties because it exhibits a spectrum of exceptional characteristics and a considerably wider chemical diversity compared to biopolymers.

This thesis is focused on the class of polymer bioconjugates based on polysaccharides – glycoconjugates, which are mainly used for biomedical application, especially for drug delivery and tissue engineering.[5] In general, glycoconjugates can exhibit a pallet of various properties because polysaccharides themselves have extremely diverse properties. In contrast with other biopolymers, polysaccharide monomeric units may be linked to each other

by different types of glycosidic bond, while the bond type has a significant effect on the polysaccharide properties and on its supramolecular structure.

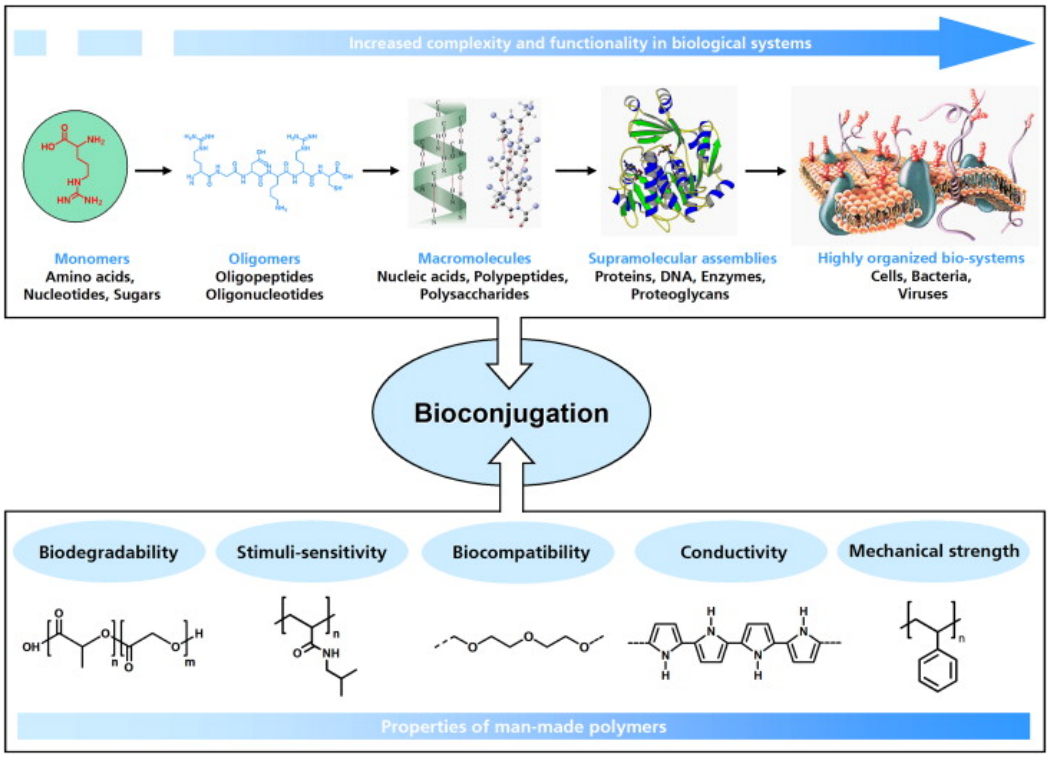

Fig. 1. The concept scheme of bioconjugation. The figure was adopted from ref.[3].

1.1 The synthesis of polymer glycoconjugate

1.1.1 The resources of polysaccharides

Although the study of polymer glycoconjugates is an important research area nowadays, the preparation of polysaccharides is relatively complicated. This is mainly caused by the fact that there is no simple automated system for the oligosaccharide synthesis unlike for proteins and nucleic acids (**Table 1**), despite that many efforts have been done in the area. The explanation of this research failure lies in the structure of the polysaccharides themselves. While the chemical synthesis of oligopeptides involves the repetitive formation of a peptide bond between *e.g.,* one activated carboxyl group and free amine, the chemical synthesis of oligosaccharides requires several suitably modified hydroxyl groups with similar reactivities to obtain the final product with desired regio- and stereoselectivity. Therefore, such synthesis often includes laborious manipulation with protecting groups and extremely long synthetic pathways. The central dogma of molecular biology (deoxyribonucleic acid → ribonucleic acid → protein) is applied for the living organisms[6] but unfortunately it is not

related to polysaccharides. They are rather biosynthesized by the post-translational processes, while their final structure is influenced by a number of factors – enzyme competition for one substrate, enzyme substrate specificity and also substrate availability. Thus, polysaccharides, including glycoproteins, are typically non-uniform molecules.[7]

Table 1. The general methods to obtain biopolymers.[8]

Biopolymer	Methods to obtain
proteins	extraction from biological material, **automated** peptide synthesis, native peptide ligation, gene overexpression, protease-catalyzed peptide synthesis
nucleic acids	extraction from biological material, **automated** oligonucleotide synthesis, polymerase chain reaction
polysaccharides	extraction from biological material, chemical synthesis, enzymatic synthesis

One of the methods to obtain polysaccharides for polymer glycoconjugate synthesis is chemical synthesis (**Table 1**), although this method is very challenging due to their structure. The formation of glycosidic bond by chemical synthesis is realized by a nucleophile ("glycosyl acceptor") which attacks an activated mono/oligosaccharide with anomeric center ("glycosyl donor"). However, for reacting the desired hydroxyl group(s) only, the other hydroxyl and amine groups have to be masked by the protecting agents (**Fig. 2**). The size, electronic properties and conformation of the protecting groups have an enormous impact on the final glycosidation reactivity and stereoselectivity; the same holds for the used solvent, temperature and activator. To improve the efficiency and stereoselectivity of glycosidation, a number of leaving anomeric groups have been developed, *e.g.,* glycosyl halides[9], glycosyl imidates[10], thioglycosides[11] or glycosyl phosphates.[12] In addition, the development of novel glycosylation agents caused a progress in sequential "one-pot" synthesis, demanding a proper combination of individual building blocks[13], while even hexasaccharides were successfully prepared by this method.[14] Nowadays, a hot topic in this field is the concept of automatic oligosaccharide solid phase synthesis, known as Glyconeer 2.1, which allows so far the synthesis of various oligosaccharides containing up to 6 units in the chain.[15]

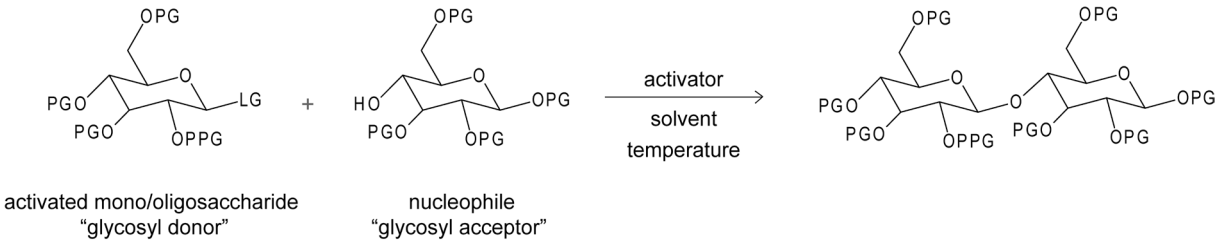

Fig. 2. The general scheme of glycosylation by chemical synthesis (PG – protecting group, LG – leaving group, PPG – "participating" protecting group). The stereochemistry of the final product depends on the nature of protecting groups, activator, solvent and temperature. Here, as an example the preparation of PG-protected disaccharide D-glucose-β-(1→4)-D-glucose is illustrated.

Another way to obtain oligo/polysaccharides is enzymatic synthesis, which exploits glycosyltransferases and glycosidases as valuable regio- and stereoselective glycosidic bond catalysts. Glycosyltransferases are responsible for the synthesis of the most glycans on the mammalian cell surface, where they transfer saccharide moieties from a corresponding "glycosyl donor" (activated nucleotide sugar) to a "glycosyl acceptor", having specific nucleophilic groups, the most often hydroxyl ones (**Fig. 3A**).[16] A large number of glycosyltransferases has already been successfully replicated and have been found to exhibit excellent binding and substrate specificity with very good yields. However, enzymatic synthesis has also some disadvantages, including the higher financial cost of nucleotide sugars as well as the fact that nucleoside diphosphate (NDP), generated during the glycosylation reaction, is an effective inhibitor of glycosyltransferase. Therefore, a multi-enzyme glycosylation method has been developed[17], requiring only a catalytic amount of nucleotide sugar because it is produced *in situ* from low-cost starting materials (**Fig. 3B**). In addition, the generated NDP is subsequently transformed into nucleotide sugar, and thus, the reaction inhibition by the product is prevented. There is still one disadvantage of enzymatic synthesis using glycosyltransferase which is its poor availability. Although many commercial glycosyltransferases are available on the market today, nevertheless, there is still a lack of their specific types for production of certain desired glycosidic linkages.

As mentioned above, in addition to glycosyltransferases, glycosidases are also used for the same purpose. In living organisms, the glycosidases are mostly responsible for the cleavage of glycosidic bonds, however, under the controlled conditions they can be used to create these linkages (**Fig. 3C**). The glycosidase substrates are inexpensive compared

to the non-economic nucleotide sugars, and moreover, the glycosidases themselves are inexpensive and stable. Nevertheless, their only disadvantage is a poor regiospecificity, leading to the formation of undesired products.[8]

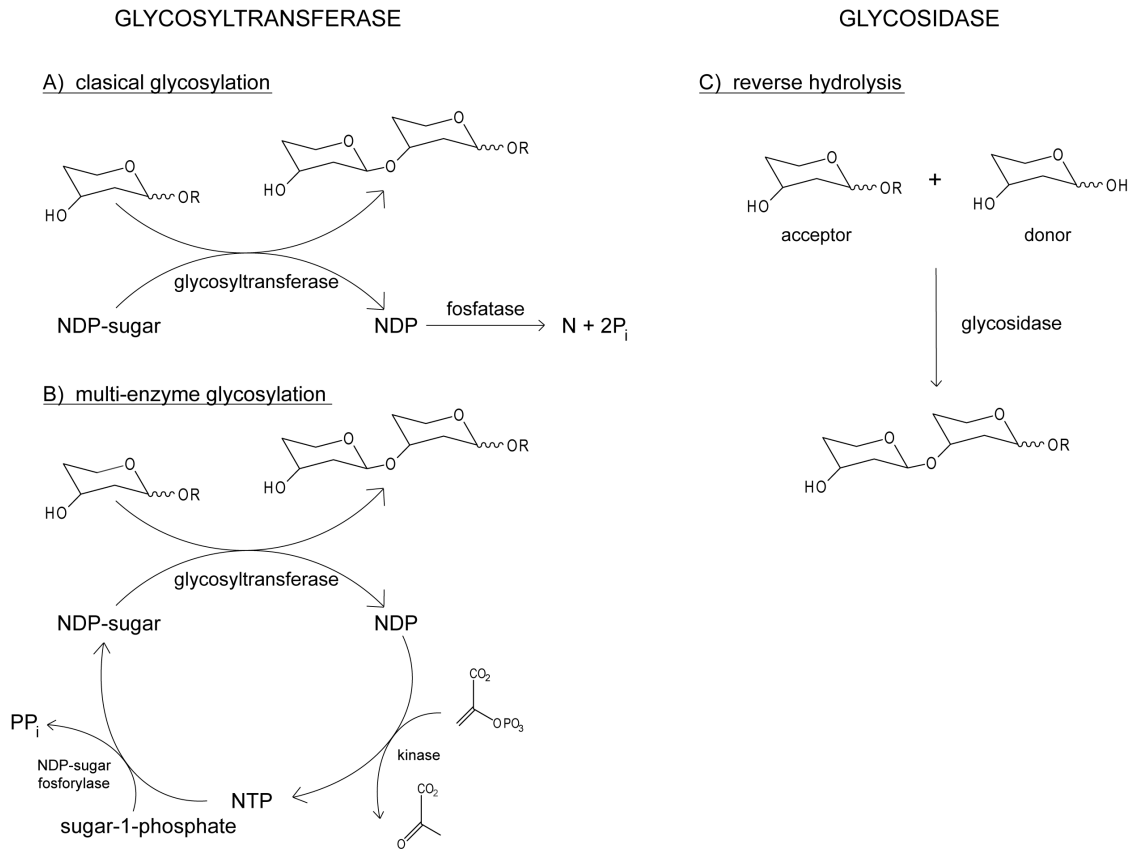

Fig. 3. The general schemes of glycosylation by enzymatic synthesis using: A) glycosyltransferase, B) glycosyltransferase and other enzymes – a multi-enzyme glycosylation and C) glycosidase (N – nucleoside, NDP – nucleoside diphosphate, NTP – nucleoside triphosphate).

The simplest and the most studied way to obtain polysaccharides is an extraction from biomaterial, although, this method quite often does not produce a sufficient amount of material with a satisfactory quality. Polysaccharides obtained by extraction are in many cases structural components of cell walls, especially of fungi, bacteria or algae. The choice of the best extraction method depends on the cell wall structure, *e.g.,* fungal cell walls contains two types of polysaccharides: fibrillar chitin (or cellulose) and water-soluble β-glucans, α-glucans and glycoproteins.[18] In the case of fungal polysaccharides, the majority of extraction methods includes at first an elimination of low-molecular weight substances using 80% ethanol solution, followed by three extraction steps using aqueous, ammonium

oxalate and sodium hydroxide solutions. The aqueous solution extraction leads to the production of water-soluble polysaccharides, which are present on the outer layer of cell walls (exopolysaccharides), protecting them against external mechanical damage. On the other hand, alkaline solution extraction produces rather water-insoluble polysaccharides, which form the inner layer of cell walls (endopolysaccharides).[19] The exact extraction method for the particular polysaccharide may differ from the general procedure described above, depending on its structure and water solubility, nevertheless, it is always necessary to disrupt the cell wall structure using appropriate extraction conditions (pH and temperature).[19] Moreover, the obtained polysaccharides are further purified by different techniques, *e.g.,* precipitations, affinity chromatography or ion-exchange chromatography. In this thesis, polysaccharide extraction was also performed to obtain the starting material for a glycoconjugate synthesis, specifically to obtain β-glucan from *Auricularia auricula-judae* and κ-carrageenan from *Kappaphycus alvarezii*.[20]

1.1.2 The synthesis of graft copolymers

The most frequently studied type of glycoconjugates are their graft copolymers, which can be prepared using three different synthetic strategies (**Fig. 4**): grafting "from", grafting "onto" and grafting "through"; the first two mentioned approaches are more often used in practice.[21] In general, the method grafting "from" is used when a higher grafting density is required. In this technique, the initiator groups are firstly introduced within the polysaccharide main chain to form a macroinitiator, and then, the graft chain growth is initiated from the polysaccharide surface in the presence of the desired monomer (**Fig. 4A**). Grafting "from" techniques is most often used for radical polymerization, where the first radicals are generated along the main polysaccharide chain by radiation or chemical initiation. Nevertheless, the disadvantages of this method are a frequent degradation of polysaccharide chains and a very limited control of the graft molecular weight and dispersity. To improve the polymerization control, special radical polymerization techniques (nitroxide-mediated polymerization[22], atom transfer radical polymerization[23] and reversible addition-fragmentation chain-transfer polymerization[24]) were developed. These controlled radical polymerizations are more tolerant to common impurities and moisture and also are compatible with a large number of functional groups. The principle of these techniques is to significantly reduce the concentration of the propagating radicals, thereby the possibility of irreversible terminations is also rapidly minimized. Becasuse the recombination rate of the radical centers

is proportional to the second power of their concentration, while the propagation rate is only directly proportional to the radical concentration, it is possible to obtain polymers with narrow molecular weight distributions in the systems with a very low amount of radical centers.

In contrast, by using the grafting "onto" technique, the living polymer chains are at first created separately and subsequently terminated by the functional groups within polysaccharide main chain (**Fig. 4B**). This technique is advantageous because the side chain polymerization proceeds apart from the polysaccharide, and thus, it does not cause any possible degradation effect. The next advantage of grafting "onto" is the opportunity to easily and precisely characterize only polymer grafts separately from the grafted polysaccharide (it is realized by a termination of the part of polymerization mixture by a low-molecular weight agent and subsequent investigation). However, this approach typically results in lower grafting densities compared to the grafting "from" approach, primarily due to the steric effect.[25] In this thesis, the grafting "onto" approach was exploited to synthesize polysaccharide-*graft*-poly(2-alkyl-2-oxazoline)s (for detailed information see *3.1 Polymer design and synthesis*).

The least-used technique for the synthesis of grafted polysaccharides is the grafting "through" approach (**Fig. 4C**). Here, a polymerizable group (most commonly a double bond) is introduced at one end of the oligo/polysaccharide chains, while these groups are then polymerized forming a main chain of the final polymer.

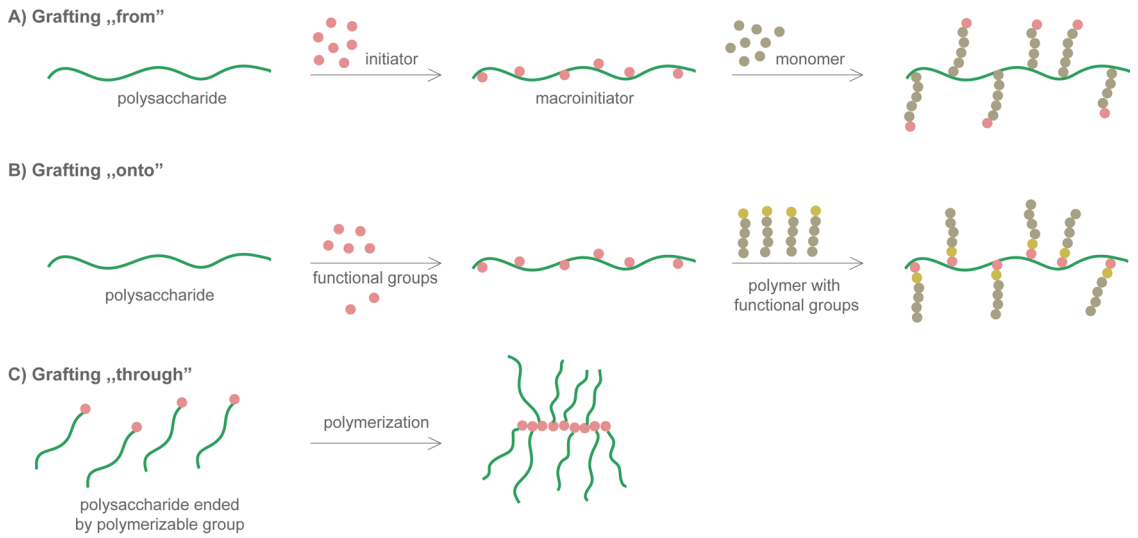

Fig. 4. The synthetic approaches for the grafted polysaccharides: A) grafting "from", B) grafting "onto" and C) grafting "through".

1.1.3 The synthesis of block copolymers

Surprisingly, only very few publications deal with the synthesis of block oligo/polysaccharide-based copolymers. The first such block copolymer was poly(ethylene oxide)-*block*-oligosaccharide prepared by the end groups "coupling" in 1984.[26] Since then, the copolymers having a synthetic block coupled to oligo/polysaccharide have been also prepared by radical[27] and enzymatic polymerization.[28] In the case of radical polymerization, a functional group is introduced at the end of the polysaccharide chain, and this group subsequently takes part in the controlled polymerization of the synthetic block. In contrast, within the enzymatic synthesis the synthetic block is firstly prepared by a conventional method, modified to bear a functional group at the end and then polymerized using enzymes (*e.g.,* potato phosphorylase[28]).

1.2 The choice of the polymers

The choice of both natural and synthetic polymers significantly influences the properties of final glycoconjugate, and thus, it plays a key role within the glycoconjugate design as well as the proposed polymer architecture.

1.2.1 The nature of the polysaccharide part

Polysaccharides consist of simple sugars (*i.e.,* monosaccharides), which are covalently linked together by *O*-glycosidic linkages in either linear or branched configuration. The polysaccharide containing only one type of monosaccharide is called homopolysaccharide (sometimes homoglycan), in contrast to the others, which are named as heteropolysaccharides (heteroglycans). In nature, they can be served for many different purposes, while the most important are a storage of energy (*e.g.,* glycogen) and a structural component (*e.g.,* cellulose). Therefore, these polysaccharides are useful for the preparation of glycoconjugates applicable especially as materials without any specific biological functions, *e.g.,* glycogen-*graft*-poly(acrylic acid) was successfully used as adsorbent for selective uptake of lead ions from aqueous solutions.[29] Moreover, these polysaccharides are also used for the preparation of hybrid polymers demanding biodegradable and biocompatible material backbone, *e.g.,* glycogen-*graft*-poly(2-alkyl-2-oxazoline)[30] or glycogen-*graft*-poly(ethyl cyanoacrylate)[31] were prepared to exhibit such properties, where the second one was specifically prepared for tissue engineering.

In general, polysaccharides display diverse biological functions. Some of them are known to exhibit immunostimulatory and anticancer properties, and these polysaccharides are most often found in mushrooms. Interestingly, in traditional Chinese medicine, mushroom extracts have been used as medicinal anticancer agents for centuries, however, it was only recently discovered that the efficient ingredients in these extracts are, except others, in particular polysaccharides.[32] These mushrooms almost exclusively belong to the class of Basidiomycetes, which have been successfully cultivated. The structure of antitumor polysaccharides and their physical properties greatly differ from each other, while, in general, polysaccharides possess high potential structural variability, resulting in their high capacity to carry biological information. Sometimes, they are bound together with peptides to form a polysaccharide-peptide complex with an increased potential antitumor activity.[33]

The most popular and studied antitumor polysaccharides are listed in **Table 2**. One class of efficient immunostimulatory polysaccharides are β-glucans[34], which are composed of glucose units linked together by 1→3 β-glycosidic bonds (**Fig. 5**). They differ in the chain length and in the branching structure, most often they contains also 1→6 β-branching.[35] Furthermore, in Japan, β-glucan from *Lentinula edodes* is already approved as an effective drug for gastric cancer therapy, used especially in the combination with fluoropyrimidines.[36] Therefore, the glycoconjugates prepared from β-glucans can be used for cancer therapy as well. The special attention must be paid to the fact that the carried chemical modifications could change the biological properties of the polysaccharide. In this thesis, β-glucan from *Auricularia auricula-judae* was exploited due to the above described immunostimulatory and antitumor activities.

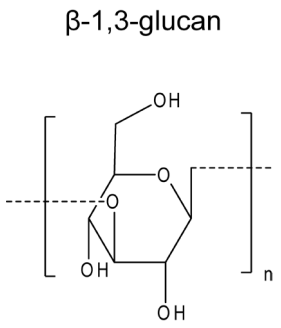

Fig. 5. The general structure of β-1,3-glucans (illustrated without any branching).

Table 2. The chosen bioactive polysaccharides with their source and bioactivity.

Source mushroom	Polysaccharide	Main bioactivity	Reference
Lentinula edodes	lentinan (β-glucan)	immunomodulating, antitumor, antiviral	37
Auricula auricularia-judae	β-glucan	immunomodulating, antitumor, anti-inflamatory	38
Ganoderma lucidum	β-glucan, glycopeptide	immunomodulating, antitumor. antioxidant, anti-decrepitude	39
Pleurotus tuber-regium	β-glucan	hepatoprotective, anti-breast cancer	40
Schizophyllum commune	schizophyllan (β-glucan)	antitumor, antiviral, antifungal	41
Grifola frondosa	grifolan (β-glucan), proteoglycan,	immunomodulating, antitumor, antiviral, hepatoprotective	42
Pleurotus ostreatus	pleuran (β-glucan), proteoglycan,	antitumor, antioxidant	43

The biologically active polysaccharides are also found in other plants. The polysaccharides extracted from macroalgae and their products are applicable in diverse areas of usage (*e.g.,* pharmaceutics, biomedicine or cosmetics) because they are known to be antiallergic, gastroprotective, neuroprotective and also antiviral[44]. Furthermore, the sulfated polysaccharides extracted from macroalgae also exhibit immunomodulatory properties[45], nevertheless, the exact principle of how they influence the immune system has not been yet fully clarified.[46] Carrageenans are sulfated linear polysaccharides, synthesized by red seaweeds, which consist of sulfated or non-sulfated galactose and 3,6-anhydrogalactose units linked together by 1→3 α- and 1→4 β-glycosidic bonds.[47] We distinguish many different types of carrageenans depending on the position and number of sulfate groups in a monomeric unit because they significantly differ in their fundamental properties. The most studied and commercially used carrageenan types are κ, ι, and λ (**Fig. 6**). The main source of κ-carrageenan is the red macroalgae *Kappaphycus alvarezii*, ι-carrageenans is extracted from *Euchema spinosum* and λ-carrageenan is found in *Gigartina* and *Chondrus sp*.[48] They are soluble in aqueous environment and form gels in specific pH and temperature, and thus, they are widely used as gelling agents in food industry, cosmetics, and pharmaceutics.[49]

Interestingly, even though they are approved as food additives[50], they may cause undesirable intestinal effects, connected probably with ulcerations and tumors.[51] In this thesis, κ-carrageenan from *Kappaphycus alvarezii* was exploited due to the known immunostimulatory and antitumor activities.[52]

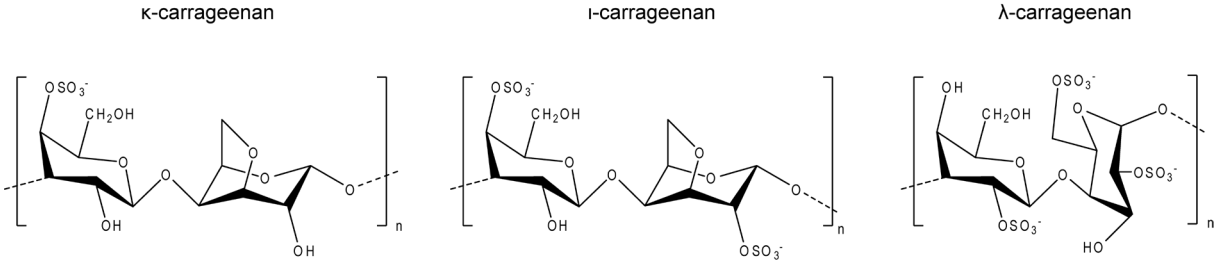

Fig. 6. The structures of κ, ι, and λ-carrageenans.

Another biologically active polysaccharide attracting attention for glycoconjugate synthesis is mannan which consists of mannose units linked together by 1→6 α-glycosidic bonds, forming a mannan backbone. The mannans vary in their branching structure, while they contain a diverse percentage of α-1,2 and α-1,3 side chains of different composition.[53] In living organisms, they bind to the mannose receptors, a part of multilectin receptor proteins, which secures a connection between innate and adaptive immunity.[54] Thus, mannan is predominantly accumulated in immune cells overexpressing the DC-SIGN (Dendritic Cell-Specific Intercellular adhesion molecule-3-Grabbing Non-integrin) receptors.[55] This phenomenon is widely exploited in various biomedical applications.

1.2.2 The nature of the synthetic polymer part

In general, hybrid polymers contain both bio- and synthetic polymeric parts. As it was discussed above, both parts have a crucial influence on the final product properties.

For glycoconjugate synthesis, there is a wide range of used synthetic polymers. Poly(ethylene oxide) (PEO) is probably one of the most widely used. It is typically synthesized using anionic ring-opening polymerization of ethylene glycol, resulting in low polymer dispersities.[56] PEO is biocompatible, non-toxic and water-soluble, even if it has a high molar mass.[57] Moreover, it is an approved substance by Food and Drug Administration to be used in food, cosmetics and pharmaceuticals.[58] In biomedical field, PEO is widely exploited to decorate bioactive molecules, protecting them from unspecific interactions with other bioactive objects.[59] This process is predominantly used to prolong a circulation time

in the bloodstream for various formulations.[60] However, several negatives of PEO have to be mentioned. It tends to accumulate in specific organs, especially with its increasing polymer molar mass.[61] Furthermore, PEO can cause an immune response because it activates the complement system, leading to hypersensitive reactions and subsequently to the anaphylactic shock.[62] Although PEO has been for a long time identified to be non-antigenic, the existence of antibody against PEO was found in approximately 20 % of Europe healthy population, resulting in the need of this antibody determination to consider an appropriate drug dosing strategy or an usage of free-PEO drugs.[63]

Recently, poly(2-alkyl-2-oxazoline)s have attracted increasing attention due to their biocompatibility and non-immunogenicity. Due to this convenient combination of properties they are predicted to be used and sometimes are already used instead of PEO in biomedical applications.[64] However, similarly like PEO, poly(2-alkyl-2-oxazoline) is not biodegradable. They are synthesized by a living cationic ring-opening polymerization of 2-alkyl-2-oxazolines using various initiation and termination agents to tune the end-groups (**Fig. 7**). The microwave-assisted synthesis was applied to optimize POXs preparation not long time ago, shortening the reaction time from days to minutes.[65] The final polymer properties can be easily fine-tuned within the limits of tolerated functionalities during the polymerization by the choice of alkyl substituent. Poly(2-methyl-2-oxazoline) is soluble in aqueous environment. If the alkyl substituent has 2 or 3 carbons (*i.e.,* ethyl, propyl and propan-2-yl), the resulting macromolecules are water-soluble with a lower critical solution temperature (LCST), which makes these polymers suitable for applications demanding such thermoresponsivity. On the other hand, the longer substituents produce rather hydrophobic macromolecules.[66] The achievable molar mass strongly depends on the used monomer. Furthermore, poly(2-ethyl-2-oxazoline) is approved by the Food and Drug Administration as a food contact agent since 2016.[67] In this thesis, poly(2-alkyl-2-oxazoline)s were extensively exploited for syntheses of new hybrid polymers, because, except for the above mentioned advantages, they are also relatively radioresistant, and thus, are suitable for the use in delivery systems that experience radiation exposure.[68]

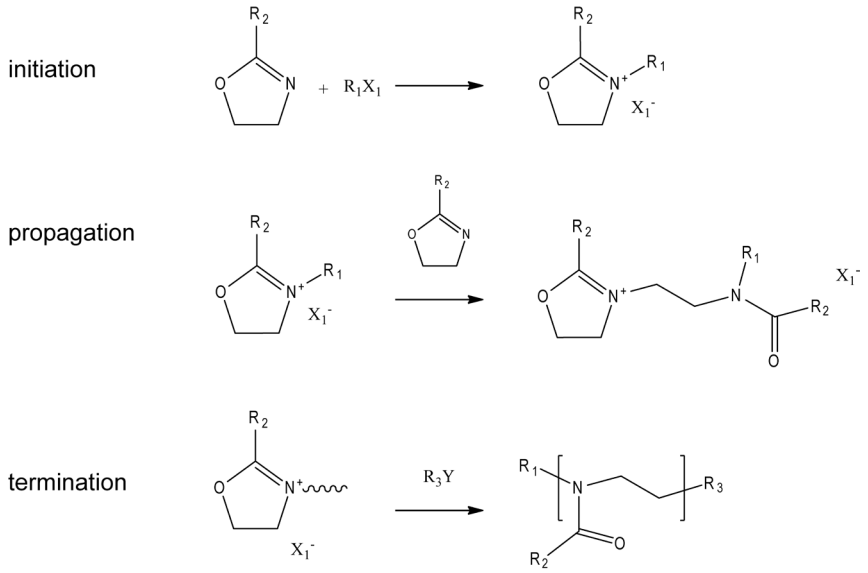

Fig. 7. The general mechanism of cationic ring-opening polymerization of 2-alkyl-2-oxazolines to form poly(2-alkyl-2-oxazoline)s.

Another frequently used polymer class, which exhibits responsivity to external stimuli, is poly(*N*-acrylamide)s. Although, the polymers are found to be non-toxic, their common use in pharmaceuticals is limited due to the possible presence of some severely toxic monomers.[69] However, the majority of monomers is classified to be not harmful. The most frequently studied and applied polymers are poly[*N*-(2-hydroxypropyl)methacrylamide] (PHPMA) and poly(*N*-isopropylacrylamide) (PNIPAm).[70] PHPMA is biocompatible, chemically stable, hydrophilic polymer, whose hydroxyl groups allow a further easy modification. It could be prepared by a free radical polymerization of *N*-(2-hydroxypropyl)methacrylamide[71], by techniques of controlled radical polymerization[72] or by a post-polymerization reaction of poly(pentafluorophenyl methacrylate), containing activated ester side chains, with 1-amino-2-propanol.[73] PNIPAm is one of the most intensively studied thermoresponsive polymers because its homopolymer displays LCST around 33 °C in aqueous environment, *i.e.,* close to the body temperature, making it suitable for biomedical applications.[74] Such polymer is water-soluble at temperatures lower than LCST and insoluble at temperatures higher than LCST; this phase separation is connected with the interruption of polymer–water hydrogen bonds.[75] Unfortunately, PHPMA as well as PNIPAm have not been yet approved by Food and Drug Administration, despite the considerable research interest and studies focused on them.

1.3. Glycoconjugates studied and used in practice

In the matter of the fact, the first commercially used glycoconjugate *Celluloid*, nitrocellulose mixed with camphor, was prepared in the Hyatt Manufacturing Company in 1870.[76] Since that time, a huge progress has been done in this research area. Nowadays, the applied ***cellulose*** modifications are numerous, including cellulose esters, ethers or copolymerized products of allyl and vinyl cellulose esters with maleic esters, which were probably the first synthesized graft copolymers of cellulose.[77] Another example of these copolymers is a cation-initiated grafting of the cellulose substrate with isobutylene and α-methyl styrene. Here, the initiator was formed *in situ* by the reaction of cellulose hydroxyl groups (Lewis base) and boron trifluoride (Lewis acid). Furthermore, cellulose was also grafted with poly(acrylonitrile), poly(methacrylonitrile) and poly(methyl methacrylate), using cellulose alcoholates as initiators.[78]

Hyaluronic acid (HA) is a linear nonsulfated glycosaminoglycan, containing 1,4-β-D-glucuronic acid and 1,3-β-*N*-acetylglucosamine. It was discovered in the cattle eye in 1934[79], however, later it was found that HA is distributed throughout the body, especially in the extracellular matrix and synovial fluids.[80] The pure HA promotes angiogenesis and also helps in wound healing, which led to its massive use in cosmetics and pharmaceuticals.[81] Furthermore, the use of HA as a biomaterial for long-terms implants was considered, nevertheless, its application is problematic due to the rapid enzymatic degradation in the body (in the human body it is degraded up to 5 g / day[82]). This is why its further modification with synthetic polymers was needed in order to reduce the degradation rate. For this purpose, HA was functionalized to bear free thiol groups and subsequently crosslinked by Michael addition with poly(ethylene glycol) diacrylate.[83] The created material is applicable for the controlled release of anti-inflammatory drugs, to increase a reepithelialization within wound healing, to stimulate a capillary growth by cytokine release[84] or as a substitute for fatty tissue.[85] Furthermore, poly(lactic-*co*-glycolic acid) was grafted onto HA, and the resulting copolymer nanoparticles were used for the targeted transport of antitumor drugs.[86] The conjugation of HA methacrylate with the diacrylate of Pluronic® F127 was also investigated using photocrosslinking effect. The formed hydrogels exhibited an interesting thermoresponsivity, showing a rapid loss of the water content in their structure with increasing temperature. This was exploited for the controlled release of human growth factors and deoxyribonucleic acid (DNA) plasmids, inducing *in vitro* transfection.[87] Similar hydrogels were produced by conjugation of HA methacrylate with the amino-functionalized

Pluronic® F127, followed by photocrosslinking with acrylate cell-adhesion domains. The subsequent encapsulation of chondrocytes by these hydrogel structures caused *in vitro* increased production of extracellular matrix proteins, especially collagen II.[87]

Chondroitin sulfate (CS) is a linear polysaccharide containing 1,3-β-*N*-acetylgalactosamine and 1,4-β-glucuronic acid, while *N*-acetylgalactosamine is sulfated in the chain at position 4 or 6 (chondroitin-4-sulfate or chondroitin-6-sulfate). CS was discovered by G. Fischer and C. Boedeker[88] in 1861, but its structure was elucidated in the beginning of the 20th century. The commercially available CS is obtained by the extraction from various natural sources, *e.g.,* cartilages of cattle, pigs or sharks. CS plays the important role in articular cartilages, where many CS chains are conjugated to one protein chain, creating a charge gradient, which reinforces the cartilage and also increases its ability to absorb burden.[89] This natural role has directed CS use in tissue engineering for the cartilage treatment. Specifically for this application, CS was first modified with glycidyl methacrylate and subsequently photocrosslinked with poly(ethylene glycol) diacrylate. Moreover, the material created by the modification of CS to have aldehyde or succinimidyl succinate groups, followed by the crosslinking with poly(vinyl alcohol-*co*-vinylamine), is used as an adhesive for corneal surgery because it exhibits minimal inflammatory responses and simultaneously it is resistant to high pressure damage.[90] This material was also studied in wound healing, and the produced hydrogel film was applied to the surface of murine wounds and also to internal injuries of the rabbit mucosa. In both cases, the treatment with these hydrogels showed a significant healing acceleration compared to the control group.[90] Another used glycoconjugate of CS is CS-*graft*-polylactide, which produces in aqueous environment the micelles suitable for chondrocyte encapsulation and targeted drug delivery.[91]

Heparin belongs to a glycosaminoglycan family of carbohydrates, consisting of variably sulfated 1,4-α,β-uronic acid and α-D-glucosamine residues. It was discovered in 1916, and since 1935 it has been clinically used as an anticoagulant.[92] Heparin is synthesized as a proteoglycan contained in the mast cells (60 – 100 kDa), which is then cleaved into smaller fragments by endoglycosidases (5 – 25 kDa).[93] Commercially, heparin is produced by an extraction of various tissues (*e.g.,* porcine or bovine intestinal mucosa) followed by numerous purification processes. The high negative charge of heparin can cause many ionic interactions with a number of proteins (growth factors, proteases, chemokines), and it has been demonstrated that such interactions can result in the structure stabilization against especially denaturation for numerous growth factors, *e.g.,* basal fibroblast growth factor

(bFGF) or vascular endothelial growth factor (VEGF). Furthermore, these interactions also increase the affinity of this complex for cellular receptors.[94] Heparin was also conjugated with polystyrene to produce material with the increased activity of growth factors VEGF and bFGF. Conjugated of heparin with PEO was used to investigated the differentiation and phenotypic response of mesenchymal stem cells and valvular interstitial cells by the capture of growth factors and other proteins binding to heparin.[95]

β-Glucans were in detail described in the section *1.2.1 The nature of polysaccharide*. They are used as stiffening agents in food and cosmetic industry. Anyway, they are generally known to have a beneficial effect on human health. For example, the intake of at least 3 g of oat β-glucan per day decreases the level of low-density lipoprotein-cholesterol and thus assists to reduce the risk of cardiovascular diseases.[96] Because β-glucans are known for their immunostimulatory and anticancer activities, also the modified β-glucans are widely studied as potential antitumor drugs. Curdlan (β-1,3-glucan), produced by fermentation of *Agrobacterium biobar*, was grafted with PEO, and the subsequently produced nanoparticles carrying the chemotherapeutic agent doxorubicin were successfully used for combined immuno- and chemotherapy.[97] A similar concept of exploiting β-glucan was used in this thesis to combine both immuno- and radiotherapy (see section *3. Results and discussion*). Moreover, the κ-carrageenan was utilized for the same purpose in this thesis.

The properties and structure of ***κ-carrageenan*** were already described in the section *1.2.1 The nature of polysaccharide*. κ-Carrageenan-*graft*-polyvinylpyrrolidone forms in aqueous environment a hydrogel, which exhibits an enhanced ability to absorb water despite of a weaker gel strength compared to the corresponding control polysaccharides.[98] Moreover, κ-carrageenan was also modified to produce pH-responsive hydrogels, κ-carrageenan-*graft*-poly(methacrylamide)s, which are designed for a controlled delivery of bioactive substances.[99] Similar system, a pH-responsive polymeric network of κ-carrageenan-*graft*-polyacrylamide and sodium alginate was successfully used for the controlled delivery of ketoprofen (a non-steroidal anti-inflammatory drug with analgesic and antipyretic effects) into the intestines.[100] Carboxymethyl derivatives of κ-carrageenan are applicable for wound healing because they are able to absorb water and exhibit antimicrobial activity. It was discovered that the substitution degree strongly affects the final wound healing ability – the higher substitution degree, the better healing results were observed.[101]

1.4 Cancer treatment

All over the world, cancer is the second leading cause of death, which is estimated to be responsible for 9.6 millions deaths in 2018.[102] In fact, it corresponds to that 1 from 6 deaths is caused by cancer. In the past, cancer was treated mainly by surgery, however, understanding of fundamental biological processes has made a revolution in cancer treatment. Nowadays, there is a number of different treatments, including chemotherapy, radiotherapy, targeted therapy or immunotherapy. These treatment methods are relatively successful, nevertheless, it is still necessary to develop and improve their efficiency, patient survival time and also a quality of life.

This thesis is focused on the polymers designed for a conceptually new cancer treatment approach, exploiting a possible synergistic effect of both immunotherapy and radiotherapy (specifically brachytherapy). Therefore, the following sections are focused only on these methods, although the cancer treatment is generally a voluminous topic.

1.4.1 Radiotherapy

Radiotherapy utilizes an ionizing radiation to kill cancer cells by a destruction of their DNA that leads to the cellular death. In general, radiation is not specific for cancer cells and, unfortunately, also damages the healthy tissue. Radiotherapy treatments are divided into two groups according to the position of the used radiation source. External beam radiotherapy uses the radiation source outside the body, while the radiation source of internal radiotherapy (brachytherapy) is placed precisely in the area requiring a treatment.

External beam radiotherapy is the most commonly used method of radiotherapy. To at least partially protect the normal tissues within the external radiotherapy treatment, the radiation beams are aimed from different exposure angles in order to intersect at the tumor site, resulting in a much higher absorbed radiation dose of tumor area compared to surrounding healthy tissues. Depending on the used radiation energy, it is possible to exploit external radiotherapy for skin cancer treatment as well as to treat deep-seated tumors (*e.g.,* prostate, bladder or brain).

As it was said above, ***brachytherapy*** exploits a localized radiation source, which is placed inside or very close to the site requiring a treatment (the word "*brachy*" means in Greek "*for short distance*"). This allows using significantly higher radiation doses because radioactivity is located only at the tumor site, and thus, the whole-body radiation exposure is minimized.[103] Therefore, brachytherapy procedure can be successful in shorter time than other

radiotherapy techniques, increasing a patient survival chance.[104] Moreover, the majority of patients are able to tolerate treatment side effects very well. Brachytherapy is most often used for solid tumor treatment. It can be realized by surgical implant, demanding two surgical interventions to place implant in and out, or by an injection of radioactive thermoresponsive polymer, which is soluble at room temperature and concurrently creates a polymer depot at the injection site due to the body temperature.[105] For this purpose, the polymers with cloud point temperature (CPT, *i.e.*, the temperature at which they start to precipitate at the given concentration) around 32 °C are suitable to use because it is guaranteed that the polymer is completely precipitated at 37 °C. The depot formation was investigated in numerous studies, *e.g.,* polymers based on poly(*N*-isopropyl acrylamide) with CPTs of approximately 33 °C, were injected intratumorally to mice and remained at the injection site for more than 10 days.[106] The brachytherapy approach utilizing a thermoresponsive polymer with CPT was exploited in this thesis.

1.4.2 Immunotherapy

Another therapy attracting interest nowadays is ***immunotherapy*** which exploits body's own immune system to eradicate tumors and also metastasis. The reason why the immune cells do not recognize and eliminate cancer cell is that in the tumor microenvironment these immune cells are rendered to be nonfunctional because tumors produce a number of immunosuppressive factors (*e.g.,* prostaglandin E2, inhibitory cytokines and others).[107] There are two main treatment strategies – passive and active immunotherapy. The success of passive therapy follows the ability of administrated anticancer monoclonal antibodies or donor T cells to cause an immediate immune reaction against cancer, bypassing the requirement of endogenous immunity activation[108], which is known to control the tumor growth.[109] Nowadays, nine monoclonal antibodies are approved drugs for the solid and hematological malignancies treatments, when they target cancer-associated proteins (EGFR, VEGF, HER2, CD20, CD52 and CD33).[108] In contrast to passive immunotherapy, the active treatment, stimulating the immune system to cause a durable antitumor immunity, seems to be still elusive. The first attempts in this field were done a long time ago, in 1891, by William Coley. He injected intratumorally live and also inactivated bacteria of *Streptococcus pyogenes* and *Serratia marcescens* to cause a spontaneous sarcoma remissions, which he had discovered in the cancer patients having erysipelas as well.[110] 'Coley's toxins' probably acted to stimulate antibacterial phagocytes, which then might kill tumor cells. In the following

40 years, some considerable immune responses were observed, however, the treatment success was rather sporadic and not reproducible. Therefore, the oncologists started to rely on surgery and also on the other newly developed methods, especially radiotherapy and chemotherapy, and the history of immunotherapy was decelerated for a while. The key role in the immune system activation is played by Toll-like receptors (TLRs), which are expressed on the leukocyte membranes, predominantly on macrophages, dendritic cells, natural killer cells and also the adaptive immunity cells (T and B lymphocytes). In general, it is believed that one of the promising approach in cancer immunotherapy could be the harnessing of TLRs[111], while this approach was applied in this thesis using polysaccharides, which trigger TLRs.

2. Aims of the thesis

1. Preparation and characterization of the novel hybrid polymers polysaccharide-*graft*-poly(2-isopropyl-2-oxazoline-*co*-2-butyl-2-oxazoline)s differing in graft length and grafting density. For this purpose, β-glucan from *Auricularia auricula-judae* and κ-carrageenan from *Kappaphycus alvarezii* were chosen as the used polysaccharides.

2. Study of thermoresponsive and potassium responsive (only for κ-carrageenan) behavior of the prepared polymers and selection of the most suitable materials for the further biomedical application from the view of thermoresponsivity (polymer has to be soluble at room temperature and to be phase-separated at 37 °C).

3. Modification of the most suitable polymer to bear at the graft ends a fluorescent dye and the moieties able to complex radioactive yttrium-90(III).

4. Fundamental *in vitro* and *in vivo* experiments of the most suitable polymer conjugate(s), studying its potential use in the immunoradiotherapy.

3. Results and discussion

3.1 β-Glucan-*graft*-poly(2-isopropyl-2-oxazoline-*co*-2-butyl-2-oxazoline)s

3.1.1 Polymer design and synthesis

We have designed a conceptually new bimodal cancer treatment, immunoradiotherapy, to exploit the possible synergistic effect of both immunotherapy and radiotherapy **(Fig. 8)**. The theoretical treatment principle is as follows: the polymer solution is injected into the tumor and, because of the its thermoresponsivity, the depot is created at the injection site, while the local action of the contained radioactivity kills the cancer cells. After the radionuclide decays, the polymer immunostimulatory part activates the immune system against the cancer cells. The increased concentration of the immune cells at the same place as the dead cancer cells (tumor debris) would lead to the recognition of the cancer cells as extraneous cells of the body. Therefore, the stimulated adaptive immunity would be able to kill the other cancer cells and metastases.

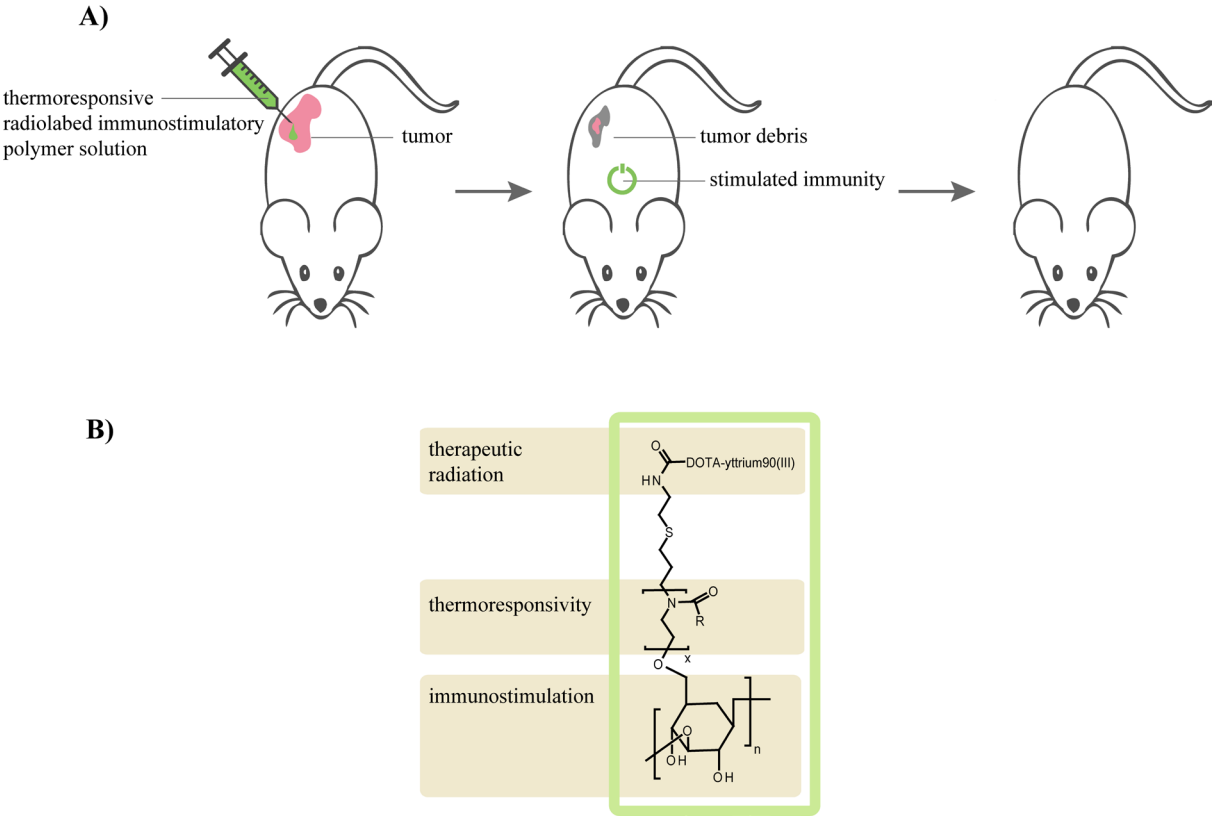

Fig. 8. A) The theoretical treatment principle of bimodal immunoradiotherapy (radiation kills the tumor cells; after the radionuclide decays, the immunostimulatory polymer part enhances the following immune response against the remaining cancer cells and metastases). B) Structure of the polymer designed to be used in immunoradiotherapy.

The polymer, β-glucan-*graft*-poly(2-isopropyl-2-oxazoline-*co*-2-butyl-2-oxazoline) (β-glucan-*graft*-POX) bearing a fluorescent dye Dyomics-615 and the complex of 1,4,7,10-tetraazacyclododecane-1,4,7,10-tetraacetic acid (DOTA) with yttrium-90(III) at the graft ends **(Fig. 8B)**, was designed to be used in such cancer treatment because it combines the known immunostimulatory and anticancer properties of β-glucan from *Auricularia auricula-judae*[38] with the POX thermoresponsivity. Yttrium-90(III) was chosen as a radiation therapy source because it has a therapeutically convenient half-life ($T_{1/2}$ = 64.1 h) and predominantly undergoes short-distance effective β^- decay. Therefore, the polymer depot labeled with yttrium-90(III) has a smaller impact on the whole body because the radiation is effective only at the depot site. Moreover, POXs are relatively radioresistant compared to the other thermoresponsive polymers, and thus, they are suitable to be used in this system.[68]

The graft length has a crucial impact on the final polymer properties; therefore, four samples of β-glucan-*graft*-POXs with a maximum achievable grafting density, differing in the graft length (G1 with the theoretical graft length 500 Da, G2 1000 Da, G3 2500 Da and G4 5000 Da), were prepared and their thermoresponsive behavior in the aqueous environment was studied.

The first step of polymer synthesis was an extraction of β-glucan from the bodies of *Auricularia auricula-judae* according to a known procedure.[20] The purified β-glucan was then grafted by a simple one-pot, two-step reaction (**Fig. 9B**) with POXs, which were separately synthesized by cationic ring-opening polymerization of 2-isopropyl-2-oxazoline and 2-butyl-2-oxazoline using allyl bromide as an initiator. Allyl bromide was selected because it brings double bonds at the graft ends, enabling further modifications, *e.g.*, radical crosslinking/copolymerization or thiol-ene click chemistry. Thereafter, the living POX ends were terminated with sodium β-glucanate, prepared separately before, to give β-glucan-*graft*-POXs. Furthermore, to study the graft properties apart, POX living ends were additionally terminated with water (instead of sodium β-glucanate) to obtain only corresponding POXs with –OH end-groups.

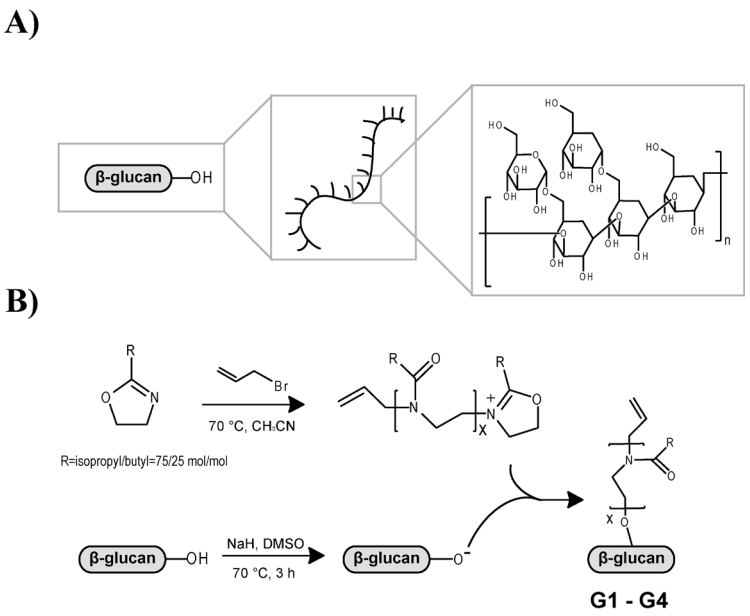

Fig. 9. A) Structure of the isolated β-glucan; B) general scheme for G1 – G4 synthesis.

The successful grafting procedure was confirmed by nuclear magnetic resonance (NMR) and by Fourier-transform infrared (FTIR) spectroscopies. The ^{1}H-NMR spectra of β-glucan-*graft*-POXs exhibited peaks, which correspond to the POX groups (POX region in **Fig. 10B**) and also to the β-glucan backbone (β-glucan region in **Fig. 10B**). The peak intensity in the β-glucan region decreased from G1 to G4, demonstrating the decreasing amount of β-glucan in the particular samples. The similar phenomenon was observed from the FTIR spectra of the grafted β-glucans (**Fig. 10A**). The peak at 1624 cm^{-1} corresponds to an amide C=O stretching vibration of the POX, confirming its presence in the final polymers.

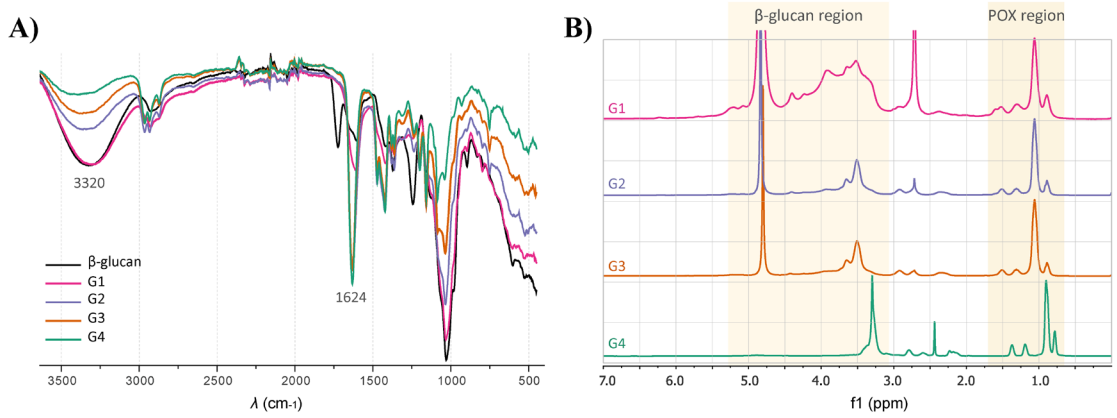

Fig. 10. A) FTIR and B) NMR spectra of the G1 – G4 polymers.

The weight-average molecular mass of grafts and of the grafted polymers was determined using size-exclusion chromatography (SEC) with multiangle light scattering (MALS) detectors (**Table 3**). The theoretical monomer ratio in the polymer grafts was selected to be $n_{\text{2-isopropyl-2-oxazoline}}$ / $n_{\text{2-butyl-2-oxazoline}}$ = 3/1 mol/mol. According to our previous experiences, POX with this monomer ratio, grafted onto polysaccharide, displays the most appropriate cloud point temperature (CPT) for biomedical application (CPT between room and body temperatures), which allows an injection of the polymer solution and a subsequent formation of the polymer depot in the organism. In this case, the depot formation is caused by the self-assembling process of the thermoresponsive polymer.[112] The actual monomer ratio $n_{\text{isopropyl}}/n_{\text{butyl}}$ in the prepared POX grafts was calculated from the ratio of the corresponding NMR peaks (integral intensities), and the obtained values were very close to the theoretical one 75/25 (**Table 3**).

Because the extracted β-glucan contained less than 0.1 wt. % nitrogen, the POX content in the synthesized polymers was calculated using the nitrogen weight content, which was determined by elemental analysis (CHN). The found POX content corresponded to the graft length (**Table 3**), the longer grafts, the higher POX content. Moreover, the POX chains were in a high excess within the grafting procedure, which probably resulted in the maximum achievable grafting density. In general, the maximum achievable density is given by the molecule conformational structure. The used β-glucan has a comb-like shape, which, interestingly, causes that the maximum achievable grafting density of shorter grafts is comparable with the one of longer grafts (from 6 to 9 glucose units per graft, **Table 3**).

Table 3. Characterization of the prepared grafted polymers.

	Theor. graft length (Da)	**Found graft length (Da)[1]**	**$n_{\text{isopropyl}}$/ n_{butyl}[2]**	**POX content (wt. %)**	**M_w (Da)[1]**	**Dispersity**	**Glucose units per graft**
G1	500	590	70/30	26	3.7×10^6	1.64	9.3
G2	1000	1140	74/26	47	6.4×10^6	1.64	7.2
G3	2500	2290	74/26	70	7.5×10^6	1.49	6.0
G4	5000	4180	73/27	80	1.6×10^7	3.70	5.9

[1] Determined by SEC-MALS,

[2] $n_{\text{isopropyl}}/n_{\text{butyl}}$ is the molar ratio of 2-isopropyl-2-oxazoline to 2-butyl-2-oxazoline incorporated in the POX grafts, determined by NMR. The theoretical one was 75/25.

3.1.2 Thermoresponsive polymer behavior

The thermoresponsive behavior of polymers G1 – G4 was studied using dynamic light scattering (DLS) in order to get detailed information about a depot formation after the polymer solution injection into the body, when using in cancer therapy.

For all polymers, the CPTs were determined in the concentration range from 1 to 25 mg/mL in phosphate-buffered saline (PBS) using DLS measurement (**Fig. 11A, B)**, which showed a dependence of polymer hydrodynamic radius R_h on the temperature. As supposed, the CPT of the prepared polymers crucially depends on the graft length – for the shortest grafts, the CPT of G1 was even not detected up to 65 °C. On the other hand, the sample G4 with the longest grafts precipitates even at room temperature. Moreover, the CPTs for a given sample decrease with the increasing concentration, while the difference between CPTs through the concentration range is influenced by the graft length. For G4 with longest grafts ($M_{n,graft(found)}$ = 4180 Da), the difference between the CPT at c = 1 mg/mL and the CPT at c = 25 mg/mL is 8 °C, while G2 ($M_{n,graft(found)}$ = 1140 Da) exhibited the difference of only 4 °C. Furthermore, these measurements revealed that the most suitable polymer for a depot formation after intratumoral injection of polymer solution is the sample G3 with the grafts of 2290 Da. The polymer G1 is not suitable because it did not show any thermoresponsivity up to 65 °C, G2 is also not useful due to the CPTs higher than 37 °C at lower concentrations, which could end in a fast dissolution of the created depot. On the other hand, the polymer G4 has too low CPTs.

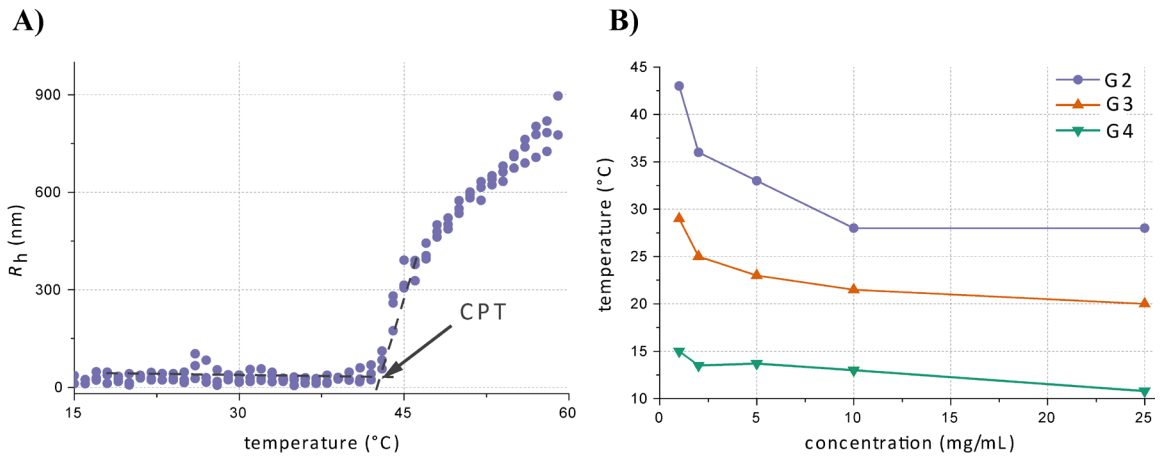

Fig. 11. A) The temperature dependence of the hydrodynamic radius R_h of G2 at concentration c = 1 mg/mL in PBS; B) CPTs of the synthesized polymers in PBS (CPT of G1 was not detected up to 65 °C).

The thermoresponsive behavior of the most suitable polymer G3 was further studied using temperature-dependent fluorescence measurements to get information about the microenvironment hydrophobicity during phase transition. This measurement exploits the aggregation-induced emission caused by a fluorescent probe, which does not emit any fluorescence in the molecularly dissolved state but it is highly fluorescent in the aggregated state (hydrophobic environment). In this case, 8-anilino-1-naphthalenesulfonic acid ammonium salt (c = 0.25 μmol/mL, λ_{ex} = 388 nm) was used as a fluorescent probe. At lower temperatures, the solution of polymer G3 (c = 10 mg/mL in PBS) exhibited only a weak fluorescence signal (**Fig. 12),** which could probably correspond to the formed aggregates from isopropyl and butyl moieties of one or very few macromolecules. However, the fluorescence intensity significantly increased at 22.5 °C, suggesting that the content of hydrophobic domains increased as well. This result is in good agreement with the result of DLS measurement, which detected the CPT of this system to be 21.5 °C. Furthermore, the fluorescence intensity was then increasing with the elevated temperature up to 32.5 °C, displaying the increasing content of hydrophobic domains and also an inter/intramolecular reorganization of the self-assembled architectures in this temperature zone. Thereafter, the fluorescence intensity was not rising with the increasing temperature, and it remained almost constant.

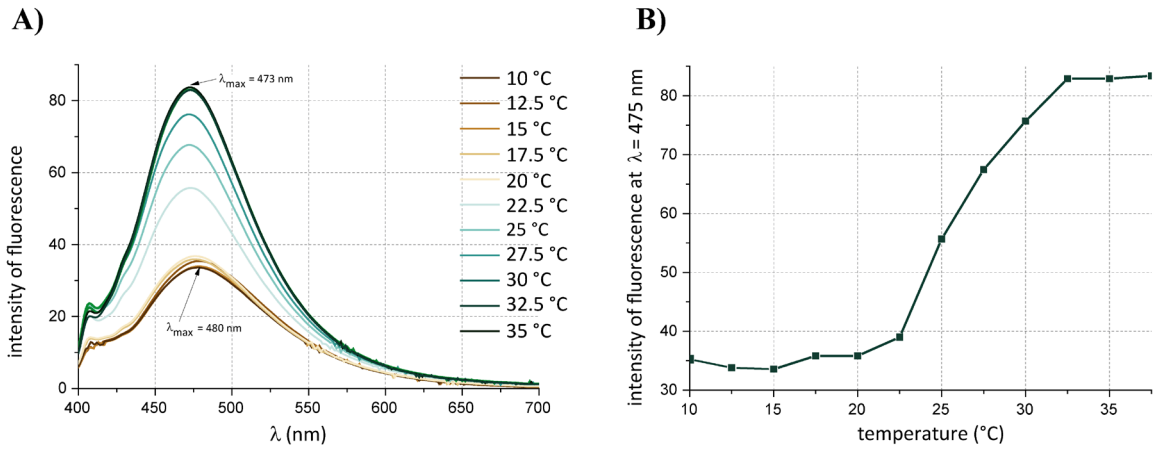

Fig. 12. A, B) The temperature-dependent fluorescence of the polymer G3 (c = 10 mg/mL in PBS) with a fluorescent probe (8-anilino-1-naphthalenesulfonic acid ammonium salt, c = 0.25 μmol/mL, λ_{ex} = 388 nm).

The thermoresponsive behavior of G3 was also characterized by high-resolution ^{1}H-NMR spectroscopy (**Fig. 13**). The intensity of signals corresponding to POX groups decreased with the increasing temperature. This phenomenon is a typical behavior for the thermoresponsive polymers, connected with the decreased mobility of POX chains at the elevated temperature, which is in analogy to literature.[113] The quantity of *p*-fraction is, in general, very useful for the temperature-dependent NMR spectra because it enables to quantitatively compare the changes that occur within the heating and cooling processes. The *p*-fraction can be calculated according to the equation (1)

$$p = 1 - \{I(T) / [I(T_0) \cdot (T_0 / T)]\} \quad (1)$$

where $I(T)$ is the integrated intensity of a signal in the spectrum at the temperature T and $I(T_0)$ is the integrated intensity of the same signal in the case when no phase separation occurs (below CPT). The *p*-fractions were calculated for POX groups (**Fig. 13B**). For all POX proton groups of G3 the phase transition begins at approximately 24 °C (c = 10 mg/mL in D_2O), which is in good agreement with the results obtained by other methods. The final *p*-fraction value (p_{max}) gives a quantitative information about the amount of the groups that participate in a phase transition. The p_{max} value was 0.69 for group "**a**" from the POX main chain and 0.76 and 0.67 for the isopropyl units "**b**" and "**c**", respectively, meaning these groups influence the phase transition similarly. However, the p_{max} values of protons from 2-butyl-2-oxazoline unit were calculated to be slightly lower, suggesting that these sections are probably more flexible in the aggregated state.

The more detailed description of β-glucan-*graft*-POXs syntheses and their thermoresponsive behavior can be found in the **Appendix 1** (see section *6. Appendixes – attached publications*).

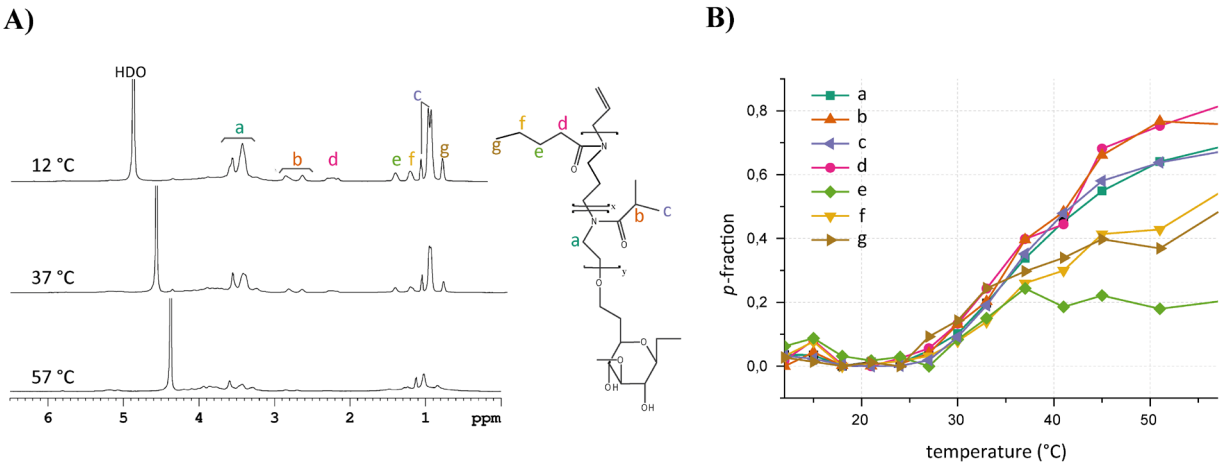

Fig. 13. A) High-resolution ^{1}H-NMR spectra of the polymer G3 (c = 10 mg/mL in D_2O) measured at 12 °C, 37 °C and 57 °C; B) the temperature-dependent p-fractions of the polymer G3 – proton groups of poly(2-isopropyl-2-oxazoline-*co*-2-butyl-2-oxazoline) (c = 10 mg/mL in D_2O).

3.1.3 Polymer modification

The most suitable polymer in the terms of thermoresponsive behavior (for a depot formation after the polymer solution injection) was selected to be the sample G3 with the graft length of 2290 Da. This polymer was further modified (**Fig. 14**) to bear at the grafts ends a fluorescent dye Dyomics-615, permitting to track the polymer fate with fluorescence imaging, and DOTA moiety, enabling its radiolabeling with yttrium-90(III) and thus its subsequent use in therapeutic experiments. The first step of such modification was incorporation of cysteamine at the graft ends using a thiol-ene click reaction (**Fig. 14**) to obtain G3-II with $–NH_2$ groups at the graft ends. Their amount was determined to be 0.17 mmol $–NH_2$ groups/g, using a 2,4,6-trinitrobenzene-1-sulfonic acid (TNBSA) assay[114]. Thereafter, $–NH_2$ groups at the graft ends were exploited to introduce the Dyomics-615 and DOTA, using the reaction with their *N*-hydroxysuccinimidyl esters (NHS-esters). The content of Dyomics-615 in the final polymer G3-III was determined spectrophotometrically ($\lambda_{absorption}$ = 621 nm, ε = 200 000 L/mol·cm) to be 0.1 wt %, and the DOTA content was detected by the chelation with Gd(III) followed by the energy-dispersive X-ray spectroscopy to be 1.72 %, meaning 0.11 mmol DOTA/g.

Similarly, the corresponding POX of length 2290 Da was modified to bear DOTA moieties at the polymer ends as well.

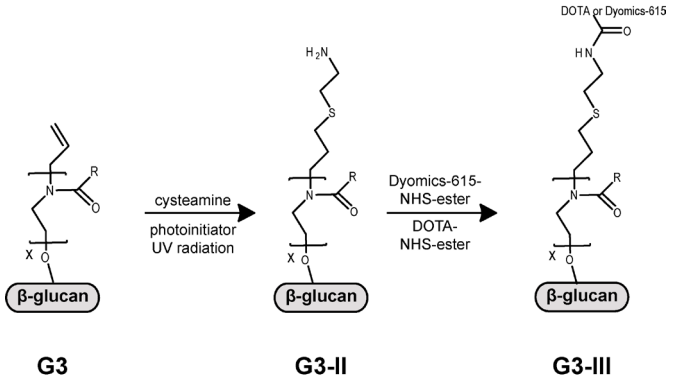

Fig. 14. The scheme of further modification of the polymer G3.

3.1.4 In vitro studies

To use the synthesized polymer G3-III in further *in vivo* experiments it must have firstly been successfully tested *in vitro*.

The polymer cytotoxicity was investigated on different cell lines (macrophages RAW 264.7, MCF7 and EL4 cancer cells) using an AlamarBlue assay, and it was found to be almost negligible for all tested cell lines, meaning the non-toxicity of the polymer G3-III.

The next *in vitro* experiment was oxidative burst response of the leukocytes assay which gives information about the polymer immunostimulatory properties. The leukocyte response after the polymer stimulation was indirectly detected using the viability decrease of *Staphylococcus (S.) aureus*, added within the experiment. The assay was done using leukocytes isolated from human whole blood, and the original non-grafted β-glucan was used as a control sample. The polymer G3-III showed the enhanced response of the leukocytes (**Fig. 15A**), which is demonstrated by the decrease of the *S. aureus* viability at the polymer concentrations corresponding to 1 and 10 μg/mL of β-glucan in the tested solutions (c = 3.4 and 34 μg/mL). Significant differences compared to the control group (no immunostimulatory properties) were statistically confirmed (c = 3.4 μg/mL, $P < 0.0065$; c = 34 μg/mL, $P < 0.0007$). The polymer G3-III exhibited similarly strong response of the leukocytes as β-glucan, considering the same amount of β-glucan. This means that grafting of β-glucan by POX does not decrease the polymer immunostimulatory properties.

β-Glucan from *Auricularia auricula-judae* enhances the production of tumor necrosis factor α (TNF-α), which is a multifunctional cytokine, playing a key role in the regulation of immune cells and influences many other actions, such as apoptosis or cell survival.[115] TNF-α was named for its antitumor properties, and it is nowadays widely studied for its potential use in cancer therapy. The production of TNF-α induced by the polymer G3-III was tested using

an enzyme-linked immunosorbent assay (ELISA) on leukocytes isolated from human whole blood (**Fig. 15**). The increased production of TNF-α was observed after the leukocyte stimulation with the polymer G3-III at the concentrations corresponding to 1 and 10 μg/mL of β-glucan (c = 3.4 and 34 μg/mL). The control group was stimulated with phorbol myristate acetate (PMA) (c = 2 μM), which is an activator of phagocytosis. Significant differences in TNF-α production by G3-III and PMA were statistically confirmed (c = 3.4 μg/mL, $P < 0.00033$; c = 34 μg/mL, $P < 0.0012$). This observation indicates an optimistic prognosis for the prospective cancer treatment by the prepared polymer.

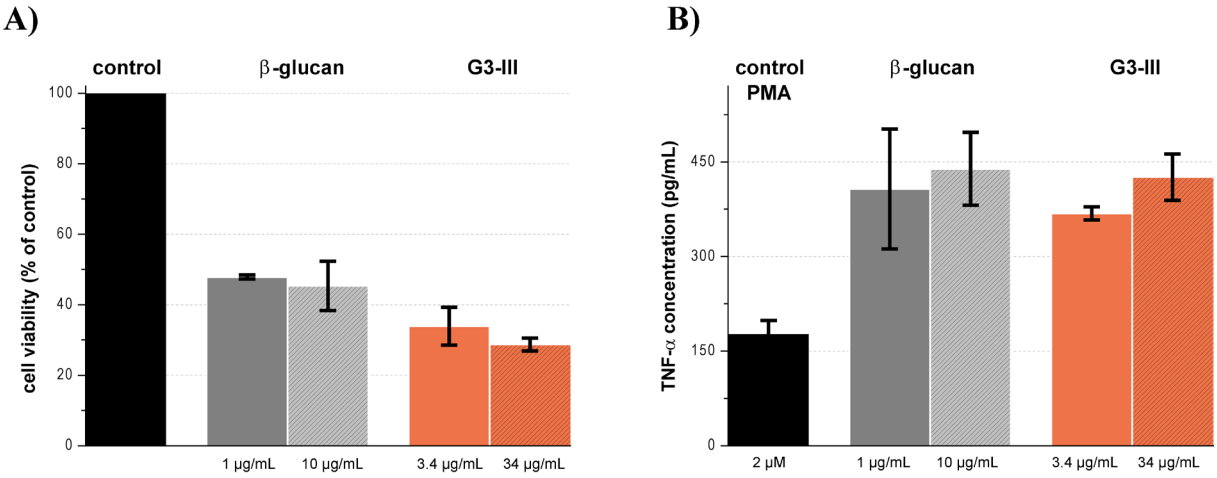

Fig. 15. A) The cell viabilities of *S. aureus* after the stimulation by β-glucan and the polymer G3-III at the concentrations corresponding to 1 and 10 μg/mL of β-glucan (for β-glucan c = 1 and 10 μg/mL and for G3-III c = 3.4 and 34 μg/mL). They correspond indirectly to the oxidative burst response of the leukocytes. B) The production of tumor necrosis factor α (TNF-α) induced by phorbol myristate acetate (PMA) as the control, β-glucan and the synthesized polymer G3-III at concentrations corresponding to 1 and 10 μg/mL of β-glucan (for β-glucan c = 1 and 10 μg/mL and for G3-III c = 3.4 and 34 μg/mL).

Thereafter, the polymer cellular uptake into macrophages and MCF7 cancer cells was studied using confocal laser scanning microscopy. The microscopy experiments revealed that the polymer G3-III was internalized into both cell lines (uptake into macrophages is visualized in **Fig. 16A**), while the data denoted that G3-III is internalized even better than the original non-grafted β-glucan that is even more pronounced after shorter incubation times

(15 min and 4 h). Therefore, the cellular internalization kinetics into the MCF7 cancer cells for β-glucan and for the polymer G3-III (β-glucan-*graft*-POX) was performed using flow cytometry (**Fig. 16B**). Anyway, MCF7 cancer cells were used because they represent a good model for drug cellular internalization *in vitro*. The observed data implies that G3-III is internalized in the cancer cells almost twice faster compared to the internalization of the original β-glucan, indicating the good cell-internalization properties of the prepared conjugate G3-III.

The *in vitro* experiments demonstrated very promising properties for cancer immunoradiotherapy, and thus, the experiments *in vivo* were subsequently performed (see below).

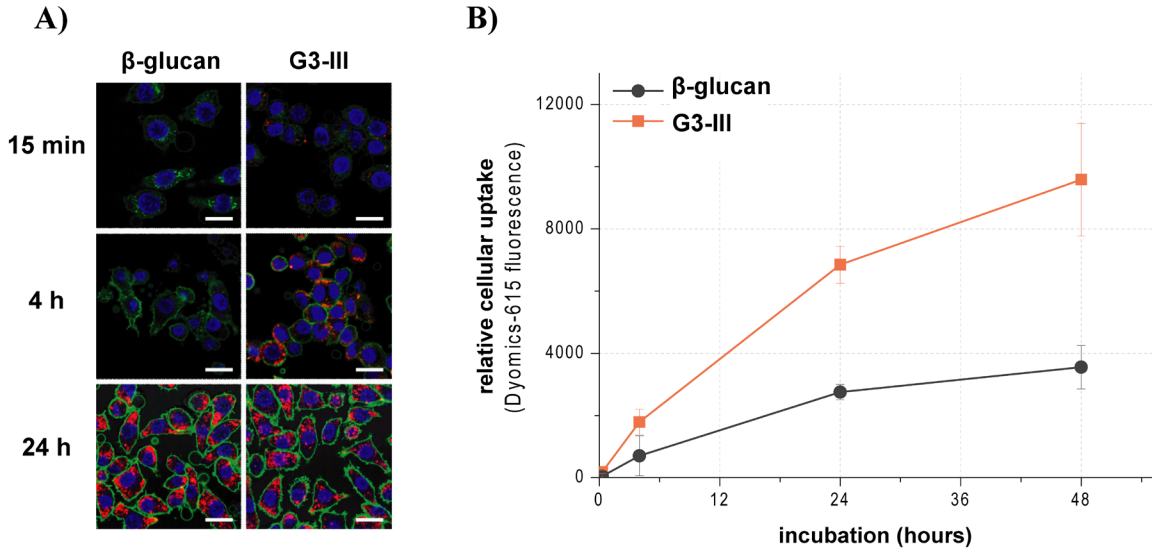

Fig. 16. A) The confocal microscopy images of β-glucan and G3-III after their incubation at the concentrations corresponding to 150 μg/mL β-glucan at 15 min, 4 h and 24 h with RAW cells. The organelle staining is shown in green (CellMask Green, cell membrane) and blue (Hoechst 33342, nucleus), the polymers are in red (Dyomics-615 dye). The scale bar is 20 μm. B) Polymer cellular uptake in the cancer cells after up to 48 h of incubation at the concentration corresponding to 50 μg/mL β-glucan.

3.1.5 Polymer radiolabeling and radiostability

For the performance of *in vivo* antitumor efficiency experiment using the prepared polymer G3-III, this polymer must be first labeled with yttrium-90(III), which, as it was said above, predominantly undergoes β^- decay, effective to the short distances (up to 1 cm in aqueous

tissue). Therefore, the created radiation operates only locally and, furthermore, its half-life time is therapeutically convenient ($T_{1/2}$ = 64.1 hours). The polymer G3-III was labeled by a chelation of DOTA groups using yttrium-90(III) chloride in ammonium acetate buffer and purified on a Sephadex® G-25 column to obtain the labeled polymer G3-III-Y with sufficient radioactivity for a subsequent therapy treatment (A = 5 MBq/mg).

In the organisms, there is a variety of different ions which can compete with yttrium-90(III) and replace it in the formed complex. Such competing ions are especially Ca^{2+} and Zn^{2+}. Moreover, in the living organism, there are also phosphates, which can complex yttrium-90(III). Therefore, the radiostability of the prepared complex DOTA-yttrium-90(III) (G3-III-Y) was studied by its incubation in the environment containing ions at the concentrations as in blood plasma (c_{Ca2+} = 1.0 mmol/L, c_{Zn2+} = 0.0153 mmol/L and $c_{phosphates}$ = 1.0 mmol/L). After a given time, the aliquot sample from the incubation mixture was taken out, and it was studied on a Sephadex® G-25 column in the comparison to yttrium-90(III) chloride. A significant leak of yttrium-90(III) from the polymer complex was not observed even after 48 h at 37 °C (**Fig. 17**), which predicts the high radiostability of the radiolabeled polymer G3-III-Y in the blood.

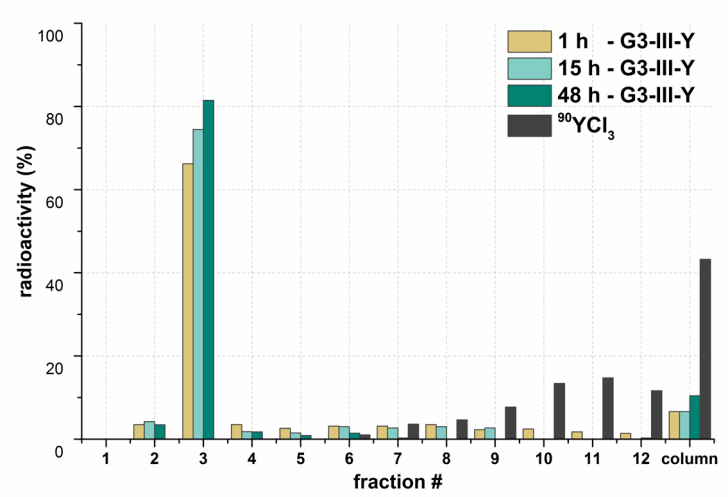

Fig. 17. The radiostability test of the polymer G3-III-Y, which was incubated for 1, 15 and 48 h under the ion concentrations as they are in blood plasma (c_{Ca2+} = 1.0 mmol/L, c_{Zn2+} = 0.0153 mmol/L and $c_{phosphates}$ = 1.0 mmol/L).

3.1.6 In vivo study

The *in vivo* study was performed after the successful *in vitro* study and also a successful radiolabeling of the prepared polymer G3-III with yttrium-90(III).

At first, the test of immune response induction was carried out. The solution of G3-III was injected into the thigh muscles of healthy mice ($n = 3$), and after 7 days the mice were sacrificed. The histological evaluation of the injection sites showed an extensive inflammation caused by the formed polymer depot (**Fig. 18**). It was represented by the round-cell inflammatory cellularization in the adipose and loose connective tissue as well as by the phlegmonous mixed inflammatory cellularization (**Fig. 18A, C, D**). Furthermore, a dystrophic calcification of the muscle fibers (**Fig. 18A, C, D**) was also observed at the injection sites that denotes a considerable inflammation. Thus, the polymer G3-III induces a non-specific immune system response, similarly as the original β-glucan. It was again discovered that grafting of the β-glucan backbone by POX chains does not significantly decrease its immunostimulatory properties (see above the section *3.2.4. In vitro studies*).

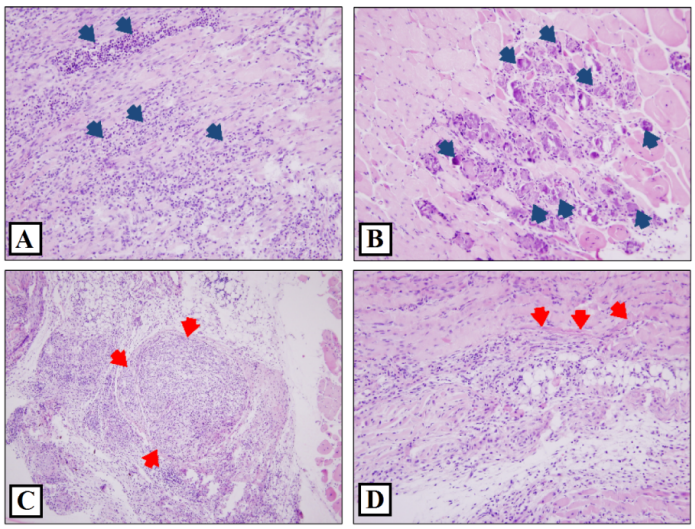

Fig. 18. Histological evaluation of the injection sites (7 days after an administration of the polymer G3-III): A) phlegmonous mixed inflammatory cellularization with the predominance of granulocytes (original magnification 200×), B) dystrophic calcification of the muscle fibers (blue arrows, original magnification 200×), C) round-cell inflammatory cellularization in adipose tissues near the nervous and vascular plexus. The nerve (red arrows) is edematous with round-cell infiltrates (original magnification 100×), D) round-cell inflammatory infiltration in the loose connective and adipose tissue reaching the dystrophic muscle fibers (red).

The antitumor efficiency of a proposed conceptually new cancer treatment – immunoradiotherapy – was studied *in vivo* using the synthesized radiolabeled polymer G3-III-Y, labeled with yttrium-90(III). For this purpose, the syngeneic murine model –

C57BL/6N mice with murine lymphoma EL4 – was exploited. To be able to confirmed a possible synergistic effect of immunoradiotherapy, the mice were separated into four groups as follows (**Fig. 19A**): 1) control group (no treatment), 2) IMMUNOtherapy (treated with β-glucan-*graft*-POX – G3-III), 3) RADIOtherapy (treated with radiolabeled POX chains with the same lengths as grafts) and 4) IMMUNORADIOtherapy (treated with radiolabeled β-glucan-*graft*-POX – G3-III-Y). Moreover, the drug dose in the particular groups was designed to be corresponding to each other – 0.3 mg of β-glucan, 0.7 mg of POX chains and radioactivity of 4 MBq per a mouse. Thus, the dose for IMMUNORADIO group was 1 mg G3-III-Y/4 MBq/mouse, for IMMUNO group was 1 mg G3-III/mouse and for RADIO group was 0.7 mg of the corresponding POX/4 MBq/mouse. To avoid a potential polymer precipitation in the needle that could have brought inhomogeneities in administration, the polymers were administrated as their DMSO solutions (50 µL DMSO/mouse) because they are soluble in DMSO without exhibiting a phase transition at elevated temperature. Moreover, this approach promotes faster polymer precipitation and a subsequent depot formation in the aqueous environment due to the cononsolvency effect.[116] The corresponding amount of DMSO was injected intratumorally also in the control group to exclude its possible effect on the tumor growth.

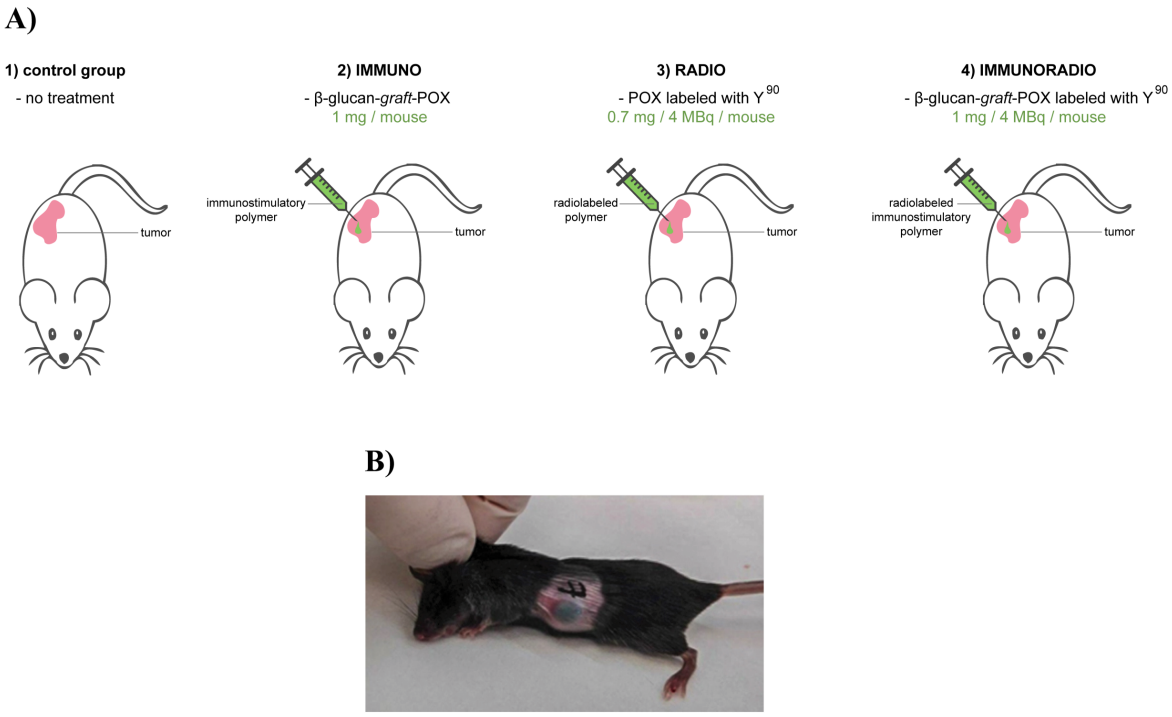

Fig. 19. A) The design of antitumor efficiency experiment, B) a mouse from IMMUNORADIO group after the polymer intratumoral administration.

The tumor growth was suppressed in all treated groups (**Fig. 20B**), and the statistically significant difference of populations ($a = 0.05$) was observed between IMMUNORADIO and control groups on day 3 and between RADIO and control groups on day 10. Moreover, growth of the primary tumor was almost blocked in the IMMUNORADIO group. Despite the fact that the difference between IMMUNO and control groups was not statistically confirmed ($a = 0.05$) up to day 20, the mean value of the tumor volume was lower from day 14.

The important quantity, informing about the treatment success, is a survival time which was also studied (**Fig. 20A**). All treated groups exhibited prolonged survival times in the comparison with the control group (24.7 ± 3.5 days). However, only a slight growth was monitored in the mean survival time in IMMUNO group (26.9 ± 4.9 days). On the other hand, two mice from RADIO group were entirely cured (treatment success: 12 %), and the mean survival time of the uncured mice from this group was considerably extended (29.8 ± 8.4 days). The treatment success in IMMUNORADIO group was significantly better because 12 mice from a total of 15 mice were observed to be cured (no trace of tumor) on day 13, nevertheless, primary and metastatic tumors again appeared in some of them. Finally, 7 mice (treatment success: 47 %) were completely cured in this group, and the mean survival time of the uncured mice was considerably prolonged (39.0 ± 6.9 days).

All the results of the antitumor efficiency experiment imply the synergistic effect of using immunoradiotherapy compared to separately used immunotherapy or radiotherapy. This phenomenon could be described by a therapy cooperation as follows: the polymer therapeutic radiation kills the cancer cells, while after the radionuclide decay, the polymer depot enhances the immune responses against remaining cancer cells.

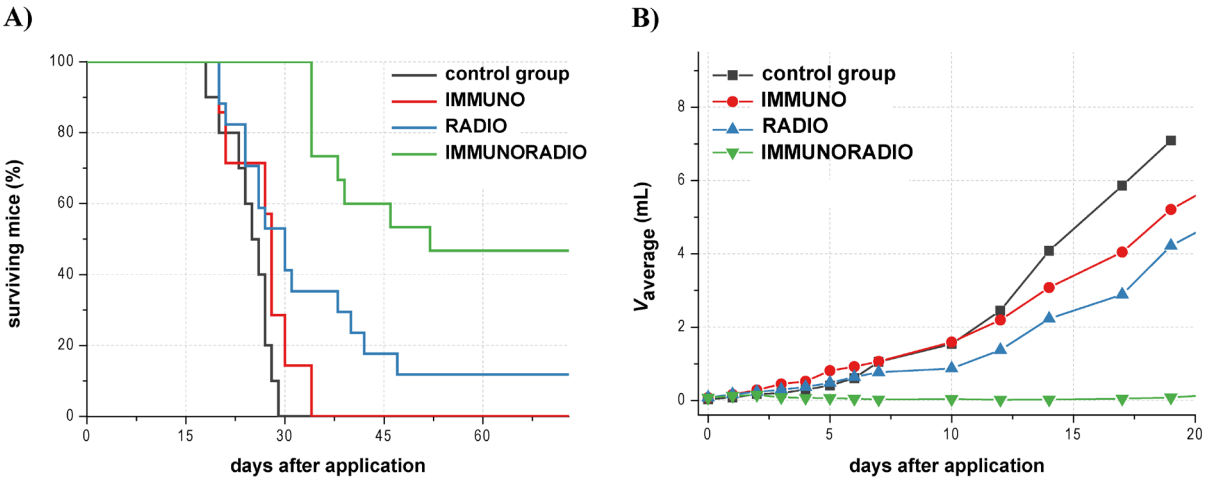

Fig. 20. The treatment effect on the: A) survival time and B) primary tumor growth.

The polymer biodistribution was studied simultaneously with the antitumor efficiency experiment (**Fig. 21**). The particular images were done by composition of X-ray images (all groups), fluorescence images of the dye Dyomics-615 (IMMUNO and IMMUNORADIO groups) and Cherenkov radiation images of yttrium-90(III) (RADIO and IMMUNORADIO groups).

The polymer G3-III-Y (IMMUNORADIO) formed a depot after the administration, staying at the injection site almost 16 days, which corresponds to 6 half-lives of yttrium-90(III). Furthermore, the presence of polymer was not observed in kidneys, livers or other body parts, confirming the theory that the polymer is slowly degraded by glycosidases into the oligomers, which are shorter than the renal threshold and gradually removed from the body. The similar observation was detected for non-radiolabeled polymer G3-III (IMMUNO). The POX polymer with the corresponding length was found at the injection site until day 5. Thereafter, the normalized Cherenkov radiaton intensity was not observed at all, confirming that the POX polymer was completely removed from the body.

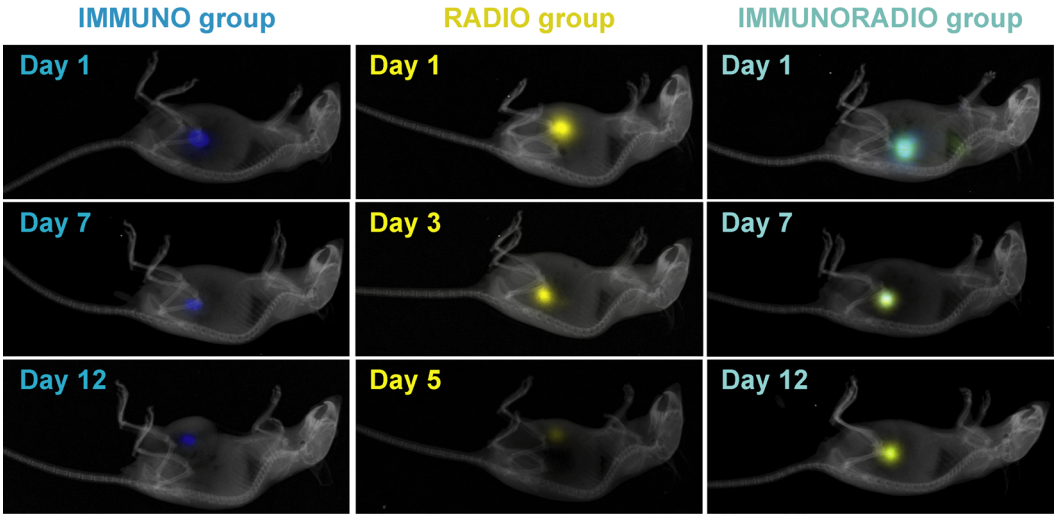

Fig. 21. The polymer biodistribution in IMMUNO, RADIO and IMMUNORADIO groups. The particular images were done by composition of X-ray images (all groups), fluorescence images of the dye Dyomics-615 (IMMUNO and IMMUNORADIO groups) and Cherenkov radiation images of yttrium-90(III) (RADIO and IMMUNORADIO groups).

The more detailed description of the modification, radiolabeling, *in vitro* and *in vivo* testing of β-glucan-*graft*-POX can be found in the **Appendix 2** (see section *6. Appendixes – attached publications*).

3.2 κ-Carrageenan-*graft*-poly(2-isopropyl-2-oxazoline-*co*-2-butyl-2-oxazoline)s

3.2.1 Polymer design and synthesis

Due to the extraordinary *in vivo* results of the previous antitumor efficiency experiment, we have decided to broaden this study and investigate the effect of particular polymer architectures of polysaccharide-*graft*-POXs on the treatment success. Therefore, we have designed κ-carrageenan-*graft*-poly(2-isopropyl-2-oxazoline-*co*-2-butyl-2-oxazoline)s. κ-Carrageenan was selected due to its interesting biological activities, specifically its considerable influence on the immune system. In general, carrageenans are frequently used as agents for the induction of experimental inflammation.[117] Moreover, they show antitumor activity and inhibition of cancer metastasis.[118]

Considering the thermoresponsive behavior of κ-carrageenan (known for gel formation at lower temperatures[119]) and POX, we supposed a kind of „schizophrenic“ thermoresponsive

behavior of κ-carrageenan-*graft*-POXs with both lower and upper critical solution temperatures. In other words, they would form a gel at lower temperatures (due to κ-carrageenan backbone) and precipitate at temperatures higher than CPT (due to POX grafts). Furthermore, the original non-grafted κ-carrageenan typically creates a large helices structure in the presence of potassium cations, and thus, the potassium responsivity is also expected to be observed in the prepared polymer solutions.

Twelve different samples of carrageenan-*graft*-poly(2-isopropyl-2-oxazoline-*co*-2-butyl-2-oxazoline)s, varying in the graft length (1000 Da – C1-C4, 2500 Da – C5-C8 and 5000 Da – C9-C12) and density, were successfully synthesized according to a procedure illustrated in **Fig. 22**. The polymer grafts were first prepared by cationic ring-opening polymerization of 2-isopropyl-2-oxazoline and 2-butyl-2-oxazoline using methyl *p*-toluenesulfonate as the initiator. The living polymer ends were terminated by sodium carrageenanate, while the part of living polymer ends were terminated with water to be able to study the corresponding grafts properties separately from the grafted polymer.

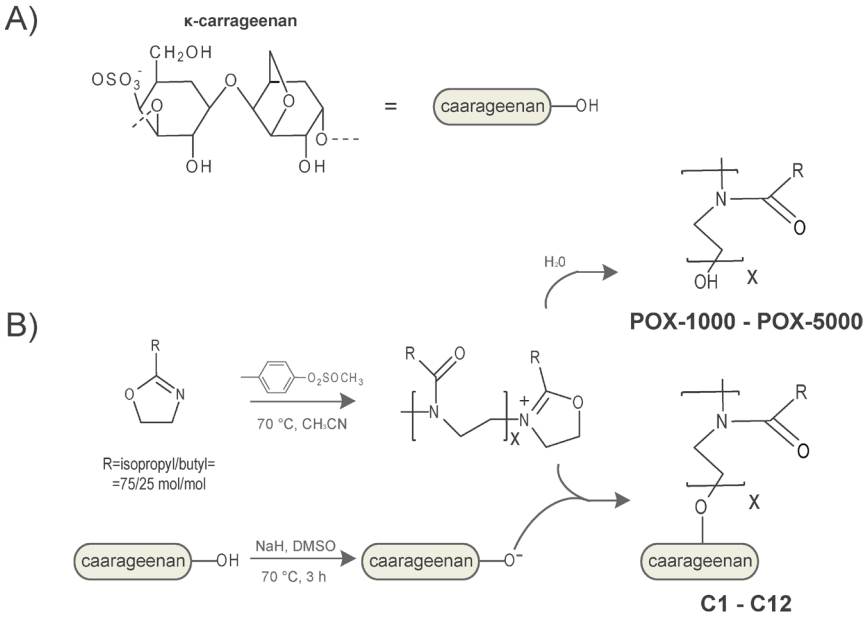

Fig. 22. A) The κ-carrageenan structure, B) general synthetic procedure for C1 – C12.

The presence of POX in the prepared grafted polymers was confirmed by NMR and elemental analysis. The weight-average polymer molecular mass was determined using SEC-MALS (**Table 4**). The theoretical monomer ratio in the polymer grafts was again chosen to be $n_{\text{2-isopropyl-2-oxazoline}}/n_{\text{2-butyl-2-oxazoline}}$ = 3/1 mol/mol, exhibiting the most convenient CPT for the polymer depot formation after an injection into the body. The found monomer ratio

in the prepared POX grafts was calculated using integral intensities of the corresponding peaks in NMR spectra, and they were very close to the theoretical ratio 75/25 (**Table 4**). Thereafter, the POX content in the prepared polymers was determined using the results of CHN elemental analysis, while the POX content accurately followed the theoretical grafting density and graft length (**Table 4**), the higher graft length, the higher POX content at the same grafting density.

Table 4. Characterization of the prepared grafted polymers.

	Theor. graft length (Da)	Found graft length (Da)[1]	$n_{isopropyl}$ /n_{butyl}[2]	POX content (wt. %)	Glucose units per graft	M_w (Da)[1]	CPT[3] (°C)
C1	1000	860	71/29	34	9.3	2.3 x 10^6	x
C2				26	13.5	1.7 x 10^6	x
C3				18	21.8	2.0 x 10^6	x
C4				8	55.0	1.0 x 10^6	x
C5	2500	1950	72/28	65	5.9	4.5 x 10^6	32
C6				60	7.2	2.0 x 10^6	30
C7				35	20.5	1.2 x 10^6	30
C8				15	59.6	9.5 x 10^5	x
C9	5000	4350	73/27	81	5.6	6.3 x 10^6	31
C10				74	8.3	5.4 x 10^6	30
C11				28	60.8	9.1 x 10^5	26
C12				15	132.1	5.3 x 10^5	26

[1] Determined by SEC-MALS,

[2] $n_{isopropyl}/n_{butyl}$ is the molar ratio of 2-isopropyl-2-oxazoline to 2-butyl-2-oxazoline incorporated in the POX grafts, determined by NMR, the theoretical one was 75/25,

[3] at c = 2.5 mg/mL in 0.15 M NaCl.

3.2.2 Thermoresponsive polymer behavior

The thermoresponsive behavior of the prepared polymers C1 – C12 was investigated using DLS in order to study the effect of graft length and grafting density on the final polymer properties, while the cooling scans of the polymers C1, C4, C6, C8, C10 and C11 (graft length of 860 Da for C1 and C4; of 1950 Da for C6 and C8 and of 4350 Da for C10 and C11; grafting density of 7 to 9 glucose units per graft for C1, C6 and C10 and of 55 to 61 glucose units per graft for C4, C8 and C11) were chosen to represent these effects (**Fig. 23**). For the shortest grafts, no polymer thermoresponsive behavior was detected, disregarding the grafting density (**Fig. 23** – C1 and C4). It denotes an existence of a minimum graft length, which is essential to launch the self-association process. Nonetheless, the thermoresponsivity

effect is more pronounced with the increasing graft length. The CPTs for all prepared polymers are shown in **Table 4**. Additionally, the effect of grafting density on the final properties could be also derived from **Fig. 23**, where the decrease in density (increase in glucose units per graft) significantly eliminates the sharpness of the phase transition, considering samples with the same graft length. This could be caused by the decreased local concentration of POX chains that form the phase-separated microdomains.

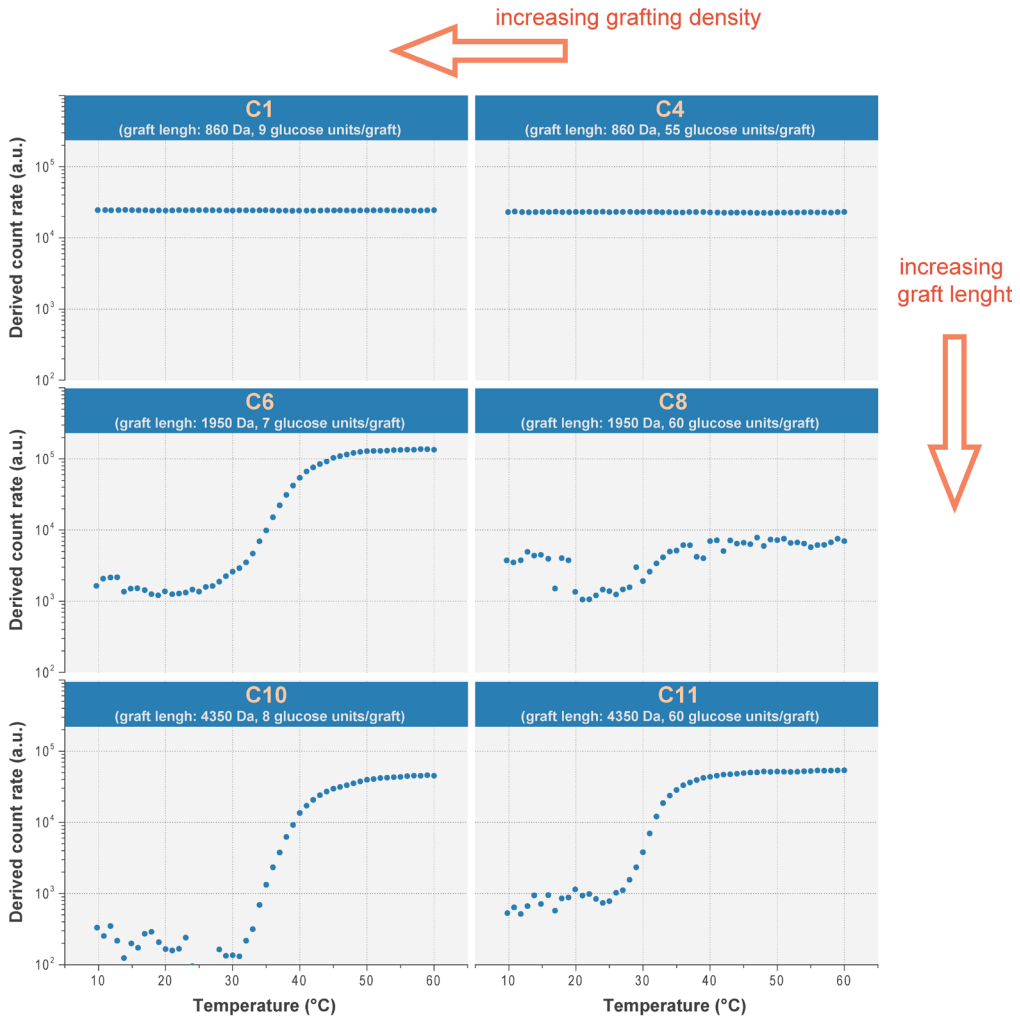

Fig. 23. A) The temperature dependences of the scattered light intensities for the polymers with different graft length (C1 and C4 – 860 Da; C6 and C8 – 1950 Da; C10 and C11 – 4350 Da) and grafting density (C1, C6 and C10 – 7 to 9 glucose units per graft; C4, C8 and C11 – 55 to 61 glucose units per graft); c = 2.5 mg/mL in 0.15 M NaCl.

To study the microenvironment hydrophobicity/hydrophilicity within a phase transition, the temperature-dependent fluorescence measurements of the polymers with the highest grafting density (C1, C5 and C9) were performed (**Fig. 24**). As it was explained in the section

3.1.2 Thermoresponsive polymer behavior, this technique utilizes the effect of aggregation-induced emission caused by a fluorescent probe, which emits fluorescence only in the aggregated state (hydrophobic environment). Again, 8-anilino-1-naphthalenesulfonic acid ammonium salt (ANSAAS, $c = 0.25$ μmol/mL, $\lambda_{ex} = 388$ nm) was used as a fluorescent probe. The measurements were done in the 0.15 M NaCl solutions to eliminate any possible effect of K^+ ions. The polymer C5 exhibited a weak fluorescence intensity at 10 °C ($\lambda_{em,max} = 489$ nm), corresponding probably to formed hydrophobic domains of isopropyl and butyl moieties from one or very few macromolecules. The peak intensity very slightly declined with the increasing temperature up to 30 °C, indicating that the content of hydrophobic domains decreased as well. At 30 °C (**Fig. 24A, B**) the peak intensity increased very sharply, exhibiting the CPT of the monitored system. The rapid increase continued up to 50 °C, demonstrating inter/intramolecular reorganization of the self-assembled structures. Moreover, the microenvironment hydrophobicity increase was confirmed by the peak maximum shift from 489 nm at 10 °C to 479 nm at 60 °C. In addition, the β-glucan-*graft*-POX, G3, showed the shift even to 473 nm at 60 °C, meaning the higher hydrophobicity of phase-separated state compared to κ-carrageenan-based polymers (see **Fig. 12**). The sample C9 exhibited a similar temperature dependence as the sample C5 (**Fig. 24B**), only the CPT was observed at lower temperature (22 °C). On the other hand, the thermoresponsivity was not detected for C1 (**Fig. 24B**). All these observations are in good agreement with the DLS measurements.

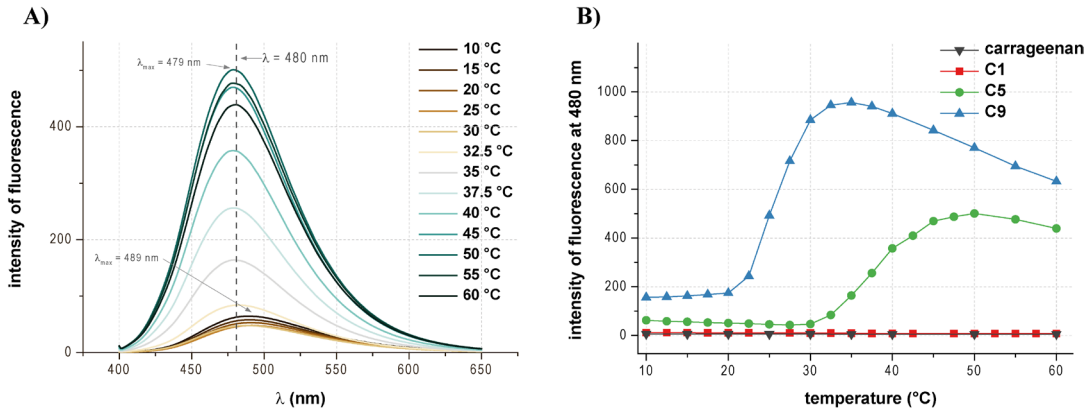

Fig. 24. A) The temperature-dependent fluorescence of C5 ($c = 2.5$ mg/mL in 0.15 M NaCl with a fluorescent probe ANSAAS), B) the temperature-dependent fluorescence of κ-carrageenan, C1, C5 and C9 emitted at 480 nm under the same experimental conditions.

To study the thermoresponsive polymer behavior in more detail, the temperature-dependent high-resolution ^{1}H-NMR spectra of the original κ-carrageenan and polymers with the highest grafting density (C1, C5 and C9) were carried out (**Fig. 25**). The solution of original κ-carrageenan (c = 2.5 mg/mL in D_2O) exhibited the increasing peak intensities with elevated temperature, and the observed broad signals at 10 and 35 °C are related to the reduced chain mobility (**Fig. 25A**), which is the typical behavior of κ-carrageenan gel at lower temperatures.[120] Nevertheless, the next temperature elevation resulted in an increased mobility of the polysaccharide chains, causing a break of the respective physical network structures.

The prepared polymers exhibited similar thermoresponsive behavior as κ-carrageenan, moreover, at elevated temperature they showed the self-assembled structures caused by POX thermoresponsivity. The NMR spectra of C9 with the longest grafts of 4350 Da (**Fig. 25B**) showed also the two contradictory phenomena with increasing temperature: an intensity enhancement of the κ-carrageenan signals (discussed in the previous paragraph) and an intensity decrease of all signals corresponding to the POX chains. In this case, the POX mobility declined so much that the peaks were no more observed in high-resolution ^{1}H-NMR spectra at 70 °C.

To quantify the changes occurring within the heating process, the *p*-fractions were calculated according to the equation (1) for all protons which were not overlapped by the water signal. In general, the *p*-fraction gives a quantitative information about group mobility at the chosen temperature compared to the highest mobility of this group through the whole measured temperature range. High value of the *p*-fractions (≈ 0.95) was observed for all signals in the solution of original κ-carrageenan at lower temperatures (**Fig. 26A**), while it was rapidly decreasing to the value around 0 in the temperature range of 30 – 40 °C, demonstrating the significantly increased mobility of the κ-carrageenan chains. In macroscopic scale, this indicates the gel/solution transition. The polymer C9 exhibited a similar trend for *p*-fractions of all protons signals related to the κ-carrageenan structure (**Fig. 26B**). Additionally, for C9, *p*-fractions of POX signals are around 0 at lower temperature, however, they started to considerably increase at 25 °C, depicting a formation of polymer aggregates (**Fig. 26B**). The observed p_{max} values (final value of *p*-fraction) for the POX groups were highly similar to each other (≈ 0.98), meaning that all POX groups have similarly limited mobility, and they participate in the aggregate formation with the elevated temperature in like manner.

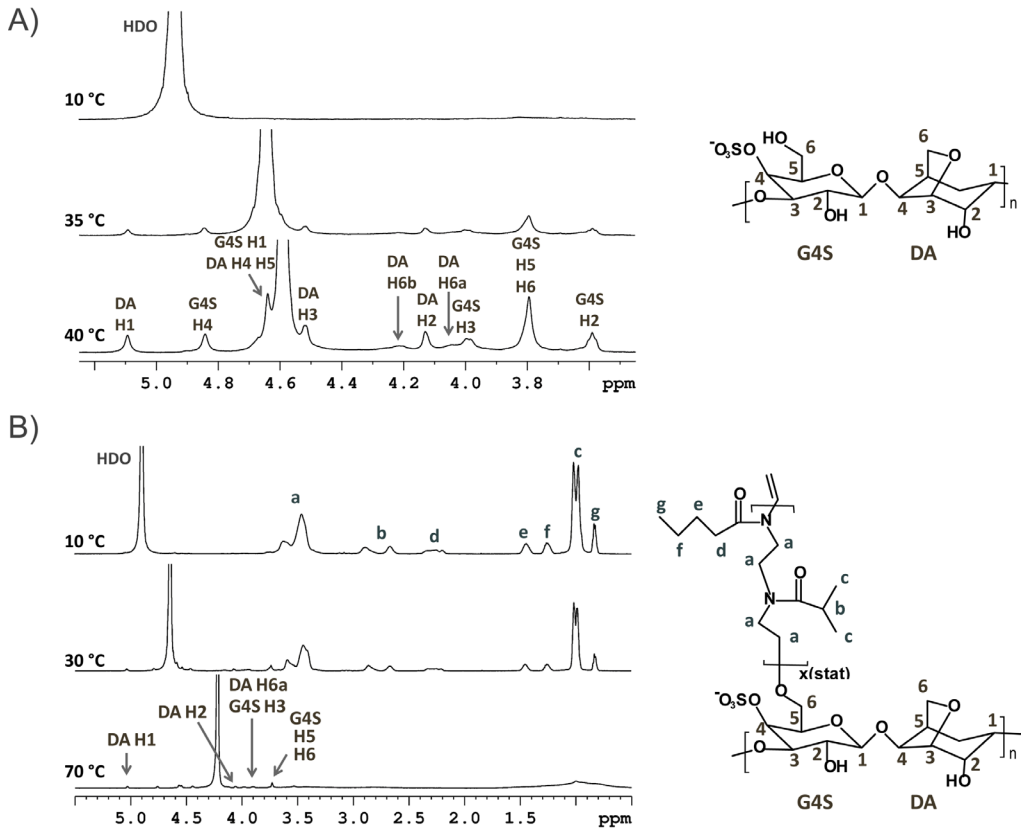

Fig. 25. ^{1}H-NMR spectra of: A) the original κ-carrageenan at 10, 35 and 40 °C and B) C9 at 10, 30 and 70 °C measured under the same conditions (c = 2.5 mg/mL in D_2O).

To quantitatively compare the thermoresponsive behavior of the original κ-carrageenan and the chosen carrageenan-*graft*-POXs (C1, C5 and C9), their temperature-dependent *p*-fractions of the DA H2 carrageenan signals (**Fig. 26C**) and POX main chain protons "**a**" (**Fig. 26D**) were selected to study because these peaks are visible through the whole temperature range. Considering the *p*-fractions of the DA H2 protons (**Fig. 26C**), the values of polymers C1, C5 and C9 at 10 °C were significantly lower than the value of original κ-carrageenan, demonstrating that POX grafting of κ-carrageenan causes a partial prevention of gel structure formation, probably due to the steric reasons. However, the samples forms a gel at 10 °C, while with the increasing temperature the *p*-fraction of the grafted polymers decreased as well up to ca 25 °C (10 °C less than for κ-carrageenan). Thereafter, the *p*-fraction values were slightly increasing with the elevated temperature, copying the trend of κ-carrageenan. On the other hand, the contradictory behavior was found for signals corresponding to the POX chains of the synthesized polymers (**Fig. 26D**). Their *p*-fractions started to increase, dependently on the POX amount – the higher POX amount, the higher final *p*-fraction value

at the same temperature and the sharper transition trend. Interestingly, DLS scans did not detect any temperature-dependent behavior for C1. However, *p*-fraction of the POX main chain protons "**a**" for C1 was only slightly increasing with the elevated temperature (**Fig. 26D**). Probably, within heating process the polymer size do not rapidly change, nevertheless, the POX mobility decreases, which probably could be caused by interactions between the hydrophobic POX groups within one macromolecule.

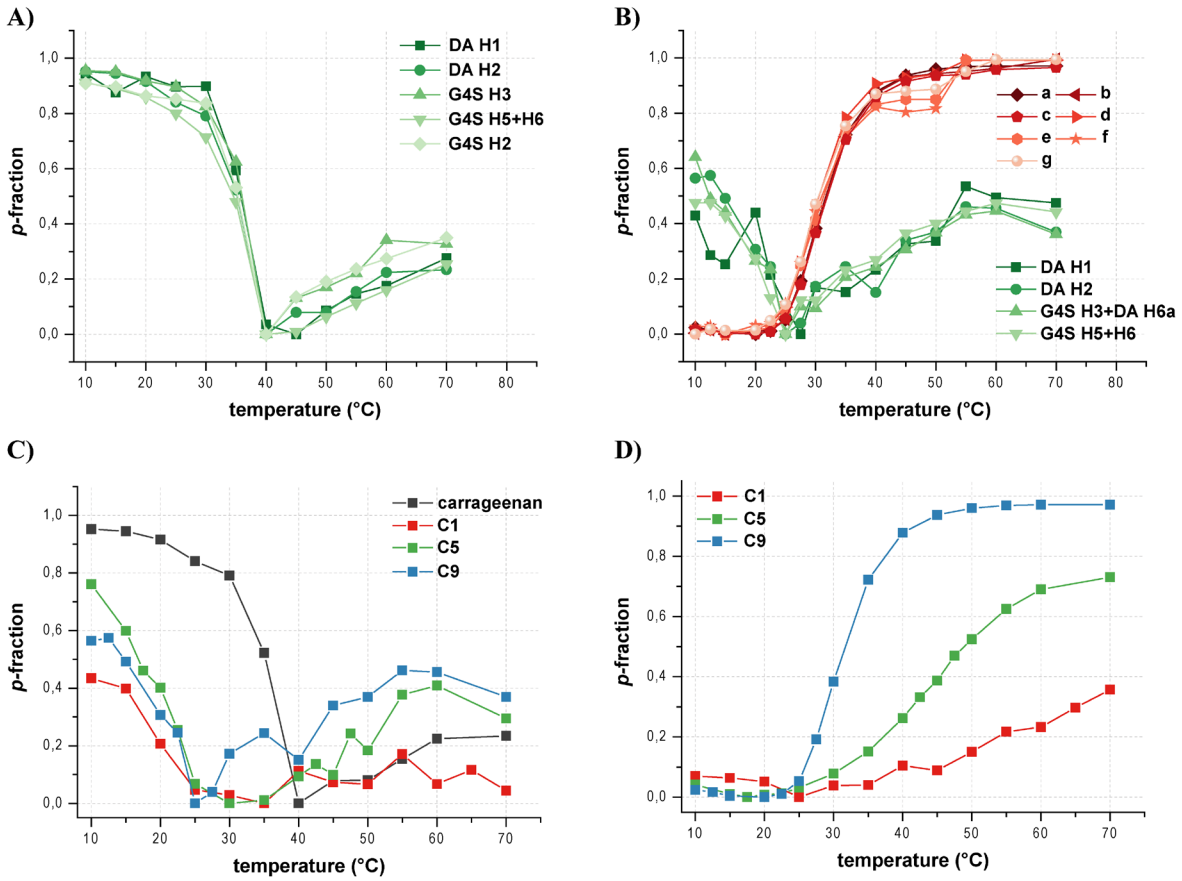

Fig. 26. A) Temperature-dependent *p*-fractions for all protons of κ-carrageenan; B) temperature-dependent *p*-fractions for all protons of C9 (signals corresponding to κ-carrageenan are in green and to POX in red); C) temperature-dependent *p*-fractions for DA H2 protons of carrageenan in the solution of κ-carrageenan, C1, C5 and C9; D) temperature-dependent *p*-fractions for POX main chain protons "**a**" in the solution of C1, C5 and C9.

In general, the interactions between carrageenan units (C1, C5 and C9) predominated at lower temperatures (**Fig. 27**), forming a gel structure, while at elevated temperature the polymer

interactions with water predominated (molecular solution) up to the CPT, when the strong hydrophobic interactions of isopropyl and butyl groups occurred, and the solution started to be turbid.

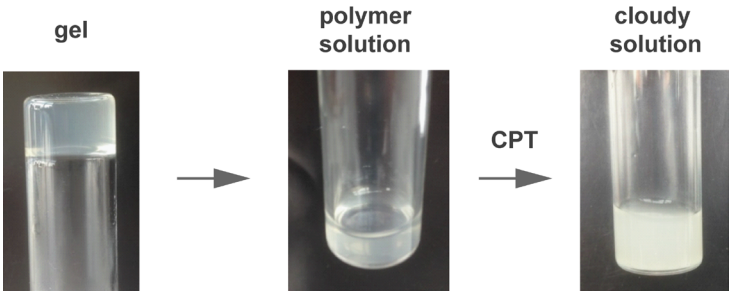

Fig. 27. The illustration of κ-carrageenan-*graft*-POX "schizophrenic" thermoresponsive behavior – a gel structure at lower temperature, while at elevated temperature it forms a polymer solution, which, at the temperature higher than the cloud point, is subsequently temperature transformed into a cloudy solution.

3.2.3 Polymer responsivity to potassium

Because the original κ-carrageenan is highly sensitive to potassium cations and in their presence forms the self-assembled structures[121], the potassium responsivity of the synthesized κ-carrageenan-*graft*-POXs was studied in their aqueous salt solutions with the same ionic strength but different potassium concentration.

The temperature-dependent DLS measurements displayed a relatively sharp phase transition of the polymer C10 in 0.15 M NaCl solution in comparison with its PBS solution (**Fig. 28**). Interestingly, PBS solution contains, besides the others, 4.5 mmol/L potassium cations and 145.5 mmol/L sodium cations, and thus, it can be said that a little amount of potassium cations changes the temperature-dependent behavior of C10. Furthermore, the DLS scan for the same polymer in 0.15 M KCl exhibited the presence of very big particles through the whole temperature range (**Fig. 28**), implying a formation of the self-assembled structures, known for the original κ-carrageenan, as it was said above. The polymer C11, having the same graft length and lower grafting density compared to C10, exhibited an analogous potassium-dependent behavior, while the difference is that the phase transition is not so steep as for C10.

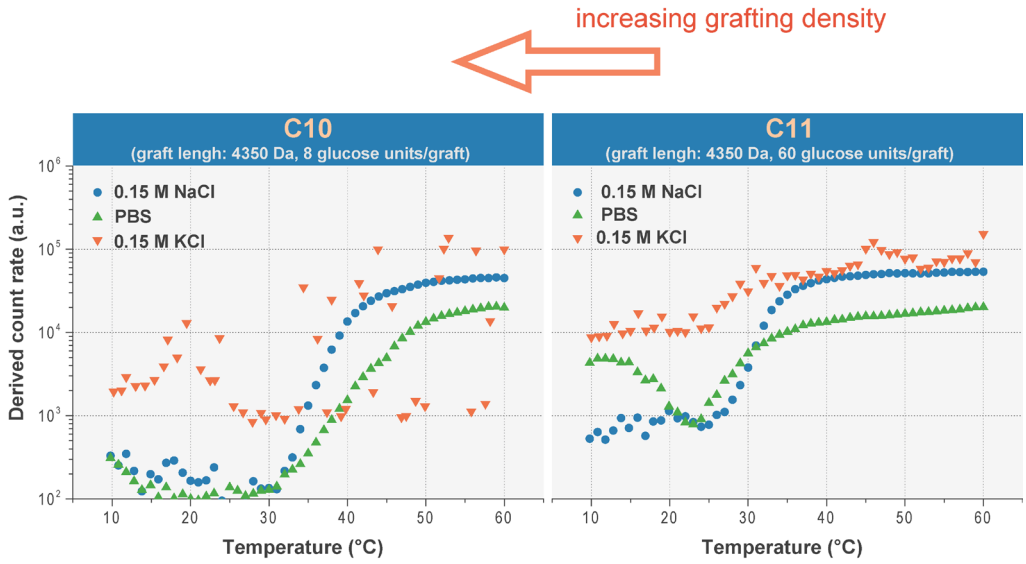

Fig. 28. The temperature dependences of the scattered light intensities for the polymers C10 and C11 (same graft length but various grafting densities) in 0.15 M NaCl, PBS and 0.15 M KCl (c = 2.5 mg/mL).

The observed polymers responsivity to potassium cations was further studied in aqueous, salt and buffer solutions at room temperature using atomic force microscopy (AFM) (**Fig. 29**). The obtained data was compared to behavior of the original κ-carrageenan: typical formation of intramolecular secondary structures in the presence of potassium cations.[121] The sample C10 with the longest grafts and grafting density of 8 glucose units per one graft exhibited the presence of random coils in aqueous environment and in the solution of 0.15 M NaCl (**Fig. 29**). Interestingly, a little amount of potassium cations in the solution of PBS (c = 4.5 mM K^+ ions) caused a formation of self-assembled structures, denoting that POX grafting does not influence the typical κ-carrageenan responsivity to the presence of K^+ ions. The polymer C10 showed very similar intermolecular structure formation in the solution of 0.15 M KCl (**Fig. 29**).

The potassium reponsivity could be useful in specific biomedical applications, *e.g.,* the injection of potassium-free polymer solution into the potassium-containing environment in the organism that can rapidly enhance the body temperature-driven phase transition.

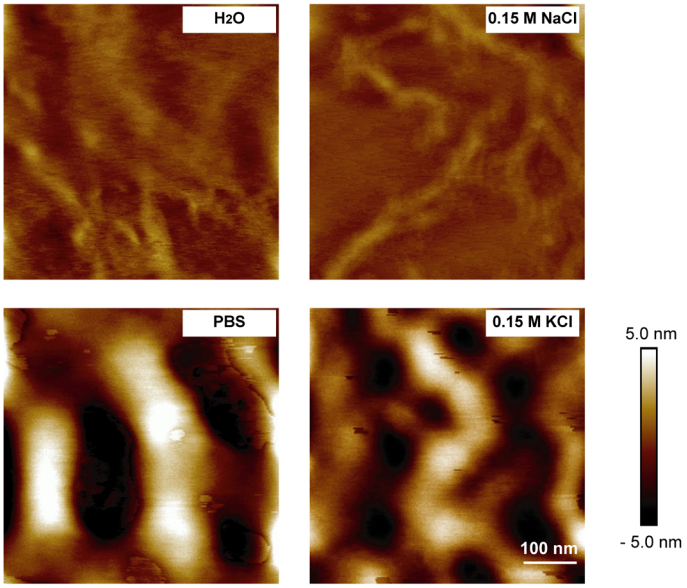

Fig. 29. The AFM height images of C10 in solutions of water, 0.15 M NaCl, PBS and 0.15 M KCl at room temperature (transferred onto mica). The scale and color bars apply to all images.

The more detailed description of κ-carrageenan-*graft*-POXs syntheses and their thermo- and potassium responsive behavior can be found in the **Appendix 3** (see section *6. Appendixes – attached publications*).

4. Conclusions

Within this work novel hybrid polysaccharides-based polymers as a potential drug system for a conceptually new bimodal immunoradiotherapy were prepared.

Specifically, β-glucan-*graft*-poly(2-isopropyl-2-oxazoline-*co*-2-butyl-2-oxazoline)s and κ-carrageenan-*graft*-poly(2-isopropyl-2-oxazoline-*co*-2-butyl-2-oxazoline)s, varying in the graft length (500 – 5000 Da) and grafting density (5 – 60 glucose units pet one graft), were successfully synthesized using β-glucan extracted from *Auricularia auricula-judae* and κ-carrageenan from *Kappaphycus alvarezii*. Their thermoresponsive behavior in the aqueous environment was studied in the context of their graft length, demonstrating an easy adjustment of the cloud point temperature by the polymer graft length choice. Moreover, κ-carrageenan-*graft*-POXs showed a potassium responsivity and also an interesting "schizophrenic" thermoresponsive behavior with both lower and upper critical solution temperatures, which were thoroughly studied in this work as well. Thereafter, the prepared polymer with the most suitable thermoresponsive properties for a depot formation after the injection of its solution was selected for the further study.

The chosen polymer (β-glucan-*graft*-POX with a maximum achievable grafting density and $M_{n,graft}$ = 2500 Da) was modified to bear a fluorescent dye Dyomics-615 and DOTA moiety at the graft ends. The *in vitro* study of this polymer showed its non-toxicity, the active cellular uptake in the cancer cells and macrophages, the oxidative burst of the leukocytes that confirm its immunostimulatory properties, and also a TNF-α production induced by the polymer. All these results motivated us to start *in vivo* experiments.

For the *in vivo* antitumor efficiency experiment on mice with EL4 lymphoma, the modified polymer was first radiolabeled with yttrium-90(III) and subsequently intratumorally administrated to form a polymer depot at the injection site, which remained at the same place for more than 12 days (polymer was gradually degraded and excluded from the body through the kidneys). The group treated with the chosen radiolabeled polymer – IMMUNORADIO group – showed a tumor growth inhibition at the treatment beginning and, furthermore, 7 out of 15 mice from this group were completely cured (treatment success: 47 %).The other mice from this group exhibited a rapidly prolonged survival time in the comparison with control group and also with the RADIO and IMMUNO groups. The *in vivo* experiment revealed a significant synergistic effect of immunoradiotherapy compared to treatment by radiotherapy or immunotherapy only.

5. References

1. Zalipsky, S. Chemistry of polyethylene glycol conjugates with biologically active molecules. *Adv. Drug Deliv. Rev.* **16,** 157–182 (1995).
2. Langer, R.; Tirrell, D. A. Designing materials for biology and medicine. *Nature* **428,** 487 (2004).
3. Lutz, J. F.; Börner, H. G. Modern trends in polymer bioconjugates design. *Prog. Polym. Sci.* **33,** 1–39 (2008).
4. Canalle, L. A.; Löwik, D. W. P. M.; van Hest, J. C. M. Polypeptide–polymer bioconjugates. *Chem. Soc. Rev.* **39,** 329–353 (2010).
5. Reis, R. L. *et al. Natural-based polymers for biomedical applications*. (Elsevier, 2008).
6. Crick, F. Central dogma of molecular biology. *Nature* **227,** 561 (1970).
7. Jenkins, N.; Parekh, R. B.; James, D. C. Getting the glycosylation right: implications for the biotechnology industry. *Nat. Biotechnol.* **14,** 975 (1996).
8. Koeller, K. M.; Wong, C. H. Synthesis of complex carbohydrates and glycoconjugates: enzyme-based and programmable one-pot strategies. *Chem. Rev.* **100,** 4465–4494 (2000).
9. Ernst, B.; Winkler, T. Preparation of glycosyl halides under neutral conditions. *Tetrahedron Lett.* **30,** 3081–3084 (1989).
10. Schmidt, R. R.; Michel, J. Facile Synthesis of α- and β-O-Glycosyl Imidates; Preparation of Glycosides and Disaccharides. *Angew. Chemie* **19**, 731–732 (1980).
11. Kaeothip, S.; Yasomanee, J. P.; Demchenko, A. V. Glycosidation of thioglycosides in the presence of bromine: mechanism, reactivity, and stereoselectivity. *J. Org. Chem.* **77,** 291–299 (2011).
12. Chu, K. *et al.* Efficient and stereoselective synthesis of α (2→ 9) oligosialic acids: from monomers to dodecamers. *Angew. Chemie Int. Ed.* **50,** 9391–9395 (2011).
13. Wu, C. Y.; Wong, C. H. Chemistry and glycobiology. *Chem. Commun.* **47,** 6201–6207 (2011).
14. Miermont, A.; Zeng, Y.; Jing, Y.; Ye, X.; Huang, X. Syntheses of LewisX and dimeric LewisX: construction of branched oligosaccharides by a combination of preactivation and reactivity based chemoselective one-pot glycosylations. *J. Org. Chem.* **72,** 8958–8961 (2007).
15. Hahm, H. S. *et al.* Automated glycan assembly using the Glyconeer 2.1 synthesizer. *Proc. Natl. Acad. Sci.* **114,** 3385–3389 (2017).
16. Leloir, L. F. Two decades of research on the biosynthesis of saccharides. *Science* **172,** 1299–1303 (1971).
17. Ichikawa, Y.; Wang, R.; Wong, C. H. *Methods in enzymology* **247,** 107–127 (1994).
18. Ruiz-Herrera, J. *Fungal cell wall: structure, synthesis, and assembly*. (CRC press, 2016).
19. Zhang, M.; Cui, S. W.; Cheung, P. C. K.; Wang, Q. Antitumor polysaccharides from mushrooms: a review on their isolation process, structural characteristics and antitumor

activity. *Trends Food Sci. Technol.* **18,** 4–19 (2007).

20. Xu, S.; Xu, X.; Zhang, L. Branching structure and chain conformation of water-soluble glucan extracted from *Auricularia auricula-juda*e. *J. Agric. Food Chem.* **60,** 3498–3506 (2012).
21. Singh, V.; Kumar, P.; Sanghi, R. Use of microwave irradiation in the grafting modification of the polysaccharides – A review. *Prog. Polym. Sci.* **37,** 340–364 (2012).
22. Hawker, C. J.; Bosman, A. W.; Harth, E. New polymer synthesis by nitroxide mediated living radical polymerizations. *Chem. Rev.* **101,** 3661–3688 (2001).
23. Matyjaszewski, K.; Xia, J. For recent reviews see Chem. *Rev* **101,** 2921 (2001).
24. Chiefari, J. *et al.* Living free-radical polymerization by reversible addition− fragmentation chain transfer: the RAFT process. *Macromolecules* **31,** 5559–5562 (1998).
25. Tizzotti, M.; Charlot, A.; Fleury, E.; Stenzel, M.; Bernard, J. Modification of polysaccharides through controlled/living radical polymerization grafting – towards the generation of high performance hybrids. *Macromol. Rapid Commun.* **31,** 1751–1772 (2010).
26. Ziegast, G.; Pfannemüller, B. Linear and star-shaped hybrid polymers, coupling of mono-and oligosaccharides to α, ω-diamino substituted poly(oxyethylene) and multifunctional amines by amide linkage. *Die Makromol. Chemie, Rapid Commun.* **5,** 373–379 (1984).
27. Schatz, C.; Louguet, S.; Le Meins, J.; Lecommandoux, S. Polysaccharide-*block*-polypeptide Copolymer Vesicles: Towards Synthetic Viral Capsids. *Angew. Chemie Int. Ed.* **48,** 2572–2575 (2009).
28. Akiyoshi, K.; Kohara, M.; Ito, K.; Kitamura, S.; Sunamoto, J. Enzymatic synthesis and characterization of amphiphilic block copolymers of poly(ethylene oxide) and amylose. *Macromol. Rapid Commun.* **20,** 112–115 (1999).
29. Pal, A. *et al.* Synthesis of glycogen and poly (acrylic acid)-based graft copolymers via ATRP and its application for selective removal of Pb^{2+} ions from aqueous solution. *Eur. Polym. J.* **66,** 33–46 (2015).
30. Pospisilova, A. *et al.* Glycogen-*graft*-poly(2-alkyl-2-oxazolines) – the new versatile biopolymer-based thermoresponsive macromolecular toolbox. *RSC Adv.* **4,** 61580–61588 (2014).
31. Vetrik, M. *et al.* Biopolymer-based degradable nanofibres from renewable resources produced by freeze-drying. *RSC Adv.* **3,** 15282–15289 (2013).
32. Tzianabos, A. O. Polysaccharide immunomodulators as therapeutic agents: structural aspects and biologic function. *Clin. Microbiol. Rev.* **13,** 523–533 (2000).
33. Cui, J.; Chisti, Y. Polysaccharopeptides of Coriolus versicolor: physiological activity, uses, and production. *Biotechnol. Adv.* **21,** 109–122 (2003).
34. Vannucci, L. *et al.* Immunostimulatory properties and antitumor activities of glucans (Review). *Int. j. Oncol.* **43**, 357–364 (2013).

35. Iannace, S.; Sorrentino, A. Bio-based and bio-inspired cellular materials. *Biofoams Sci. Appl. Bio-Based Cell. Porous Mater.* **1** (2015).
36. Ina, K.; Kataoka, T.; Ando, T. The use of lentinan for treating gastric cancer. *Anti-Cancer Agents Med. Chem. (Formerly Curr. Med. Chem. Agents)* **13,** 681–688 (2013).
37. Chihara, G. The antitumor polysaccharide Lentinan: an overview. *Manip. host Def. Mech. Excerpta Med, Int Congr Ser* **576** (1981).
38. Ukai, S. *et al.* Polysaccharides in fungi. XIII. Antitumor activity of various polysaccharides isolated from Dictyophora indusiata, Ganoderma japonicum, Cordyceps cicadae, Auricularia auricula-judae, and Auricularia species. *Chem. Pharm. Bull.* **31,** 741–744 (1983).
39. Mizuno, T. The extraction and development of antitumor-active polysaccharides from medicinal mushrooms in Japan. *Int. J. Med. Mushrooms* **1,** 9–29 (1999).
40. Solomko, E. F. The physiology-biochemical properties and biosynthetic activities of higher Basidiomycetes mushroom *Pleurotus ostreatus. Dr. Sci. thesis, NG Kholodny Inst. Bot. Acad. Sci. Ukr.* 49–63 (1992).
41. Yamamoto, T.; Yamashita, T.; Tsubura, E. Inhibition of pulmonary metastasis of Lewis lung carcinoma by a glucan, Schizophyllan. *Invasion Metastasis* **1,** 71–84 (1981).
42. Mizuno, T.; Zhuang, C. *Maitake*, *Grifola frondosa*: pharmacological effects. *Food Rev. Int.* **11,** 135–149 (1995).
43. Zhang, M.; Cheung, P. C. K.; Zhang, L. Evaluation of mushroom dietary fiber (nonstarch polysaccharides) from sclerotia of *Pleurotus* tuber-regium (Fries) singer as a potential antitumor agent. *J. Agric. Food Chem.* **49,** 5059–5062 (2001).
44. Wijesekara, I.; Pangestuti, R.; Kim, S. K. Biological activities and potential health benefits of sulfated polysaccharides derived from marine algae. *Carbohydr. Polym.* **84,** 14–21 (2011).
45. Dominguez, H. *Functional ingredients from algae for foods and nutraceuticals*. (Elsevier, 2013).
46. Lee, S. H. *et al.* Anti-inflammatory effect of fucoidan extracted from Ecklonia cava in zebrafish model. *Carbohydr. Polym.* **92,** 84–89 (2013).
47. Laurienzo, P. Marine polysaccharides in pharmaceutical applications: an overview. *Mar. Drugs* **8,** 2435–2465 (2010).
48. Florez, N. *et al.* Algae Polysaccharides Chemical Characterization and their Role in the Inflammatory Process. *Curr. Med. Chem.* **24,** 149–175 (2017).
49. Hernandez-Carmona, G.; Freile-Pelegrín, Y.; Hernández-Garibay, E. *Functional Ingredients from Algae for Foods and Nutraceuticals* 475–516 (Elsevier, 2013).
50. van de Velde, F. *et al.* Coil–helix transition of ι-carrageenan as a function of chain regularity. *Biopolym. Orig. Res. Biomol.* **65,** 299–312 (2002).
51. Liu, J.; Zhan, X.; Wan, J.; Wang, Y.; Wang, C. Review for carrageenan-based pharmaceutical

biomaterials: favourable physical features versus adverse biological effects. *Carbohydr. Polym.* **121,** 27–36 (2015).

52. Raman, M.; Doble, M. κ-Carrageenan from marine red algae, *Kappaphycus alvarezii* – A functional food to prevent colon carcinogenesis. *J. Funct. Foods* **15,** 354–364 (2015).
53. Yamabhai, M.; Sak-Ubol, S.; Srila, W.; Haltrich, D. Mannan biotechnology: from biofuels to health. *Crit. Rev. Biotechnol.* **36,** 32–42 (2016).
54. Ferreira, S. A.; Coutinho, P. J. G.; Gama, F. M. Self-assembled nanogel made of mannan: synthesis and characterization. *Langmuir* **26,** 11413–11420 (2010).
55. Cui, Z.; Hsu, C. H.; Mumper, R. J. Physical characterization and macrophage cell uptake of mannan-coated nanoparticles. *Drug Dev. Ind. Pharm.* **29,** 689–700 (2003).
56. Brocas, A. L.; Mantzaridis, C.; Tunc, D.; Carlotti, S. Polyether synthesis: From activated or metal-free anionic ring-opening polymerization of epoxides to functionalization. *Prog. Polym. Sci.* **38,** 845–873 (2013).
57. Kjellander, R.; Florin, E. Water structure and changes in thermal stability of the system poly(ethylene oxide)–water. *J. Chem. Soc. Faraday Trans. 1 Phys. Chem. Condens. Phases* **77,** 2053–2077 (1981).
58. Alconcel, S. N. S.; Baas, A. S.; Maynard, H. D. FDA-approved poly(ethylene glycol)–protein conjugate drugs. *Polym. Chem.* **2,** 1442–1448 (2011).
59. Abuchowski, A.; Van Es, T.; Palczuk, N. C.; Davis, F. F. Alteration of immunological properties of bovine serum albumin by covalent attachment of polyethylene glycol. *J. Biol. Chem.* **252,** 3578–3581 (1977).
60. Schöttler, S. *et al.* Protein adsorption is required for stealth effect of poly(ethylene glycol)- and poly(phosphoester)-coated nanocarriers. *Nat. Nanotechnol.* **11,** 372 (2016).
61. Rudmann, D. G.; Alston, J. T.; Hanson, J. C.; Heidel, S. High molecular weight polyethylene glycol cellular distribution and PEG-associated cytoplasmic vacuolation is molecular weight dependent and does not require conjugation to proteins. *Toxicol. Pathol.* **41,** 970–983 (2013).
62. Szebeni, J. Complement activation-related pseudoallergy: a new class of drug-induced acute immune toxicity. *Toxicology* **216,** 106–121 (2005).
63. Armstrong, J. K. *et al.* Antibody against poly(ethylene glycol) adversely affects PEG-asparaginase therapy in acute lymphoblastic leukemia patients. *Cancer* **110,** 103–111 (2007).
64. Knop, K.; Hoogenboom, R.; Fischer, D.; Schubert, U. S. Poly(ethylene glycol) in drug delivery: pros and cons as well as potential alternatives. *Angew. chemie Int. Ed.* **49,** 6288–6308 (2010).
65. Wiesbrock, F.; Hoogenboom, R.; Abeln, C. H.; Schubert, U. S. Single-Mode Microwave Ovens as New Reaction Devices: Accelerating the Living Polymerization of

2-Ethyl-2-Oxazoline. *Macromol. Rapid Commun.* **25,** 1895–1899 (2004).

66. Weber, C.; Hoogenboom, R.; Schubert, U. S. Temperature responsive bio-compatible polymers based on poly(ethylene oxide) and poly(2-oxazoline)s. *Prog. Polym. Sci.* **37,** 686–714 (2012).
67. Englert, C. *et al.* Pharmapolymers in the 21st Century: Synthetic Polymers in Drug Delivery Applications. *Prog. Polym. Sci.* **87,** 107–164 (2018).
68. Sedlacek, O. *et al.* Thermoresponsive polymers for nuclear medicine: Which polymer is the best? *Langmuir* **32,** 6115–6122 (2016).
69. King, D. J.; Noss, R. R. Toxicity of polyacrylamide and acrylamide monome. *Rev. Environ. Health* **8,** 3–16 (1989).
70. Sheftel, V. O. *Handbook of toxic properties of monomers and additives*. (CRC Press, 1995).
71. Kopeček, J.; Bazilová, H. Poly[*N*-(2-hydroxypropyl)methacrylamide] – Radical polymerization and copolymerization. *Eur. Polym. J.* **9,** 7–14 (1973).
72. Scales, C. W.; Vasilieva, Y. A.; Convertine, A. J.; Lowe, A. B.; McCormick, C. L. Direct, controlled synthesis of the nonimmunogenic, hydrophilic polymer, poly(*N*-(2-hydroxypropyl) methacrylamide) via RAFT in aqueous media. *Biomacromolecules* **6,** 1846–1850 (2005).
73. Gibson, M. I.; Fröhlich, E.; Klok, H. Postpolymerization modification of poly(pentafluorophenyl methacrylate): Synthesis of a diverse water-soluble polymer library. *J. Polym. Sci. Part A Polym. Chem.* **47,** 4332–4345 (2009).
74. Wei, H.; Cheng, S. X.; Zhang, X. Z.; Zhuo, R. X. Thermo-sensitive polymeric micelles based on poly(*N*-isopropylacrylamide) as drug carriers. *Prog. Polym. Sci.* **34,** 893–910 (2009).
75. Sun, T.; Qing, G. Biomimetic smart interface materials for biological applications. *Adv. Mater.* **23,** 57–77 (2011).
76. Theisen, E. The history of nitrocellulose as a film base. *J. Soc. Motion Pict. Eng.* **20,** 259–262 (1933).
77. Tsubokawa, N.; Iida, T.; Takayama, T. Modification of cellulose powder surface by grafting of polymers with controlled molecular weight and narrow molecular weight distribution. *J. Appl. Polym. Sci.* **75,** 515–522 (2000).
78. Prasad, K.; Mehta, G.; Meena, R.; Siddhanta, A. K. Hydrogel-forming agar-*graft*-PVP and κ-carrageenan-*graft*-PVP blends: Rapid synthesis and characterization. *J. Appl. Polym. Sci.* **102,** 3654–3663 (2006).
79. Meyer, K.; Palmer, J. W. The polysaccharide of the vitreous humor. *J. Biol. Chem.* **107,** 629–634 (1934).
80. Lapčík, L.; Lapcik, L.; De Smedt, S.; Demeester, J.; Chabrecek, P. Hyaluronan: preparation, structure, properties, and applications. *Chem. Rev.* **98,** 2663–2684 (1998).
81. Necas, J.; Bartosikova, L.; Brauner, P.; Kolar, J. Hyaluronic acid (hyaluronan): a review. *Vet. Med. (Praha).* **53,** 397–411 (2008).

82. Stern, R. Hyaluronan catabolism: a new metabolic pathway. *Eur. J. Cell Biol.* **83,** 317–325 (2004).

83. Zhang, J.; Skardal, A.; Prestwich, G. D. Engineered extracellular matrices with cleavable crosslinkers for cell expansion and easy cell recovery. *Biomaterials* **29,** 4521–4531 (2008).

84. Peattie, R. A. *et al.* Stimulation of *in vivo* angiogenesis by cytokine-loaded hyaluronic acid hydrogel implants. *Biomaterials* **25,** 2789–2798 (2004).

85. Flynn, L.; Prestwich, G. D.; Semple, J. L.; Woodhouse, K. A. Adipose tissue engineering with naturally derived scaffolds and adipose-derived stem cells. *Biomaterials* **28,** 3834–3842 (2007).

86. Saravanakumar, G. *et al.* Hydrotropic hyaluronic acid conjugates: synthesis, characterization, and implications as a carrier of paclitaxel. *Int. J. Pharm.* **394,** 154–161 (2010).

87. Kim, M. R.; Park, T. G. Temperature-responsive and degradable hyaluronic acid/Pluronic composite hydrogels for controlled release of human growth hormone. *J. Control. Release* **80,** 69–77 (2002).

88. Fischer, G.; Boedeker, C. Künstliche Bildung von Zucker aus Knorpel (Chondrogen), und über die Umsetzung des genossenen Knorpels im menschlichen Körper. *Justus Liebigs Ann. Chem.* **117,** 111–118 (1861).

89. Chahine, N. O.; Chen, F. H., Hung; C. T.; Ateshian, G. A. Direct measurement of osmotic pressure of glycosaminoglycan solutions by membrane osmometry at room temperature. *Biophys. J.* **89,** 1543–1550 (2005).

90. Strehin, I.; Nahas, Z.; Arora, K.; Nguyen, T.; Elisseeff, J. A versatile pH sensitive chondroitin sulfate–PEG tissue adhesive and hydrogel. *Biomaterials* **31,** 2788–2797 (2010).

91. Abbas, A. K.; Lichtman, A. H. H.; Pillai, S. *Cellular and molecular immunology E-book*. (Elsevier Health Sciences, 2014).

92. Jorpes, E. The chemistry of heparin. *Biochem. J.* **29,** 1817 (1935).

93. Tipson, R. S.; Horton, D. Advances in carbohydrate chemistry and biochemistry **43** (1985).

94. Neufeld, G.; Cohen, T.; Gengrinovitch, S.; Poltorak, Z. Vascular endothelial growth factor (VEGF) and its receptors. *FASEB J.* **13,** 9–22 (1999).

95. Benoit, D. S. W.; Collins, S. D.; Anseth, K. S. Multifunctional hydrogels that promote osteogenic human mesenchymal stem cell differentiation through stimulation and sequestering of bone morphogenic protein 2. *Adv. Funct. Mater.* **17,** 2085–2093 (2007).

96. Ho, H. V. T. *et al.* A systematic review and meta-analysis of randomized controlled trials of the effect of konjac glucomannan, a viscous soluble fiber, on LDL cholesterol and the new lipid targets non-HDL cholesterol and apolipoprotein B, 2. *Am. J. Clin. Nutr.* **105,** 1239–1247 (2017).

97. Lehtovaara, B. C.; Verma, M. S.; Gu, F. X. Synthesis of curdlan-*graft*-poly(ethylene glycol) and formulation of doxorubicin-loaded core–shell nanoparticles. *J. Bioact. Compat. Polym.* **27,**

3–17 (2012).

98. Krässig, H. Cellulose: Structure, Accessibility, and Reactivity Gordon and Breach Sci. (*Publ. Switz.*, 1993).

99. Pourjavadi, A.; Sadeghi, M.; Hosseinzadeh, H. Modified carrageenan. 5. Preparation, swelling behavior, salt-and pH-sensitivity of partially hydrolyzed crosslinked carrageenan-*graft*-polymethacrylamide superabsorbent hydrogel. *Polym. Adv. Technol.* **15,** 645–653 (2004).

100. Kulkarni, R. V.; Boppana, R.; Mohan, G. K.; Mutalik, S.; Kalyane, N. V. pH-responsive interpenetrating network hydrogel beads of poly(acrylamide)-*graft*-carrageenan and sodium alginate for intestinal targeted drug delivery: Synthesis, *in vitro* and *in vivo* evaluation. *J. Colloid Interface Sci.* **367,** 509–517 (2012).

101. Fan, L. *et al.* Synthesis, characterization and properties of carboxymethyl kappa carrageenan. *Carbohydr. Polym.* **86,** 1167–1174 (2011).

102. Smith, R. A. *et al.* Cancer screening in the United States, 2018: A review of current American Cancer Society guidelines and current issues in cancer screening. *CA. Cancer J. Clin.* **68,** 297–316 (2018).

103. Stephens, S. O.; Feder, B. H.; Haymond, H. R.; George, F. W. Dose rate relationships in brachytherapy: An *in vivo* evaluation. *Int. J. Radiat. Oncol. Biol. Phys.* **2,** 137 (2016).

104. Stewart, A. J.; Jones, B. Radiobiologic concepts for brachytherapy. *Brachytherapy Appl. Tech. Devlin PM (ed). Lippincott Williams &Wilkins, Philadelphia* (2007).

105. Hruby, M.; Pouckova, P.; Zadinova, M.; Kucka, J.; Lebeda, O. ;Thermoresponsive polymeric radionuclide delivery system – An injectable brachytherapy. *Eur. J. Pharm. Sci.* **42,** 484–488 (2011).

106. Kučka, J.; Hrubý, M.; Lebeda, O. Biodistribution of a radiolabelled thermoresponsive polymer in mice. *Appl. Radiat. Isot.* **68,** 1073–1078 (2010).

107. Chen, W.; Konkel, J. E. TGF-β and 'adaptive'Foxp3+ regulatory T cells. *J. Mol. Cell Biol.* **2,** 30–36 (2009).

108. Mellman, I.; Coukos, G.; Dranoff, G. Cancer immunotherapy comes of age. *Nature* **480,** 480 (2011).

109. Baxevanis, C. N.; Perez, S. A. Endogenous immunity at the forefront of tumor dormancy. *Futur. Sci. OA* **1,** (2015).

110. Hall, S. S. A Commotion in the Blood: Life, Death, and the Immune System, Henry Holt and Company. *Inc., New York* (1997).

111. Rakoff-Nahoum, S.; Medzhitov, R. Toll-like receptors and cancer. *Nat. Rev. Cancer* **9,** 57–63 (2009).

112. Diab, C.; Akiyama, Y.; Kataoka, K.; Winnik, F. M. Microcalorimetric study of the temperature-induced phase separation in aqueous solutions of poly(2-isopropyl-2-oxazolines).

Macromolecules **37,** 2556–2562 (2004).

113. Konefał, R.; Spěváček, J.; Jäger, E.; Petrova, S. Thermoresponsive behaviour of terpolymers containing poly(ethylene oxide), poly (2-ethyl-2-oxazoline) and poly (ε-caprolactone) blocks in aqueous solutions: an NMR study. *Colloid Polym. Sci.* **294,** 1717–1726 (2016).
114. G. T, H. Bioconjugate techniques. (1996).
115. Villares, A.; Mateo-Vivaracho, L.; Guillamón, E. Structural features and healthy properties of polysaccharides occurring in mushrooms. *Agriculture* **2,** 452–471 (2012).
116. Hruby, M. *et al.* New bioerodable thermoresponsive polymers for possible radiotherapeutic applications. **119,** 25–33 (2007).
117. Morris, C. J. Carrageenan-induced paw edema in the rat and mouse. *Inflamm. Protoc.* 115–121 (2003).
118. Campo, V. L.; Kawano, D. F.; da Silva, D. B.; Carvalho, I. Carrageenans: Biological properties, chemical modifications and structural analysis – A review. *Carbohydr. Polym.* **77,** 167–180 (2009).
119. Funami, T. *et al.* Influence of molecular structure imaged with atomic force microscopy on the rheological behavior of carrageenan aqueous systems in the presence or absence of cations. *Food Hydrocoll.* **21,** 617–629 (2007).
120. Hermansson, A. M.; Eriksson, E.; Jordansson, E. Effects of potassium, sodium and calcium on the microstructure and rheological behaviour of kappa-carrageenan gels. *Carbohydr. Polym.* **16,** 297–320 (1991).
121. Schefer, L.; Adamcik, J.; Diener, M.; Mezzenga, R. Supramolecular chiral self-assembly and supercoiling behavior of carrageenans at varying salt conditions. *Nanoscale* **7,** 16182–16188 (2015).

6. Appendixes – attached publications

Publications declaration

Hereby the author of this thesis declares her contribution to the work. Lenka Loukotová performed all polymer syntheses and the physico-chemical characterization, including DLS, fluorescence measurement, SEC, UV-Vis spectrophotometry. The NMR measurements were performed by R. Konefal. The *in vitro* experiments of the prepared samples were done by collaborating biologists from the Institute of Macromolecular Chemistry AS CR (K. Venclíková, A. Hocherl, D. Machová, O. Šebestová Janoušková). The *in vivo* testing was performed by Lenka Loukotová under the supervision of J. Kučka and collaborating biologists from the Center for Advanced Preclinical Imaging, First Faculty of Medicine, Charles University in Prague (P. Francová, T. Heizer, P. Páral, V. Kolářová, L. Šefc).

List of appendixes – publications included into this thesis

Appendix 1

Loukotová, L.; Konefał, R.; Venclíková, K.; Machová, D.; Janoušková, O.; Rabyk, M.; Netopilík, M.; Mázl Chánová, E.; Štěpánek, P.; Hrubý, M. Hybrid thermoresponsive graft constructs of fungal polysaccharide β-glucan: Physico-chemical and immunomodulatory properties, *Eur. Polym. J.* **106**, 117 – 127 (2018). IF = 3.741.

Appendix 2

Loukotová, L.; Kučka, J.; Rabyk, M.; Höcherl, A.; Venclíková, K.; Janoušková, O.; Páral, P.; Kolářová, V.; Heizer, T.; Šefc, L.; Štěpánek, P.; Hrubý, M. Thermoresponsive β-glucan-based polymers for bimodal immunoradiotherapy–Are they able to promote the immune system? *J. Control. Release* **268**, 78 – 91 (2017). IF = 7.877.

Appendix 3

Loukotová, L.; Bogomolova, A.; Konefał, R.; Špírková, M.; Štěpánek, P.; Hrubý, M. Hybrid κ-carrageenan-based polymers showing "schizophrenic" lower and upper critical solution temperatures and potassium responsivity, *Carbohydr. Polym.*, submitted article. IF = 5.158.

Appendix 4

Loukotová, L.; Hrubý, M. Polysacharidy jako stavební bloky hybridních kopolymerů, *Chem. Listy* **112**, 497 – 507 (2018). IF = 0.260.

Appendix 1

Loukotová, L.; Konefał, R.; Venclíková, K.; Machová, D.; Janoušková, O.; Rabyk, M.; Netopilík, M.; Mázl Chánová, E.; Štěpánek, P.; Hrubý, M. Hybrid thermoresponsive graft constructs of fungal polysaccharide β-glucan: Physico-chemical and immunomodulatory properties, *Eur. Polym. J.* **106**, 117 – 127 (2018). IF = 3.741.

European Polymer Journal 106 (2018) 118–127

Contents lists available at ScienceDirect

European Polymer Journal

journal homepage: www.elsevier.com/locate/europolj

Hybrid thermoresponsive graft constructs of fungal polysaccharide β-glucan: Physico-chemical and immunomodulatory properties

L. Loukotová, R. Konefał, K. Venclíková, D. Machová, O. Janoušková, M. Rabyk, M. Netopilík, E. Mázl Chánová, P. Štěpánek, M. Hrubý*

Institute of Macromolecular Chemistry AS CR, v. v. i., Heyrovsky sq. 2, Prague 162 06, Czech Republic

ARTICLE INFO

Keywords:
β-glucan
Polyoxazoline
Multimodal cancer therapy
Thermoresponsivity

ABSTRACT

We describe a family of thermoresponsive hybrid biodegradable peptidoglycan-like polymers, β-glucan-*graft*-poly(2-isopropyl-2-oxazoline-*co*-2-butyl-2-oxazoline)s, in the context of their physical, chemical and biological properties. Four polymer samples, differing in the polyoxazoline graft length (500–5000 Da), were synthesized using β-glucan extracted from *Auricularia auricula-judae*, which is known for its anticancer and immunomodulatory activities. The thermoresponsive behaviour of the prepared polymers were thoroughly studied using dynamic light scattering, fluorescence and magnetic resonance measurements, demonstrating an easy adjustment of the cloud point temperature by the graft length. Moreover, all samples show nontoxicity *in vitro*. The assay of oxidative burst of the polymorphonuclears established that the polymer immunostimulatory properties are not significantly influenced by their graft length considering the same amount of β-glucan. Thus, we showed that the desired immunostimulatory properties are not decreased by the polyoxazoline grafting of β-glucan, even they are not influenced by the graft length of the polyoxazoline chains. Therefore, for the intended application the final graft length can be chosen considering the polymer thermoresponsive properties only, while not influencing their immunostimulatory properties.

1. Introduction

Hybrid polymers composed of natural and synthetic building blocks attract increasing interest due to their outstanding functional properties. These polymers combine the advantageous properties of natural polymers (biodegradability, sustainability and environmentally friendly nature) with those of synthetic polymers (tailorability, processability and economical synthesis) [1]. An important class of such polymers includes polysaccharide-based materials, which are widely used in drug delivery and tissue engineering because of their biocompatibility, biodegradability and bioactivity. Moreover, polysaccharides have a diverse range of physico-chemical properties based on their monosaccharide constituents, composition and their source [2].

An easy way to obtain hybrid polysaccharide-based polymers with controlled material properties is by the grafting of synthetic monomers/polymers onto a polysaccharide chain; for example, the amphiphilic copolymer curdlan-*graft*-poly(ethylene oxide) was prepared for delivery of the chemotherapeutic drug doxorubicin [3], and methoxy poly (ethylene oxide)-*graft*-chitosan was prepared for wound healing [4]. Furthermore, novel stimuli-responsive grafted polysaccharides, which possess a lower critical solution temperature (LCST), were prepared by grafting of poly(*N*-isopropylacrylamide) onto *O*-carboxymethyl-*O*-hydroxypropyl guar gum [5] or by grafting of a thermoresponsive polymer onto glycogen [6]. These types of polymers exhibited reversible and rapid phase transitions, applicable for temperature-responsive drug release systems.

In general, β-glucan polysaccharides are subjects of numerous researches because of their immunomodulatory and anticancer properties [7]. Moreover, in Japan, licensed β-glucans extracted from *Lentinula edodes* (lentinan) are already used as effective drugs in gastric cancer therapy, usually in combination with fluoropyrimidines [8]. β-Glucan from the mushroom *Auricularia auricula-judae* shows anticancer properties as well and, interestingly, it exhibits a unique self-assembly behaviour in the aqueous environments, forming hollow nanofibers [9]. It was identified that this β-glucan contains β-1,3- and β-1,6-glycosidic bonds, and has a comb-like shape with short branches. The branches are hydrophilic, allowing good solubility in water, but relatively hydrophobic nature of −OH side of C2 of glucose main-chain units causes the formation of the closed triangular hydrogen-bonding network [9].

Recently, the cancer immunoradiotherapy was successfully

* Corresponding author.
E-mail address: mhruby@centrum.cz (M. Hrubý).

https://doi.org/10.1016/j.eurpolymj.2018.07.004
Received 16 January 2018; Received in revised form 22 June 2018; Accepted 3 July 2018
Available online 04 July 2018
0014-3057/

demonstrated on mice bearing EL4 tumour using thermoresponsive polysaccharide-based system – β-glucan-*graft*-polyoxazoline [10]. This treatment was designed to exploit a potential synergistic effect of both therapies, while the *in vivo* study demonstrated such effect with very promising treatment success. However, for deeper understanding of this synergy, a detailed research is needed. The aim of this work was to investigate the properties of β-glucan-*graft*-polyoxazolines in the context of the graft length, especially their thermoresponsivity, which has an influence on the correct drug administration, and their immunostimulatory properties, which play a crucial role in the final treatment success. We have synthesized four β-glucan-*graft*-poly(2-isopropyl-2-oxazoline-*co*-2-butyl-2-oxazoline)s with various graft lengths (500–5000 Da) and maximum achievable grafting density. The thermoresponsive properties of these samples were studied using dynamic light scattering, nuclear magnetic resonance and aggregation-induced emission. Moreover, the immunostimulatory properties of prepared polymers were studied using oxidative burst of the polymorphonuclears assay in the context of their graft length, which is extremely important for a dose design of a treatment.

2. Materials and methods

2.1. Materials

β-Glucan was extracted from the bodies of *Auricularia auricula-judae* according to Ref. [9]. The isolated β-glucan exhibited the molecular weight $M_w = 2.5 \times 10^6$ Da ($I = 1.85$). 2-Butyl-2-oxazoline and 2-isopropyl-2-oxazoline were synthesized according to Ref. [11]. Diethyl ether, dimethyl sulfoxide, sodium chloride and toluene were purchased from Lachner Ltd. (Neratovice, Czech Republic). 2,4,6-Trinitrobenzene 1-sulfonic acid (TNBSA) solution was purchased from Thermo Fisher Scientific (Prague, Czech Republic). Spectra/Por dialysis membranes (molecular weight cut-off, MWCO, 6–8 kDa) were purchased from P-LAB (Prague, Czech Republic). All other chemicals were purchased from Sigma Aldrich Ltd. (Prague, Czech Republic). The chemicals were used without further purification unless stated otherwise.

2.2. Polymer synthesis

2.2.1. Preparation of β-glucan-graft-poly(2-isopropyl-2-oxazoline-co-2-butyl-2-oxazoline), theoretical molecular weight of polyoxazoline (POX) grafts $M_{n,graft} = 500$ Da (G1)

2-Isopropyl-2-oxazoline (1.000 mL, 8.4 mmol), 2-butyl-2-oxazoline (0.367 mL, 2.8 mmol) and allyl bromide (0.242 mL, 2.8 mmol) were mixed with 2 mL anhydrous acetonitrile, and the reaction mixture was stirred overnight at 70 °C under argon atmosphere. β-Glucan (0.20 g) was dissolved in 12 mL anhydrous dimethylsulfoxide, and the solution was azeotropically dried by the multiple addition of anhydrous toluene (10 mL). Sodium hydride (0.34 g of 60% dispersion in mineral oil, 8.4 mmol) was added to the β-glucan solution, and the mixture was stirred for 3 h at 70 °C. Both solutions were then mixed, except for 0.2 mL of the POX solution. The resulting mixture was stirred overnight at 70 °C. Water (10 mL) was added to the reaction mixture, which was then washed twice with diethyl ether to remove the mineral oil. The aqueous layer was dialyzed (MWCO 6–8 kDa) against water for 72 h and freeze-dried to give the desired product G1 (yield 175.1 mg).

The remaining 0.2 mL POX solution was mixed with 0.1 mL water and purified on a Sephadex® LH-20 column using methanol as the mobile phase, followed by evaporation of the solvent to obtain only the corresponding polymer grafts terminated with −OH groups.

^{1}H NMR of POX grafts (300 MHz, CD_3CN), δ (ppm): 0.89 ($-CH_2-CH_2-CH_2-C\mathbf{H_3}$), 1.02 ($-CH-(C\mathbf{H_3})_2$), 1.31 ($-CH_2-CH_2-C\mathbf{H_2}-CH_3$), 1.51 ($-CH_2-C\mathbf{H_2}-CH_2-CH_3$), 2.35 ($-C\mathbf{H_2}-CH_2-CH_2-CH_3$), 2.76 ($-CH-(CH_3)_2$), 3.40 ($-N-C\mathbf{H_2}-CH_2-$, $CH_2=CH-C\mathbf{H_2}-POX-$), 5.17 ($C\mathbf{H_2}=CH-CH_2-POX-$), 5.85 ($CH_2=C\mathbf{H}-CH_2-POX-$). Size-exclusion chromatography (SEC) of POX grafts: $M_n = 590$ Da, $I = 1.06$.

^{1}H NMR of G1 (300 MHz, D_2O), δ (ppm): 0.89 (POX: $-CH_2-CH_2-CH_2-C\mathbf{H_3}$), 1.06 (POX: $-CH-(C\mathbf{H_3})_2$), 1.30 (POX: $-CH_2-CH_2-C\mathbf{H_2}-CH_3$), 1.52 (POX: $-CH_2-C\mathbf{H_2}-CH_2-CH_3$), 2.37 ($-C\mathbf{H_2}-CH_2-CH_2-CH_3$), 2.7–2.9 ($-CH-(CH_3)_2$), 3.3–5.2 (POX: $-N-C\mathbf{H_2}-CH_2-$, glucose). ^{13}C NMR of G1 (75 MHz, D_2O, 4,4-dimethyl-4-silapentane-1-sulfonic acid, DSS, as standard), δ (ppm): 16, 21, 32, 41, 48, 63, 68, 69, 72, 76, 79, 81, 103, 107, 179, 184. Elemental analysis of G1: C 42.01%, H 6.22%, N 2.32%. Infrared spectroscopy (IR) of G1 (KBr): 3312 (ν_{O-H}), 2922 (ν_{C-H}), 1611 ($\nu_{C=O}$), 1422, 1363, 1033, 897. SEC of G1: $M_w = 3.7 \times 10^6$ Da, $I = 1.64$.

According to the procedure described above, we prepared four types of β-glucan-*graft*-polyoxazolines differing in graft length, starting from 500 Da (sample G1) up to 5000 Da (sample G4).

2.2.2. Preparation of β-glucan-graft-poly(2-isopropyl-2-oxazoline-co-2-butyl-2-oxazoline), theoretical molecular weight of POX grafts $M_{n,graft} = 1000$ Da (G2)

The general procedure is described in Section 2.2.1 *Preparation of β-glucan-graft-poly(2-isopropyl-2-oxazoline-co-2-butyl-2-oxazoline), theoretical molecular weight of POX grafts $M_{n,graft} = 500$ Da*. Here, the starting mixture contained allyl bromide (0.121 mL, 1.4 mmol), 2-isopropyl-2-oxazoline (1.000 mL, 8.4 mmol) and 2-butyl-2-oxazoline (0.367 mL, 2.8 mmol). The resulting polymer was denoted G2 (yield 235.2 mg).

^{1}H NMR of POX grafts (300 MHz, CD_3CN), δ (ppm): 0.89 ($-CH_2-CH_2-CH_2-C\mathbf{H_3}$), 1.02 ($-CH-(C\mathbf{H_3})_2$), 1.30 ($-CH_2-CH_2-C\mathbf{H_2}-CH_3$), 1.50 ($-CH_2-C\mathbf{H_2}-CH_2-CH_3$), 2.35 ($-C\mathbf{H_2}-CH_2-CH_2-CH_3$), 2.52 ($-CH-(CH_3)_2$), 3.46 ($-N-C\mathbf{H_2}-CH_2-$, $CH_2=CH-C\mathbf{H_2}-POX-$), 5.19 ($C\mathbf{H_2}=CH-CH_2-POX-$), 5.79 ($CH_2=C\mathbf{H}-CH_2-POX-$). SEC of POX grafts: $M_n = 1140$ Da, $I = 1.11$.

^{1}H NMR of G2 (300 MHz, D_2O), δ (ppm): 0.89 (POX: $-CH_2-CH_2-CH_2-C\mathbf{H_3}$), 1.06 (POX: $-CH-(C\mathbf{H_3})_2$), 1.31 (POX: $-CH_2-CH_2-C\mathbf{H_2}-CH_3$), 1.51 (POX: $-CH_2-C\mathbf{H_2}-CH_2-CH_3$), 2.36 ($-C\mathbf{H_2}-CH_2-CH_2-CH_3$), 2.7–2.9 ($-CH-(CH_3)_2$), 3.3–5.2 (POX: $-N-C\mathbf{H_2}-CH_2-$, glucose). ^{13}C NMR of G2 (75 MHz, D_2O, DSS), δ (ppm): 16, 21, 30, 32, 35, 41, 46, 48, 62, 68, 69, 72, 75, 76, 79, 80, 105, 107, 122, 179, 183. Elemental analysis of G2: C 49.03%, H 7.95%, N 5.51%. IR of G2 (KBr): 3340 (ν_{O-H}), 2965 (ν_{C-H}), 2933 (ν_{C-H}), 2871 (ν_{C-H}), 1630 ($\nu_{C=O}$), 1472, 1422, 1380, 1363, 1235, 1200, 1156, 1034, 897. SEC of G2: $M_w = 6.4 \times 10^6$ Da, $I = 1.64$.

2.2.3. Preparation of β-glucan-graft-poly(2-isopropyl-2-oxazoline-co-2-butyl-2-oxazoline), theoretical molecular weight of POX grafts $M_{n,graft} = 2500$ Da (G3)

The general procedure is described in Section 2.2.1 *Preparation of β-glucan-graft-poly(2-isopropyl-2-oxazoline-co-2-butyl-2-oxazoline), theoretical molecular weight of POX grafts $M_{n,graft} = 500$ Da*. Here, the starting mixture contained allyl bromide (48 μL, 0.56 mmol), 2-isopropyl-2-oxazoline (1.000 mL, 8.4 mmol) and 2-butyl-2-oxazoline (0.367 mL, 2.8 mmol). The resulting polymer was denoted G3 (yield 315.1 mg).

^{1}H NMR of POX grafts (300 MHz, CD_3CN), δ (ppm): 0.88 ($-CH_2-CH_2-CH_2-C\mathbf{H_3}$), 1.02 ($-CH-(C\mathbf{H_3})_2$), 1.30 ($-CH_2-CH_2-C\mathbf{H_2}-CH_3$), 1.50 ($-CH_2-C\mathbf{H_2}-CH_2-CH_3$), 2.31 ($-C\mathbf{H_2}-CH_2-CH_2-CH_3$), 2.68 ($-CH-(CH_3)_2$), 3.39 ($-N-C\mathbf{H_2}-CH_2-$). SEC of POX grafts: $M_n = 2290$ Da, $I = 1.19$.

^{1}H NMR of G3 (300 MHz, D_2O), δ (ppm): 0.89 (POX: $-CH_2-CH_2-CH_2-C\mathbf{H_3}$), 1.06 (POX: $-CH-(C\mathbf{H_3})_2$), 1.31 (POX: $-CH_2-CH_2-C\mathbf{H_2}-CH_3$), 1.51 (POX: $-CH_2-C\mathbf{H_2}-CH_2-CH_3$), 2.36 ($-C\mathbf{H_2}-CH_2-CH_2-CH_3$), 2.7–2.9 ($-CH-(CH_3)_2$), 3.3–5.2 (POX: $-N-C\mathbf{H_2}-CH_2-$, glucose). ^{13}C NMR of G3 (75 MHz, D_2O, DSS), δ (ppm): 16, 21, 25, 29, 33, 35, 45, 46, 49, 68, 69, 72, 76, 78, 81, 106, 179, 183. Elemental analysis of G3: C 52.50%, H 8.32%, N 6.91%. IR of G3 (KBr): 3365 (ν_{O-H}), 2965 (ν_{C-H}), 2933 (ν_{C-H}), 2871 (ν_{C-H}), 1631 ($\nu_{C=O}$), 1472, 1423, 1380, 1362, 1236, 1200, 1158, 1085, 1037. SEC of G3: $M_w = 7.5 \times 10^6$ Da, $I = 1.49$.

2.2.4. Preparation of β-glucan-graft-poly(2-isopropyl-2-oxazoline-co-2-butyl-2-oxazoline), theoretical molecular weight of POX grafts $M_{n,graft}$ = 5000 Da (G4)

The general procedure is described in Section 2.2.1 *Preparation of β-glucan-graft-poly(2-isopropyl-2-oxazoline-co-2-butyl-2-oxazoline), theoretical molecular weight of POX grafts $M_{n,graft}$ = 500 Da*. Here, the starting mixture contained allyl bromide (24 μL, 0.28 mmol), 2-isopropyl-2-oxazoline (1.000 mL, 8.4 mmol) and 2-butyl-2-oxazoline (0.367 mL, 2.8 mmol). In contrast to the general procedure, dialysis was performed at 10 °C (the CPT in this case is below room temperature) to maximize the purification efficiency. The resulting polymer was denoted G4 (yield 451.8 mg).

^{1}H NMR of POX grafts (300 MHz, CD_3CN), δ (ppm): 0.88 ($-CH_2-CH_2-CH_2-C\mathbf{H_3}$), 1.01 ($-CH-(C\mathbf{H_3})_2$), 1.29 ($-CH_2-CH_2-C\mathbf{H_2}-CH_3$), 1.49 ($-CH_2-C\mathbf{H_2}-CH_2-CH_3$), 2.33 ($-C\mathbf{H_2}-CH_2-CH_2-CH_3$), 2.55 ($-CH-(CH_3)_2$), 3.39 ($-N-C\mathbf{H_2}-CH_2-$). SEC of POX grafts: M_n = 4180 Da, I = 1.20.

^{1}H NMR of G4 (600 MHz, dimethyl sulfoxide, DMSO), δ (ppm): 0.89 (POX: $-CH_2-CH_2-CH_2-C\mathbf{H_3}$), 1.02 (POX: $-CH-(C\mathbf{H_3})_2$), 1.30 (POX: $-CH_2-CH_2-C\mathbf{H_2}-CH_3$), 1.50 (POX: $-CH_2-C\mathbf{H_2}-CH_2-CH_3$), 2.36 ($-C\mathbf{H_2}-CH_2-CH_2-CH_3$), 2.7–2.9 ($-CH-(CH_3)_2$), 3.3–5.2 (POX: $-N-C\mathbf{H_2}-CH_2-$, glucose). ^{13}C NMR of G4 (150 MHz, DMSO), δ (ppm): 14, 20, 22, 27, 29, 32, 34, 43, 45, 46, 60, 65, 69, 73, 76, 104, 173, 177. Elemental analysis of G4: C 52.50%, H 8.32%, N 6.91%. IR of G4 (KBr): 3400 (ν_{O-H}), 2965 (ν_{C-H}), 2933 (ν_{C-H}), 2871 (ν_{C-H}), 1632 ($\nu_{C=O}$), 1472, 1420, 1380, 1363, 1236, 1198, 1158, 1086, 1039. SEC of G4: $M_w = 1.6 \times 10^7$ Da, I = 3.70.

2.3. Polymer characterization

^{1}H NMR and ^{13}C NMR spectra were obtained on a Bruker Avance DPX-300 spectrometer and on a Bruker Avance III 600 spectrometer (both Bruker Co., Austria). Fourier transform infrared (FT-IR) measurements were carried out on a Perkin-Elmer Paragon 1000PC spectrometer (Perkin-Elmer Co., USA) equipped with a Specac MKII Golden Gate single attenuated total reflection (ATR) system (Perkin-Elmer Co., USA). Elemental analysis was performed on a Perkin-Elmer Series II CHNS/O Analyzer 2400 (PE Systems Ltd., Czech Republic) instrument.

The molecular weights of the grafts were determined by SEC, which was composed of a Deltachrom SDS030 pump (Watrex Co., Prague, Czech Republic), an autosampler MIDAS (Spark HOLLAND B.V., Netherlands), two PL gel MIXED-B-LS (10 μm) columns and an evaporative light-scattering detector ELS-1000 (Polymer Laboratories, USA). *N,N*-Dimethylformamide was used as the mobile phase, and commercial alkyne-terminated poly(2-ethyl-2-oxazoline)s served as the calibration standards. The molecular weights of the prepared polymers were also determined using the same SEC arrangement with dual detection by an Optilab t-rEX refractive index detector and DAWN Heleos II multiangle light-scattering (MALS) detectors (both Wyatt Technology Corporation, USA). Dimethyl sulfoxide was used as the mobile phase. To compare the measured molecular weights of the products, static light scattering (SLS) was performed as well. SLS was carried out on an ALV instrument equipped with a 30 mW He—Ne laser (vertically polarized light at λ = 632.8 nm) in the angular range of 30–150°. The Zimm plot procedure was used for M_w determination.

The CPTs of the polymers were determined in phosphate-buffered saline (PBS) solution over a concentration range of 1–25 mg/mL using the dynamic light scattering (DLS) technique. The temperature dependence of the polymer hydrodynamic radius (R_h) (volume mean) was measured on a Zetasizer Nano-ZS, Model ZEN3600 (Malvern Instruments, UK) at the scattering angle θ = 173° from 5 to 65 °C with a heating rate of 1 °C/min (using the DTS software – version 6.20 for data evaluation). After each heating step, three R_h measurements were performed. The CPTs were also studied using fluorescence measurements on a RF 5302 Shimadzu spectrofluorometer (Shimadzu, Japan). The temperature-dependent behaviour of the polymers in aqueous solution was also studied by ^{1}H NMR measurements recorded on a Bruker Avance III 600 spectrometer (Bruker Co., Austria) operating at 600.2 MHz with a width of 90°, pulse of 10 μs, relaxation delay of 10 s, acquisition time of 2.18 s, and 16 scans. The integrated intensities were determined with the spectrometer integration software with an accuracy of ± 1%. Before measurement, the samples were equilibrated at the given temperature for at least 10 min. The temperature dependences of the ^{1}H spin-spin relaxation times T_2 of HDO and the copolymer blocks were measured using the CPMG pulse sequence $90^\circ_x-(t_d-180^\circ_y-t_d)_n$-acquisition [14]. The relaxation delay between scans was 100 s, the acquisition time was 2.84 s, and 2 scans were performed. The relative error of T_2 did not exceed ± 5%. The polymer phase transition was also studied using differential scanning calorimetry (DSC). DSC analyses were carried out on a Perkin Elmer DSC 8500 calorimeter with nitrogen purge gas (20 $cm^3\,min^{-1}$). The analyses were performed in a cycle heating/cooling – heating from 5 °C to 55 °C at 3 $°C/min^{-1}$.

Samples for atomic force microscopy (AFM) characterization were prepared on freshly cleaved mica. The polymer was dissolved in water (1 mg/mL) and equilibrated at temperatures 15 and 37 °C. A drop of the sample solution was placed on the mica substrate and quickly dried under vacuum. All images were acquired using a Dimension ICON atomic force microscope (Bruker Co., USA) under air in Peak Force Tapping mode: 256 × 256 pixel topography scans were taken using etched MPP silicon tips (TAP150A, Bruker Co., USA) with a typical spring constant k = 5 N/m, Peak Force frequency of 2 kHz and scan rates in the range of 0.5–0.9 Hz. The Nano Scope Analysis software (Bruker Co., USA) was used for image processing.

2.4. Biological studies

2.4.1. Cell lines and isolated white blood cells

Murine BALB/C monocyte macrophage cell line J774A.1 (Sigma Aldrich, Prague, Czech Republic) was cultured in Dulbecco's modified Eagle medium (DMEM) supplemented with 100 unit of penicillin and 100 μg/mL streptomycin, 2 mM glutamine and 10% fetal bovine serum (all from Thermo Fisher Scientific, Prague, Czech Republic). The cell line was cultivated in a humidified incubator at 37 °C with 5% CO_2.

White blood cells were isolated from the human whole blood (kindly provided by Military Hospital, Prague, Czech Republic) after the lysis of erythrocytes according following protocol: the whole blood (1 mL) was mixed with the Lysis solution (14 mL; 1.5 M NH_4Cl, 100 mM $NaHCO_3$, 10 mM ethylenediaminetetraacetic acid, pH = 7.3) for 10 min at room temperature (RT). The mixture was centrifuged (300 × *g*, 5 min, RT), and the pellets were washed with ice cold PBS (5 mL) followed by next centrifugation (300 × *g*, 5 min, 8 °C). The cells were resuspended in Hank's balanced salt solution (HBSS) Ca^{2+}/Mg^{2+} (0.137 M NaCl, 5.4 mM KCl, 0.44 mM KH_2PO_4, 5.55 mM glucose, 0.34 mM Na_2HPO_4, 0.8 mM $MgSO_4$, 1.26 mM $CaCl_2$, 4.17 mM $NaHCO_3$).

2.4.2. Cytotoxicity

Cell viability was determined using Alamar Blue® cell viability reagent (Life Technologies, Prague, Czech Republic) on monocyte macrophage cell line according to the manufacturer protocol. Cells J774A.1 were seeded into 96-well plates (in triplicates, density: 10^4 cells/well) in 100 μL of media 24 h prior to the treatment. The medium was then replaced by 100 μL of serial dilution of polymers (G2 – G4) in complete cell culture medium. The cells were subsequently incubated for 24 h in 5% CO_2 at 37 °C. Then, 10 μL of Alamar Blue reagent was added to each well and incubated for 4 h in 5% CO_2 at 37 °C. Resazurin (Alamare Blue reagent) is metabolized in viable cell to the high fluorescent compound resorufin, which was measured using the Synergy Neo plate reader (Bio-Tek, Prague, Czech Republic) at $570nm_{Ex}/600nm_{Em}$. Non-treated cells were used as a positive control and the cells killed by 0.03% hydrogen peroxide were used as negative control. Each concentration was

measured in triplicates in three independent experiments.

2.4.3. Oxidative burst assay

The white blood cells were seeded into 96-well plate in 100 µL HBSS in the density of 150,000 cells per well immediately after the isolation. The samples G2, G3 and G4 were added at the concentrations corresponding to 100 and 10 µg/mL ß-glucan. Original ß-glucan was used as a control. The change in hydrogen peroxide concentration was measured by the detection of luminol chemiluminescence (150 µM) on MicroBeta2 (PerkinElmer, Prague, Czech Republic) after the stimulation with phorbol 12-myristate 13-acetate (PMA, 10 µg/mL) or no stimulation, respectively. The procedure was repeated in three independent experiments in duplicates.

The statistical analysis of data was conducted using Origin® 9 software (OriginLab Corporation, MA, USA) using ANOVA test at the significance level of $\alpha = 0.05$.

3. Results and discussion

β-Glucan-*graft*-polyoxazolines combine the thermoresponsivity and the biocompatibility of POXs with the biodegradability, self-assembled structure, bioactivity and immunostimulatory properties of β-glucan. Because of these exceptional properties, we have designed them to be used in cancer immunoradiotherapy, while the successful treatment, showing synergistic effect, of both therapies was demonstrated *in vivo* [10]. However, a detailed study of these polymers is necessary, especially the relation between the thermoresponsivity (needed for the correct administration – a formation of the polymer depot after the intratumoural injection of polymer solution) and their bioactivity (for the knowledge of the expected treatment success). The polymer immunostimulatory properties can be influenced by the POX chains, namely, by a possible steric hindrance of the active moieties. Therefore, these crucial immunostimulatory properties were studied in the context of graft length and the thermoresponsive properties on four samples of β-glucan-*graft*-poly(2-isopropyl-2-oxazoline-*co*-2-butyl-2-oxazoline)s with a maximum achievable grafting density – G1 with the theoretical graft length 500 Da, G2 1000 Da, G3 2500 Da and G4 5000 Da.

3.1. Synthesis and characterization

The initial β-glucan was extracted from *Auricularia auricula-judae* according to Ref. [9]. The grafted polymers were prepared using this β-glucan by a simple one-pot, two-step synthesis (Fig. 1B). At first, all polymer grafts were synthesized by the cationic ring-opening polymerization of 2-isopropyl-2- oxazoline and 2-butyl-2-oxazoline using allyl bromide as an initiator, as the use of allyl bromide introduces a double bond at the graft ends, allowing further modifications, *e.g.*, thiol-click chemistry or radical crosslinking/copolymerization. Secondly, the living graft ends were terminated with sodium β-glucanate to give β-glucan-*graft*-poly(2-isopropyl-2-oxazoline-*co*-2-butyl-2-oxazoline). Additionally, the living ends were terminated with water to obtain the corresponding POX grafts with −OH groups at the ends, allowing us to study the graft properties.

The successful grafting procedure was confirmed by ^{1}H NMR spectroscopy as well as by infrared spectroscopy. The nuclear magnetic resonance (NMR) spectra of the grafted β-glucans show peaks corresponding to POX chains consisting of 2-isopropyl-2-oxazoline units and 2-butyl-2-oxazoline units (POX region in Fig. 2B) as well as peaks corresponding to the β-glucan backbone (polysaccharide region in Fig. 2B). The NMR intensity decrease in the polysaccharide region from G1 to G4 demonstrates the decreasing content of β-glucan in the sample. Moreover, all grafts have allyl groups at the ends (from the initiator), while in the sample G1, the presence of allyl groups was confirmed by NMR. However, in the spectra of polymers G2, G3 and G4, the signals corresponding to the allyl groups were weak (longer grafts contain comparably fewer end groups). In the IR spectra of the grafted β-glucans (Fig. 2A), the peak at 1624 cm^{-1} corresponds to an amide C=O stretching vibration of the POX grafts. In addition, the peak at 3320 cm^{-1} corresponds to the −OH groups of the β-glucan moiety. This peak intensity decreases from G1 to G4, indicating that the β-glucan content in the samples decreases as well.

The graft lengths were determined using SEC. Aliquots of the polymerization mixtures were quenched with water instead of the β-glucanate solution to study only the corresponding grafts (Table 1). The graft lengths are close to the desired theoretical values. Moreover, the dispersity is also acceptable; in all cases, it is lower than 1.20.

The theoretical molar ratio of the monomers in resulting polymer grafts was selected to be $n_{\text{isopropyloxazoline}}/n_{\text{butyloxazoline}} = 3/1$ mol/mol because, according to our previous experience, this monomer ratio exhibits the most appropriate CPT to obtain a material that has a CPT between room and body temperatures, *i.e.*, allowing injection of the molecular solution and subsequent formation of the self-assembled

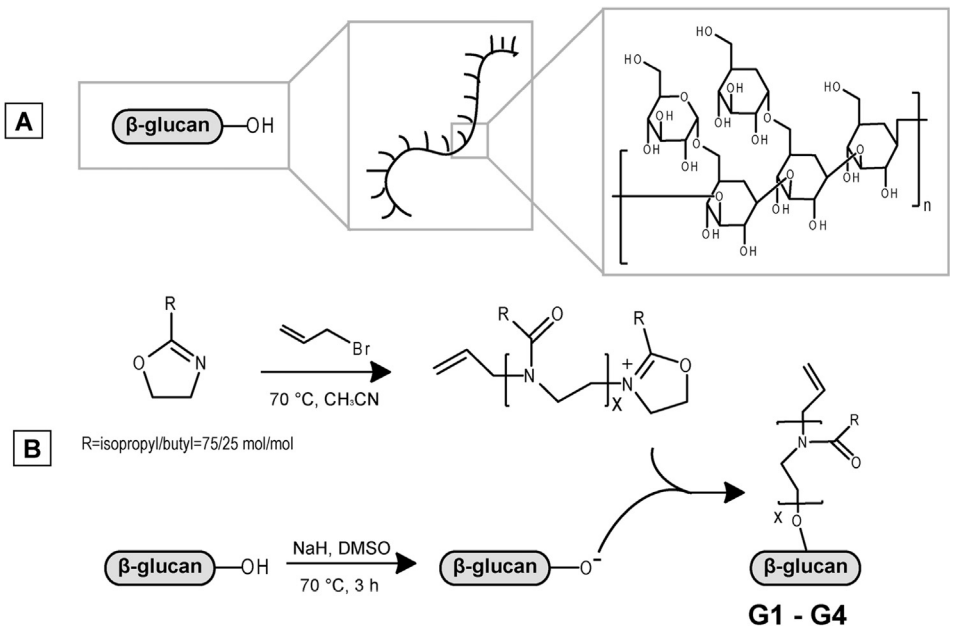

Fig. 1. (A) Structure of the isolated β-glucan; (B) general synthetic procedure.

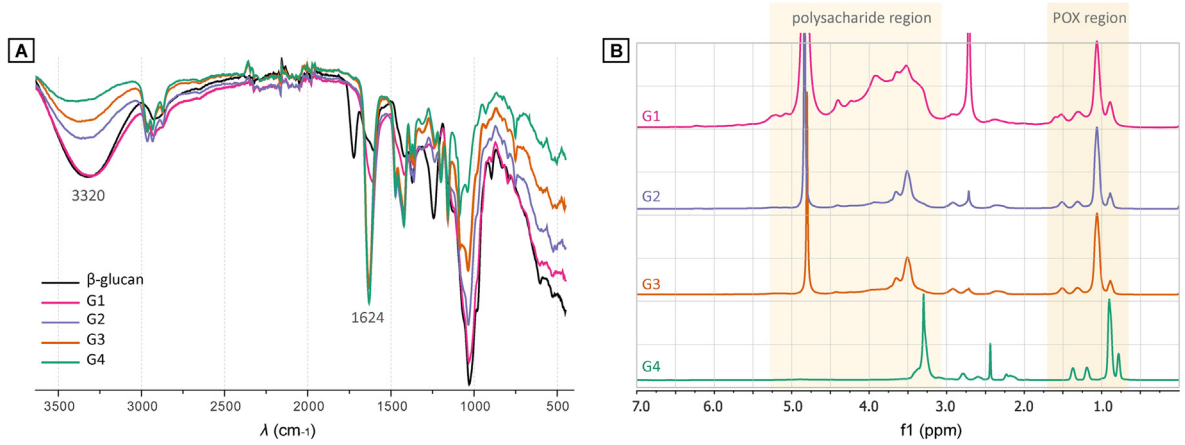

Fig. 2. (A) FT-IR spectra and (B) NMR spectra of polymers G1 – G4.

Table 1
Characterization of the POX polymers, representing the grafts contained in the prepared polymers.

Sample	$M_{n,theor}$ (Da)	$M_{n,found}$ (Da)	Dispersity	n_{butyl}/n_{propyl} [a]
G1 graft	500	590	1.06	70/30
G2 graft	1000	1140	1.11	74/26
G3 graft	2500	2290	1.19	74/26
G4 graft	5000	4180	1.20	73/27

[a] n_{butyl}/n_{propyl} is the molar ratio of 2-isopropyl-2-oxazoline to 2-butyl-2-oxazoline incorporated in the POX grafts, determined by NMR.

structures in organism due to the thermoresponsive behaviour of the material [12]. Moreover, the presence of 2-butyl-2-oxazoline in the grafts prevents the crystallization of homopolymer poly(2-isopropyl-2-oxazoline) after heating, which could results in an insoluble non-thermoresponsive product [13]. The actual ratio of monomeric units in the resulting POX grafts was calculated according to Eq. (1):

$$n_{isopropyl}/n_{butyl} = (I_{\delta=1.02ppm}/6)/(I_{\delta=1.31ppm}/2) \quad (1)$$

where $n_{isopropyl}/n_{butyl}$ is the molar ratio of 2-isopropyl-2-oxazoline to 2-butyl-2-oxazoline incorporated in the POX grafts; $I_{\delta=1.02\ ppm}$ is the intensity of the peak at 1.02 ppm, corresponding to the $-CH-(CH_3)_2$ group of 2-isopropyl-2-oxazoline and $I_{\delta=1.31\ ppm}$ is the peak intensity at 1.31 ppm corresponding to $-CH_2-CH_2-CH_2-CH_3$ group of 2-butyl-2-oxazoline. The theoretical ratio $n_{isopropyl}/n_{butyl}$ for all grafts was supposed to be 75/25, and the obtained ratios are very close to the theoretical ones (Table 1).

To eliminate the presence of unbound POX grafts, the polymer solutions were dialyzed using cellulose membranes with a molecular weight cut-off of 6–8 kDa, that is well above the maximal molecular weight of the prepared grafts. The dialysis of G4 was performed at lower temperature (10 °C) to ensure the solubility of unbound longer POX grafts with a CPT lower than room temperature. Because the starting β-glucan contained less than 0.1 wt% nitrogen, the content of POX in the prepared polymers could be calculated using the weight content of nitrogen, determined by elemental analysis (CHN). The weight content of POX w_{POX} in the resulting polymer was calculated according to Eq. (2):

$$w_{POX} = (w_N/w_{N,ox}) \times 100\% \quad (2)$$

where w_N is the content of nitrogen in the resulting polymer and $w_{N,ox}$ is the theoretical content of nitrogen in the corresponding POX grafts. The weight content of POX nicely corresponds to the graft length (Table 2). During the grafting procedure, POX chains were added in high excess, resulting in the maximum achievable grafting density. In general, the grafting limit is determined by the spatial and conformational properties of the β-glucan structure. The number of glucose units per graft was calculated to be the same for all samples (from 6 to 9 glucose units per graft), and therefore, the maximum achievable grafting density was reached for all samples. Interestingly, the comb-like shape of β-glucan causes the maximum achievable grafting density of longer grafts to be comparable with the maximum grafting density of shorter grafts. In other words, a significant difference in the maximum achievable grafting density for different graft lengths, ranging from 500 to 5000 Da, was not found.

To determine the weight-average molecular weight of the prepared polymers, SEC-MALS and SLS measurements were performed (Table 2). According to SEC-MALS, the increasing weight-average molecular weight of the prepared polymers correspond to the increasing weight content of the POX grafts, from 3.7×10^6 Da for G1 up to 1.6×10^7 Da for G4. The weight-average molecular weight of the initial (non-grafted) β-glucan was found to be 2.5×10^6 Da, which is in good agreement with the literature (β-glucan, denoted as AF1, in DMSO, $M_w = 2.07 \times 10^6$ Da) [9]. The theoretical molecular weights of the polymers were calculated by considering the M_w of β-glucan and the particular weight content of POX grafts (Table 2), and these values correspond well to the molecular weights found by SEC-MALS for all samples. The chromatograms showed unimodal curves of the prepared polymers and no presence of unreacted POX grafts (Fig. S1 in the

Table 2
Characterization of the prepared grafted polymers.

	POX content (wt%)	$M_{w,theor}$ (Da)[a]	$M_{w,found}$ (Da)[b]	Dispersity	$M_{w,found}$ (Da)[c]	Glucose units per graft
G1	26	3.4×10^6	3.7×10^6	1.64	4.0×10^6	9.3
G2	47	4.7×10^6	6.4×10^6	1.64	5.2×10^6	7.2
G3	70	8.3×10^6	7.5×10^6	1.49	7.5×10^6	6.0
G4	80	1.3×10^7	1.6×10^7	3.70	1.9×10^7	5.9

[a] Theoretical value calculated from the weight content of POX.
[b] Determined by SEC-MALS.
[c] Determined by SLS.

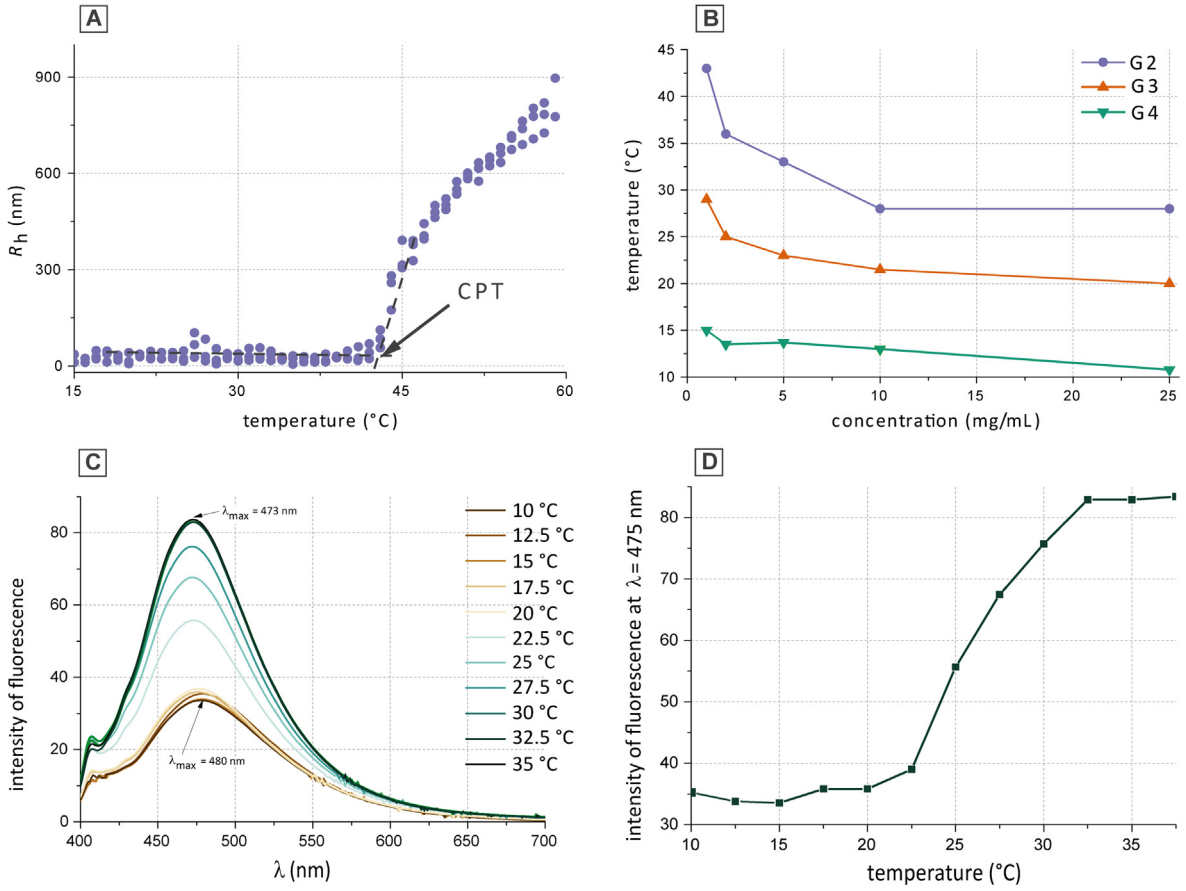

Fig. 3. (A) Temperature dependence of the R_h (volume mean) of G2 polymer particles in solution at a concentration c = 1 mg/mL in PBS; (B) CPTs of the prepared polymers (CPT of G1 was not detected up to 65 °C). The standard deviation of 3 independent measurements was below 5%. (C and D) The temperature-dependent fluorescence of G3 at the concentration c = 10 mg/mL in PBS. The standard deviation of 3 independent measurements was below 5%.

Supplementary Figures). The dispersity for all samples was found to be ~1.5, which is typical for polysaccharides isolated from biomaterials, with an exception of G4, where the dispersity was measured to be ca 3.70. SLS measurements showed that the weight-average molecular weight increased from 4.0 × 10^6 Da for G1 up to 1.9 × 10^7 Da for G4 (Table 2), confirming the increase of weight content of the POX grafts. These results are in good agreement with the M_w obtained by SEC-MALS.

Supplementary data associated with this article can be found, in the online version, at https://doi.org/10.1016/j.eurpolymj.2018.07.004.

3.2. Thermoresponsive polymer behaviour

The polymer hydrodynamic radius (R_h) as a function of temperature was measured using DLS to determine the CPT of the solution at a given concentration. The R_h was measured for all prepared polymers in the concentration range from 1 to 25 mg/mL in PBS. As an example of these measurements, the temperature dependence of the R_h (volume mean) of G2 at a concentration of 1 mg/mL in PBS (Fig. 3A) shows that the polymer volume average R_h in the solution (below CPT) is approximately 30 nm, while at 43 °C, the R_h begins to increase (at CPT). All observed CPTs of the grafted β-glucans at different concentrations (1–25 mg/mL in PBS) show a significant dependence of the solution behaviour on the graft length (Fig. 3B). For the shortest grafts (G1 with $M_{n,graft(found)}$ = 590 Da), the CPT was even not detected up to 65 °C. On the other hand, the sample with the longest grafts (G4 with $M_{n,graft(found)}$ = 4180 Da) precipitates at room temperature (20 °C), even in relatively low concentrations. As expected, the CPTs of the prepared polymers decrease with increasing concentration, which, for a given sample, corresponds to the POX content in the solution as much as to the increasing content of hydrophobic alkyl groups. It can also be seen that the concentration dependence of the CPT is influenced by the graft length. For G2 ($M_{n,graft(found)}$ = 1140 Da), the difference between the CPT at c = 1 mg/mL and the CPT at c = 25 mg/mL is approximately 8 °C, while the sample with the longer grafts, G4 ($M_{n,graft(found)}$ = 4180 Da), showed a difference of only 4 °C in the CPTs at the same concentration values. Therefore, the influence of longer grafts on solution behaviour of whole final macromolecule is more pronounced than in case of the shorter grafts.

In terms of polymer suitability for body administration (formation of the polymer depot after the intratumoural injection of polymer solution), sample G1 is not suitable because it did not show any thermoresponsive behaviour (up to 65 °C). The polymer G2 is also not suitable due to CPT higher than 37 °C at lower concentrations, which could result in not creating of polymer depot or its faster dissolution. G3 and G4 are suitable for polymer depot formation. However, G4 has quite low CPT, which, on the other hand, causes its precipitation even at room temperature at high concentration. Therefore, the best candidate for administration is G3 with grafts of 2500 Da.

The R_h measurement provides the information about the particle sizes, nevertheless, it does not inform about hydrophobicity of the microenvironment before, during and after a transition. Therefore, the temperature-dependent fluorescence was measured to determine the formation of hydrophobic domains in the solution of the polymer G3 (c = 10 mg/mL in PBS) (Fig. 3C and D). This measurement utilizes the aggregation-induced emission caused by a low-fluorescent probe in the molecularly dissolved state and a highly fluorescent probe in the aggregate state in a hydrophobic environment. 8-Anilino-1-

naphthalenesulfonic acid ammonium salt (c = 0.25 µmol/mL, λ_{ex} = 388 nm) was used as a probe. No difference in fluorescence intensity was observed at lower temperatures (below CPT, Fig. 3C and D), indicating that the hydrophobic domains come from the isopropyl and butyl moieties of one macromolecule (or very few). At 22.5 °C, the fluorescence intensity significantly increased, which indicates that the content of hydrophobic domains increased as well. This fact is in good agreement with the DLS measurement, which determined the CPT of this system (G3, c = 10 mg/mL in PBS) to be 21.5 °C. Moreover, the fluorescence intensity increased up to 32.5 °C, indicating a higher content of hydrophobic domains and possible inter/intramolecular reorganization of the self-assembled structures in this temperature region. Thereafter, the fluorescence intensity remained constant, and no change in fluorescence intensity was revealed with further increases in temperature (above 32.5 °C). In addition, the peak maximum in the fluorescence spectrum shifted to shorter wavelengths (from 480 to 473 nm) during the temperature elevation, confirming the increase in the microenvironment hydrophobicity.

The temperature-dependent behaviour of the polymer G3 was also characterized by NMR. The high-resolution ^{1}H NMR spectra of G3 (c = 10 mg/mL in D_2O) were measured over a temperature range from 12 to 57 °C (Fig. 4A). Peak assignments of the various types of protons in POXs are shown in the spectrum measured at 12 °C. The chemical structure of the polymer is shown in the same figure on the right of the spectra. The broad unmarked signals between δ = 3–4.5 ppm and $\delta \approx$ 5 ppm are related to β-glucan protons. The signal "**a**" is related to the −N−C**H$_2$**− groups of poly(2-isopropropyl-2-oxazoline-*co*-2-butyl-2-oxazoline), which form the graft main chain. The protons present in the −CO−**CH**−$(CH_3)_2$ and −CO−CH−$(\mathbf{CH_3})_2$ groups of the 2-isopropropyl-2-oxazoline monomeric unit are marked as "**b**" and "**c**". The −CO−⊖**CH$_2$**−CH_2−CH_2−CH_3, −CO−CH_2−**CH$_2$**−CH_2−CH_3, −CO−⊖CH_2−CH_2−**CH$_2$**−CH_3 and −CO−CH_2−CH_2−CH_2−**CH$_3$** groups of the 2-butyl-2-oxazoline monomeric unit correspond to the peaks "**d**", "**e**", "**f**" and "**g**", respectively. The main change observed in the spectra is that the intensity of the signals related to POXs decreases with increasing temperature. The broadening and disappearance of the peak, corresponding to the thermoresponsive polymer, are connected with the decreased mobility of the POX chains under increasing temperature in analogy to Ref. [14]. To quantitatively characterize the changes that occur during the heating and cooling processes, the p-fraction of groups with significantly reduced mobility was calculated from the integrated intensities in the ^{1}H NMR spectra using the following Eq. (3): [14]

$$p = 1-\{I(T)/[I(T_0)\cdot(T_0/T)]\} \quad (3)$$

where $I(T)$ is the integrated intensity of a given polymer signal in the spectrum at a given temperature T and $I(T_0)$ is the integrated intensity of this signal when no phase separation occurs (below the transition). The calculated p-fractions for particular POX groups in G3 (c = 10 mg/mL in D_2O) at various temperatures are shown in Fig. 4B. The phase transition begins at 24 °C for all POX protons, which is in good agreement with other methods. The final p-fraction values (p_{max}) give quantitative information about the amount of the groups that participate in a phase transition. The p_{max} value was 0.69 for group "**a**" from the POX main chain and 0.76 and 0.67 for the isopropyl units "**b**" and "**c**", respectively. Therefore, the −N−**CH$_2$**− groups of the POX main chain and the isopropyl groups influence the phase transition similarly. However, the p_{max} value of "**d**" protons in the butyl monomer unit was calculated to be 0.81, while for "**e**", the value was 0.54, for "**f**", 0.20 (this value may be affected by the broadening of signal "**c**"), and for "**g**", 0.48. The higher p_{max} values for the POX main chain and for the side groups of the 2-isopropyl-2-oxazoline unit suggest that these sections of the polymer are less mobile in the hydrophobic center of the formed nanoparticles, while the side groups of the 2-butyl-2-oxazoline unit are probably more flexible. A comparison of the heating and cooling processes for the "**a**" protons in the POX main chain (−N−**CH$_2$**−) is shown in Fig. S2 in the Supplementary Figures. The fully reversible behaviour is confirmed by the nearly identical phase transition curves and corresponding CPTs for the heating and cooling processes. Such comparison for the other groups in POX confirm the same reversibility of the phase transition processes (data is not shown).

The signals of the polysaccharide section remain unchanged, showing that only the poly(2-alkyl-2-oxazoline) section participates in the temperature-induced phase separation, with a negligible effect on the hydrophilic polysaccharide section. However, the polysaccharide section influences the thermoresponsive behaviour of the poly(2-alkyl-2-oxazoline) section, especially when the grafts are short (see above).

Consequently, NMR relaxation measurements were performed to provide information about the water behaviour and polymer-solvent interactions (hydration) during the phase transition. It is well known that the spin-spin relaxation times T_2 of water (HDO protons or D_2O deuterons) are especially useful in this respect [15]. Fig. S3 in the Supplementary Figures shows the temperature (full circles) and time dependence (full squares) at 57 °C of the ^{1}H spin-spin relaxation time T_2 of the HDO in G3 D_2O solution (c = 10 mg/mL). The low T_2 value (0.56 s at 12 °C) of HDO molecules gives information about the strong interactions (H-bonding) between the solvent and polymer G3, which reduce the solvent mobility. Further T_2 value increase under the temperature elevation is connected to the phase separation, increasing of p-fraction, reduced POX mobility and a microenvironment change from hydrophilic to hydrophobic. With increasing p-fraction, more POX chains break the hydrogen bonds with water, increasing mobility. Furthermore, keeping the sample at 57 °C for 12 h causes almost no

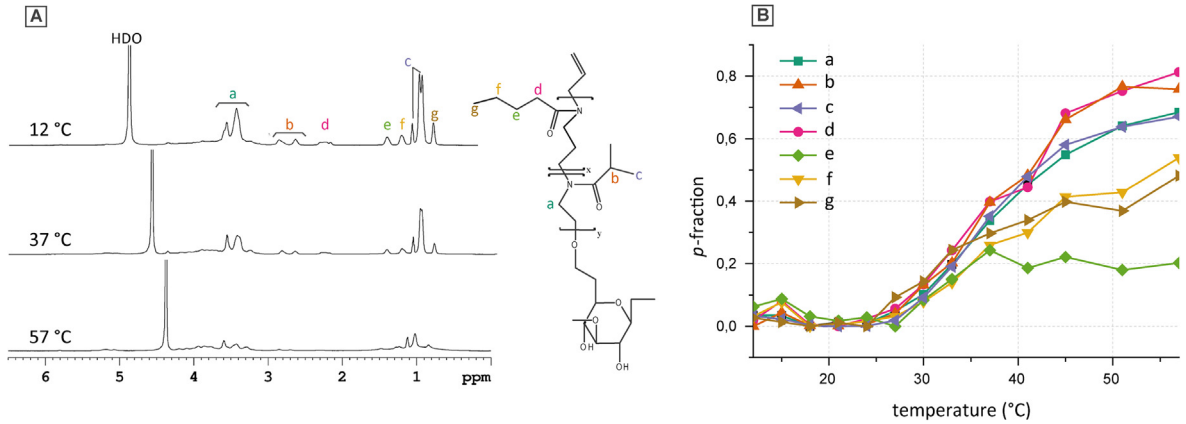

Fig. 4. (A) High-resolution ^{1}H NMR spectra of G3 (c = 10 mg/mL in D_2O) measured at 12 °C, 37 °C and 57 °C; (B) temperature-dependence of the p-fraction for various proton groups in the poly(2-isopropyl-2-oxazoline-*co*-2-butyl-2-oxazoline) unit of G3 (c = 10 mg/mL in D_2O) – during the heating process. The standard deviation of 3 independent measurements was below 5%.

change in T_2, suggesting that the polymer system is stable during this period.

All the methods used for solution behaviour and CPT characterization are in good agreement for the G3 sample at $c = 10$ mg/mL. Both DLS and fluorescence measurements were performed in PBS, while NMR was measured in D_2O, and thus, the higher ionic strength in PBS could slightly influence the results. This fact was confirmed by CPT measurements of this sample ($c = 10$ mg/mL) using DLS at both solvents – deuterium oxide and PBS (see Fig. S4 in the Supplementary Figures). Overall, the CPT of G3 at $c = 10$ mg/mL was determined to be 21.5 °C using DLS, 22.5 °C using fluorescence measurement with an aggregation-induced emission probe and 24 °C using NMR. DLS evidently shows the CPT as a point of aggregate formation based on the hydrodynamic radius, and fluorescence measurement exhibits the CPT as a point of aggregate formation based on the formation of hydrophobic domains, through it is possible that the formed small aggregates are still soluble. On the other hand, NMR shows the CPT as a point at which the aggregates begin to be insoluble, which is why the CPT determined by this technique for the same sample and concentration could be slightly higher.

The polymer phase transition was also investigated using differential scanning calorimetry. However, the transition was not observed for all polymers because the energy released/needed during the phase transition was probably negligible in comparison with the energy needed/released for the temperature change of water (see Fig. S5 in the Supplementary Figures).

3.3. Self-assembled polymer structures

The shape change during the phase transition of G3 was investigated by atomic force microscopy (AFM) in comparison to original β-glucan. The samples were transferred from 15 °C and 37 °C water solutions onto freshly cleaved mica substrates and characterized under the ambient conditions (Fig. 5). β-Glucan from *Auricularia auricula-judae* showed the presence of the typical fibres in their aqueous solutions, which is in good agreement with literature [9], and it also exhibited no significant difference in the structure within the temperature change ($R_{RMS,15\,°C} = 1.2$ nm; $R_{RMS,37\,°C} = 1.5$ nm). The G3 sample prepared at 15 °C exhibited a distinct, almost homogenous pattern with a root-mean-squared roughness $R_{RMS} = 0.5$ nm and a particle size of approximately 50 nm, which is in good agreement with the DLS measurement. In addition, a small portion of larger particles (approximately 100 nm) was observed, which can be attributed to the aggregates of a few macromolecules. On the other hand, the sample prepared at 37 °C had an increased surface roughness ($R_{RMS} = 2.9$ nm) and an enlarged ellipsoidal particles (approximately 500 nm). Such particles correspond well to the polymer aggregates at higher temperatures. Therefore, the poly(2-alkyl-2-oxazoline) grafts disturb the formation of typical nanofibers of the original β-glucan in aqueous solution, most likely due to the steric hindrance preventing the formation of intermolecular hydrogen bonds, which are essential for the nanofiber formation.

3.4. Biological studies

The sample G1 was not included in the following *in vitro* study because it did not show any thermoresponsive properties up to 65 °C, and thus, this polymer is completely unusable for intended application (formation of a polymer depot after injection from a polymer solution) because, interestingly, β-glucan administrated intratumourally is more anticancer efficient due to its close contact to tumour cells [16]. The cytotoxicity of the other prepared polymers (G2 – G4) was studied on murine BALB/C monocyte macrophage cell line J774A.1 using an AlamarBlue assay. The polymer cytotoxicity values were detected to be negligible at low concentrations for this cell line. Moreover, the half maximal inhibitory concentration (IC_{50}) was not found for all polymers up to the concentration $c = 0.5$ mg/mL (see Fig. S6 in the Supplementary Figures), which is, in general, sufficiently high concentration for biomedical application (it corresponds approximately to 2.5 g of polymer dissolved in the blood of an average adult).

The oxidative burst response of the polymorphonuclears, isolated from human blood, upon the incubation with the synthesized polymers

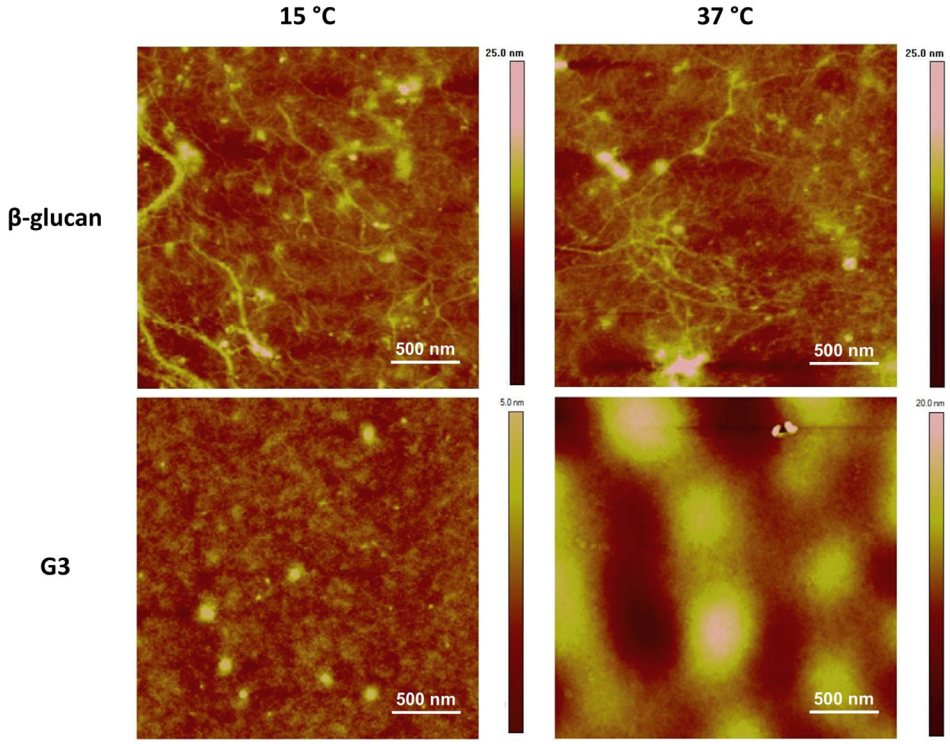

Fig. 5. The AFM topography images of β-glucan and G3 transferred from aqueous solutions at 15 °C and 37 °C onto fresh mica.

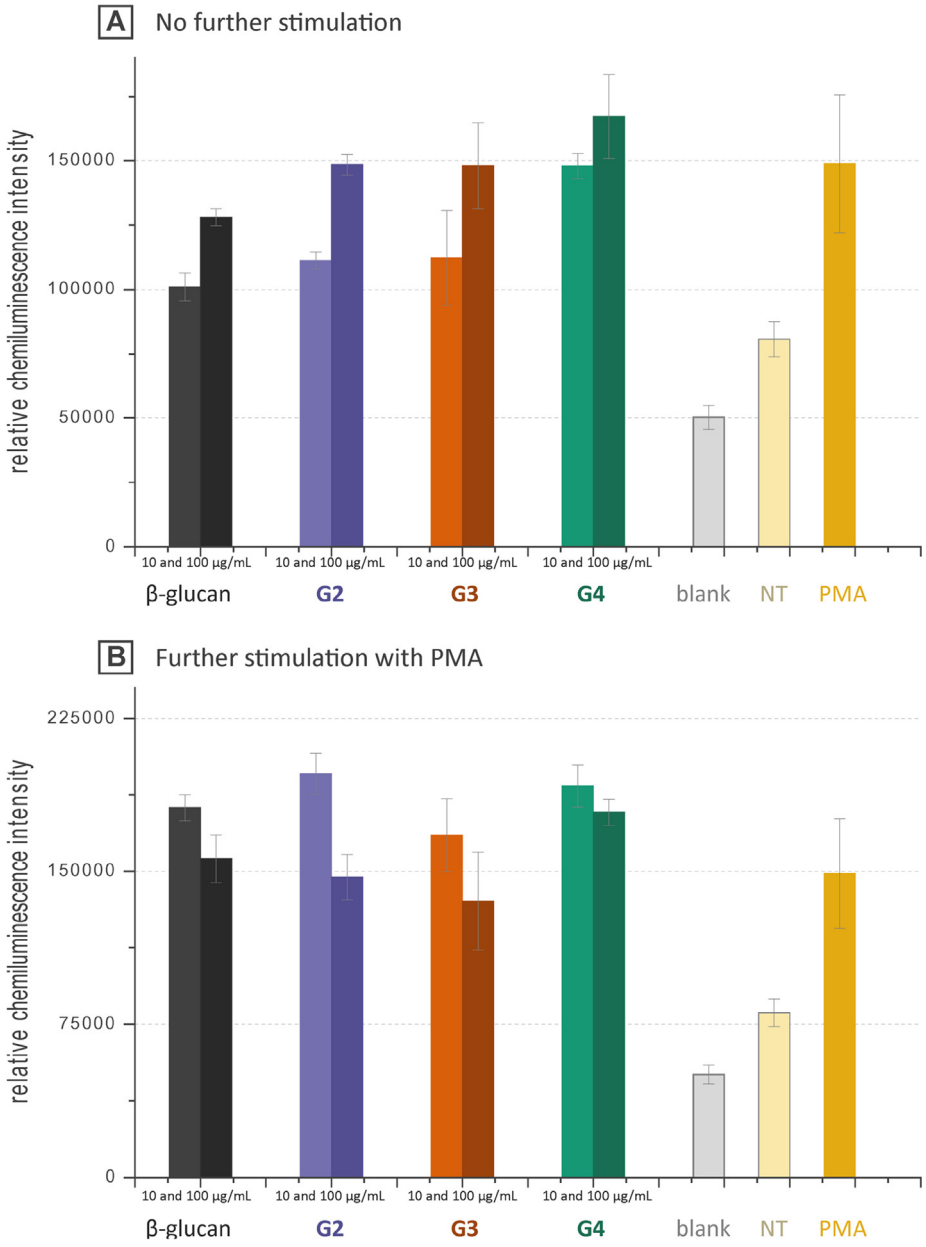

Fig. 6. The oxidative burst response of the polymorphonuclears upon the incubation with the polymers at their concentrations 10 and 100 µg/mL: (A) with no further stimulation and (B) with further stimulation by phorbol 12-myristate 13-acetate (PMA). Produced hydrogen peroxide was indirectly measured by addition of luminol, which was determined by chemiluminescence. NT is a non-treated control and PMA is a positive control.

was studied using the chemiluminescent detection of produced hydrogen peroxide by luminol. The oxidative burst response was studied with and without further addition of PMA as a stimulating agent for the burst, respectively. Regarding to the no further stimulation (no addition of PMA), all samples induced the oxidative burst response at the concentrations that correspond to 100 µg/mL ß-glucan (Fig. 6A). The induced oxidative burst was statistically confirmed to be significant in comparison with the non-treated (NT) controls (for G2 $P < 0.00026$, for G3 $P < 0.00619$ and for G4 $P < 0.00231$). Moreover, G2 induced the statistically significant oxidative burst also at the concentration that corresponds to 10 µg/mL ß-glucan ($P < 0.00452$). At this lower concentration, the samples G3 and G4 did not cause statistically significant oxidative burst compared to NT controls. However, the oxidative burst of G3 and G4 is in absolute values comparable with those of G2.

The oxidative burst response at concentration 10 µg/mL ß-glucan is measurable but not significant compared to NT cells and there is a potential for further stronger stimulation. Therefore, the assay was done again using further PMA addition (Fig. 6B), while only samples at the concentration 10 µg/mL ß-glucan showed a strong response to PMA. The samples stimulated with G2, G3 and G4 at the concentration 100 µg/mL ß-glucan showed no further burst increase, suggesting that the polymorphonuclears already reached their maximum response only by ß-glucan stimulation. This observation could be helpful in future determination of an ideal therapeutic concentration of the polymers.

Anyway, β-glucan-*graft*-polyoxazolines (G2 – G4) displayed the slightly higher oxidative burst than the non-grafted β-glucan considering the same amount of β-glucan. Moreover, G4 (the longest grafts) showed the highest oxidative burst (Fig. 6), however, these differences were observed only in absolute values but they were not statistically significant. Therefore, it can be said that the graft length did not influence significantly the caused oxidative burst by polymer considering the same amount of β-glucan. Thus, *in vitro* study demonstrated that the immunostimulatory properties of β-glucan-*graft*-polyoxazolines, firstly intended for immunoradiotherapy, but also usable in a wide range of

biomedical applications, are not significantly influenced by the graft length of POX chains considering the same amount of β-glucan. In other words, the grafting of β-glucan by POX could cause a steric hindrance of active β-glucan moieties, and thus it could have an influence on the final polymer immunostimulatory properties, which are crucial for the treatment success. However, this phenomenon was not observed. Therefore, for the intended application the final graft length can be chosen only considering the polymer thermoresponsive properties independently of their ability to stimulate the immune system.

4. Conclusion

We have successfully synthesized β-glucan-*graft*-poly(2-isopropyl-2-oxazoline-*co*-2-butyl-2-oxazoline)s differing in the polyoxazoline graft length (500–5000 Da, maximum achievable grafting density) using β-glucan extracted from *Auricularia auricula-judae* by a one-pot, two-step synthesis. Such polymers are biodegradable, thermoresponsive and can be easily chemically functionalized due to the presence of allyl group at the graft ends. The thermoresponsive properties of the prepared polymers were studied in the context of graft length, denoting an easy adjustment of the solution behaviour by the graft length variation. Moreover, all samples show nontoxicity *in vitro*. The assay of oxidative burst of the polymorphonuclears established that the polymer immunostimulatory properties are not significantly influenced by their graft length, considering the same amount of β-glucan. Therefore, the required immunostimulatory properties are not decreased by the polyoxazoline grafting of β-glucan, even they are not influenced by the graft length of the polyoxazoline chains. Thus, for the intended application the final graft length can be chosen only considering the polymer thermoresponsive properties independently of their ability to stimulate the immune system. This result is very important not only for the dose design in immunoradiotherapy treatment.

Acknowledgements

Financial support from the Czech Science Foundation (grants # 16-02870S (P. Š., L. L.) and 16-03156S (M. H.)); the Ministry of Health of the Czech Republic (grant # 15-25781a) and the Ministry of Education, Youth and Sports (grant # 7AMB16FR042) is gratefully appreciated. The authors also acknowledge the Charles University in Prague for the opportunity of doctoral studies for L. Loukotová. The authors thank to Dr. Jana Kredatusová for the differential scanning calorimetry measurements.

References

[1] M. Lu, B. Xie, J. Kang, F.-C. Chen, Yang, Z. Peng, Chem. Mater. 17 (2005) 402–408.
[2] C. Alvarez-Lorenzo, B. Blanco-Fernandez, A.M. Puga, A. Concheiro, Adv. Drug. Deliv. Rev. 65 (2013) 1148–1171.
[3] B.C. Lehtovaara, M.S. Verma, F.X. Gu, J. Bioact. Compat. Polym. 27 (2012) 3–17.
[4] X. Li, K. Nan, L. Li, Z. Zhang, H. Chen, Carbohydr. Polym. 88 (2012) 84–90.
[5] H.Y. Shi, L.M. Zhang, Carbohydr. Polym. 67 (2007) 337–342.
[6] A. Pospisilova, S.K. Filippov, A. Bogomolova, S. Turner, O. Sedlacek, N. Matushkin, Z. Cernochova, P. Stepanek, M. Hruby, RSC Adv. 4 (2014) 61580–61588.
[7] X. Meng, H. Liang, L. Luo, Carbohydr. Res. 424 (2016) 30–41.
[8] K. Ina, T. Kataoka, T. Ando, Anti-Cancer Agents Med. Chem. 13 (2013) 681–688.
[9] S. Xu, X. Xu, L. Zhang, J. Agric. Food Chem. 60 (2012) 3498–3506.
[10] L. Loukotova, J. Kucka, M. Rabyk, A. Hocherl, K. Venclikova, O. Janouskova, P. Paral, V. Kolarova, T. Heizer, L. Sef, P. Stepanek, M. Hruby, J. Controlled, Release 268 (2017) 78–91.
[11] Y. Seo, A. Schulz, Y. Han, Z. He, H. Bludau, X. Wan, J. Tong, T.K. Bronich, M. Sokolsky, R. Luxenhofer, R. Jordan, A.V. Kabanov, Polym. Adv. Technol. 26 (2015) 837–850.
[12] M. Hruby, S.K. Fillippov, J. Panek, M. Novakova, H. Mackova, J. Kucka, D. Vetvicka, K. Ulbrich, Macromol. Biosci. 10 (2010) 916–924.
[13] R. Obeid, T. Fumihiko, F.M. Winnik, Macromolecules 42 (2009) 5818–5828.
[14] R. Konefal, J. Spevacek, E. Jager, S. Petrova, Colloid Polym. Sci. 294 (2016) 1717–1726.
[15] M. Rusu, S. Wohlrab, D. Kuckling, H. Mohwald, M. Schonhoff, Macromolecules 39 (2006) 7358–7363.
[16] V.E.C. Ooi, F. Liu, Curr. Med. Chem. 7 (2000) 715–729.

Appendix 2

Loukotová, L.; Kučka, J.; Rabyk, M.; Höcherl, A.; Venclíková, K.; Janoušková, O.; Páral, P.; Kolářová, V.; Heizer, T.; Šefc, L.; Štěpánek, P.; Hrubý, M. Thermoresponsive β-glucan-based polymers for bimodal immunoradiotherapy–Are they able to promote the immune system? *J. Control. Release* **268**, 78 – 91 (2017). IF = 7.877.

Journal of Controlled Release 268 (2017) 78–91

Contents lists available at ScienceDirect

Journal of Controlled Release

journal homepage: www.elsevier.com/locate/jconrel

Thermoresponsive β-glucan-based polymers for bimodal immunoradiotherapy – Are they able to promote the immune system?

Lenka Loukotová[a], Jan Kučka[a], Mariia Rabyk[a], Anita Höcherl[a], Kristýna Venclíková[a], Olga Janoušková[a], Petr Páral[b,c], Věra Kolářová[b], Tomáš Heizer[c], Luděk Šefc[b], Petr Štěpánek[a], Martin Hrubý[a,*]

[a] Institute of Macromolecular Chemistry AS CR, v. v. i., Heyrovsky sq. 2, Prague 162 06, Czech Republic
[b] Charles University in Prague, First Faculty of Medicine, Center for Advanced Preclinical Imaging, Salmovska 3, Prague 120 00, Czech Republic
[c] Charles University in Prague, First Faculty of Medicine, Institute of Pathological Physiology, U Nemocnice 5, Prague 128 53, Czech Republic

ARTICLE INFO

Keywords:
β-glucan
Polyoxazoline
Multimodal cancer therapy
Immunotherapy
Radiotherapy

ABSTRACT

A conceptually new bimodal immunoradiotherapy treatment was demonstrated using thermoresponsive polymer β-glucan-*graft*-poly(2-isopropyl-2-oxazoline-*co*-2-butyl-2-oxazoline) bearing complexes of 1,4,7,10-tetraazacyclododecane-1,4,7,10-tetraacetic acid with yttrium-90(III) at the graft ends. The behavior of this thermoresponsive polymer in aqueous solutions was studied, and it showed the appropriate cloud point temperature for brachytherapy applications. The polymer was tested *in vitro*, and it exhibited nontoxicity and active uptake into cancer cells and macrophages with colocalization in the lysosomes and macrophagosomes. Moreover, the observed oxidative burst response of the leukocytes established the immunostimulatory properties of the polymer, which were also studied *in vivo* after injection into the thigh muscles of healthy mice. The subsequent histological evaluation revealed the extensive immune activation reactions at the site of injection. Furthermore, the production of tumor necrosis factor α induced by the prepared polymer was observed *in vitro*, denoting the optimistic prognosis of the treatment. The biodistribution study *in vivo* indicated the formation of the polymer depot, which was gradually degraded and excluded from the body. The radiolabeled polymer was used during *in vivo* antitumor efficiency experiments on mice with EL4 lymphoma. The immunoradiotherapy group (treated with the radiolabeled polymer) demonstrated the complete inhibition of tumor growth during the beginning of the treatment. Moreover, 7 of the 15 mice were completely cured in this group, while the others exhibited significantly prolonged survival time compared to the control group. The *in vivo* experiments indicated the considerable synergistic effect of using immunoradiotherapy compared to separately using immunotherapy or radiotherapy.

1. Introduction

Cancer immunotherapy has recently gained increasing interest because it has great potential for systemic eradicating tumors and metastases exploiting the body's own immune system. The advantages of a such treatment include fewer and less severe side effects compared to other types of treatment [1]. So far, cancer immunotherapy has exhibited a limited therapeutic efficiency; the immune response is, except for a few cases, weak and short-lived because cancer in its advanced stages has tools to avoid the immune reactions [2]. In other words, the immune cells could theoretically recognize and eliminate the cancer cells but the tumor produces a wide range of immunosuppressive factors (*e.g.*, prostaglandin E2 and inhibitory cytokines) [3], and thus, in the tumor microenvironment, the immune cells have very limited efficiency [4]. One of the promising approaches in immunotherapy is the targeting tumor cells *via* monoclonal antibodies, which is well-tolerated treatment modality for many tumor patients but the clinical trials revealed quite disappointing results, mainly due to their low efficiency [5]. To improve the efficiency, the bispecific antibodies (BiAbs) targeting both cancer and T cells were designed, combining the specificities of two antibodies into a one molecule [6]. This approach allowed them to redirect and stimulate T-cells against antigen expressing tumor cells, in contrast with the conventional antibodies, which are not able to do that because T cells lack Fc receptors [7]. Several examples using these types of BiAbs have been reported, however, more clinical trials, which would show the therapy efficiency, are needed. Moreover, the

* Corresponding author.
E-mail address: mhruby@centrum.cz (M. Hrubý).

http://dx.doi.org/10.1016/j.jconrel.2017.10.010
Received 16 July 2017; Received in revised form 9 October 2017; Accepted 10 October 2017
Available online 12 October 2017

disadvantage of BiAbs is their significantly challenging production and very strict storage conditions [7]. Anyway, a special role in the immune system is played by Toll-like receptors (TLRs), and the harnessing of the immune cells *via* TLRs could be another promising approach in immunotherapy [8].

In traditional Chinese medicine, mushroom extracts are used as a medicinal agent for cancer treatment. The most efficient extract components are immunostimulatory polysaccharides, especially β-glucans [9]. All β-glucans are composed of glucose units linked together by 1 → 3 β-glycosidic bonds, and they vary in their branching structure and chain length [10]. Many of them show anticancer and immunomodulatory activities [11]. Previous *in vitro* studies have demonstrated that β-glucans trigger immune cells *via* receptors TLR-2/6 and Dectin-I [12]. Moreover, in Japan, licensed β-glucans extracted from *Lentinula edodes* (lentinan) already exist as effective drugs in gastric cancer therapy, usually used in combination with fluoropyrimidines [13]. Interestingly, β-glucan administered intratumorally is more anticancer efficient probably due to its close contact to tumor cells resulting in local immune responses and the nonspecific killing of tumor cells [14]. However, the therapeutic efficiency of β-glucan still needs to be improved.

Brachytherapy is a commonly used method for the treatment of solid tumors. Unlike standard radiation therapy, it allows using much higher radiation doses because the drug is delivered only to the tumor site; therefore, the whole-body radiation exposure is minimized [15]. Previous studies have shown that thermoresponsive polymers are advantageous carriers of radiation emitter due to their behavior in aqueous solutions [16]. Such polymers are soluble in aqueous solutions at lower temperatures, while they precipitate at higher temperatures (*i.e.*, above the cloud point temperature – CPT). Our previous *in vivo* study proved that the depots formed after the polymer solution injection (polymers based on poly(*N*-isopropyl acrylamide)), exhibiting a CPT of approximately 33 °C, remained at the site of application for > 10 days [17], and thus, these polymers are appropriate for brachytherapy applications instead of that time used implants, which must be surgically embedded and also removed after the radionuclide decay. Highly defined polymers with analogous tunable thermoresponsive properties are poly(2-alkyl-2-oxazoline)s (POXs). They have attracted attention due to their biocompatibility, bioinspired polypeptide-like structure and tunable polymer properties [18]. Moreover, POXs are relatively radioresistant; therefore, they are suitable for use in delivery systems that experience radiation exposure [19]. The weak point of brachytherapy is its inability to kill metastases. Thus, the development of multimodal treatments is necessary.

We designed a conceptually new bimodal immunoradiotherapy treatment using the thermoresponsive immunostimulatory radiolabeled polymer. The principle of the treatment is as follows: radiation kills the tumor cells, and after the radionuclide decays, the immunomodulator enhances an immune response against the tumor cell debris and metastases. Such treatment exhibits following advantages: non-surgical drug administration by the polymer solution injection, the local radiation therapy with minimal radiation exposure to the rest of the body and the enhanced local immunotherapy with harnessing T cells against cancer cells and metastases. Moreover, the polymer is degradable in the body because the glycosidases convert it into metabolites that are smaller than the renal threshold (~45 kDa [20]) and are thus excludable by kidneys. As an immunoradiotherapeutic, the novel β-glucan-*graft*-poly(2-isopropyl-2-oxazoline-*co*-2-butyl-2-oxazoline) polymer bearing complexes of 1,4,7,10-tetraazacyclododecane-1,4,7,10-tetraacetic acid (DOTA) and yttrium-90(III) at the graft ends ($M_{n,graft}$ = 2500 Da, with a maximum achievable graft density) was synthesized using β-glucan extracted from the bodies of *Auricularia auricula-judae*. The thermoresponsive polymer behavior in aqueous solutions was studied, and its biological properties (cytotoxicity, oxidative burst response of the leukocytes, production of tumor necrosis factor α, cellular uptake) were tested *in vitro*. The polymer biodistribution and anticancer efficiency experiment, which indicates the effectiveness of the immunoradiotherapy, were studied *in vivo* using mice with EL4 tumors. Moreover, to study the effect of the immunoradiotherapy in comparison with using only radiotherapy, a polymer that was analogous to the grafts was prepared and used in the same *in vivo* anticancer efficiency experiment. The excellent synergy of the immunoradiotherapy was demonstrated, curing ~50% of the mice in the immunoradiotherapy group without any significant side effects.

2. Materials and methods

2.1. Materials

2-Butyl-2-oxazoline and 2-isopropyl-2-oxazoline were synthesized according to ref. [21]. β-Glucan was extracted from bodies of *Auricularia auricula-judae* as described in ref. [22]. Diethyl ether, dimethyl sulfoxide, sodium chloride and toluene were purchased from Lachner Ltd. (Neratovice, Czech Republic). 1,4,7,10-Tetraazacyclododecane-1,4,7,10-tetraacetic acid mono-*N*-hydroxysuccinimide ester (DOTA-NHS-ester) was purchased from Macrocyclics, Inc. (Plano, USA). Dyomics-615-NHS-ester was purchased from Dyomics GmbH (Jena, Germany). 2,4,6-Trinitrobenzene 1-sulfonic acid (TNBSA) solution was purchased from Thermo Fisher Scientific (Prague, Czech Republic). Dialysis membranes Spectra/Por (molecular weight cut-off (MWCO) 6–8 kDa) were purchased from P-LAB (Prague, Czech Republic). All other chemicals were purchased from Sigma Aldrich Ltd. (Prague, Czech Republic). The chemicals were used without further purification unless stated otherwise.

2.2. Synthesis and preparation

2.2.1. Preparation of β-glucan-graft-poly(2-isopropyl-2-oxazoline-co-2-butyl-2-oxazoline) with a theoretical molecular weight of POX grafts $M_{n,graft}$ = 2500 Da (G-I and POX-I)

Allyl bromide (96 μL, 1.12 mmol) was added to a solution of 2-isopropyl-2-oxazoline (2.000 mL, 16.8 mmol) and 2-butyl-2-oxazoline (0.734 mL, 5.6 mmol) in 4 mL of anhydrous acetonitrile, and the reaction mixture was stirred overnight at 70 °C under an argon atmosphere (POX solution). β-Glucan (0.20 g, $M_w = 2.5 \cdot 10^6$ Da, I = 1.85) was dissolved in 12 mL of anhydrous dimethyl sulfoxide, and this solution was then azeotropically dried using anhydrous toluene. Thereafter, sodium hydride (0.30 g of a 60% dispersion in mineral oil, 4.5 mmol) was added to the β-glucan solution, and the mixture was stirred for 3 h at 70 °C. One half of a POX solution was mixed with the β-glucanate solution, and the resulting mixture was stirred overnight at 70 °C. Water (10 mL) was added to the reaction mixture, and it was twice washed with diethyl ether to remove the mineral oil. The aqueous layer was dialyzed (MWCO 6–8 kDa) against water for 72 h and freeze-dried to give the desired product marked as G-I (315.1 mg).

The second half of the POX mixture was mixed with water (0.5 mL), purified on a Sephadex® LH-20 column using methanol as the mobile phase and evaporated to give polymer POX-I (1.32 g).

^{1}H NMR of POX-I (300 MHz, CD_3CN), δ (ppm): 0.88 ($-CH_2-CH_2-CH_2-\mathbf{CH_3}$), 1.02 ($-CH-(\mathbf{CH_3})_2$), 1.30 ($-CH_2-CH_2-\mathbf{CH_2}-CH_3$), 1.50 ($-CH_2-\mathbf{CH_2}-CH_2-CH_3$), 2.31 ($-\mathbf{CH_2}-CH_2-CH_2-CH_3$), 2.68 ($-\mathbf{CH}-(CH_3)_2$), 3.39 ($-N-\mathbf{CH_2}-CH_2-$). Size-exclusion chromatography (SEC) of POX-I: M_n = 2290 Da, I = 1.19.

^{1}H NMR of G-I (300 MHz, D_2O), δ (ppm): 0.89 (POX: $-CH_2-CH_2-CH_2-\mathbf{CH_3}$), 1.06 (POX: $-CH-(\mathbf{CH_3})_2$), 1.31 (POX: $-CH_2-CH_2-\mathbf{CH_2}-CH_3$), 1.51 (POX: $-CH_2-\mathbf{CH_2}-CH_2-CH_3$), 2.36 ($-\mathbf{CH_2}-CH_2-CH_2-CH_3$), 2.7–2.9 ($-\mathbf{CH}-(CH_3)_2$), 3.3–5.2 (POX: $-N-\mathbf{CH_2}-CH_2-$, glucose). ^{13}C NMR of G-I (75 MHz, D_2O, 4,4-dimethyl-4-silapentane-1-sulfonic acid (DSS) as standard), δ (ppm): 16, 21, 25, 29, 33, 35, 45, 46, 49, 68, 69, 72, 76, 78, 81, 106, 179, 183. Elemental analysis of G-I: C 52.50%, H 8.32%, N 6.91%. IR of G-I (KBr): 3365 (ν_{O-H}), 2965 (ν_{C-H}), 2933 (ν_{C-H}), 2871 (ν_{C-H}), 1631 ($\nu_{C=O}$),

1472, 1423, 1380, 1362, 1236, 1200, 1158, 1085, 1037. SEC of G-I: $M_w = 7.5 \cdot 10^6$ Da, $I = 1.49$.

2.2.2. Cysteamine incorporation on the graft ends of G-I (G-II)

G-I (250 mg, 0.22 mmol/g of allyl groups) was dissolved in water (17 mL) containing cysteamine (250 mg, 3.25 mmol) and hydrochloric acid (36%, 265 μL, 3.25 mmol). The solution of 2-hydroxy-2-methylpropiophenone (50 μL dissolved in 150 μL of ethanol) was added, and the reaction mixture was cooled to 0 °C and irradiated using a UV lamp (TESLA RVK 6 × 125 W) for 60 min. The solution of sodium carbonate (10%, 17 mL) was added, and the aqueous layer was washed with diethyl ether, dialyzed (MWCO 6–8 kDa) against water for 48 h and freeze-dried to give the product G-II (172 mg). The content of the $-NH_2$ groups was determined using a TNBSA assay according to ref. [23] (0.17 mmol/g of $-NH_2$ groups).

^{1}H NMR of G-II (600 MHz, DMSO), δ (ppm): 0.84 (POX: $-CH_2-CH_2-CH_2-C\mathbf{H_3}$), 0.96 (POX: $-CH-(C\mathbf{H_3})_2$), 1.25 (POX: $-CH_2-CH_2-C\mathbf{H_2}-CH_3$), 1.43 (POX: $-CH_2-C\mathbf{H_2}-CH_2-CH_3$), 2.29 ($-C\mathbf{H_2}-CH_2-CH_2-CH_3$), 2.66 ($-S-CH_2-C\mathbf{H_2}-NH_2$), 2.8–3.1 (POX: $-C\mathbf{H}-(CH_3)_2$, $-S-C\mathbf{H_2}-CH_2-NH_2$), 3.3–5.2 (POX: $-N-C\mathbf{H_2}-CH_2-$, glucose). ^{13}C NMR of G-II (150 MHz, DMSO), δ (ppm): 14, 20, 22, 25, 27, 29, 31, 43, 45, 46, 66, 70, 73, 76, 104, 173, 176. Elemental analysis of G-II: C 53.20%, H 8.35%, N 6.57%, S 0.87%. IR of G-II (KBr): 3345 (ν_{O-H}), 2964 (ν_{C-H}), 2930 (ν_{C-H}), 2871 (ν_{C-H}), 1630 ($\nu_{C=O}$), 1472, 1422, 1382, 1362, 1239, 1201, 1158, 1037. SEC of G-II: $M_w = 6.7 \cdot 10^6$ Da, $I = 1.45$.

2.2.3. Conjugation of Dyomics-615 and DOTA with the amino groups of G-II (G-III)

The G-II sample (150 mg, 0.026 mmol of $-NH_2$ groups), $Na_2HPO_4 \cdot 12\ H_2O$ (0.707 g, 1.98 mmol) and KH_2PO_4 (45 mg, 0.33 mmol) were dissolved in water (11 mL), and the solution was cooled to 0 °C. Dyomics-615-NHS-ester was added (0.75 mg, 0.0011 mmol), and the mixture was stirred for 1 h at 0 °C. Thereafter, DOTA-NHS-ester (32 mg, 0.050 mmol) was added, and the reaction mixture was stirred overnight at room temperature. The crude product was twice purified on a Sephadex® G-25 column using ice water as the mobile phase and freeze-dried to give product G-III (132 mg).

^{1}H NMR of G-III (600 MHz, DMSO), δ (ppm): 0.79 (POX: $-CH_2-CH_2-CH_2-C\mathbf{H_3}$), 0.90 (POX: $-CH-(C\mathbf{H_3})_2$), 1.19 (POX: $-CH_2-CH_2-C\mathbf{H_2}-CH_3$), 1.37 (POX: $-CH_2-C\mathbf{H_2}-CH_2-CH_3$), 2.23 ($-C\mathbf{H_2}-CH_2-CH_2-CH_3$), 2.53 ($-S-CH_2-C\mathbf{H_2}-NH-$), 2.7–3.3 (POX: $-C\mathbf{H}-(CH_3)_2$, $-S-C\mathbf{H_2}-CH_2-NH-$), 3.4–5.2 (POX: $-N-C\mathbf{H_2}-CH_2-$, glucose). ^{13}C NMR of G-III (150 MHz, DMSO), δ (ppm): 14, 20, 22, 27, 29, 31, 43, 45, 46, 60, 66, 70, 73, 76, 103, 173, 177. IR of G-III (KBr): 3287 (ν_{O-H}), 2966 (ν_{C-H}), 2932 (ν_{C-H}), 2871 (ν_{C-H}), 1630 ($\nu_{C=O}$), 1474, 1419, 1381, 1362, 1240, 1200, 1156, 1037, 978. SEC of G-III: $M_w = 8.8 \cdot 10^6$ Da, $I = 1.38$.

The content of Dyomics-615 was determined spectrophotometrically to be 0.1 wt% ($\lambda_{absorption} = 621$ nm and $\varepsilon = 200{,}000$ L/mol·cm). To determine the content of the DOTA moieties, the product G-III was chelated with Gd(III) according to the following procedure: product G-III (12 mg), ammonium acetate (40 mg, 0.52 mmol) and gadolinium(III) chloride hexahydrate (8 mg, 0.52 mmol) were dissolved in water (1 mL), and the reaction mixture was stirred overnight at room temperature. The crude product was twice purified on a Sephadex® G-25 column using ice water as the mobile phase and freeze-dried to obtain G-III-Gd (10 mg). The content of Gd(III) was determined to be 1.72% using energy-dispersive X-ray spectroscopy (EDS), meaning that the DOTA content in the polymer G-III was 0.11 mmol/g.

2.2.4. Modification of POX-I (POX-II and POX-III)

The POX-I polymer (0.50 g) was dissolved in water (10 mL) with cysteamine (0.50 g, 6.5 mmol) and hydrochloric acid (36%, 530 μL, 6.5 mmol). The solution of 2-hydroxy-2-methylpropiophenone (100 μL dissolved in 300 μL of ethanol) was added, and the reaction mixture was cooled to 0 °C and irradiated with a UV lamp (TESLA RVK 6 × 125 W) for 15 min. The solution of sodium carbonate (10%, 34 mL) was added, and the aqueous layer was washed with diethyl ether and freeze-dried. The crude product was purified on a Sephadex® LH-20 column using methanol as the mobile phase and evaporated to give the product POX-II (330 mg).

The content of the $-NH_2$ groups was determined using a TNBSA assay [23] (0.08 mmol/g of $-NH_2$ groups).

^{1}H NMR of POX-II (600 MHz, CH_3OD), δ (ppm): 0.92 ($-CH_2-CH_2-CH_2-C\mathbf{H_3}$), 1.08 ($-CH-(C\mathbf{H_3})_2$), 1.34 ($-CH_2-CH_2-C\mathbf{H_2}-CH_3$), 1.55 ($-CH_2-C\mathbf{H_2}-CH_2-CH_3$), 2.40 ($-C\mathbf{H_2}-CH_2-CH_2-CH_3$), 2.7–3.1 ($-C\mathbf{H}-(CH_3)_2$, $-S-C\mathbf{H_2}-CH_2-NH_2$, $-S-CH_2-C\mathbf{H_2}-NH_2$), 3.51 ($-N-C\mathbf{H_2}-CH_2-$).

Polymer POX-II (100 mg, 0.006 mmol of $-NH_2$ groups), $Na_2HPO_4 \cdot 12\ H_2O$ (1.081 g, 3.03 mmol) and KH_2PO_4 (67 mg, 0.49 mmol) were dissolved in water (5 mL), and the solution was cooled to 0 °C. DOTA-NHS-ester (35 mg, 0.055 mmol) was added, and the reaction mixture was stirred overnight. The crude product was twice purified on a Sephadex® LH-20 column using methanol as the mobile phase, followed by solvent evaporation to obtain product POX-III (91 mg).

^{1}H NMR of POX-III (600 MHz, CH_3OD), δ (ppm): 0.87 ($-CH_2-CH_2-CH_2-C\mathbf{H_3}$), 1.03 ($-CH-(C\mathbf{H_3})_2$), 1.31 ($-CH_2-CH_2-C\mathbf{H_2}-CH_3$), 1.51 ($-CH_2-C\mathbf{H_2}-CH_2-CH_3$), 2.37 ($-C\mathbf{H_2}-CH_2-CH_2-CH_3$), 2.7–3.1 ($-C\mathbf{H}-(CH_3)_2$, $-S-C\mathbf{H_2}-CH_2-NH-$, $-S-CH_2-C\mathbf{H_2}-NH-$), 3.46 ($-N-C\mathbf{H_2}-CH_2-$). ^{13}C NMR of POX-III (600 MHz, CH_3OD), δ (ppm): 14, 20, 23, 28, 31, 33, 44, 45, 47, 176, 179, 180. SEC of POX-III: $M_n = 2330$ Da, $I = 1.16$.

To determine the DOTA content, POX-III was chelated with Gd(III) according to the procedure as described above in the Section 2.2.3. *Conjugation of Dyomics-615 and DOTA with amino groups of G-II (G-III)*. The DOTA content in polymer POX-III was found to be 0.07 mmol/g.

2.2.5. Preparation of the β-glucan conjugate with Dyomics-615 (B-III)

β-Glucan (250 mg, 1.40 mmol glucose units, $M_w = 2.5 \cdot 10^6$ Da, $I = 1.85$) and sodium hydroxide (125 mg, 3.13 mmol) were dissolved in water (20 mL), and the mixture was cooled to 0 °C. Allyl bromide (80 μL, 0.924 mmol) was added, and it was stirred for 10 h at 0 °C, followed by stirring overnight at room temperature. Acetic acid (458 μL, 8.00 mmol) was added, and the solution was dialyzed (MWCO 6–8 kDa) against water for 48 h and freeze-dried to give product B-I (230 mg).

^{1}H NMR of B-I (600 MHz, D_2O), δ (ppm): 3.10–4.80 (glucose), 5.23 (glucose), 5.51 ($-CH=C\mathbf{H_2}$), 5.93 ($-C\mathbf{H}=CH_2$).

The degree of functionalization (f, number of allyl moieties per D-glucose unit) was calculated from the ^{1}H NMR spectrum according to the following equation: $f = I_{\delta\ =\ 5.93\ ppm}/I_{\delta\ =\ 5.23\ ppm}$, where $I_{\delta\ =\ 5.93\ ppm}$ is the peak integral belonging to the $-C\mathbf{H}=CH_2$ at $\delta = 5.93$ ppm and $I_{\delta\ =\ 5.23\ ppm}$ is the peak integral belonging to the acetal hydrogen on position 1 of the D-glucose unit at $\delta = 5.23$ ppm. Here, f is 0.27, meaning that polymer B-I contains, on average, 0.27 allyl moieties per D-glucose unit.

Polymer B-I (200 mg) was dissolved in water (20 mL) containing cysteamine (250 mg, 3.25 mmol) and hydrochloric acid (36%, 265 μL, 3.25 mmol). The solution of 2-hydroxy-2-methylpropiophenone (50 μL dissolved in 150 μL of ethanol) was added, and the reaction mixture was cooled to 0 °C and irradiated using a UV lamp (TESLA RVK 6 × 125 W) for 60 min. The solution of sodium carbonate (10%, 15 mL) was added, and then the aqueous layer was washed with diethyl ether, dialyzed (MWCO 6–8 kDa) against water for 48 h and freeze-dried. The dried product was purified on a Sephadex® G-25 column using water as the mobile phase and freeze-dried to give the product B-II (140 mg).

The content of the $-NH_2$ groups was determined using a TNBSA assay [23] (0.33 mmol/g of $-NH_2$ groups).

^{1}H NMR of B-II (600 MHz, D_2O), δ (ppm): 2.64

(−S−CH_2−$\mathbf{CH_2}$−NH_2), 2.93 (−S−$\mathbf{CH_2}$−CH_2−NH_2), 3.10–4.80 (glucose), 5.23 (glucose).

Polymer B-II (100 mg, 0.033 mmol of –NH_2 groups), $Na_2HPO_4 \cdot 12\ H_2O$ (0.470 g, 1.31 mmol) and KH_2PO_4 (30 mg, 0.22 mmol) were dissolved in water (15 mL) and the solution was cooled to 0 °C. Dyomics-615-NHS-ester was added (1 mg, 0.0015 mmol) and the mixture was stirred overnight at room temperature. The crude product was twice purified on a Sephadex® G-25 column using water the mobile phase and freeze-dried to give product B-III (88 mg). The amount of Dyomics-615 was determined spectrophotometrically (0.05 wt%, $\lambda_{absorption}$ = 621 nm, ε = 200,000 L/mol·cm).

^{1}H NMR of B-III (600 MHz, D_2O), δ (ppm): 2.57 (−S−CH_2−$\mathbf{CH_2}$−NH−), 2.91 (−S−$\mathbf{CH_2}$−CH_2−NH−) 3.30–4.80 (glucose), 5.23 (glucose). ^{13}C NMR of B-III (600 MHz, D_2O, DSS), δ (ppm): 63, 68, 72 75, 76, 78, 80, 106. SEC of B-III: $M_w = 2.6 \cdot 10^6$ Da, I = 1.70.

2.3. Characterization

The ^{1}H NMR and ^{13}C NMR measurements were carried out on a Bruker Avance DPX-300 spectrometer and on a Bruker Avance III 600 spectrometer (both Bruker Co., Austria). Fourier transform infrared (FT-IR) spectra were obtained on a Perkin-Elmer Paragon 1000PC spectrometer (Perkin-Elmer Co., USA) equipped with the Specac MKII Golden Gate single attenuated total reflection (ATR) system (Perkin-Elmer Co., USA). The elemental analysis was performed on a Perkin-Elmer Series II CHNS/O Analyzer 2400 (PE Systems Ltd., Czech Republic) instrument.

The molecular weight of the POXs was determined using SEC; the system contained a Deltachrom SDS030 pump (Watrex Co., Prague, Czech Republic), a MIDAS autosampler (Spark HOLLAND B.V., Netherlands), two columns (PL gel MIXED-B-LS, 10 μm) and an ELS-1000 evaporative light-scattering detector (Polymer Laboratories, USA). *N*,*N*-Dimethylformamide was used as the mobile phase, and commercial alkyne terminated poly(2-ethyl-2-oxazoline)s were used as the calibration standards. The molecular weight of the prepared β-glucan-based polymers was determined using the same SEC system with dual detection: an Optilab t-rEX refractive index detector and DAWN Heleos II multiangle light-scattering detectors (MALSs) (both from Wyatt Technology Corporation, USA). Dimethyl sulfoxide was used as the mobile phase.

The polymer cloud point temperatures (CPTs) were determined in their phosphate-buffered saline (PBS) solutions at a polymer concentration c = 1 mg/mL using a dynamic light scattering (DLS) technique. The temperature dependence of the polymer hydrodynamic radius (R_h) was measure from 5 to 65 °C with a heating rate of 1 °C/min at a scattering angle of θ = 173° on a Zetasizer Nano-ZS, Model ZEN3600 (Malvern Instruments, UK), using DTS software (version 6.20) for data evaluation. After each heating step, three measurements were performed.

2.4. In vitro studies

2.4.1. Cell lines and cell culture

The mouse macrophages RAW 264.7 (kindly provided by Zdeňka Syrová, PhD., First Faculty of Medicine, Charles University, Prague, Czech Republic), mouse lymphoma EL4 cells (ATCC, Lomianki, Poland) and human mammary gland adenocarcinoma MCF7 cells (kindly provided by Institute of Biotechnology AS CR, Prague, Czech Republic) were cultured according to the ATCC protocol in Dulbecco's Modified Eagle's Medium (DMEM) supplemented with 10% fetal bovine serum, 100 u of penicillin and 100 μg/mL of streptomycin (all from Thermo Fisher Scientific, Prague, Czech Republic). *Staphylococcus aureus* cells (kindly provided by Karel Holada, PhD., First Faculty of Medicine, Charles University, Prague, Czech Republic) were incubated on Luria broth (LB) agar (Sigma Aldrich, Prague, Czech Republic). White blood cells were isolated from human whole blood (kindly provided by Military Hospital, Prague, Czech Republic) after the lysis of erythrocytes as follows: the whole blood (1 mL) was mixed with the Lysis solution (14 mL; 1.5 M NH_4Cl, 100 mM $NaHCO_3$, 10 mM ethylenediaminetetraacetic acid, pH = 7.3) for 4 min at room temperature (RT). The mixture was centrifuged (300 × *g*, 5 min, RT), and the pellets were washed with cold PBS (5 mL) followed by centrifugation (300 × *g*, 5 min, 2 °C). The pellets were then suspended in Roswell Park Memorial Institute (RPMI) medium (Gibco, Invitrogen, California, USA), representing the white blood cells.

2.4.2. Cytotoxicity

After overnight incubation of the RAW 264.7, EL4 and MCF7 cells on 96-well plates, the polymer G-III was added in a concentration range from 0.049 up to 100 μg/mL (3 wells for each cell line and each concentration), and the cells were incubated at 37 °C for 72 h. The cell viability was determined using an AlamarBlue Assay (ThermoScientific, Prague, Czech Republic) following manufacturer's instructions. The half maximal inhibitory concentration (IC_{50}) was calculated from the dose-response curves.

2.4.3. Microbicidal assay

A microbicidal assay was used to estimate the oxidative burst of the leukocytes upon incubation with polymers G-III and B-III. White blood cells isolated from human whole blood were seeded in a 96-well plate (50,000 cells/well). Phorbol 12-myristate 13-acetate as a positive control (PMA, c = 2 μM) and polymers G-III and B-III were added to the wells (3 wells for each sample and each concentration) at concentrations corresponding to 1 and 10 μg/mL β-glucan (c = 3.4 and 34 μg/m G-III, c = 1 and 10 μg/mL B-III). The plate was incubated for 30 min at 37 °C. The overnight culture of *Staphylococcus aureus* was added to the cells at the multiplicity of infection (MOI) of 5. The samples were further incubated for 60 min at 37 °C. The growth colonies of surviving bacteria were enumerated, and the bacterial viability was calculated from the colony counts. The untreated sample was established as a reference value. This assay was repeated three times.

2.4.4. Enzyme-linked immunosorbent assay (ELISA)

The defrozen white blood cells isolated from human whole blood were seeded in a 96-well plate (40,000 cells/well), and the prepared polymers G-III and B-III were added to the wells (2 wells for each sample and each concentration) at concentrations corresponding to 1 and 10 μg/mL β-glucan (c = 3.4 and 34 μg/mL G-III, c = 1 and 10 μg/mL B-III). PMA (c = 2 μM) was used as a control. The plate was incubated for 2 h at 37 °C. Lipopolysaccharide (LPS) derived from *Escherichia coli* 026:B6 (eBioscience, ThermoFisher, Prague, Czech Republic) was added to all wells (c = 1 μg/mL), and the plate was further incubated for 16 h at 37 °C. Tumor necrosis factor-α (TNF-α) was detected using an ELISA (Invitrogen, California, USA) assay, which was performed according to the manufacturer's instructions. The TNF-α concentration in the samples was calculated by extrapoling to the standard curve plotted from the dilution of the TNF-α standard. The statistical analysis of the data was conducted using Origin® 9 software (OriginLab Corporation, MA, USA). The variance analysis (ANOVA) calculations were performed at the significance level of a = 0.05.

2.4.5. Cellular uptake measured using flow cytometry

MCF7 cells were seeded in 24-well plates (7000 cells/cm^2) in triplicates and left to attach overnight. The conjugates G-III and B-III were added to the cells at concentrations corresponding to 50 μg/mL β-glucan (c = 167 μg/mL G-III, c = 50 μg/mL B-III) and incubated with the cells for 0.25, 4, 24 and 48 h in a volume of 1 mL. The cells were then detached and suspended in 0.5% bovine serum albumin for analysis in a BD FACSverse™ flow cytometer (BD Biosciences, San Jose, USA). The fluorescence of the Dyomics-615 ($\lambda_{emission}$ = 641 nm) was detected in the APC channel and a minimum of 10,000 cells was measured.

2.4.6. Cellular uptake studied using microscopy

The MCF7 (12,000 cells/cm^2) and RAW (33,000 cells/cm^2) cells were seeded at the bottom of a polylactide-coated 4-chamber glass dish and left to adhere overnight. For the time-dependent uptake study, the cells were incubated with the conjugates G-III and B-III at a concentration corresponding to 150 μg/mL β-glucan (c = 500 μg/mL G-III, c = 150 μg/mL B-III) for 0.25 h and at a concentration corresponding to 50 μg/mL β-glucan (c = 167 μg/mL G-III, c = 50 μg/mL B-III) for 4 and 24 h. The cells were then washed and cooled on ice, stained briefly with Hoechst 33342 and CellMask™ Green (both purchased from Molecular Probes, Eugene, USA) at 4 × of the recommended working concentration (see the manufacturer's protocol) and fixed in 3% formaldehyde solution. The cells were imaged using an Olympus FV 10 confocal laser scanning microscope (Olympus Czech Group, s.r.o, Prague, Czech Republic) using a 60 × oil objective. The signal detection was observed in channels Ch1 (Hoechst 33342, exc. 405 nm, em. 450/50 nm), Ch2 (CellMask™ Green, exc. 488 nm, em. 550/100 nm), and Ch3 (Dyomics-615, exc. 635 nm, em. 700/100 nm).

For lysosome colocalization visualization, RAW cells were incubated for 4 h with conjugate G-III at a concentration corresponding to 50 μg/mL β-glucan (c = 167 μg/mL G-III). The cells were then incubated for 10 min with 1 μM Lyso Sensor Blue/Yellow (purchased from Molecular Probes, Eugene, USA). During the last 2 min of incubation, Hoechst 33342 and CellMask™ Green were added. The RAW cells were visualized rapidly without fixation. Two separate scans, for the lysomarker (Lyso Sensor Blue/Yellow, exc. 458 nm, em. 630/100 nm) and for the other dyes (see above, Ch1-Ch3), were conducted.

To investigate the energy-dependence of the internalization process, the RAW cells were deprived of energy by incubation at low temperature. The cells were preincubated for 20 min at 4 °C prior to the addition of G-III at a concentration corresponding to 50 μg/mL β-glucan (c = 167 μg/mL G-III) and incubated for 45 min at 4 °C. The cells were then stained, fixated and visualized as described above.

2.5. Radiolabeling and radiostability

2.5.1. Radiolabeling of G-III and POX-III with $^{90}YCl_3$ (G-III-Y and POX-III-Y)

The polymer G-III (45 mg) was dissolved in 0.5 M ammonium acetate (1 mL) and yttrium-90(III) chloride solution (7.5 μL in 0.05 M hydrochloric acid, A = 207 MBq, M.G.P. spol. s r.o., Zlin, Czech Republic) was added. The reaction mixture was incubated for 2 h under continuous shaking at 20 °C. The labeled polymer was purified on a Disposable PD-10 Desalting Column (GE Healthcare, BioTech a.s., Prague, Czech Republic) using ice water as the mobile phase and freeze-dried to obtain product G-III-Y (25 mg, A = 127 MBq). The radioactivity measurement was performed on a calibrated ionizing chamber BQM-4 (Konsorcium BQM, Prague, Czech Republic).

Similarly, the POX-III polymer (25 mg) was dissolved in 0.5 M ammonium acetate (1 mL) and yttrium-90(III) chloride solution (5 μL in 0.05 M hydrochloric acid, A = 138 MBq) was added. The reaction mixture was incubated for 2 h under continuous shaking at 20 °C. The labeled polymer was purified on a Sephadex® LH-20 column using methanol as the mobile phase, followed by an evaporation process to produce POX-III-Y (16.8 mg, A = 123 MBq).

2.5.2. In vivo stability estimation of the G-III-Y polymer in a metal ion solution representing blood

Polymer G-III-Y (5 mg, A = 25 MBq) was dissolved in 0.5 M ammonium acetate (1.6 mL), and the competing ion solution (400 μL of aqueous solution containing NaCl 750 mmol/L, $MgSO_4$ 50 mmol/L, $CaCl_2$ 5.0 mmol/L, KH_2PO_4 5.0 mmol/L and $ZnSO_4$ 0.0765 mmol/L) was added. The reaction mixture was incubated for 48 h at 37 °C. After 1, 15 and 48 h, successively, the samples (500 μL) were taken out and cooled down, and the polymer samples were purified on a Disposable PD-10 Desalting Column using ice 0.5 M ammonium acetate as the mobile phase. The particular fractions (1.5 mL) were collected, and their radioactivities were measured as described above. The identical separation process (on a Disposable PD-10 Desalting Column using ice 0.5 M ammonium acetate as the mobile phase) was performed with yttrium-90(III) chloride solution (0.1 μL in 0.05 M HCl, A = 10 MBq) in 0.5 M ammonium acetate (500 μL) and the radioactivity of particular fractions (1.5 mL) was measured as well.

2.6. In vivo experiments

The experiments described below were performed in the accordance with The Law of Animal Protection against Cruelty (Act No. 359/2012) of the Czech Republic, which is fully compatible with the corresponding European Union directives.

All *in vivo* experiments were performed using C57BL/6N strain female mice (8 weeks old, purchased from AnLab Ltd., Prague, Czech Republic). They were housed in accordance to the approved guidelines (in individually ventilated cages with the sterilized bedding, 12:12 h light-dark cycle at temperature 22 ± 1 °C and humidity 60 ± 5%), food and water were given *ad libitum*.

2.6.1. Immune response induction test

Polymer G-III (1 mg in 50 μL DMSO) was injected into the muscles of healthy mice (n = 3). The mice were sacrificed 7 days after application, and the injection sites were histologically evaluated.

2.6.2. Antitumor efficiency and biodistribution

The antitumor efficiency of β-glucan-*graft*-poly(2-alkyl-2-oxazoline) labeled with yttrium-90(III) was evaluated using mice with syngeneic T cell mouse lymphoma. The precultivated EL4 mouse lymphoma cells (purchased from First Faculty of Medicine, Charles University, Prague, Czech Republic) were applied subcutaneously (10^5 cells per animal) in a mixture with BD Matrigel™ (I.T.A.-Interact, Ltd., Prague, Czech Republic) into the shaved area above the right leg of the mouse to produce continuously growing tumors.

When the tumor sizes had reached the diameter of approximately 5 mm (after 5 days), the mice (n = 49) were randomly divided into 4 groups – control and groups called the immunotherapy group (IMMUNO), radiotherapy group (RADIO) and immunoradiotherapy group (IMMUNORADIO) – and the therapeutic treatment regimen was started. In the control group (n = 10), DMSO was administered intratumorally (50 μL of DMSO per mouse); in the IMMUNO group (n = 7), the polymer G-III was administered intratumorally (1 mg of G-III/50 μL of DMSO/mouse); in the RADIO group (n = 17) the polymer POX-III-Y was administered intratumorally (0.7 mg of POX-III-Y/4 MBq/50 μL of DMSO/mouse) and in the IMMUNORADIO group (n = 15), the polymer G-III-Y was administered intratumorally (1 mg of G-III-Y/4 MBq/50 μL of DMSO/mouse). The tumor sizes were regularly measured using a caliper in two perpendicular diameters, and the tumor volume (V) was calculated according to the following equation: $V = \pi \cdot a \cdot b^2/6$ (a = longer diameter, b = shorter diameter). The survival time was regularly scored. The data statistical evaluation was conducted using OriginPro 8.1 software (OriginLab Corporation, MA, USA). The calculation of variance analysis (ANOVA) was performed at the significance level of α = 0.05.

The polymer biodistribution was studied simultaneously with the antitumor efficiency experiment. Two mouse were randomly chosen from each group (IMMUNO, RADIO, IMMUNORADIO), and the screens of X-ray imaging (all groups), fluorescence imaging for dye Dyomics-615 using excitation filter 630 nm and emission filter 700 nm (groups IMMUNO and IMMUNORADIO) and Cherenkov radiation imaging for yttrium-90(III) (groups RADIO and IMMUNORADIO) were completed using the Xtreme *In Vivo* Imaging System (Bruker BioSpin, Ettlingen, Germany) on days 1, 2, 3, 5, 7, 9, 12 and 16. The study was performed in anesthesia of 2% isoflurane (Aerrane, Baxter, UK) in air. As a background the image of an X-ray screen for all mice was used. The X-ray

dose from a single short exposition was negligible and couldn't affect the tumor growth. The image merge and analysis were done using Fiji software [24].

During the antitumor efficiency experiment, the important blood parameters of mice, especially the white blood cell parameters, were monitored to evaluate their health conditions. Three mice were randomly chosen from each group, and their blood samples were collected as follows: the first samples were taken before the EL4 cells application (*i.e.,* from healthy mice), the second samples before the start of a treatment (*i.e.*, from the mice with growing tumors), and the subsequent samples were taken twice a week for the next two months. All blood samples (~100 μL) were collected using a retro-orbital bleeding technique with a capillary containing saturated ethylenediaminetetraacetate solution (~3 μL). The whole blood cell staining technique was used. The blood cells (50 μL of a blood suspension) were stained with the mixture of fluorochrome-conjugated antibodies: anti-CD45 (panleukocyte marker), anti-Mac1 +/Gr1 + (marker of granulocytes/monocytes), anti-B220 (marker of B-lymphocytes), anti-CD4 and anti-CD8 (markers of T-lymphocytes); all antibodies were purchased from Biolegend (San Diego, USA). Thereafter, the blood cell solutions were incubated with the antibodies for 20 min at 0 °C in the dark, and they were analyzed using a FACS Canto II flow cytometer (BD Biosciences, San Jose, USA). Flow cytometry data were analyzed and evaluated using FlowJo software (Tree Star, Oregon, USA). The gating strategy is shown in Fig. S7 (see in the Supplementary material).

3. Results and discussion

A conceptually new bimodal cancer treatment was designed to exploit the synergistic effect of immunotherapy and radiotherapy. The theoretical treatment principle is shown in Fig. 1. After injecting our polymer solution into the tumor, the polymer depot is created, and the local action of the radioactive polymer kills the cancer cells. After the radionuclide decays, the immunostimulatory part of the polymer activates the immune system against the cancer cells. Theoretically, the increased concentration of immune cells at the same place as the tumor debris (dead cancer cells) would lead to the recognition of the cancer cells as extraneous cells in the body, and thus, the stimulated adaptive immunity would be able to kill the remaining cancer cells and metastases.

The structure of the final polymer product (G-III-Y) – β-glucan-*graft*-poly(2-isopropyl-2-oxazoline-*co*-2-butyl-2-oxazoline) bearing Dyomics-615 and complex DOTA-yttrium-90(III) at the graft ends (Fig. 2) – was designed for use in immunoradiotherapy. For this purpose, the resulting polymer was required to be immunostimulatory and thermoresponsive and to contain a therapeutic radiation source. As an immunostimulatory backbone, β-glucan extracted from *Auricularia auricula-judae* was chosen because it is widely known for its immunostimulatory and anticancer activity [25]. Poly(2-isopropyl-2-oxazoline-*co*-2-butyl-2-oxazoline) was chosen as a thermoresponsive moiety because, according to our previous experiences, when grafted onto polysaccharides, it exhibits the most appropriate CPT [26]. Furthermore, POXs are relatively radioresistant compared to the other thermoresponsive polymers, and thus they are suitable for use in this

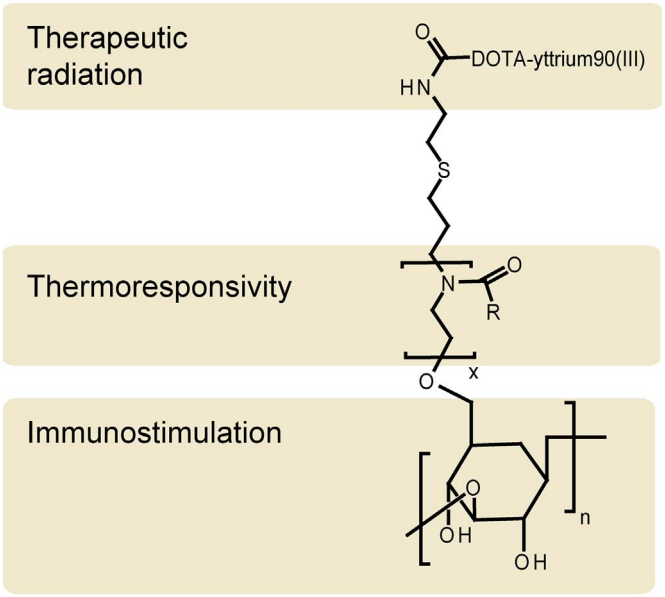

Fig. 2. The structure of the polymer G-III-Y, designed for use in immunoradiotherapy.

system [19]. As a radiation therapy source, yttrium-90(III) was chosen because it dominantly undergoes β^- decay, which is only effective at short distances, and has a relatively short half-life ($T_{1/2}$ = 64.1 h). Therefore, when used as a part of the polymer depot it causes a smaller impact on the whole body because the radiation is localized only at the site of this depot.

3.1. Synthesis, preparation and characterization

The schemes of all synthetic procedures are illustrated in Fig. 3. The used β-glucan was first extracted from *Auricularia auricula-judae* according to ref. [22]. The polymer grafts were synthesized using cationic ring-opening polymerization of 2-isopropyl-2-oxazoline and 2-butyl-2-oxazoline using allyl bromide as the initiator. The use of allyl bromide provides double bonds at the graft ends, allowing further modifications. The theoretical monomer molar ratio of the resulting polymer grafts was chosen to be $n_{\text{isopropyloxazoline}}/n_{\text{butyloxazoline}}$ = 3/1 and the theoretical polymer length was chosen to be $M_{\text{n,graft(theoretical)}}$ = 2500 Da because this monomer ratio and graft length exhibited the most appropriate CPTs after grafting onto the polysaccharides [26]. The living ends of the POX grafts were terminated with sodium β-glucanate to produce the desired polymer β-glucan-*graft*-poly(2-alkyl-2-oxazoline) (G-I), and in addition, they were terminated with water to obtain POX polymer (POX-I) that have the same length as the POX grafts of the polymer G-I.

First, POX-I, representing the polymer grafts, was characterized. To determine the number-average molecular weight, size-exclusion chromatography (SEC) measurements were conducted using *N,N*-dimethylformamide as the mobile phase. The molecular weight of the POX-I was $M_{\text{n,graft(found)}}$ = 2290 Da, which was very close to the

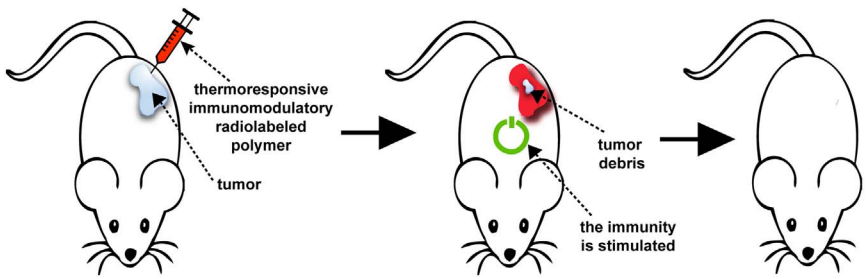

Fig. 1. The principle of bimodal immunoradiotherapy: radiation kills the tumor cells; after the radionuclide decays, the immunomodulator enhances the following immune response against the remaining cancer cells and metastases.

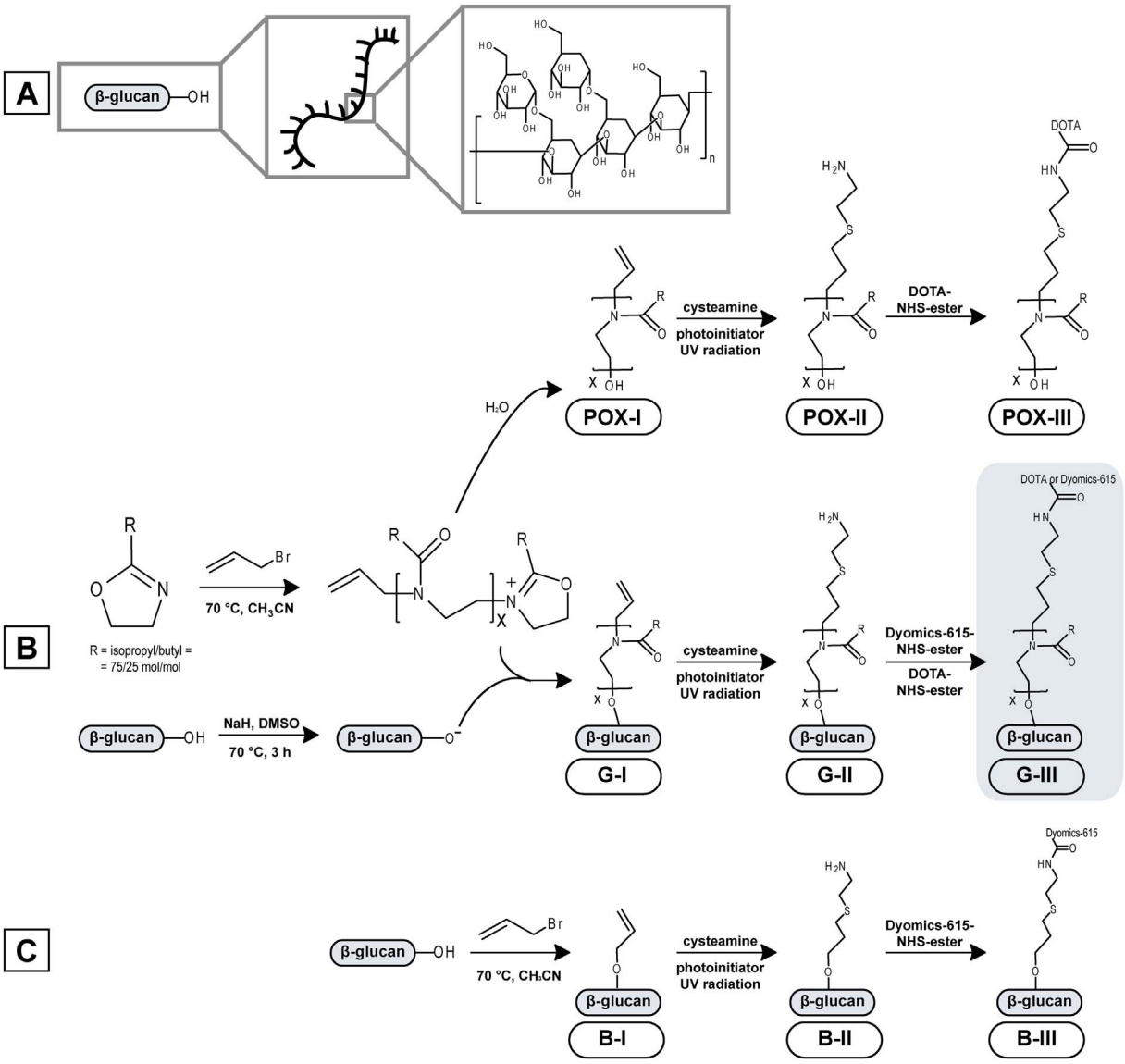

Fig. 3. A) The structure of the isolated β-glucan, B) the synthetic procedure for POX-III and G-III, C) the synthetic procedure for B-III.

theoretical value of 2500 Da; the dispersity was found to be 1.19. To determine the monomer ratio of the POX-I, ^{1}H NMR spectroscopy was used, and the monomer ratio was calculated according to Eq. (1):

$$\frac{n_{\text{isopropyl}}}{n_{\text{butyl}}} = \frac{\frac{1}{6}\cdot I_{\delta=1.02\ \text{ppm}}}{\frac{1}{2}\cdot I_{\delta=1.31\ \text{ppm}}} \quad (1)$$

where $n_{\text{isopropyl}}/n_{\text{butyl}}$ is the molar ratio of 2-isopropyl-2-oxazoline and 2-butyl-2-oxazoline incorporated in the POX-I, $I_{\delta\ =\ 1.02\ \text{ppm}}$ is the peak integral at 1.02 ppm corresponding to the $-CH-(C\mathbf{H_3})_2$ group coming from 2-isopropyl-2-oxazoline and $I_{\delta\ =\ 1.31\ \text{ppm}}$ is the peak integral at 1.31 ppm corresponding to the $-CH_2-CH_2-C\mathbf{H_2}-CH_3$ group from 2-butyl-2-oxazoline. The monomer ratio for POX-I was determined to be $n_{\text{isopropyl}}/n_{\text{butyl}}$ = 74/26, that was very close to theoretical value of $n_{\text{isopropyl}}/n_{\text{butyl}}$ = 75/25.

The successful grafting process of β-glucan, which resulted in polymer G-I, was confirmed using ^{1}H NMR spectroscopy. Because the starting composition of β-glucan contained < 0.1 wt% nitrogen, the weight content of the POX grafts in sample G-I could be calculated using the weight content of nitrogen determined from the elemental analysis (CHN). The POX weight content, w_{POX}, in the polymer was calculated according to Eq. (2):

$$w_{\text{POX}} = \frac{w_{\text{N}}}{w_{\text{N,POX}}}\cdot 100\% \quad (2)$$

where w_{N} is the nitrogen content in the resulting polymer and $w_{\text{N,POX}}$ is the theoretical nitrogen content in the POX graft. The weight content of POX in G-I was determined to be 70%, which corresponded to the density of one graft per 5.5 glucose units. This was the maximum achievable grafting density because the grafting process was performed in a high molar excess of POX grafts. In general, the grafting limit was established by the spatial and conformational limitations of the β-glucan structure. According to the SEC-MALS measurements (using dimethyl sulfoxide (DMSO) as the mobile phase), the weight-average molecular weight of G-I was measured to be $M_{\text{w,found}} = 7.5\cdot 10^6$ Da, which was in good agreement with the theoretical value $M_{\text{w,theory}} = 8.3\cdot 10^6$ Da, calculated considering the weight content of POX in polymer (70%) and the molecular weight of the starting (non-grafted) β-glucan $M_{\text{w,found}} = 2.5\cdot 10^6$ Da (consistent with literature [22], in which β-glucan extracted from *Auricularia auricula-judae* had $M_{\text{w}} = 2.07\cdot 10^6$ Da in DMSO).

To study the temperature-dependent behavior and CPTs of both

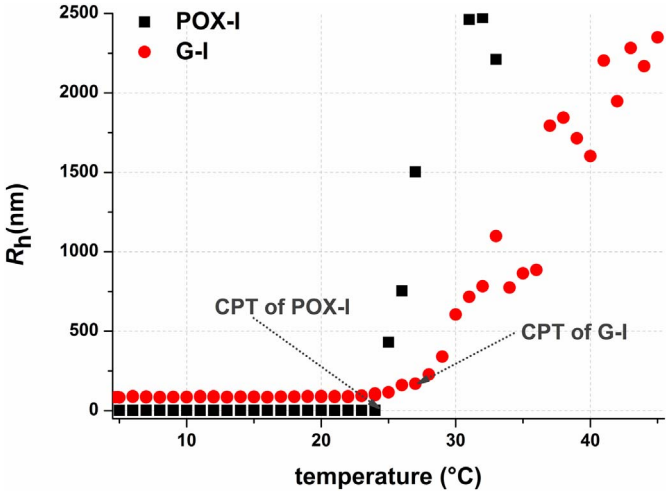

Fig. 4. Temperature-dependence of the hydrodynamic radius, R_h, (volume mean) of POX-I and G-I at c = 1 mg/mL in PBS.

polymers (G-I and POX-I), dynamic light scattering was measured at the concentration of c = 1 mg/mL in phosphate-buffered saline (PBS) (Fig. 4). According to the measured intensity (attenuator index: 11) and size, POX-I was practically molecularly dissolved below the CPT, while at 24 °C, the average hydrodynamic radius, R_h, (volume mean) of POX-I began to increase sharply (CPT). Similarly, the average R_h of G-I was approximately 100 nm, while the CPT occurred at 27 °C when it started to increase. The difference between CPTs is in a good agreement with the theory because G-I was composed of 70% POX grafts (represented by POX-I) and 30% of the β-glucan backbone, and thus, the CPT of POX-I should have been lower than the CPT of G-I at the same concentration. Moreover, the temperature-dependent phase transition of G-I did not occur as rapidly as that of POX-I, which was caused by the hydrophilic polysaccharide backbone present in the G-I sample. In conclusion, both polymers (G-I and POX-I) have CPTs lower than ca 33 °C (c = 1 mg/mL) and they are completely insoluble at 37 °C. Therefore, they are suitable for use in brachytherapy based on their temperature-dependent behavior.

Due to their appropriate CPTs, both polymers were modified to bear Dyomics-615 and DOTA moieties at the graft ends. First, cysteamine was incorporated at the graft ends using a thiol-ene click reaction (Fig. 3) to obtain polymers G-II and POX-II with –NH_2 groups at the graft ends. The content of the –NH_2 groups was determined using a 2,4,6-trinitrobenzene-1-sulfonic acid (TNBSA) assay [23] (G-II – 0.17 mmol/g of −NH_2 groups, POX-II – 0.08 mmol/g of −NH_2 groups). After, the Dyomics-615 and DOTA were introduced at the graft ends using the reaction between their *N*-hydroxysuccinimidyl ester (NHS-ester) and −NH_2 groups at the graft ends to obtain G-III and POX-III (only with DOTA). The content of Dyomics-615 was detected spectrophotometrically ($\lambda_{absorption}$ = 621 nm, ε = 200,000 L/mol·cm) to be 0.1 wt% for G-III (POX-III was conjugated only with DOTA-NHS-ester). The DOTA content in the polymers was determined using chelation with Gd(III) followed by energy-dispersive X-ray spectroscopy EDS. The content of Gd(III) in polymer G-III was measured to be 1.72%, indicating 0.11 mmol/g of DOTA, and 1.16% in POX-I, indicating 0.07 mmol/g of DOTA.

The presence of DOTA in the resulting polymers was necessary because it enabled polymer complexation with the radioactive yttrium-90(III) for subsequent use in therapeutic *in vivo* experiments. The fluorescent dye, Dyomics-615, was incorporated into the resulting polymer in order to study the polymer *in vitro* and *in vivo*.

Moreover, a β-glucan conjugate (B-III) with Dyomics-615 was synthesized (Fig. 3) as a control sample for *in vitro* testing. First, the hydroxyl groups of β-glucan were alkylated with allyl bromide in an alkaline aqueous solution. The degree of functionalization, f, (number of allyl groups per D-glucose unit) was calculated from the ^{1}H NMR spectrum according to Eq. (3):

$$f = I_{\delta=5.93\ ppm}/I_{\delta=5.23\ ppm} \quad (3)$$

where $I_{\delta\ =\ 5.93\ ppm}$ is the peak integral at δ = 5.93 ppm corresponding to −C**H**=CH_2 and $I_{\delta\ =\ 5.23\ ppm}$ is the peak integral at δ = 5.23 ppm corresponding to the acetal hydrogen on position 1 of the D-glucose unit. Here, f is 0.27, meaning that polymer B-I contains, on average, 0.27 allyl moieties per D-glucose unit. After, cysteamine was incorporated to produce B-II (0.33 mmol/g of −NH_2 groups). Finally, B-II was reacted with Dyomics-615-NHS-ester to produce polymer B-III containing 0.05 wt% Dyomics-615 (determined spectrophotometrically: $\lambda_{absorption}$ = 621 nm and ε = 200,000 L/mol·cm).

3.2. In vitro study

3.2.1. Cytotoxicity

The cytotoxicity of polymer G-III was studied on different cell lines (macrophages RAW 264.7, MCF7 and EL4 cancer cells) using an AlamarBlue assay. The polymer cytotoxicity was detected to be nearly negligible at low concentrations for all cell lines. Moreover, the half maximal inhibitory concentration (IC_{50}) of G-III was calculated to be relatively high (354.12 μg/mL for the RAW cells, 427.79 μg/mL for the MCF7 cells and 152.5 μg/mL for the EL4 cells), denoting the non-toxicity of polymer G-III.

3.2.2. Oxidative burst response of the leukocytes

The oxidative burst activation caused by polymer G-III was tested using leukocytes isolated from human whole blood, while polymer B-III was used as a control that represented non-grafted β-glucan. The response of the leukocytes after polymer stimulation was indirectly determined using the viability decrease of *Staphylococcus (S.) aureus*, which was added during the experiment. Both polymers showed the enhanced response of the leukocytes (Fig. 5A). The non-grafted β-glucan (B-III, c = 1 and 10 μg/mL) exhibited the decreased viability of *S. aureus* up to 45% compared to the control group (c = 1 μg/mL, P < 0.0001; c = 10 μg/mL, P < 0.016). Furthermore, the grafted β-glucan (G-III, c = 3.4 and 34 μg/mL) demonstrated an even higher decrease in the *S. aureus* viability at polymer concentrations corresponding to the same amount of β-glucan in the tested solutions, while the differences compared to the control group were statistically confirmed (c = 3.4 μg/mL, P < 0.0065; c = 34 μg/mL, P < 0.0007). Polymer G-III exhibited slightly stronger immune activation compared to non-grafted β-glucan (B-III), considering the same amount of contained β-glucan. This result was attributed to their significantly different sizes at 37 °C, since the non-grafted β-glucan (B-III) had similar R_h as that at 20 °C (~60 nm, c = 1 mg/mL), and the grafted β-glucan (G-III) formed macroscopic phase-separated aggregates that were a few times bigger than the non-grafted β-glucan aggregates.

3.2.3. Production of tumor necrosis factor α (TNF-α)

The TNF-α production induced by the prepared polymers (B-III and G-III) was tested using an enzyme-linked immunosorbent assay (ELISA) on the leukocytes isolated from human whole blood (Fig. 5B). Both β-glucan (B-III) and grafted β-glucan (G-III) at concentrations corresponding to 1 and 10 μg/mL of β-glucan increased the TNF-α production compared to the control group containing phorbol 12-myristate 13-acetate (PMA) (c = 2 μM), an activator of phagocytosis. The significant differences in the TNF-α expression were detected by comparison of the samples activated by B-III or G-III with the samples activated by PMA (B-III, c = 1 μg/mL, P < 0.029; c = 10 μg/mL, P < 0.0038; G-III, c = 3.4 μg/mL, P < 0.00033; c = 34 μg/mL, P < 0.0012).

Generally, TNF-α is a multifunctional cytokine that plays a key role in many functions, such as apoptosis or cell survival. TNF-α was named for its antitumor properties, and for cancer therapy, it is currently used

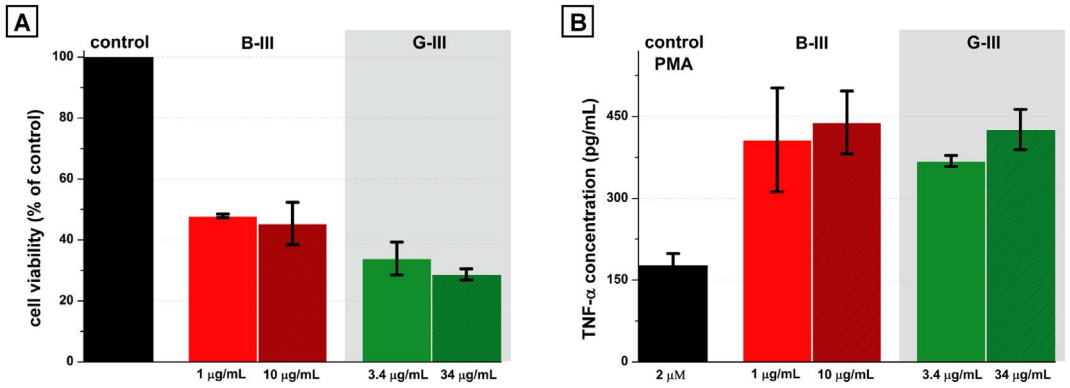

Fig. 5. A) The cell viabilities of *S. aureus* after the stimulation of polymers B-III and G-III at concentrations corresponding to 1 and 10 μg/mL of β-glucan; the cell viabilities correspond indirectly to the oxidative burst response of the leukocytes, B) the tumor necrosis factor α (TNF-α) production induced by phorbol 12-myristate 13-acetate (PMA) as the control and by the prepared polymers (B-III is β-glucan with the fluorescent dye and G-III is β-glucan-*graft*-POX with the fluorescent dye).

in the regional treatment of locally advanced soft tissue sarcomas and metastatic melanomas [27]. Therefore, the observed TNF-α production induced by the prepared polymer indicates an optimistic prognosis for cancer treatment.

3.2.4. Cellular uptake measured using flow cytometry

To compare the cellular internalization kinetics between β-glucan (B-III) and β-glucan-*graft*-poly(2-alkyl-2-oxazoline) (G-III) in the cancer cells, both polymers were added to the cancer cells (MCF7) for up to 48 h at a concentration corresponding to 50 μg/mL β-glucan (c = 167 μg/mL G-III, c = 50 μg/mL B-III), and the cellular uptake was measured using flow cytometry (Fig. 6). In general, MCF7 cells are a good model for representing a drug cellular internalization into cancer cells *in vitro*. The obtained flow cytometry data indicated that the polymer G-III internalized in the cancer cells (MCF7) with more than doubled efficiency compared to that of the non-grafted β-glucan B-III. This result demonstrates the good cell-internalization properties of the prepared conjugate G-III.

3.2.5. Cellular uptake study using microscopy

The conjugates (B-III and G-III) were visualized inside the RAW cells (macrophages) and MCF7 (cancer) cells using a confocal laser scanning microscope after incubation times of 15 min, 4 h and 24 h. The microscopy studies showed that both B-III and G-III were internalized in the macrophages (Fig. 7A) and MCF7 cells (Fig. 7B). The data indicated that the carrier system (G-III) was internalized better in the cell lines than the non-grafted β-glucan (B-III) and was especially visible after shorter incubation times (15 min and 4 h). This finding is in good agreement with the flow cytometry data, which also showed a higher uptake of G-III. Significant differences between the intracellular distribution patterns were not observed. The cellular uptake in the macrophages was very high and exceeded the uptake in the MCF7 cells. This behavior can be explained by the phagocytic activity of RAW cells as specialized macrophages.

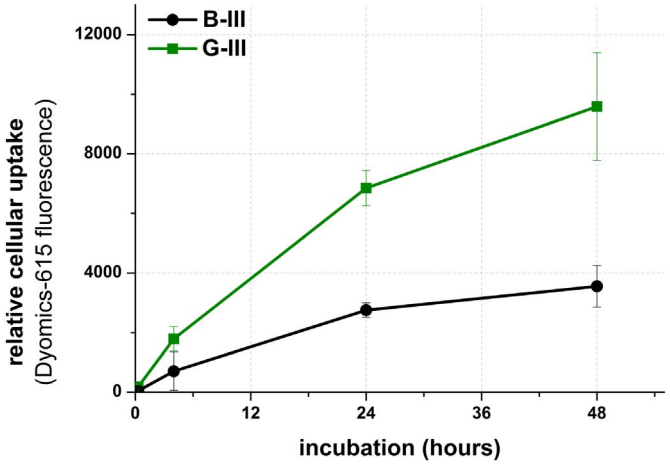

Fig. 6. Polymer cellular uptake in the cancer cells (MCF7) after up to 48 h of incubation at a concentration corresponding to 50 μg/mL β-glucan (c = 167 μg/mL G-III, c = 50 μg/mL B-III). The given data was based on 3 independent experiments (n = 3) and normalized to the same fluorescence intensity for both polymers.

3.2.6. Microscopy colocalization of G-III in the RAW cells

For a better view of the interactions between G-III and the macrophages, a marker for acidic organelles was applied to visualize the colocalization of the G-III conjugate in the macrophagosomes. The RAW cells were incubated for 4 h with G-III and imaged after staining the macrophagosomes (Fig. 8). The colocalization experiment showed that the vast amount of the detected Dyomics-615 fluorescence colocalized with the lysosensor signals, indicating that polymer G-III indeed accumulated in the lysosomes and macrophagosomes. Energy-independent insertion of G-III in the cells *via* an endocytosis-independent process was not observed, which would have resulted in a large amount of freely distributed G-III polymer in the cytoplasm.

To further disprove the cell-inserting activity of the polymers (B-III and G-III) the RAW cells were incubated at 4 °C under the deprivation of energy (Fig. S4 in the Supplementary material). This experimental setup excludes the fact that the strong internalization in the RAW cells was supported by the energy-independent cell-penetrating activity of both polymers. After 45 min of incubation at 4 °C, internalization of both B-III and G-III in the RAW cells was not detected, confirming that the high uptake rate of both polymers (G-III and B-III) in the RAW cells was predominantly an active internalization process that occurred *via* macrophagocytosis and the lysosomal pathway, as indicated by the lysosensor staining.

3.3. Radiolabeling and radiostability

Polymers labeled with yttrium-90(III) were utilized because yttrium-90(III) dominantly undergoes β^- decay, which is only effective up to short distances (up to 1 cm in water tissue), and thus, the radiation acts only locally. Moreover, it has a therapeutically convenient half-life ($T_{1/2}$ = 64.1 h). Both polymers B-III and G-III were labeled with yttrium-90(III) in ammonium acetate buffer, and the products were purified on a Disposable PD-10 Desalting Column (Sephadex® G-25, G-III-Y) and on a Sephadex® LH-20 column (POX-III-Y). The separation process of the radiolabeled polymers from the uncomplexed yttrium-90(III) chloride was effective (see Fig. S5 in the Supplementary material). The radiolabeled polymers were prepared with sufficient radioactivity for therapy treatment: G-III-Y (25 mg, A = 127 MBq) and

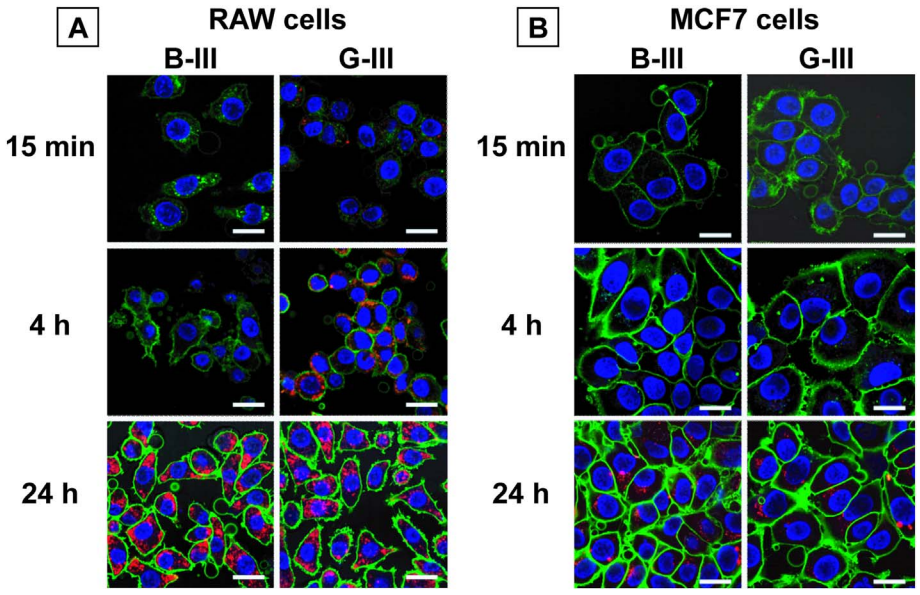

Fig. 7. The confocal microscopy images of polymers G-III and B-III after incubation at concentrations corresponding to 150 μg/mL β-glucan (c = 500 μg/mL G-III, c = 150 μg/mL B-III) at 15 min, 4 and 24 h with A) RAW cells; B) MCF7 cells. For both images, organelle staining is shown in green (CellMask Green, cell membrane) and blue (Hoechst 33342, nucleus), and the polymers are in red (Dyomics-615 dye). The scale bar is 20 μm. (For interpretation of the references to colour in this figure legend, the reader is referred to the web version of this article.)

POX-III-Y (16.8 mg, A = 123 MBq).

However, in living organisms, there are many various ions that can compete with yttrium-90(III) and replace it in the DOTA complex. The most risky competing ions are Ca^{2+} and Zn^{2+} (which can be complexed with DOTA) and phosphates (which can complex yttrium-90(III)), and thus, the stability of the radiolabeled G-III-Y was studied in an environment containing ions at concentrations similar to their concentrations in blood plasma (c_{Ca2+} = 1.0 mmol/L, c_{Zn2+} = 0.0153 mmol/L and $c_{phosphates}$ = 1.0 mmol/L, for further experimental details see the Section 2.5.2). The radiolabeled polymer was incubated with the ion solution mentioned above at 37 °C, and the polymer radiostability was investigated using SEC (the standard deviation of radioactivity measurement was not > 5%). The polymer fractions showed approximately same relative radioactivity after the incubation of 1, 15 and 48 h. Therefore, a significant leakage of yttrium-90(III) from the labeled polymer was not detected even after 48 h at 37 °C, that predicted the high stability of the yttrium-90(III)-labeled polymer (G-III-Y) in the blood environment.

3.4. *In vivo study*

The experiments described below were performed in accordance with The Law of Animal Protection against Cruelty (Act No. 359/2012) of the Czech Republic, which is fully compatible with the corresponding European Union directives.

3.4.1. *Immune response induction test*

The biological behavior of polymer G-III in the context of immune response induction was studied *in vivo* after its injection into the thigh muscles of healthy mice. The histological evaluation was performed 7 days after the polymer injection (Fig. 9). The created polymer depot caused considerable inflammation at the site of injection, as represented by the phlegmonous mixed inflammatory cellularization and the round-cell inflammatory cellularization in the loose connective and adipose tissue. Moreover, dystrophic calcification of the muscle fibers (Fig. 9B) was found at the injection sites, denoting the extensive inflammation. Therefore, it could be said that polymer G-III induced a similar non-specific immune system response as the non-grafted β-glucan. Hence, the grafting procedure probably did not significantly reduce the immunostimulatory properties of the β-glucan backbone, which is in good agreement with the results from assay of the oxidative burst response of the leukocytes, tested *in vitro* (see above the Section 3.2.2. *Oxidative burst response of the leukocytes*).

3.4.2. *Antitumor efficiency and biodistribution*

The anticancer efficiency of the prepared G-III-Y polymer, which represented its immunoradiotherapy ability, was evaluated in the syngeneic lymphoma mouse models – C57BL/6N mice with mouse lymphoma EL4. Moreover, the synergistic effect of the immunoradiotherapy (treatment with radiolabeled β-glucan-*graft*-POX) in comparison with only immunotherapy (treatment by β-glucan-*graft*-POX) and radiotherapy (treatment by radiolabeled POX chains having the same lengths as grafts) was studied. Thus, the polymer dose in particular groups was designed to be consistent, corresponding to a dose of 0.3 mg of β-glucan, 0.7 mg of POX chains and a radioactivity of 4 MBq per a mouse. Therefore, the dose in the IMMUNORADIO group was 1 mg of G-III-Y/4 MBq/mouse, the dose in the IMMUNO group was 1 mg G-III/mouse and the dose in the RADIO group was 0.7 mg of POX-

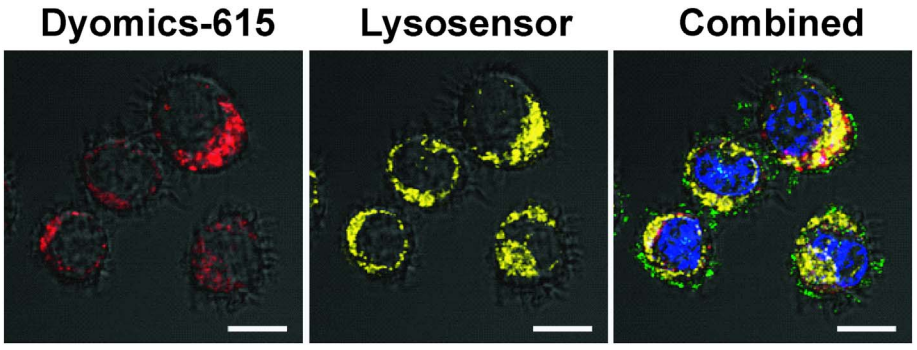

Fig. 8. The confocal microscopy images of G-III in the RAW cells after incubation at a concentration corresponding to 50 μg/mL β-glucan (c = 167 μg/mL G-III) for 4 h. From left to right: the fluorescence of the Dyomics-615 dye representing the G-III polymer (red) and the lysosensor localized macrophagosomes (yellow). On the right, the combined image of the G-III polymer (red), macrophagosomes (yellow), nucleus (blue, Hoechst 33342) and cell membranes (green, CellMask™ Green) is shown. The scale bar is 10 μm. (For interpretation of the references to colour in this figure legend, the reader is referred to the web version of this article.)

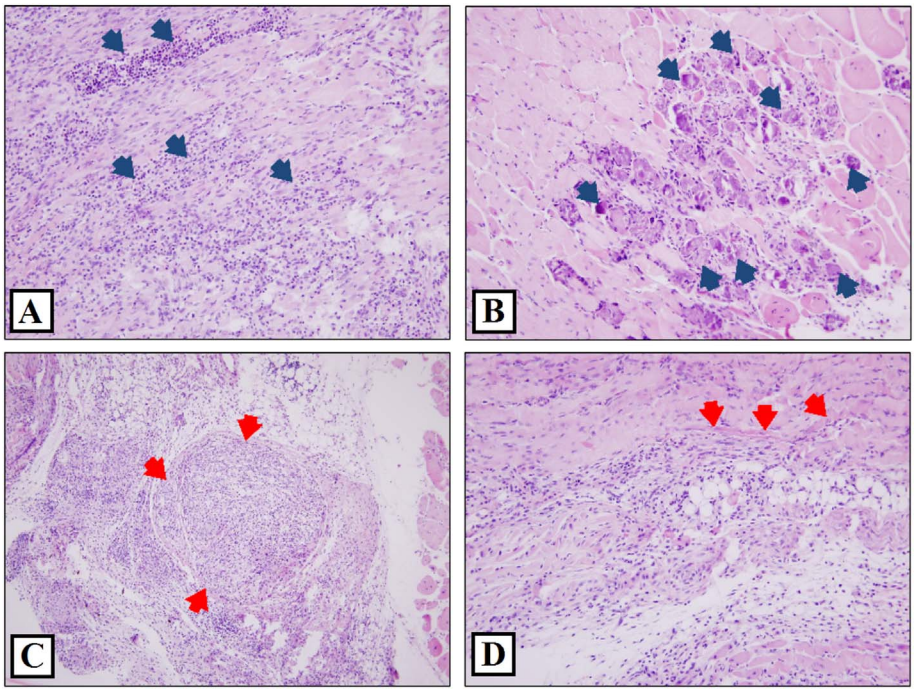

Fig. 9. Histological evaluation of the G-III polymer in the muscle tissue (7 days after the administration): A) phlegmonous mixed inflammatory cellularization with the predominance of granulocytes (original magnification 200 ×); B) dystrophic calcification of the muscle fibers (blue arrows, original magnification 200 ×); C) round-cell inflammatory cellularization in adipose tissues near the nervous and vascular plexus. The nerve (red arrows) is edematous with round-cell infiltrates (original magnification 100 ×); D) round-cell inflammatory infiltration in the loose connective and adipose tissue reaching the dystrophic muscle fibers (red). (For interpretation of the references to colour in this figure legend, the reader is referred to the web version of this article.)

III/4 MBq/mouse. All polymers were administered in their DMSO solutions (50 μL of DMSO/mouse) because these polymers are generally soluble in DMSO without exhibiting any CPT (no precipitation at higher temperatures). This approach avoids possible polymer precipitation in the injection needle during the application, which could have resulted in administered inhomogeneities in the study. However, the use of DMSO instead of water did not change the desirable polymer properties [16]. Furthermore, DMSO promotes polymer precipitation in the aqueous environments of the organisms due to the cononsolvency effect [28]. To exclude any possible effects of DMSO on the tumor growth, DMSO was also administered intratumorally in the control group (50 μL of DMSO/mouse).

During the antitumor efficiency experiment, the polymer biodistribution was studied in all treated groups. The images (Fig. 10) were composed using screen superposition with the X-ray images (all groups), fluorescence images of the Dyomics-615 dye (in the IMMUNO and IMMUNORADIO groups) and Cherenkov radiation images of yttrium-90(III) (in the RADIO and IMMUNORADIO groups). The G-III-Y polymer (IMMUNORADIO) created a polymer depot immediately after its injection, while the polymer remained at the site of injection > 12 days (12 days correspond to *ca.* 4.5 half-lives of the yttrium-90(III)). However, a presence of the polymer G-III-Y at the injection site was found to be negligible on day 16. Moreover, the presence of the polymer in other parts of body was not detected, even in the kidneys or livers, meaning that polymer G-III-Y slowly degraded and was consequently removed from the mouse body. This result is in good agreement with the theory because G-III-Y was designed to be gradually decomposed by glycosidases into oligomers shorter than the renal threshold in order to be excluded by kidneys. As expected, the similar biodistribution result was observed for polymer G-III (IMMUNO), confirming that in this case, radiation did not significantly influence the polymer biodistribution (comparing G-III-Y and G-III). A different situation was monitored for polymer POX-III-Y (RADIO) which was observed at the site of injection only until day 5. Thereafter, Cherenkov radiation (normalized for the half-life of yttrium-90(III)) was not detected in the mouse body, indicating POX-III was fully removed from the body on day 6. Interestingly, POX-III exhibited a lower CPT than G-III, while the created polymer depot of POX-III-Y was eliminated from the body after a shorter time than that of G-III-Y. This fact was probably caused due to the considerably lower molecular weight of POX-III (POX-III M_n = 2290 Da; G-III $M_w = 7.5 \cdot 10^6$ Da).

Regarding the tumor growth, growth inhibition was observed in all

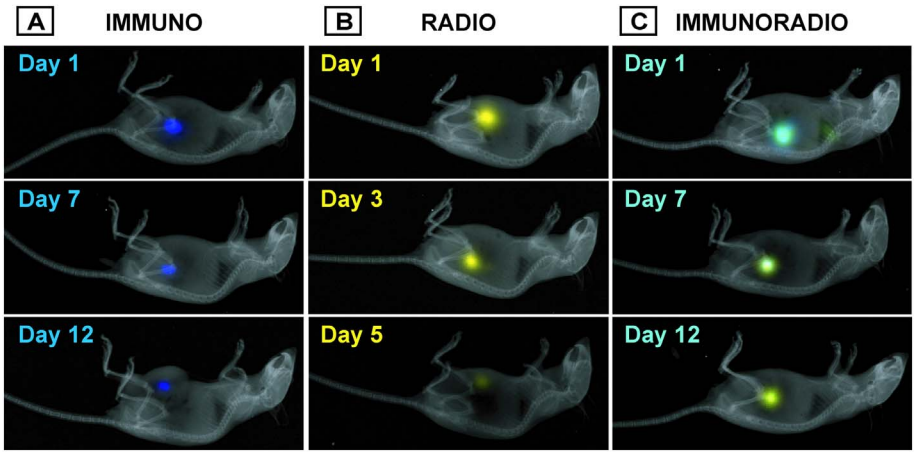

Fig. 10. Biodistribution of the polymers: A) G-III administered in the IMMUNO group (the composed images were made superimposing screens from the X-ray imaging and fluorescence imaging of the Dyomics-615 dye); B) POX-III-Y administered in the RADIO group (the composed images were made superimposing screens from the X-ray imaging and Cherenkov radiation imaging of yttrium-90(III)); C) G-III-Y administered in the IMMUNORADIO group (the composed images were made superimposing screens from the X-ray imaging, fluorescence imaging of the Dyomics-615 dye and Cherenkov radiation imaging of yttrium-90(III)).

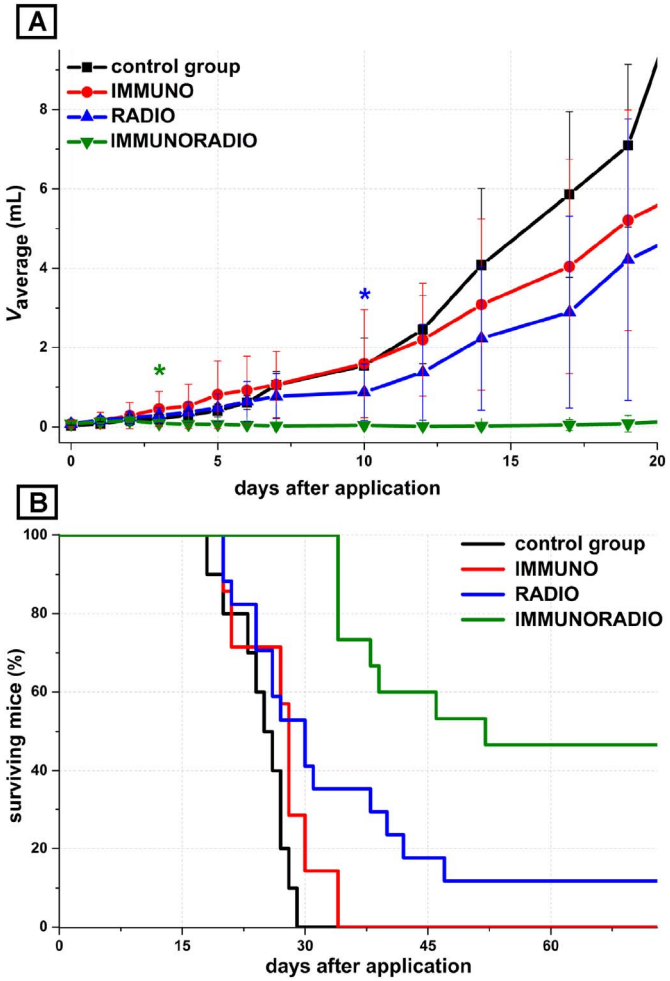

Fig. 11. The *in vivo* effects of the particular treatments on the: A) primary tumor growth and B) survival time. The treatment doses were as follows: control group – 50 μL of DMSO/mouse, IMMUNO group – 1 mg of G-III/50 μL DMSO/mouse, RADIO group – 0.7 mg of POX-III/4 MBq/50 μL DMSO/mouse and IMMUNORADIO group – 1 mg of G-III-Y/4 MBq/50 μL DMSO/mouse. The green asterisk (A) marks the time from when the populations of control and IMMUNORADIO groups were statistically different (day 3), and the blue asterisk (A) denotes the time from when the populations of control and RADIO groups were statistically different (day 10). (For interpretation of the references to colour in this figure legend, the reader is referred to the web version of this article.)

treated groups compared to the control group (Fig. 11A), while the primary tumor growth was almost stopped in the IMMUNORADIO group. The substantial difference in the tumor volumes at the significance level of $\alpha = 0.05$ was detected between the control and IMMUNORADIO groups on day 3 and between the control and RADIO groups on day 10. However, between the control and IMMUNO groups, the tumor growth inhibition was not statistically confirmed at the significance level of $\alpha = 0.05$ up to day 20, but the mean value of the tumor volume was lower compared to the control group on day 14 (Fig. 11A).

The survival time was also monitored for all groups (Fig. 11B). In general, the treated groups demonstrated longer survival times compared to the control group (24.7 ± 3.5 days). In the IMMUNO group, only a slight increase in the average survival time was observed (26.9 ± 4.9 days). In contrast, in the RADIO group 2 mice (from a total of 17 mice, treatment success: 12%) were completely cured on day 13, while the average survival time of the uncured mice (15 mice) was prolonged to 29.8 ± 8.4 days. The situation was considerably better in the IMMUNORADIO group because 12 cured mice (from a total of 15 mice) without any evidence of tumors were observed on day 13. Unfortunately, the primary tumors appeared again in 2 mice, and metastatic tumors appeared in armpits of 3 originally cured mice. Therefore, 7 mice (from a total of 15 mice, treatment success: 47%) were completely cured in the IMMUNORADIO group and the average survival time of the uncured mice (8 mice) was significantly prolonged to 39.0 ± 6.9 days.

During the antitumor efficiency experiment, the important blood parameters of mice, especially a composition of the white blood cells (WBCs), were monitored to evaluate their health conditions within the experiment (Fig. 12). The blood samples of 3 randomly chosen mice from each group were taken before the cancer cells injection (*i.e.,* from healthy mice), before the start of a treatment (*i.e.,* from the mice with growing tumors) and then during a treatment. The lymphoma growth resulted in a transient decrease of the WBC count during the initial tumor growth process (ca 5 days after the cancer cell injection), followed by a significant increase until reaching a maximum count, which was a few times higher than a WBC count of healthy mice, and this maximum count was observed close to the mouse death. Moreover, the CD4 and CD8 T-lymphocytes decreased their blood percentage amount with the tumor growth, however, this decrease was not significant in the absolute count but it resulted from a considerable increase of granulocytes and monocytes, observed during the tumor growth. The B-lymphocyte absolute count decreased to the approximately one half of the original value during an early tumor growth (within first week), and then they remained at the same low level. Anyway, no significant differences in the WBC parameters were indicated between the control and the treated mice with the tumors. Nevertheless, the mice that cured the tumors in the IMMUNORADIO group were clearly distinguishable from the others due to their normalization of the blood counts (Fig. 12). The further blood parameters related to the red blood cells and platelets were not affected by the tumor growth and the treatment (see Fig. S6 in the Supplementary material).

All the results of the *in vivo* anticancer efficiency experiments indicate the synergistic effect of immunoradiotherapy. This synergy could be explained using a hypothesis of the cooperating therapies as follows: the therapeutic radiation of the polymer kills the cancer cells, and after the decay of the radionuclide, the polymer causes stronger immune responses against cancer cells at the tumor site. Thus, the combined immunoradiotherapy brings better prognosis in the healing process. More detailed biological studies are needed to further understand the principles of the observed synergistic effect.

4. Conclusion

A novel thermoresponsive polymer β-glucan-*graft*-poly(2-isopropyl-2-oxazoline-*co*-2-butyl-2-oxazoline) (maximum achievable graft density, $M_{n,graft}$ = 2500 Da) bearing complexes of DOTA-yttrium-90(III) and the fluorescent dye Dyomics-615 at the graft ends was successfully prepared, using β-glucan extracted from *Auricularia auricula-judae*, as a potential drug system for a conceptually new bimodal immunoradiotherapy treatment. The thermoresponsive polymer behavior was studied in aqueous solutions and demonstrated the appropriate CPT for polymer depot formation after injection into the body. The *in vitro* tests exhibited the non-toxicity of the polymer and its active cellular uptake into cancer cells and macrophages with colocalization in lysosomes and macrophagosomes. Furthermore, the oxidative burst of the leukocytes and the *in vivo* immune response induction experiments confirmed the immunostimulatory properties of the polymer. Additionally, the production of TNF-α induced by the polymer (G-III) was detected *in vitro*. The *in vivo* antitumor efficiency and polymer biodistribution were characterized using mice with EL4 lymphoma. The polymer (G-III-Y) created a depot after injection, and the depot remained at the site > 12 days. However, after 16 days, a presence of the polymer G-III-Y at the injection site was found to be negligible, and thus, the polymer was gradually degraded and excluded from the body through the kidneys. The immunoradiotherapy group (treated with the radiolabeled polymer) demonstrated the complete inhibition of the

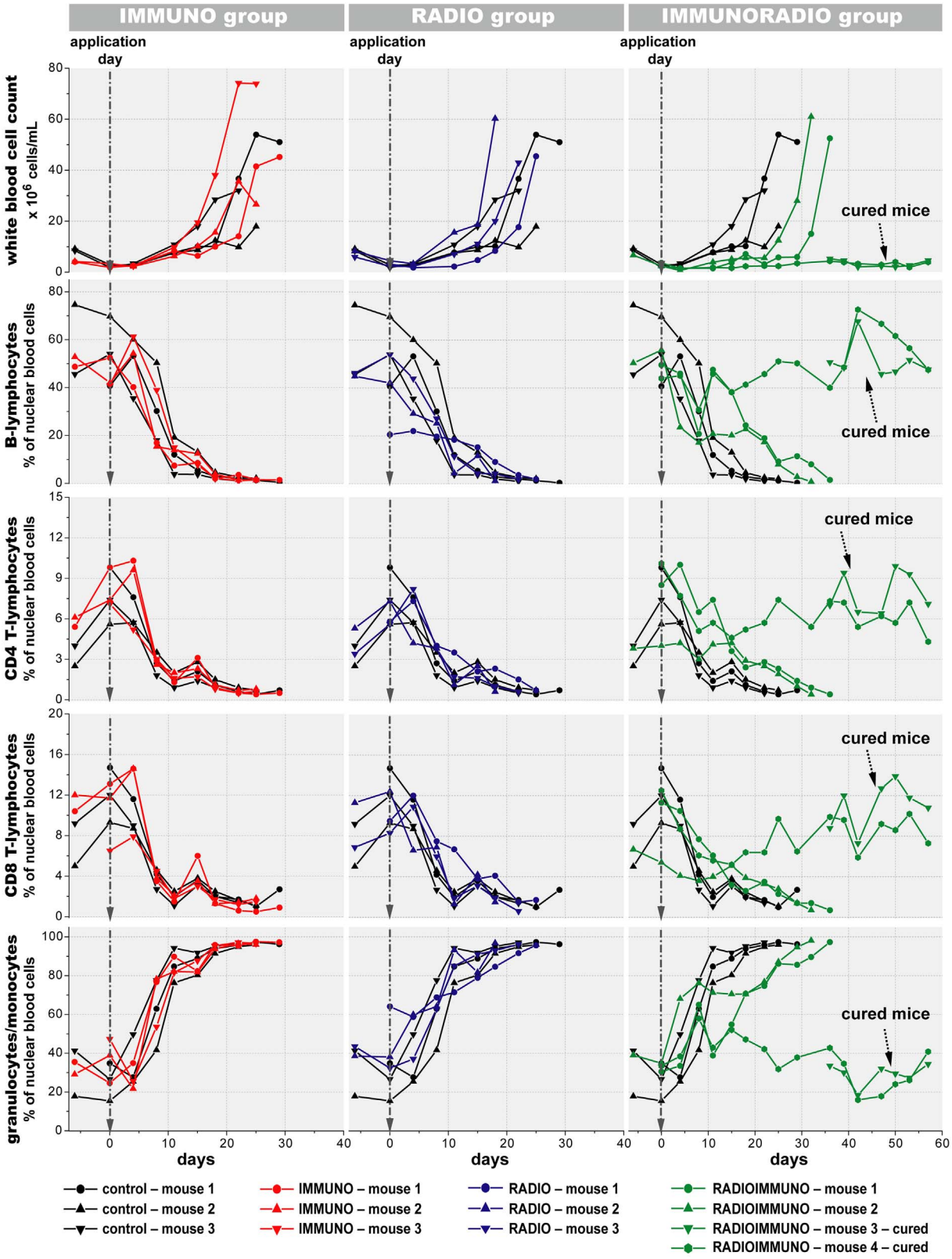

Fig. 12. The white blood cell counts and their composition (B-lymphocytes, CD4 T-lymphocytes, CD8 T-lymphocytes and granulocytes/monocytes) in the blood before and during each treatment (IMMUNO group – red lines, RADIO group – blue lines, IMMUNORADIO group – green lines) in a comparison with the control group (black lines). Three mice from each experimental group (four mice from the IMMUNORADIO group) were monitored. The curves completed earlier correspond to the death of the animal during the experiment. (For interpretation of the references to colour in this figure legend, the reader is referred to the web version of this article.)

tumor growth during the beginning of the treatment. Furthermore, 7 out of the 15 mice were completely cured in this group, while the others exhibited a significantly prolonged survival time compared to the control group. Interestingly, the tested blood parameters of the mice that cured the tumors in the immunoradiotherapy group revealed their blood count normalization, and therefore, these mice were clearly

distinguishable from the others.

Importantly, the *in vivo* experiments indicated the considerable synergistic effect of using immunoradiotherapy compared to using only immunotherapy or radiotherapy.

Acknowledgements

The financial support of the Czech Science Foundation (grants # 16-02870S and 16-03156S), the Ministry of Health of the Czech Republic (grant # 15-25781a) and the Ministry of Education, Youth and Sports (grants # 7AMB16FR042, LM2015062-CzechBioImaging, and SVV 260371/2017) is gratefully appreciated. The authors thank to Dr. Olga Trhlíková for the elemental analysis measurements.

Appendix A. Supplementary data

Supplementary data to this article can be found online at https://doi.org/10.1016/j.jconrel.2017.10.010.

References

[1] K. Shao, S. Singha, X. Clemente-Casares, S. Tsai, Y. Yang, P. Santamaria, Nanoparticle-based immunotherapy of cancer, ACS Nano 9 (2014) 16–30.
[2] Y.A. Alpizar, B. Chain, M.K. Collins, J. Greenwood, D. Katz, H.J. Stauss, N.A. Mitchison, Ten years of progress in vaccination against cancer: the need to counteract cancer evasion by dual targeting in future therapies, Cancer Immunol. Immunother. 60 (2011) 1127–1135.
[3] W. Chen, J.E. Konkel, TGF-β and "adaptive"Foxp3 + regulatory T cells, J. Mol. Cell Biol. 2 (2010) 30–36.
[4] R. Kim, M. Emi, K. Tanabe, K. Arihiro, Tumor-driven evolution of immunosuppressive networks during malignant progression, Cancer Res. 66 (2006) 5527–5536.
[5] C.A. White, R.L. Weaver, A.J. Grillo-López, Antibody-targeted immunotherapy for treatment of malignancy, Annu. Rev. Med. 52 (2001) 125–145.
[6] P. Kufer, R. Lutterbüse, P.A. Baeuerle, A revival of bispecific antibodies, Trends Biotechnol. 22 (2004) 238–244.
[7] C. May, P. Sapra, H.P. Gerber, Advances in bispecific biotherapeutics for the treatment of cancer, Biochem. Pharmacol. 84 (2012) 1105–1112.
[8] S. Rakoff-Nahoum, R. Medzhitov, Toll-like receptors and cancer, Nat. Rev. Cancer 9 (2009) 57–64.
[9] L. Vannucci, J. Krizan, P. Sima, D. Stakheev, F. Caja, L. Rajsiglova, V. Horak, M. Saieh, Immunostimulatory properties and antitumor activities of glucans, Int. J. Oncol. 43 (2013) 357–364.
[10] A. Bacic, G.B. Fincher, B.A. Stone, Chemistry, Biochemistry, and Biology of 1-3 Beta Glucans and Related Polysaccharides, Academic Press, San Diego, 2009, pp. 5–46.
[11] M. Novak, V. Vetvicka, β-glucans, history, and the present: immunomodulatory aspects and mechanisms of action, J. Immunotoxicol. 5 (2008) 47–57.
[12] G.C. Chan, W.K. Chan, D.M. Sze, The effects of β-glucan on human immune and cancer cells, J. Hematol. Oncol. 2 (2009) 2–25.
[13] K. Ina, T. Kataoka, T. Ando, The use of lentinan for treating gastric cancer, Anti Cancer Agents Med. Chem. 13 (2013) 681–688.
[14] V.E.C. Ooi, F. Liu, Immunomodulation and anti-cancer activity of polysaccharide-protein complexes, Curr. Med. Chem. 7 (2000) 715–729.
[15] S.O. Stephens, B.H. Feder, H.R. Haymond, F.W. George, Dose rate relationships in brachytherapy: an in-vivo evaluation, Int. J. Radiat. Oncol. Biol. Phys. 2 (2016) 137.
[16] M. Hruby, P. Pouckova, M. Zadinova, J. Kucka, O. Lebeda, Thermoresponsive polymeric radionuclide delivery system – an injectable brachytherapy, Eur. J. Pharm. Sci. 42 (2011) 484–488.
[17] J. Kucka, M. Hruby, O. Lebeda, Biodistribution of a radiolabelled thermoresponsive polymer in mice, Appl. Radiat. Isot. 68 (2010) 1073–1078.
[18] R. Hoogenboom, H. Schlaad, Bioinspired poly(2-oxazoline)s, Polymers 3 (2011) 467–488.
[19] O. Sedlacek, P. Cernoch, J. Kucka, R. Konefal, P. Stepanek, M. Vetrik, T.P. Lodge, M. Hruby, Thermoresponsive polymers for nuclear medicine: which polymer is the best? Langmuir 32 (2016) 6115–6122.
[20] M. Kissel, P. Peschke, V. Subr, K. Ulbrich, J. Schuhmacher, J. Debus, E. Friedrich, Synthetic macromolecular drug carriers: biodistribution of poly [(*N*-2-hydroxypropyl) methacrylamide] copolymers and their accumulation in solid rat tumors, PDA J. Pharm. Sci. Technol. 55 (2001) 191–201.
[21] Y. Seo, A. Schulz, Y. Han, Z. He, H. Bludau, X. Wan, J. Tong, T.K. Bronich, M. Sokolsky, R. Luxenhofer, R. Jordan, A.V. Kabanov, Poly(2-oxazoline) block copolymer based formulations of taxanes: effect of copolymer and drug structure, concentration, and environmental factors, Polym. Adv. Technol. 26 (2015) 837–850.
[22] S. Xu, X. Xu, L. Zhang, Branching structure and chain conformation of water-soluble glucan extracted from Auricularia auricula-judae, J. Agric. Food Chem. 60 (2012) 3498–3506.
[23] G.T. Hermanson, Bioconjugate Techniques, (1996).
[24] J. Schindelin, I. Arganda-Carreras, E. Frise, V. Kaynig, M. Longair, T. Pietzsch, S. Preibisch, C. Rueden, S. Saalfeld, B. Schmid, Fiji: an open-source platform for biological-image analysis, Nat. Methods 9 (2012) 676–682.
[25] X. Meng, H. Liang, L. Luo, Antitumor polysaccharides from mushrooms: a review on the structural characteristics, antitumor mechanisms and immunomodulating activities, Carbohydr. Res. 424 (2016) 30–41.
[26] A. Pospisilova, S.K. Filippov, A. Bogomolova, S. Turner, Glycogen-*graft*-poly(2-alkyl-2-oxazolines)–the new versatile biopolymer-based thermoresponsive macromolecular toolbox, RSC Adv. 4 (2014) 61580–61588.
[27] R. van Horssen, T.L.M. ten Hagen, A.M.M. Eggermont, TNF-α in cancer treatment: molecular insights, antitumor effects, and clinical utility, Oncologist 11 (2006) 397–408.
[28] M. Hruby, J. Kucka, O. Lebeda, H. Mackova, M. Babic, C. Konak, M. Studenovsky, A. Sikora, J. Kozempel, K. Ulbrich, New bioerodable thermoresponsive polymers for possible radiotherapeutic applications, J. Control. Release 119 (2007) 25–33.

Appendix 3

Loukotová, L.; Bogomolova, A.; Konefał, R.; Špírková, M.; Štěpánek, P.; Hrubý, M. Hybrid κ-carrageenan-based polymers showing "schizophrenic" lower and upper critical solution temperatures and potassium responsivity, *Carbohydr. Polym*., submitted article. IF = 5.158.

HYBRID κ-CARRAGEENAN-BASED POLYMERS SHOWING "SCHIZOPHRENIC" LOWER AND UPPER CRITICAL SOLUTION TEMPERATURES AND POTASSIUM RESPONSIVITY

L. Loukotová[a], A. Bogomolova[a], R. Konefal[a], M. Špírková[a], P. Štěpánek[a], M. Hrubý[a]*

[a]Institute of Macromolecular Chemistry AS CR, v. v. i., Heyrovsky sq. 2, Prague, 162 06, Czech Republic

*Corresponding author, e-mail: mhruby@centrum.cz

Graphical abstract

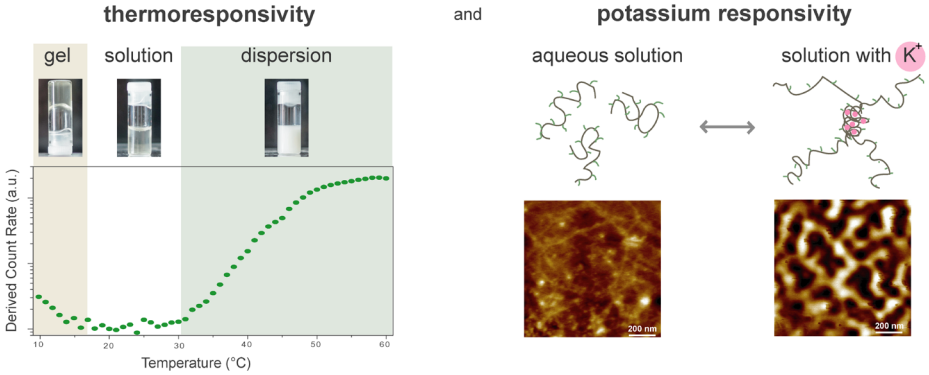

Abstract

Multiresponsive hybrid biodegradable systems of κ-carrageenan-*graft*-poly(2-isopropyl-2-oxazoline-*co*-2-butyl-2-oxazoline)s with unique combination of responsivities to external stimuli were synthesized and studied. The polymer thermoresponsive behavior proved the existence of both lower and upper critical solution temperatures in aqueous milieu, forming gel at lower temperature, molecularly dissolved solution at room temperature and cloudy nanophase-separated dispersion at elevated temperature. The limit temperatures can easily be adjusted by the polyoxazoline grafts length and grafting density. Moreover, the polymer behavior is additionally dependent on the concentration of potassium ions. The polymers behave similarly as the original κ-carrageenan, and thus, the poly(2-alkyl-2-oxazoline) grafts do not decrease the ability of the κ-carrageenan to form the self-assembled structures. Molecular principles beyond this multistimuli-responsive behavior were elucidated with the use of dynamic light scattering, magnetic resonance and fluorescence measurements as well as atomic force microscopy. These polymers could be used in a wide range of biological applications demanding thermo- and potassium-responsivity.

Keywords: carrageenan; polyoxazoline; LCST; UCST; potassium responsivity

CPT	cloud point temperature
DLS	dynamic light scattering
LCST	lower critical solution temperature
NMR	nuclear magnetic resonance
PBS	phosphate-buffered saline
POX	poly(2-alkyl-2-oxazoline)
SEC	size-exclusion chromatography
SLS	static light scattering
UCST	upper critical solution temperature

1. Introduction

Adaptive materials, represented by responsive gels, shape-memory polymers or elastomers, have been actively developed nowadays due to their high application potential in material science, medicine or biology (Stuart et al., 2010),(Ma, Guo, Anderson, & Langer, 2013). Here in many cases, diverse environment-sensitive polymeric nanoparticles are used. Such particles can precipitate, dissolve or swell as a response to an external or internal stimulus (*e.g.* temperature, pH, light or specific ion concentration) (Meng, Zhong, & Feijen, 2009). For instance, the pH-responsive polymers are designed to release a drug inside the tumor, exploiting the fact that the solid tumor tissue shows slightly acidic environment (pH 6.5 – 7.2) in comparison to the blood and the normal tissues (physiological pH 7.4) (Chen, Meng, Li, Ji, & Zhong, 2009). Another example of environment-sensitive polymers is thermoresponsive polymers, which are envisioned in a wide range of biological applications, exploiting the temperature difference of a body and its surroundings, *e.g*. controlled drug delivery and release (Hrubý et al., 2005), smart surfaces (Hatakeyama, Kikuchi, Yamato, & Okano, 2007) or bioseparation processes (Shamim, Hong, Hidajat, & Uddin, 2007).

The thermoresponsive polymers exhibit sudden changes in their solubility at either a lower critical solution temperature (LCST) or an upper critical solution temperature (UCST), while those with the LCST behavior in the aqueous solutions are in abundance. Such behavior is based on the extensive hydrogen bonding interactions between polymers and surrounding water molecules at lower temperatures, while upon heating, the hydrogen bonds with water are disrupted and the intra-/intermolecular bonding and hydrophobic domain interactions become more preferable, resulting in a transition in their solubility (Fujishige, Kubota, & Ando, 1989). The earliest report of thermoresponsive phase transition of poly(*N*-isopropylacrylamide) (PNIPAM) is dated to 1967 (Priest, Murray, Nelson, & Hoffman, 1987), however, nowadays various polymers are known to possess such property. One of these polymer classes attracting increasing interest is poly(2-alkyl-2-oxazoline)s (POXs). They are highly defined polypeptide-like polymers with easily tunable thermoresponsive properties (Hoogenboom & Schlaad, 2011). Moreover, POXs are biocompatible and relatively radioresistant in comparison with other thermoresponsive polymers (Sedláček et al., 2016).

On the other hand, also the polymers that exhibit reduced solubility upon cooling (those with UCST) are a topic of increasing interest last years. An interesting example of such polymers is polysaccharide carrageenan, which is present in a random coil conformation in hot solutions, while upon cooling it is transformed into a gel due to the formation of rigid helical rods (Funami et al., 2007). Moreover, the helices of κ-carrageenan further aggregates in the presence of K^+ ions form a stable gel (Gulrez, Al-Assaf, & Phillips, 2011). Additionally, the carrageenans are commonly known to show interesting biological activities, especially they can influence the immune system. Therefore, they are often used as agents for the induction of experimental inflammation (Morris, 2003), and they exhibit antitumor activity, inhibition of cancer metastasis and complement activation (Campo, Kawano, da Silva, & Carvalho, 2009). κ-Carrageenan oligosaccharides from *Kappaphycus striatum* and their different chemical modifications were successfully tested on S180-bearing mice, showing the antitumor and immunomodulation effects (Yuan, Song, Li, Li, & Liu, 2011).

We have designed a novel thermoresponsive and potassium-responsive system – κ-carrageenan-*graft*-poly(2-isopropyl-2-oxazoline-*co*-2-butyl-2-oxazoline), which would combine the UCST behavior and potassium responsivity of carrageenan and LCST behavior of poly(2-isopropyl-2-oxazoline-*co*-2-butyl-2-oxazoline). Such polymers would be usable in a wide range of applications demanding thermo- and potassium responsivity as well as the described above biological properties of κ-carrageenan. To study them and understand their behavior is a crucial point for their subsequent applications. In this study, the thermoresponsive properties of κ-carrageenan-*graft*-poly(2-isopropyl-2-

oxazoline-*co*-2-butyl-2-oxazoline)s were studied in the context of their grafting density and length using dynamic light scattering, nuclear magnetic resonance, fluorescence measurement and atomic force microscopy to elucidate molecular interaction background beyond the observed phenomena of stimuli responsivity. The main aim of this article is the elucidation of the principles and structure-solution behavior relationships of stimuli-dependent κ-carrageenan-*graft*-poly(2-isopropyl-2-oxazoline-*co*-2-butyl-2-oxazoline)s that should allow to fine-tune the responsivity of such systems to temperature and potassium ion concentration changes as needed in a more general applicable manner.

2. Experimental

2.1 Materials

Diethyl ether, dimethyl sulfoxide, sodium chloride and toluene were purchased from Lachner Ltd. (Neratovice, Czech Republic). Dialysis membranes Spectra/Por (molecular weight cut-off (MWCO) 6 –8 kDa) were purchased from P-LAB (Prague, Czech Republic). 2-Butyl-2-oxazoline and 2-isopropyl-2-oxazoline were synthesized according to ref. (Seo et al., 2015). All other chemicals were purchased from Sigma Aldrich Ltd. (Prague, Czech Republic). The commercial κ-carrageenan was purchased from Sigma Aldrich Ltd. (catalogue number: C1013, CAS: 9000-07-1). Its molecular weight was determined using static light scattering to be M_w = 543 kDa ± 15% and the radius of gyration to be R_g = 107 nm. The type composition of this commercial κ-carrageenan was checked using both nuclear magnetic resonance (NMR) and Fourier-transform infrared spectroscopy (FTIR) (Turquois, Acquistapace, Vera, & Welti, 1996), showing the composition is 84 % κ-carrageenan and 16 % ι-carrageenan (see **Fig. S1** in the Supplementary Material). The chemicals were used without further purification unless stated otherwise.

2.2 Synthesis of carrageenan-*graft*-poly(2-isopropyl-2-oxazoline-*co*-2-butyl-2-oxazoline)s – $M_{n,theor,grafts}$ = 1000 Da.

2.2.1 Sample C1

Methyl *p*-toluenesulfonate (2.0005 g, 10.8 mmol) was added to a solution of 2-isopropyl-2-oxazoline (7.000 mL, 61.9 mmol) and 2-butyl-2-oxazoline (2.616 mL, 20.6 mmol) in 10 mL of anhydrous acetonitrile, and the reaction mixture was stirred overnight at 70 °C under an argon atmosphere. This solution was named as POX-1000 solution. The POX-1000 solution (1 mL) was mixed with water (1 mL), and the crude product was purified on a Sephadex® LH-20 column using methanol as the mobile phase and evaporated to give polymer POX-1000 (385 mg).

Carrageenan (0.50 g, $M_w = 5.4 \times 10^5$ Da) was dissolved in 35 mL of anhydrous dimethyl sulfoxide, and this solution was then azeotropically dried using anhydrous toluene. Sodium hydride (0.50 g of 60% dispersion in mineral oil, 16.7 mmol) was added to the carrageenan solution, and the mixture was stirred for 3 h at 70 °C. The POX-1000 solution (7.00 mL) was then mixed with the carrageenan solution, and the resulting mixture was stirred overnight at 70 °C. Water (35 mL) was added to the reaction mixture, and it was twice washed with diethyl ether to remove the mineral oil. The aqueous layer was dialyzed (MWCO 6 – 8 kDa) against water for 72 h and freeze dried to give the desired product C1 (546 mg).

^{1}H-NMR of POX-1000 (600 MHz, acetone), δ (ppm): 0.88 (–CH_2–CH_2–CH_2–***CH_3***), 1.03 (–CH–(***CH_3***)$_2$), 1.32 (–CH_2–CH_2–***CH_2***–CH_3), 1.53 (–CH_2–***CH_2***–CH_2–CH_3), 2.33 (–***CH_2***–CH_2–CH_2–CH_3), 2.7–2.9 (–***CH***–$(CH_3)_2$), 3.48 (–N–***CH_2***–CH_2–). Size-exclusion chromatography (SEC) of POX-1000: M_n = 860 Da, I = 1.08.

^{1}H-NMR of C1(600 MHz, dimethyl sulfoxide – DMSO), δ (ppm): 0.85 (–CH_2–CH_2–CH_2–***CH_3***), 0.97 (–CH–(***CH_3***)$_2$), 1.23 (–CH_2–CH_2–***CH_2***–CH_3), 1.45 (–CH_2–***CH_2***–CH_2–CH_3), 2.25 (–***CH_2***–CH_2–CH_2–CH_3), 2.63–2.97 (–***CH***–$(CH_3)_2$), 3.25 (G4S: H2 – for the proton peaks assignments see **Fig. 4B**), 3.38 (–N–***CH_2***–CH_2–), 3.52 (G4S: H6), 3.66 (G4S: H3), 3.82 (DA: H2, H6), 4.14 (DA:

H3), 4.35 (DA: H4, H5, G4S: H1), 4.45 (G4S: H4), 4.97 (DA: H1). ^{13}C-NMR of C1 (600 MHz, DMSO), δ (ppm): 13.87, 19.80, 21.93, 27.00, 28.95, 31.49, 44.90, 59.92, 68.88, 69.90, 70.74, 73.84, 75.90, 78.67, 94.66, 103.41, 172.56, 176.78. Elemental analysis of C1: C 41.03 %, H 6.51 %, N 3.93 %. SEC of C1: $M_w = 2.3 \times 10^6$ Da, $I = 1.94$.

2.2.2 Sample C2

The general procedure is described above in the section *2.2.1 Sample C1*. Here, the POX-1000 solution (5.00 mL) was mixed with the carrageenan solution. The resulting polymer was marked as C2 (438 mg).

^{1}H-NMR of C2 (300 MHz, DMSO), δ (ppm): 0.85 (–CH_2–CH_2–CH_2–***CH_3***), 0.96 (–CH–(***CH_3***)$_2$), 1.23 (–CH_2–CH_2–***CH_2***–CH_3), 1.43 (–CH_2–***CH_2***–CH_2–CH_3), 2.27 (–***CH_2***–CH_2–CH_2–CH_3), 2.63–2.97 (–***CH***–$(CH_3)_2$), 3.25 (G4S: H2), 3.37 (–N–***CH_2***–CH_2–), 3.51 (G4S: H6), 3.66 (G4S: H3), 3.81 (DA: H2, H6), 4.15 (DA: H3), 4.36 (DA: H4, H5, G4S: H1), 4.45 (G4S: H4), 4.97 (DA: H1). ^{13}C-NMR of C2 (300 MHz, DMSO), δ (ppm): 13.86, 19.78, 21.91, 27.00, 28.95, 31.51, 44.94, 59.92, 68.90, 69.94, 70.77, 73.84, 75.87, 78.69, 94.66, 103.40, 172.56, 176.80. Elemental analysis of C2: C 37.07 %, H 6.08 %, N 3.05 %. SEC of C2: $M_w = 1.7 \times 10^6$ Da, $I = 2.02$.

2.2.3 Sample C3

The general procedure is described above in the section *2.2.1 Sample C1*. Here, the POX-1000 solution (2.50 mL) was mixed with the carrageenan solution. The resulting polymer was marked as C3 (398 mg).

^{1}H-NMR of C3 (600 MHz, DMSO), δ (ppm): 0.84 (–CH_2–CH_2–CH_2–***CH_3***), 0.96 (–CH–(***CH_3***)$_2$), 1.23 (–CH_2–CH_2–***CH_2***–CH_3), 1.43 (–CH_2–***CH_2***–CH_2–CH_3), 2.25 (–***CH_2***–CH_2–CH_2–CH_3), 2.63–2.97 (–***CH***–$(CH_3)_2$), 3.25 (G4S: H2), 3.42 (–N–***CH_2***–CH_2–), 3.51 (G4S: H6), 3.66 (G4S: H3), 3.82 (DA: H2, H6), 4.14 (DA: H3), 4.35 (DA: H4, H5, G4S: H1), 4.45 (G4S: H4), 4.97 (DA: H1). ^{13}C-NMR of C3 (600 MHz, DMSO), δ (ppm): 13.89, 19.82, 21.93, 27.11, 28.97, 30.99, 44.77, 59.94, 68.89, 69.89, 70.75, 73.86, 75.87, 78.69, 94.61, 103.42, 172.66, 176.59. Elemental analysis of C3: C 35.22 %, H 5.70 %, N 2.15 %. SEC of C3: $M_w = 2.0 \times 10^6$ Da, $I = 2.02$.

2.2.4 Sample C4

The general procedure is described above in the section *2.2.1 Sample C1*. Here, the POX-1000 solution (0.75 mL) was mixed with the carrageenan solution. The resulting polymer was marked as C4 (379 mg).

^{1}H-NMR of C4 (600 MHz, DMSO), δ (ppm): 0.84 (–CH_2–CH_2–CH_2–***CH_3***), 0.97 (–CH–(***CH_3***)$_2$), 1.23 (–CH_2–CH_2–***CH_2***–CH_3), 1.45 (–CH_2–***CH_2***–CH_2–CH_3), 2.25 (–***CH_2***–CH_2–CH_2–CH_3), 2.63–2.97 (–***CH***–$(CH_3)_2$), 3.25 (G4S: H2), 3.38 (–N–***CH_2***–CH_2–), 3.52 (G4S: H6), 3.66 (G4S: H3), 3.82 (DA: H2, H6), 4.14 (DA: H3), 4.35 (DA: H4, H5, G4S: H1), 4.45 (G4S: H4), 4.97 (DA: H1). ^{13}C-NMR of C4 (600 MHz, DMSO), δ (ppm): 13.87, 19.80, 21.93, 27.00, 28.95, 31.49, 44.90, 59.94, 68.89, 69.89, 70.74, 73.87, 75.88, 78.69, 94.57, 103.42, 172.56, 176.78. Elemental analysis of C4: C 32.48 %, H 5.31 %, N 0.97 %. SEC of C4: $M_w = 1.0 \times 10^6$ Da, $I = 1.55$.

2.3 Synthesis of carrageenan-*graft*-poly(2-isopropyl-2-oxazoline-*co*-2-butyl-2-oxazoline)s – $M_{n,theor,grafts}$ = 2500 Da.

2.3.1 Sample C5

Methyl *p*-toluenesulfonate (0.8060 g, 4.3 mmol) was added to a solution of 2-isopropyl-2-oxazoline (7.000 mL, 61.9 mmol) and 2-butyl-2-oxazoline (2.616 mL, 20.6 mmol) in 10 mL of anhydrous acetonitrile, and the reaction mixture was stirred overnight at 70 °C under an argon atmosphere. This solution was named as POX-2500 solution. The POX-2500 solution (1 mL) was mixed with water (1 mL), and the crude product was purified on a Sephadex® LH-20 column using methanol as the mobile phase and evaporated to give polymer POX-2500 (0.4020 g).

Carrageenan (0.50 g) was dissolved in 35 mL of anhydrous dimethyl sulfoxide, and this solution was then azeotropically dried using anhydrous toluene. Sodium hydride (0.50 g of 60% dispersion in mineral oil, 16.7 mmol) was added to the carrageenan solution, and the mixture was stirred for 3 h at 70 °C. The POX-2500 solution (9.00 mL) was then mixed with the carrageenan solution and the resulting mixture was stirred overnight at 70 °C. Water (35 mL) was added to the reaction mixture, and it was twice washed with diethyl ether to remove the mineral oil. The aqueous layer was dialyzed (MWCO 6 –8 kDa) against water for 72 h and freeze dried to give the desired product C5 (438 mg).

^{1}H-NMR of POX-2500 (600 MHz, acetone), δ (ppm): 0.89 (–CH_2–CH_2–CH_2–C***H₃***), 1.04 (–CH–(C***H₃***)$_2$), 1.33 (–CH_2–CH_2–C***H₂***–CH_3), 1.54 (–CH_2–C***H₂***–CH_2–CH_3), 2.32 (–C***H₂***–CH_2–CH_2–CH_3), 2.7–2.9 (–C***H***–$(CH_3)_2$), 3.49 (–N–C***H₂***–CH_2–). SEC of POX-2500: M_n = 1950 Da, I = 1.15.

^{1}H-NMR of C5 (300 MHz, DMSO), δ (ppm): 0.84 (–CH_2–CH_2–CH_2–***CH₃***), 0.95 (–CH–(***CH₃***)$_2$), 1.24 (–CH_2–CH_2–***CH₂***–CH_3), 1.42 (–CH_2–***CH₂***–CH_2–CH_3), 2.27 (–***CH₂***–CH_2–CH_2–CH_3), 2.63–2.97 (–***CH***–$(CH_3)_2$), 3.44 (–N–***CH₂***–CH_2–), 3.66 (G4S: H3), 3.81 (DA: H2, H6), 4.14 (DA: H3), 4.36 (DA: H4, H5, G4S: H1), 4.45 (G4S: H4), 4.97 (DA: H1). ^{13}C-NMR of C5 (300 MHz, DMSO), δ (ppm): 13.86, 19.79, 21.92, 27.04, 28.96, 31.52, 44.90, 59.93, 68.90, 69.92, 70.77, 73.84, 75.87, 78.72, 94.65, 103.42, 172.55, 176.78. Elemental analysis of C5: C 50.84 %, H 8.26 %, N 7.59 %. SEC of C5 $M_w = 4.5 \cdot 10^6$ Da, I = 2.06.

2.3.2 Sample C6

The general procedure is described above in the section *2.3.1 Sample C5*. Here, the POX-2500 solution (5.00 mL) was mixed with the carrageenan solution. The resulting polymer was marked as C6 (438 mg).

^{1}H-NMR of C6 (600 MHz, DMSO), δ (ppm): 0.84 (–CH_2–CH_2–CH_2–***CH₃***), 0.96 (–CH–(***CH₃***)$_2$), 1.25 (–CH_2–CH_2–***CH₂***–CH_3), 1.43 (–CH_2–***CH₂***–CH_2–CH_3), 2.25 (–***CH₂***–CH_2–CH_2–CH_3), 2.63–2.97 (–***CH***–$(CH_3)_2$), 3.25 (G4S: H2), 3.38 (–N–***CH₂***–CH_2–), 3.67 (G4S: H3), 3.82 (DA: H2, H6), 4.14 (DA: H3), 4.35 (DA: H4, H5, G4S: H1), 4.45 (G4S: H4), 4.97 (DA: H1). ^{13}C-NMR of C6 (600 MHz, DMSO), δ (ppm): 13.87, 19.80, 21.93, 27.00, 28.95, 31.49, 44.90, 59.92, 68.88, 69.90, 70.74, 73.84, 75.90, 78.67, 94.66, 103.41, 172.56, 176.78. Elemental analysis of C6: C 49.51 %, H 8.00 %, N 7.06 %. SEC of C6: $M_w = 2.0 \cdot 10^6$ Da, I = 1.60.

2.3.3 Sample C7

The general procedure is described above in the section *2.3.1 Sample C5*. Here, the POX-2500 solution (2.50 mL) was mixed with the carrageenan solution. The resulting polymer was marked as C7 (438 mg).

^{1}H-NMR of C7 (600 MHz, DMSO), δ (ppm): 0.84 (–CH_2–CH_2–CH_2–***CH₃***), 0.96 (–CH–(***CH₃***)$_2$), 1.25 (–CH_2–CH_2–***CH₂***–CH_3), 1.42 (–CH_2–***CH₂***–CH_2–CH_3), 2.26 (–***CH₂***–CH_2–CH_2–CH_3), 2.63–2.97 (–***CH***–$(CH_3)_2$), 3.24 (G4S: H2), 3.41 (–N–***CH₂***–CH_2–), 3.51 (G4S: H6), 3.66 (G4S: H3), 3.82 (DA: H2, H6), 4.14 (DA: H3), 4.35 (DA: H4, H5, G4S: H1), 4.45 (G4S: H4), 4.97 (DA: H1). ^{13}C-NMR of C7 (600 MHz, DMSO), δ (ppm): 13.89, 19.81, 21.93, 27.05, 28.96, 31.49, 44.84, 59.95, 68.90, 69.90, 70.75, 73.84, 75.87, 78.71, 94.62, 103.42, 172.42, 176.81. Elemental analysis of C7: C 41.01 %, H 6.81 %, N 4.05 %. SEC of C7: $M_w = 1.2 \cdot 10^6$ Da, I = 2.08.

2.3.4 Sample C8

The general procedure is described above in the section *2.3.1 Sample C5*. Here, the POX-2500 solution (0.75 mL) was mixed with the carrageenan solution. The resulting polymer was marked as C8 (438 mg).

^{1}H-NMR of C8 (600 MHz, DMSO), δ (ppm): 0.84 (–CH_2–CH_2–CH_2–***CH₃***), 0.96 (–CH–(***CH₃***)$_2$), 1.22 (–CH_2–CH_2–***CH₂***–CH_3), 1.43 (–CH_2–***CH₂***–CH_2–CH_3), 2.25 (–***CH₂***–CH_2–CH_2–CH_3), 2.63–2.97 (–***CH***–$(CH_3)_2$), 3.24 (G4S: H2), 3.40 (–N–***CH₂***–CH_2–), 3.51 (G4S: H6), 3.66 (G4S: H3), 3.81 (DA:

H2, H6), 4.14 (DA: H3), 4.35 (DA: H4, H5, G4S: H1), 4.45 (G4S: H4), 4.97 (DA: H1). ^{13}C-NMR of C8 (600 MHz, DMSO), δ (ppm): 13.88, 19.81, 21.95, 27.00, 28.97, 31.48, 44.85, 59.94, 68.90, 69.90, 70.75, 73.85, 75.87, 78.66, 94.61, 103.42, 172.54, 176.81 Elemental analysis of C8: C 35.16 %, H 5.87 %, N 1.80 %. SEC of C8: $M_w = 9.5 \cdot 10^5$ Da, $I = 2.15$.

2.4 Synthesis of carrageenan-*graft*-poly(2-isopropyl-2-oxazoline-*co*-2-butyl-2-oxazoline)s – $M_{n,theoretical,grafts}$ = 5000 Da.

2.4.1 Sample C9

Methyl *p*-toluenesulfonate (0.4030 g, 2.1 mmol) was added to a solution of 2-isopropyl-2-oxazoline (7.000 mL, 61.9 mmol) and 2-butyl-2-oxazoline (2.616 mL, 20.6 mmol) in 10 mL of anhydrous acetonitrile, and the reaction mixture was stirred overnight at 70 °C under an argon atmosphere. This solution was named as POX-5000 solution. The POX-5000 solution (1 mL) was mixed with water (1 mL), and the crude product was purified on a Sephadex® LH-20 column using methanol as the mobile phase and evaporated to give polymer POX-5000 (0.3935 g).

Carrageenan (0.50 g) was dissolved in 35 mL of anhydrous dimethyl sulfoxide, and this solution was then azeotropically dried using anhydrous toluene. Sodium hydride (0.50 g of 60% dispersion in mineral oil, 16.7 mmol) was added to the carrageenan solution, and the mixture was stirred for 3 h at 70 °C. The POX-5000 solution (9.00 mL) was then mixed with the carrageenan solution and the resulting mixture was stirred overnight at 70 °C. Water (35 mL) was added to the reaction mixture, and it was twice washed with diethyl ether to remove the mineral oil. The aqueous layer was dialyzed (MWCO 6 – 8 kDa) against water for 72 h and freeze dried to give the desired product C9 (438 mg).

^{1}H-NMR of POX-5000 (600 MHz, acetone), δ (ppm): 0.89 (–CH_2–CH_2–CH_2–C***H*****$_3$**), 1.04 (–CH–(C***H*****$_3$**)$_2$), 1.34 (–CH_2–CH_2–C***H*****$_2$**–CH_3), 1.54 (–CH_2–C***H*****$_2$**–CH_2–CH_3), 2.32 (–C***H*****$_2$**–CH_2–CH_2–CH_3), 2.7–2.9 (–C***H***–$(CH_3)_2$), 3.49 (–N–C***H*****$_2$**–CH_2–). SEC of POX-5000: M_n = 4350 Da, I = 1.10.

^{1}H-NMR of C9 (600 MHz, DMSO), δ (ppm): 0.84 (–CH_2–CH_2–CH_2–***CH*****$_3$**), 0.96 (–CH–(***CH*****$_3$**)$_2$), 1.25 (–CH_2–CH_2–***CH*****$_2$**–CH_3), 1.43 (–CH_2–***CH*****$_2$**–CH_2–CH_3), 2.25 (–***CH*****$_2$**–CH_2–CH_2–CH_3), 2.63–2.97 (–***CH***–$(CH_3)_2$), 3.37 (–N–***CH*****$_2$**–CH_2–), 3.66 (G4S: H3), 3.82 (DA: H2, H6), 4.15 (DA: H3), 4.34 (DA: H4, H5, G4S: H1), 4.45 (G4S: H4), 4.97 (DA: H1). ^{13}C-NMR of C9 (600 MHz, DMSO), δ (ppm): 13.85, 19.78, 21.92, 27.00, 28.94, 31.49, 44.91, 59.96, 68.80, 69.92, 70.86, 73.67, 75.94, 78.76, 94.74, 103.58, 172.38, 176.76. Elemental analysis of C9: C 56.20 %, H 8.77 %, N 9.50 %. SEC of C9: $M_w = 6.3 \cdot 10^6$ Da, I = 1.57.

2.4.2 Sample C10

The general procedure is described above in the section *2.4.1 Sample C9*. Here, the POX-5000 solution (5.00 mL) was mixed with the carrageenan solution. The resulting polymer was marked as C10 (438 mg).

^{1}H-NMR of C10 (300 MHz, DMSO), δ (ppm): 0.85 (–CH_2–CH_2–CH_2–***CH*****$_3$**), 0.96 (–CH–(***CH*****$_3$**)$_2$), 1.23 (–CH_2–CH_2–***CH*****$_2$**–CH_3), 1.42 (–CH_2–***CH*****$_2$**–CH_2–CH_3), 2.26 (–***CH*****$_2$**–CH_2–CH_2–CH_3), 2.63–2.97 (–***CH***–$(CH_3)_2$), 3.40 (–N–***CH*****$_2$**–CH_2–), 3.65 (G4S: H3), 3.81 (DA: H2, H6), 4.14 (DA: H3), 4.35 (DA: H4, H5, G4S: H1), 4.45 (G4S: H4), 4.97 (DA: H1). ^{13}C-NMR of C10 (300 MHz, DMSO), δ (ppm): 13.84, 19.76, 21.91, 27.00, 28.96, 31.49, 44.91, 59.89, 68.86, 69.90, 70.74, 73.88, 75.91, 78.71, 94.71, 103.36, 172.50, 176.72. Elemental analysis of C10: C 54.40 %, H 8.40 %, N 8.77 %. SEC of C10: $M_w = 5.4 \cdot 10^6$ Da, I = 1.42.

2.4.3 Sample C11

The general procedure is described above in the section *2.4.1 Sample C9*. Here, the POX-5000 solution (2.50 mL) was mixed with the carrageenan solution. The resulting polymer was marked as C11 (438 mg).

^{1}H-NMR of C11 (300 MHz, DMSO), δ (ppm): 0.85 (–CH_2–CH_2–CH_2–***CH_3***), 0.96 (–CH–(***CH_3***)$_2$), 1.23 (–CH_2–CH_2–***CH_2***–CH_3), 1.42 (–CH_2–***CH_2***–CH_2–CH_3), 2.27 (–***CH_2***–CH_2–CH_2–CH_3), 2.63–2.97 (–***CH***–$(CH_3)_2$), 3.51 (–N–***CH_2***–CH_2–), 3.81 (DA: H2, H6), 4.14 (DA: H3), 4.36 (DA: H4, H5, G4S: H1), 4.46 (G4S: H4), 4.97 (DA: H1). ^{13}C-NMR of C11 (300 MHz, DMSO), δ (ppm): 13.84, 19.78, 21.92, 27.01, 28.96, 31.50, 44.87, 59.92, 68.89, 69.91, 70.76, 73.85, 75.87, 78.68, 94.64, 103.40, 172.59, 176.78.Elemental analysis of C11: C 40.64 %, H 6.32 %, N 3.33 %. SEC of C11: $M_w = 9. \cdot 10^5$ Da, $I = 1.89$.

2.4.4 Sample C12

The general procedure is described above in the section *2.4.1 Sample C9*. Here, the POX-5000 solution (0.75 mL) was mixed with the carrageenan solution. The resulting polymer was marked as C12 (438 mg).

^{1}H-NMR of C12 (300 MHz, DMSO), δ (ppm): 0.85 (–CH_2–CH_2–CH_2–***CH_3***), 0.96 (–CH–(***CH_3***)$_2$), 1.23 (–CH_2–CH_2–***CH_2***–CH_3), 1.45 (–CH_2–***CH_2***–CH_2–CH_3), 2.25 (–***CH_2***–CH_2–CH_2–CH_3), 2.63–2.97 (–***CH***–$(CH_3)_2$), 3.38 (–N–***CH_2***–CH_2–), 3.65 (G4S: H3), 3.81 (DA: H2, H6), 4.14 (DA: H3), 4.36 (DA: H4, H5, G4S: H1), 4.45 (G4S: H4), 4.97 (DA: H1). ^{13}C-NMR of C12 (300 MHz, DMSO), δ (ppm): 13.81, 19.72, 21.93, 27.01, 28.95, 31.48, 44.99, 59.91, 68.85, 69.90, 70.73, 73.87, 75.84, 78.67, 94.64, 103.39, 172.66, 176.70.. Elemental analysis of C12: C 36.36 %, H 5.60 %, N 1.81 %. SEC of C12: $M_w = 5.3 \cdot 10^6$ Da, $I = 1.68$.

2.5 Characterization

^{1}H-NMR, ^{13}C-NMR spectra and the temperature dependences of ^{1}H-NMR spectra were recorded on a Bruker Avance DPX-300 spectrometer and on a Bruker Avance III 600 spectrometer (both Bruker Co., Austria). The width of 90° pulse was 10 μs, the relaxation delay 10 s, the acquisition time 2.18 s and 16 scans were performed. The integrated intensities were determined using the spectrometer integration software with an accuracy of ±1 %. Before measurement the samples were equilibrated at the desired temperature for at least 10 min. Fourier transform infrared (FTIR) measurements were carried out on a Perkin-Elmer Paragon 1000PC spectrometer (Perkin-Elmer Co., USA) equipped with a Specac MKII Golden Gate single attenuated total reflection (ATR) system (Perkin-Elmer Co., USA). Elemental analysis was performed on a Perkin-Elmer Series II CHNS/O Analyzer 2400 (PE Systems Ltd., Czech Republic) instrument.

The molecular weights of the grafts were determined by size exclusion chromatography (SEC) using an HPLC Ultimate 3000 system (Dionex, USA) equipped with a SEC column (TSKgel SuperAW3000 150 × 6 mm, 4 μm) and three detectors: UV/VIS, refractive index (RI) Optilab®-rEX and multi-angle light scattering (MALS) DAWN EOS (Wyatt Technology Co., USA). The mixture (80:20 volume %) of methanol and sodium acetate buffer (0.3 M, pH = 6.5) was used as the mobile phase. The molecular weight of the prepared polymers was determined using the same SEC system, here, equipped with a PL gel MIXED-B-LS (10 μm) column. The solution of lithium bromide in dimethyl sulfoxide (0.1 M) was used as the mobile phase. Static light scattering was carried out on an ALV instrument equipped with a 30 mW He-Ne laser (vertically polarized light at $\lambda = 632.8$ nm) in the angular range of 30 – 150 °. The Zimm plot procedure was used for M_w determination.

The CPTs of the polymers were determined in 0.15 M NaCl solution at 2.5 mg/mL using the dynamic light scattering technique. The temperature dependence of the polymer hydrodynamic radius (R_h) was measured on a Zetasizer Nano-ZS, Model ZEN3600 (Malvern Instruments, UK) at the scattering angle $\theta = 173°$ from 10 to 65 °C with a heating rate of 1 °C/min (using the DTS software – version 6.20 for data evaluation). The thermoresponsive behavior of the polymers was also studied using fluorescence measurements on a RF 5302 Shimadzu spectrofluorometer (Shimadzu, Japan). The samples for atomic force microscopy (AFM) characterization were prepared on freshly cleaved mica. The polymer was

dissolved in water (0.5 mg/mL) and equilibrated at room temperature overnight. The cleaved mica was soaked in a polymer solution and quickly dried under vacuum. All images were acquired using a Dimension Icon® Atomic Force Microscope System (Bruker Co., USA) under air in the tapping mode: 256 × 256 pixel topography and phase scans were with an SSS-NCHR probe, Super Sharp Silicon™–SPM-Sensor from NanoSensors™ Switzerland with a spring constant of 33 Nm^{-1}, resonant frequency of 388 kHz and tip radius of curvature of 2 nm. The size of obtained square scans was in the range from 0.25 to 2500 μm^2 at scan rates from 0.4 to 1 Hz. The Nano Scope Analysis software (Bruker Co., USA) was used for image processing.

3. Results and discussion

The prepared polymers κ-carrageenan-*graft*-poly(2-isopropyl-2-oxazoline-*co*-2-butyl-2-oxazoline)s were designed as the novel stimuli-responsive biodegradable peptidoglycan-like polymers, which exhibit two phase transition through the temperature range – the gelation point at lower temperatures (due to the κ-carrageenan backbone) and the cloud point temperature (CPT) at higher temperatures (due to the polyoxazoline grafts). Moreover, the polymers were supposed to be potassium-responsive as the original κ-carrageenan, which forms a stable gel in the presence of K^+ ions. These polymers are intended to be used in a wide range of biological and medical applications demanding thermo- and potassium-responsivity.

3.1 Synthesis and characterization

For all the synthesis was used the commercial κ-carrageenan, which has molecular weight M_w = 543 kDa ± 15% and the radius of gyration R_g = 107 nm (determined using static light scattering). The type composition of the sample was checked using both nuclear magnetic resonance (NMR) and Fourier-transform infrared spectroscopy (FTIR). The measure spectra are in the **Fig. S1** in the Supplementary Material. ^{1}H-NMR spectra revealed the ratio of the contained κ-carrageenan to ι-carrageenan (rκ), which was calculated according to the equation (1):

$$r\kappa = 100 * I\kappa / (I\iota + I\kappa) \quad (1)$$

where Iι and Iκ are intensities of the signals DA2S H1 and DA H1, respectively (**Fig. S1A** in the Supplementary Material). Therefore, the used κ-carrageenan contains 84 % of κ-carrageenan and 16 %of ι-carrageenan (Van de Velde, Knutsen, Usov, Rollema, & Cerezo, 2002). Moreover, FTIR spectrum of the sample exhibited the presence of both κ-carrageenan and ι-carrageenan (**Fig. S1B** in the Supplementary Material), however, the peaks typical for λ-carrageenan (830 and 820 cm^{-1}) were not observed, and thus, its contain in the used sample is negligible (Turquois et al., 1996).

All polymer grafts were synthesized by cationic ring opening polymerization of 2-isopropyl-2-oxazoline and 2-butyl-2-oxazoline with methyl *p*-toluenesulfonate as an initiator. The living graft ends were terminated with sodium carrageenanate to give carrageenan-*graft*-poly(2-isopropyl-2-oxazoline-*co*-2-butyl-2-oxazoline). In a separate vessel, the living ends were terminated with water to obtain polyoxazoline (POX) grafts with corresponding lengths and with –OH ending groups, which allowed us to study the corresponding graft properties separately from the properties of the grafted polymers.

The general synthetic procedure for all polymers is illustrated in **Fig. 1**. We have successfully prepared twelve different samples of carrageenan-*graft*-poly(2-isopropyl-2-oxazoline-*co*-2-butyl-2-oxazoline)s varying in the graft length and density (1000 Da – C1-C4, 2500 Da – C5-C8 and 5000 Da – C9-C12) in order to study the temperature-dependent solution behavior in the context of graft length and grafting density.

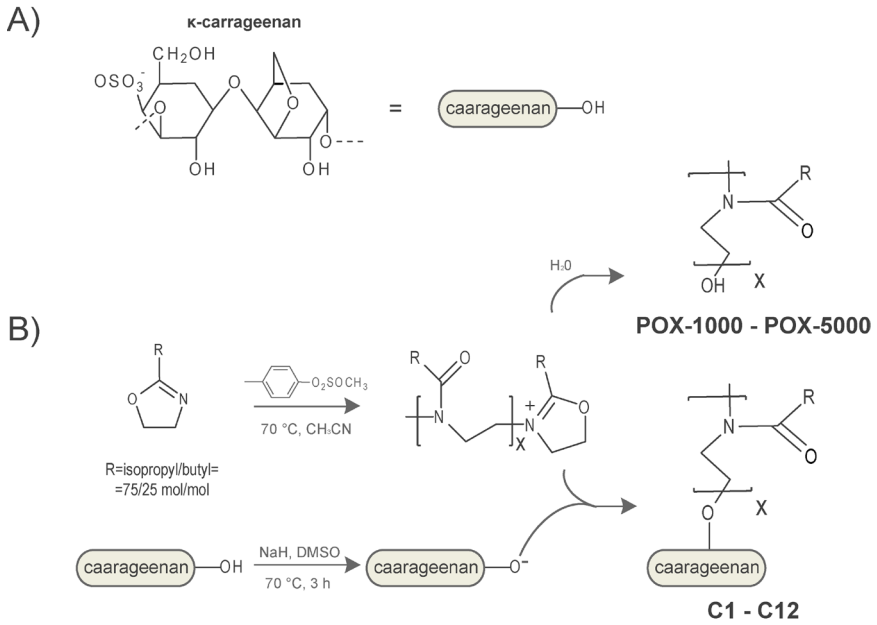

Figure 1. A) Structure of κ-carrageenan, B) general synthetic scheme for polymers C1 – C12.

Firstly, the POX polymers (POX-1000, POX-2500, POX-5000) representing corresponding polymer grafts were studied separately from the final polymers (**Table 1**). It was realized by a termination of the aliquot samples of the polymerization mixtures with water instead of adding them into a carrageenate solution. The molecular weights of particular POX grafts were determined using size-exclusion chromatography (SEC). The found graft lengths were close to the theoretical values. Furthermore, the dispersity was in all cases lower than 1.15.

Table 1. Characterization of the polymers representing the grafts contained in the prepared polymers.

Sample	$M_{n,graft\ (theor)}$ (Da)	$M_{n,graft\ (found)}$ (Da)	Dispersity	$n_{isopropyl}/n_{butyl}$ [1] (theoretically 75/25)
POX-1000	1000	860	1.08	71/29
POX-2500	2500	1950	1.15	72/28
POX-5000	5000	4350	1.10	73/27

[1] $n_{isopropyl}/n_{butyl}$ is the molar ratio of 2-isopropyl-2-oxazoline and 2-butyl-2-oxazoline in the POX grafts determined by NMR.

The theoretical molar ratio of the monomers in the resulting polymer grafts was selected to be $n_{isopropyloxazoline}/n_{butyloxazoline}$ = 3/1 mol/mol because this monomer ratio exhibited the most appropriate CPTs to obtain a material which has CPT between room and body temperatures (Hruby et al., 2010). The found ratio of monomeric units in the resulting POX grafts was calculated according to the equation (2):

$$n_{isopropyl}/n_{butyl} = (I_{\delta = 1.02\ ppm}/6)/(I_{\delta = 1.31\ ppm}/2) \quad (2)$$

where $n_{isopropyl}/n_{butyl}$ is the molar ratio of 2-isopropyl-2-oxazoline and 2-butyl-2-oxazoline incorporated in the POX grafts, $I_{\delta = 1.02\ ppm}$ is the peak intensity at 1.02 ppm corresponding to the –CH–(C$\boldsymbol{H_3}$)$_2$ group of 2-isopropyl-2-oxazoline and $I_{\delta = 1.31\ ppm}$ is the peak intensity at 1.31 ppm corresponding to –CH$_2$–CH$_2$–C$\boldsymbol{H_2}$–CH$_3$ group of 2-butyl-2-oxazoline. The theoretical ratio $n_{isopropyl}/n_{butyl}$ of all grafts was supposed to be 75/25, while the obtained ratios are very close to the theoretical ones (**Table 1**).

To separate the unbound POX grafts from the grafted polymers, the polymer solutions were dialyzed using the membranes with molecular weight cut-off 6 – 8 kDa, which is well above the maximal molecular weight of the prepared grafts. The dialysis of the samples C9 – C12 was made at lower temperatures (about 10 °C) to assure the solubility of unbound longer POX grafts, which could have CPTs lower than room temperature. Anyway, cloud point temperature is the temperature at which macroscopically observable phase separation occurs; LCST is the temperature minimum in the CPT versus concentration chart.

The content of POX in the prepared polymers was calculated using the weight content of nitrogen according to the equation (3):

$$w_{POX} = (w_N/w_{N,ox})\cdot 100\% \quad (3)$$

where w_N is the content of nitrogen in the resulting polymer, determined by elemental analysis (CHN), and $w_{N,ox}$ is the theoretical content of nitrogen in the corresponding POX grafts. The weight content of POX corresponded nicely to the graft lengths for all samples (**Table 2**). Moreover, during the synthesis of the samples C1, C5 and C9, the grafts were in a high excess, which probably resulted in the maximum achievable grafting density. This was confirmed by the number of glucose units per one graft (**Table 2**), which was calculated to be the same for these samples (from 6 to 9 glucose units per one graft). The others samples were synthesized using a lower molar ratios of living POX/carrageenate compared to the samples C1, C5 and C9; therefore, the obtained number of glucose units per one graft was higher (lower grafting density).

Table 2. Characterization of the prepared grafted polymers.

Sample	Found graft length (Da)	POX content (wt. %)	Glucose units per one graft	$M_{w,found}$ [1] (Da)	CPT [2] (°C)
C1	860	34	9.3	2.3×10^6	x
C2		26	13.5	1.7×10^6	x
C3		18	21.8	2.0×10^6	x
C4		8	55.0	1.0×10^6	x
C5	1950	65	5.9	4.5×10^6	32
C6		60	7.2	2.0×10^6	30
C7		35	20.5	1.2×10^6	30
C8		15	59.6	9.5×10^5	x
C9	4350	81	5.6	6.3×10^6	31
C10		74	8.3	5.4×10^6	30
C11		28	60.8	9.1×10^5	26
C12		15	132.1	5.3×10^5	26

[1] Determined by SEC-MALS.
[2] at c = 2.5 mg/mL in 0.15 M NaCl

3.2. Polymer thermoresponsive behavior – light scattering experiments

For a better understanding of the synthesized grafted polymer behavior, the molecular characteristics of the original carrageenan and the polymer grafts were firstly studied separately using static light scattering (SLS) and dynamic light scattering (DLS) techniques. To prevent any association between κ-carrageenan and potassium molecules in phosphate buffered saline (PBS), the SLS experiment was performed in potassium-free 0.15 M NaCl at 40 °C. The resulting Zimm-plot (see **Fig. S3** in the Supplementary Material) provided molecular weight of the original κ-carrageenan M_w = 543 kDa (± 15%) and its radius of gyration R_g = 107 nm. The temperature-dependent DLS scans of original κ-carrageenan were performed at two particular aqueous environments, in PBS and sodium chloride

solutions, while the temperature DLS scan of pure POX polymer, corresponding to the grafts, was investigated in water and PBS, respectively. The PBS solution was here used as a model of the physiological conditions. However, considering the chemical composition of PBS solution (0.137 M NaCl, 0.0027 M KCl, 0.01 M Na_2HPO_4, 0.0018 M KH_2PO_4) and potassium-responsivity of carrageenan, the 0.15 M NaCl solution was further also used as a reference to exclude the effect of K^+ ions. During the cooling process of carrageenan solution in PBS (**Fig. 2**), the intensity growth was found at 24 °C, and is attributed to a gelation process, which occurs as a consequence of the adaptation of polysaccharide chain to a helix conformation stabilized by the hydrogen bounds (Schefer, Adamcik, Diener, & Mezzenga, 2015). In the helix conformation, the sulfate groups of carrageenan are located at the periphery of helix backbone. Therefore, they could participate in the electrostatic stabilization of the full molecule. However, the presence of certain cations in the solution, such as K^+, acting as gelation agent and resulting in the formation of ionic clusters, leads up to the formation of 3D-network. As it is visible in **Fig. 2**, the transition of the carrageenan solution in NaCl is at the same concentration smoother than in PBS; however, the salt type does not affect the transition temperature onset significantly. The explanation of that phenomenon could be that the polysaccharide chains are transformed into a coil/helix conformation, dependently on the external temperature change, and in the presence of potassium cations the structures are additionally cross-linked, changing the response intensity but not its onset. In the case of POX polymers, corresponding to the polymer grafts, the intensity increase was observed at 40 °C in aqueous solution and at 35 °C in PBS solution (**Fig. 2**), while it is attributed with self-assembly process or so-called CPT, typical for poly(2-alkyl-2-oxazoline) family with isopropyl substituents (Hoogenboom et al., 2008). The shift in the transition temperature would be considered in the context of the Hofmeister series (Zhang, Furyk, Bergbreiter, & Cremer, 2005), where the influence of salts on the CPT is related with a salting-in or salting-out effect. Therefore, we claim the existence of salting-out effect for the current system that is also consistent with the literature data for the similar systems (Bao, Li, Leong, & Gan, 2010). Thus, we expect to detect double-responsive temperature behavior for the final carrageenan-*graft*-poly(2-isopropyl-2-oxazoline-*co*-2-butyl-2-oxazoline)s – a cloud point temperature (at elevated temperature) and a gelation point (at lower temperature), while it would show a molecularly dissolved solution between these two temperatures.

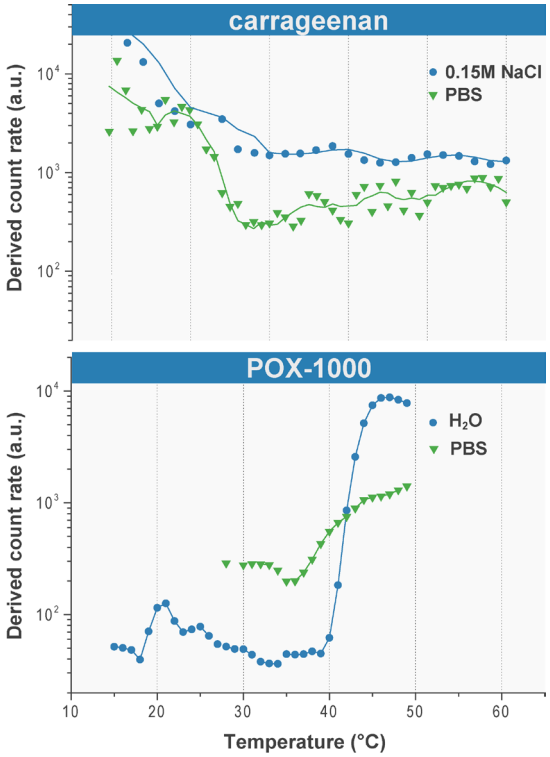

Figure 2. The temperature-dependent DLS measurement in the solution of carrageenan (c = 2.5 mg/mL) and POX-1000 – poly(2-isopropyl-2-oxazoline-*co*-2-butyl-2-oxazoline) (c = 2.5 mg/mL) with the length of 860 Da.

The temperature-dependent behavior of all prepared grafted polymers was studied using DLS. The cooling trends of polymers C1, C4, C6, C8, C10 and C11 (**Fig. 3**) were chosen to display the temperature-dependent effect of two particular factors: graft length (C1 and C4 – 860 Da; C6 and C8 – 1950 Da; C10 and C11 – 4350 Da) and grafting density (C1, C6 and C10 – 7 to 9 glucose units per graft; C4, C8 and C11 – 55 to 61 glucose units per graft). No significant temperature dependence was found for the shortest graft length, disregarding the number of the attached grafts on the polymer (**Fig. 3 –** C1 and C4). This result implies that there is a threshold in the minimum graft length needed to launch the self-association process, due to primarily hydrophobic nature of interactions driving it. However, the more pronounced temperature dependence is observed with the increasing graft length. According to the previous temperature-dependent behavior study of the individual components, the phase transition occurring at ca 30 °C for samples C5 – C12 corresponds to the self-assembly process of POX chains. The CPT values for all synthesized polymers are shown in **Table 2**. Interestingly, the transition onset in all cases starts for the final grafted polymer at lower temperature than for the pure corresponding POX polymer. Explanation of this phenomenon would be that the polymer chemical structure results in a high local concentration of the POX grafts, which, therefore, promotes the association process (the dependence of CPT on a local concentration of poly(2-alkyl-2-oxazoline)s). Besides the influence of graft length, the effect of grafting density could also be deduced from the **Fig. 3**. The decrease in amount of the grafts per polymer molecule, meaning the increase in glucose units per a graft value and the decrease in grafting density, remarkably reduces the sharpness of the phase transition, comparing the samples with the same graft length, probably by decreasing the probability of the occurrence of sufficiently high local concentration of POX to form the phase-separated microdomains.

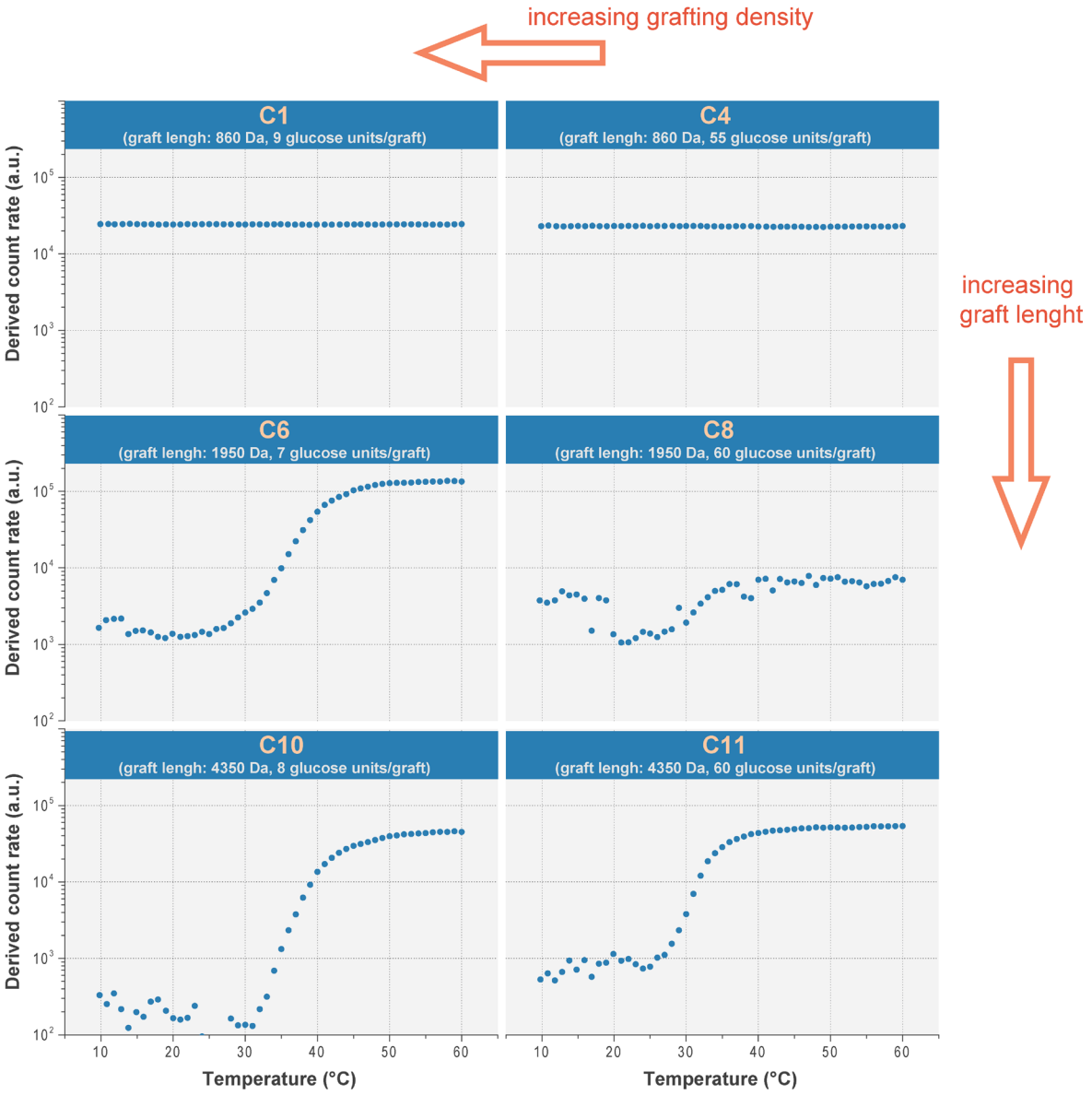

Figure 3. The temperature dependences of scattered light intensities for the synthesized polymers (c = 2.5 mg/mL in 0.15 M NaCl). The graphs display the temperature-dependent effect of two particular factors: graft length (C1 and C4 – 860 Da; C6 and C8 – 1950 Da; C10 and C11 – 4350 Da) and grafting density (C1, C6 and C10 – 7 to 9 glucose units per graft; C4, C8 and C11 – 55 to 61 glucose units per graft). The standard deviation of 3 independent measurements was below 5 %.

3.3. Polymer thermoresponsive behavior characterization with nuclear magnetic resonance (NMR)

The temperature-dependent behavior of the chosen polymers was also characterized by NMR. Firstly to be able to compare the temperature dependence of the synthesized polymers, high-resolution ^{1}H-NMR spectra of the original κ-carrageenan (c = 2.5 mg/mL in D_2O) were measured at 10, 35 and 40 °C (**Fig. 4A**), while the intensity of all κ-carrageenan signals increased with the increasing temperature. Additionally, the spectrum of κ-carrageenan measured at 70 °C is shown in **Fig. S4** (see the Supplementary Material). The measured broad signals at 10 and 35 °C correspond to a reduced mobility of κ-carrageenan chains in the gel, while the gel formation is typical for κ-carrageenan at

lower temperatures (Hermansson, Eriksson, & Jordansson, 1991). However, the temperature increase causes an elevated mobility of the polysaccharide chains that subsequently results in a break of the respective physical network structures.

Thereafter, the polymers with the highest grafting density, differing in the graft length (C1, C5 and C9), were chosen to be studied using high-resolution ^{1}H-NMR under the similar instrumental conditions as the pure carrageenan above (at 10, 30 and 70 °C, c = 2.5 mg/mL in D_2O). The measured spectra of polymer C9 (with the longest grafts of 4350 Da) is shown as a typical example of the behavior of the prepared polymers (**Fig. 4B**). The signal "**a**" is related to –NC**H$_2$**– groups of the poly(2-isopropyl-2-oxazoline-*co*-2-butyl-2-oxazoline) (graft main chain). The groups –COC**H**– and C**H$_3$**– of the 2-isopropyl-2-oxazoline units (side chain protons) are marked as "**b**" and "**c**", while the side chain groups –COC**H$_2$**–, –COCH$_2$C**H$_2$**–, –C**H$_2$**CH$_3$ and –C**H$_3$** of 2-butyl-2-oxazoline units correspond to peaks "**d**", "**e**", "**f**" and "**g**", respectively. During the measurements, two contradictory effects were observed with an increase of temperature: intensity increase of the κ-carrageenan signals, discussed above, and intensity decrease of all signals related to the POX part. This broadening and almost disappearance of the peaks corresponding to a thermoresponsive part of the polymer is connected to the decreased mobility of the POX chains at elevated temperature. Here, the mobility of POX chains at 70 °C decreased so much that they were no more detected in high-resolution ^{1}H-NMR spectra. A similar effect was already reported for the other LCST-showing thermoresponsive polymer systems (Konefał, Spěváček, & Černoch, 2018).

The changes occurring within the heating process can be quantified using a calculation of the *p*-fraction values for the groups with a reduced mobility, according to the equation (4):

$$p = 1 - \frac{I(T)}{I(T_0) \times \frac{T_0}{T}} \tag{4}$$

where $I(T)$ is the integrated intensity of the given polymer signal in the spectrum at the given absolute temperature T and $I(T_0)$ is the integrated intensity of this signal in the case of maximal mobility of the polymer segments at the absolute temperature T_0. Therefore, the value of $p(T_0)$ is 0 in the case of the maximal peak intensity.

The temperature dependences of the *p*-fraction values were calculated for all measured signals which were not overlapped by the water signal during the heating process (**Fig. 5**). For the pure carrageenan solution (**Fig. 5A**), the *p*-fraction of all signals exhibited pretty high value (≈0.95) at low temperatures that drastically dropped to the value around 0 in the temperature range 30 – 40 °C. Then, these *p*-fractions were slightly increasing with the growing temperature up to the value of 0.2 at 70 °C (the final measurement temperature). As it was discussed above, at lower temperature the carrageenan chains have a reduced mobility caused by the strong interactions of the polysaccharide chains and the solvent (gel form), while the radical drop of *p*-fraction is connected with the re-established chain mobility connected to the break of the physical network structure. For the polymer C9 (**Fig. 5B**), the similar behavior was observed for all proton signals corresponding to the carrageenan structure. In addition, the *p*-fraction of polyoxazoline signals was calculated to be around 0 at lower temperature, and it started to elevate at 25 °C, representing a formation of polymer aggregates. The p_{max} (final value of *p*-fraction) gives quantitative information about the fraction which participates in the phase transition. The p_{max} values for the POX groups "**a**", "**b**", "**c**", "**d**", "**e**", "**f**" and "**g**" were almost same, ca 0.98, meaning all POX groups are similarly restricted in their mobility and form aggregates. The temperature dependences of the *p*-fraction values for polymers C1 and C5 are shown in **Fig. S5** and **S6** (see the Supplementary Material).

The temperature-dependent *p*-fraction values of the DA H2 carrageenan protons (**Fig. 5C**) and POX main chain protons "**a**" (**Fig. 5D**) were chosen to quantitatively study thermoresponsive behavior of the original carrageenan and the chosen carrageenan-*graft*-POXs (these protons are easily visible

through the whole temperature range). Related to the *p*-fractions of the DA H2 signals (**Fig. 5C**), the initial value at 10 °C is for the synthesized polymers significantly lower than for the original carrageenan, which implies that the presence of POX grafts on the carrageenan macromolecules partially prevents the gelation process of the polysaccharide, most plausibly due to the steric reasons. Moreover, the minimum *p*-fraction values for the grafted polymers were found at 25 °C which is ca 10 °C less than for the carrageenan. Furthermore, POX chains started a phase separation at this temperature because the *p*-fractions of the prepared polymers began to increase, dependently on the polymer composition (the higher POX amount, the higher final *p*-fraction value). The exception was for polymer C1 which did not show any significant increase of the *p*-fraction with the growing temperature (from 25 °C) that is in good agreement with the DLS measurements, which exhibited no temperature dependence of the polymer size. Considering *p*-fractions of POX main chain protons "**a**" (**Fig. 5D**), a phase transition of the prepared polymers depends on their POX content. The polymer C9, having the highest POX content (81 wt. %), showed the sharp transition, the highest p_{max} value (0.98) and CPT around 26 °C. The samples C1 and C5 with lower amount of POX (34 and 65 wt. %, respectively) exhibited a broader transition and lower p_{max} value at the same concentration (0.41 for C1 and 0.70 for C5). Interestingly, DLS measurement did not revealed any temperature dependence for the sample C1. However, *p*-fraction of the POX main chain protons "**a**" for C1 displayed increased value with the growing temperature (**Fig. 5D**). This means that within the heating process the polymer size is not dramatically changing but the mobility of its POX chains is decreasing, probably due to the interactions between the hydrophobic POX groups within one polymer chain.

In general, the interactions between carrageenan units (C1, C5 and C9) predominated at lower temperature, while with increasing temperature the interactions of polymer and water prevailed up to the CPT, when the strong hydrophobic interactions of isopropyl and butyl moieties took place.

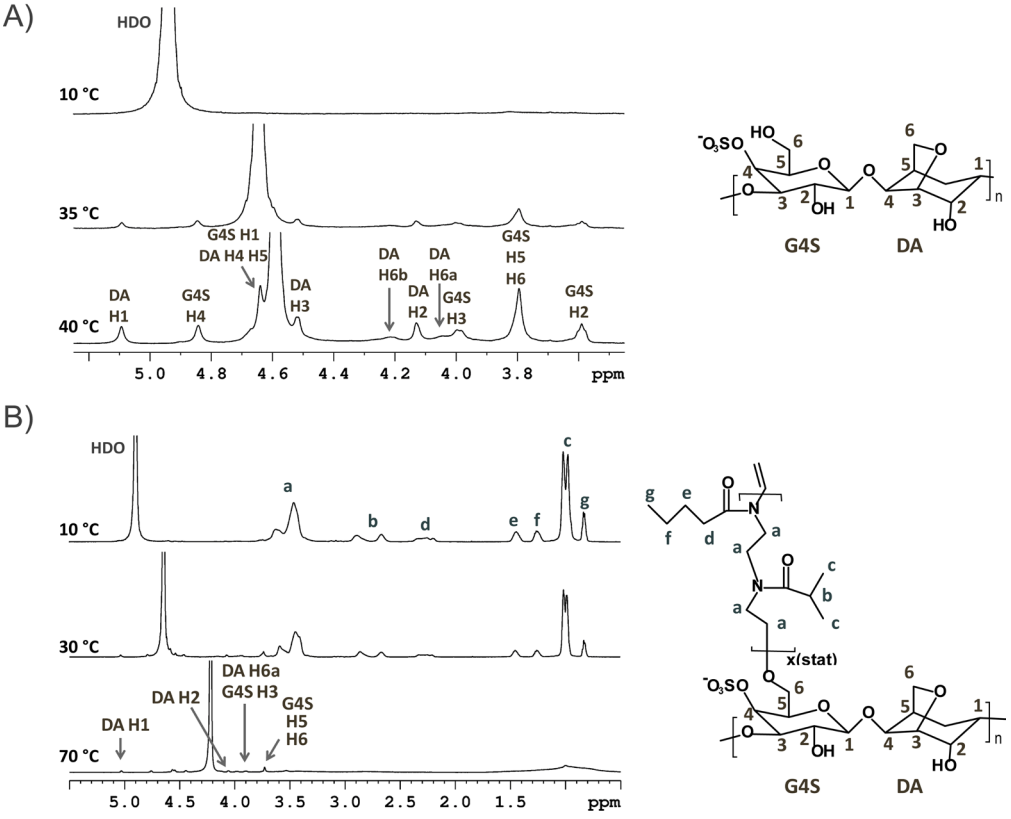

Figure 4. ^{1}H-NMR spectra of: A) original κ-carrageenan (c = 2.5 mg/mL in D_2O) measured at 10, 35 and 40 °C and B) C9 (c = 2.5 mg/mL in D_2O) measured at 10, 30 and 70 °C under the same instrumental conditions.

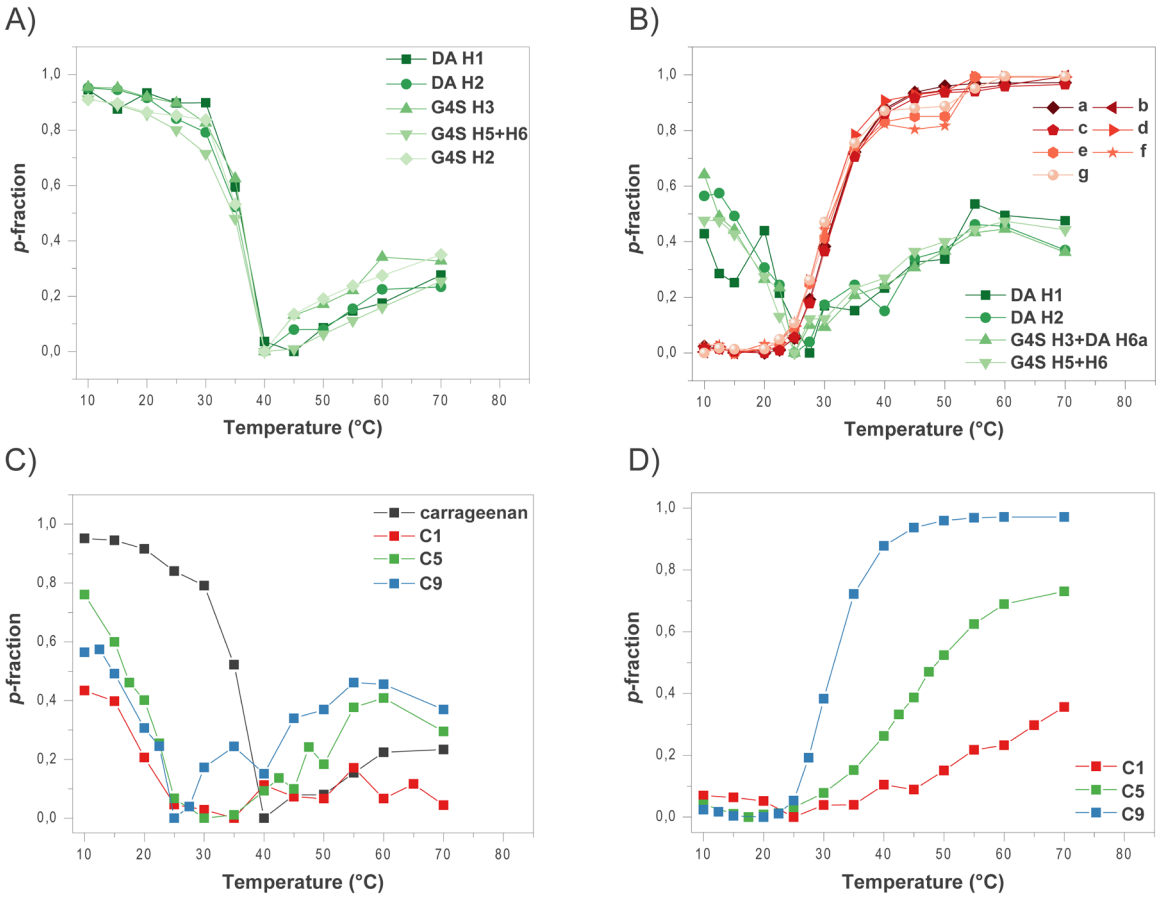

Figure 5. A) Temperature dependences of *p*-fractions for various proton groups of original carrageenan (c = 2.5 mg/mL in D_2O). B) Temperature dependences of *p*-fractions for various proton groups of C9 (c = 2.5 mg/mL in D_2O). C) Temperature dependences of *p*-fraction for DA H2 proton carrageenan group in the solution of: original carrageenan (black), C1 (red), C5 (green) and C9 (blue) (c = 2.5 mg/mL in D_2O). D) Temperature dependences of *p*-fraction for POX main chain protons "**a**" in the solution of: C1 (red), C5 (green) and C9 (blue) (c = 2.5 mg/mL in D_2O). The standard deviation of 3 independent measurements was below 5 %.

3.3. Polymer thermoresponsive behavior – fluorescence measurements

The DLS measurement provides the information about the particle sizes and the NMR gives information about the mobility of particular groups, nevertheless, they do not inform about hydrophobicity/hydrophilicity of the microenvironment before, during and after a transition.

Thus, the temperature-dependent fluorescence measurement was utilized to study the formation of hydrophobic domains during the phase-transition of pure carrageenan and of the polymers with the highest grafting density, (C1, C5 and C9), which differ in the graft length. The fluorescence measurement exploits the aggregation-induced emission caused by a fluorescent probe, which is not fluorescent in the molecularly dissolved state, however, it is a highly fluorescent in the aggregated state in a hydrophobic environment. In this case, 8-anilino-1-naphthalenesulfonic acid ammonium salt (ANSAAS, c = 0.25 µmol/mL, λ_{ex} = 388 nm) was used as a fluorescent probe, and the measurement were performed in the 0.15 M NaCl solutions to exclude the possible effect of K^+ ions. The sample C5 (**Fig. 6A,B**) showed a low intensity fluorescent peak ($\lambda_{em,max}$ = 489 nm) at 10 °C, which probably corresponds to the formation of hydrophobic domains, coming from isopropyl and butyl groups of one macromolecule (or very few). With the increasing temperature the peak intensity slightly decreased up

to 30 °C, meaning that the amount of hydrophobic domains slightly decrease as well. The explanation for this phenomenon could be following: the sample C5 has a gel-like structure at 10 °C, and thus the mobility of isopropyl and butyl groups is reduced; therefore, the amount of hydrophobic domains formed within one macromolecule at one moment is higher than in a solution, in which it is transformed with the increasing temperature. At 30 °C (**Fig. 6A,B**), the fluorescence peak intensity of C5 started to significantly increase up to 50 °C, indicating the CPT of the system and inter/intramolecular reorganization of the self-assembled structures. The peak maximum detected at 60 °C shifted to 479 nm (from 489 nm), confirming the growth in the microenvironment hydrophobicity. These observations are in good agreement with the DLS and NMR studies, which indicated very similar CPTs at the same conditions (32 and 30 °C, respectively). Almost identical comparable situation was observed for the polymer C9 (**Fig. 6B**). The temperature-dependent formation of the hydrophobic domains was not revealed for the sample C1 as well as the for original carrageenan (**Fig. 6B**), which is also in good agreement with DLS and NMR measurements.

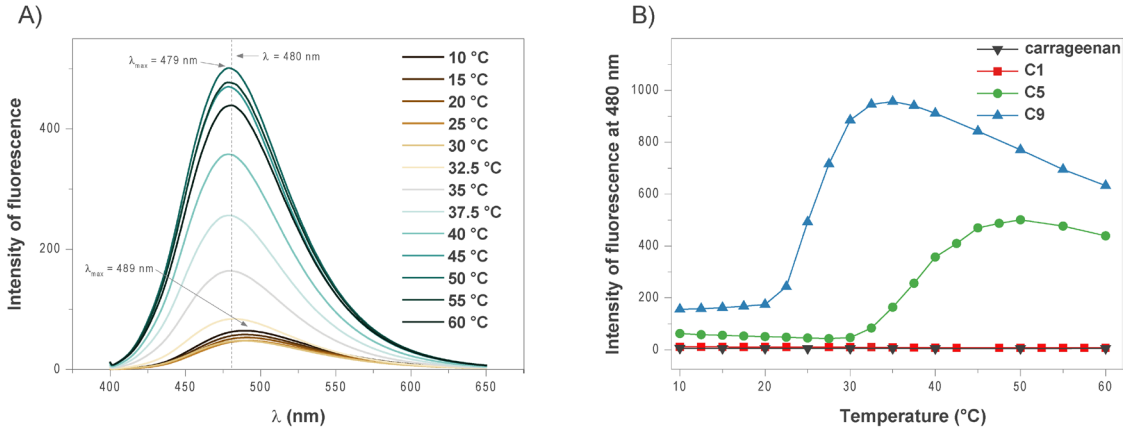

Figure 6. A) The temperature-dependent fluorescence of C5 (c = 2.5 mg/mL in 0.15 M NaCl with a fluorescence probe ANSAAS, λ_{ex} = 388 nm). B) The temperature-dependent fluorescence emission at 480 nm of the original carrageenan, C1, C5 and C9 (c = 2.5 mg/mL in 0.15 M NaCl with a fluorescence probe ANSAAS, λ_{ex} = 388 nm). The standard deviation of 3 independent measurements was below 5 %.

3.4. Polymer responsivity to potassium

In order to study the influence of the potassium ions on the polymer thermoresponsive behavior and on the formation of self-assembled structures, the dynamic light scattering measurements and atomic force microscopy were performed in the polymer solution of different salts with the same ionic strength, but varying in the potassium concentration.

The sample C10 (**Fig. 7**) exhibited a relatively sharp phase transition in a solution of 0.15 M NaCl compared to in a PBS solution, which is an interesting phenomenon, considering that NaCl is the main component of a PBS solution, exceeding almost 14 times the other components. However, the onset of the phase transition was not significantly influenced, comparing 0.15 M NaCl and PBS. Moreover, the scan for the polymer C10 was also performed in 0.15 M KCl (**Fig. 7**), but this measurement provided only very big particles, denoting the possible formation of self-assembled structure as it is typical for the original κ-carrageenan (Schefer et al., 2015). The polymer C11 (**Fig. 7**), which has the same graft length but lower grafting density in comparison to the sample C10, showed a similar behavior. In PBS, the onset of its phase transition only slightly shifted to the lower temperature and the transition is not as steep as in the case of 0.15 M NaCl. Furthermore, the bigger structures were observed at lower temperature in PBS, which implies the similar behavior as original carrageenan. The formation of

bigger structures through the whole measured temperature range was observed in the polymer solution of 0.15 M KCl (**Fig. 7**).

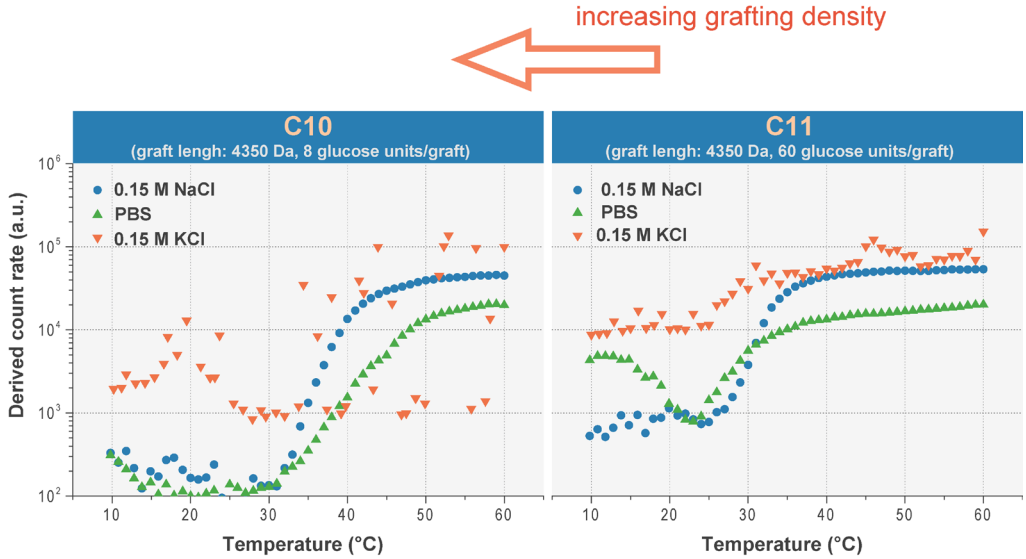

Figure 7. The temperature dependences of scattered light intensities for the polymers C10 and C11 (same graft length but different grafting density), measured in 0.15 M NaCl, PBS and 0.15 M KCl (c = 2.5 mg/mL). The standard deviation of 3 independent measurements was below 5 %.

The effect of pottasium ions on the formation of self-assembled structures was further investigated using atomic force microcopy (AFM). The samples were transferred from aqueous, salt and buffer solutions, respectively, at room temperatures onto the freshly cleaved mica substrate and characterized under the ambient conditions (**Fig. 8**). For the original κ-carrageenan the countercation-dependent formation of intramolecular secondary structures is a typical behavior, especially sensitive to the presence of K^+ ions (in lesser extent also to Ca^{2+} ions) (Schefer et al., 2015), coming from the electrostatic repulsion among the negatively charged carrageenan sulphate groups, which are compensated by cooperative chelation of the countercations. It was realized (**Fig. 8** and **Fig. S7** in the Supplementary Material) that the polymer C10 (the longest grafts of 4350 Da, grafting density: 8 glucose units per one graft) forms the structures of random coils in a purely aqueous solution and in the solution of 0.15 M NaCl at room temperature. However, it self-assembles into the bigger structures in the solutions of PBS (containing 4.5 mM K^+ ions) and 0.15 M KCl, and thus, the driving force for the self-assembly is the presence of potassium cations. This fact implies that POX grafts do not influence the κ-carrageenan behavior in response to the presence of K^+ ions in the solution.

The practical use of potassium responsivity may be as follow: the injection of potassium-free solution of such polymers into the inherently potassium-containing environment of organism may significantly enhance the body temperature-driven phase separation when an *in situ* formation of injectable depot/implant is needed (injectable brachytherapy, local drug depots, local immunomodulator injections/vaccine adjuvants *etc.*).

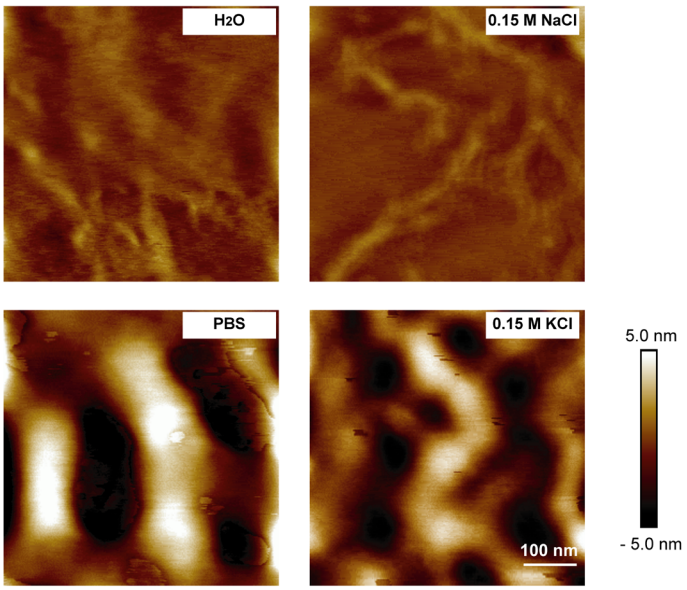

Figure 8. Representative AFM height images of C10 transferred from aqueous, 0.15 M NaCl, PBS and 0.15 M KCl solutions at room temperature onto the freshly cleaved mica. The scale and color bars apply to all images.

4. Conclusion

Novel polymers with lower and upper critical solution temperatures, κ-carrageenan-*graft*-poly(2-isopropyl-2-oxazoline-*co*-2-butyl-2-oxazoline)s (M_n = 500 – 5000 Da, grafting density from 6 to 130 glucose units per one graft), were successfully prepared using a one-pot, two-step synthesis. The "schizophrenic" thermoresponsive behavior of the synthesized polymers was thoroughly studied, showing the existence of a gel form at lower temperature, the molecularly dissolved solution at room temperature and the cloudy solution at elevated temperature, while the limit temperatures can be easily tuned by the grafting density and graft length. However, the minimal graft length of the prepared polymers to exhibit a described above thermoresponsive behavior was found to be 1950 Da. Furthermore, the polymer exhibited potassium responsivity as the original κ-carrageenan, forming relatively big self-assembled structures in the presence of K^+ ions, which denotes that the POX grafts do not influence the carrageenan behavior in the ion solution.

The extraordinary properties can be used in a wide range of biological application demanding thermo- and potassium-responsivity with the synergy between each other. Some of them show a CPT under the body temperature; therefore, they can be usable, for example, as a material for polymer depot, formed after the injection into the body from the polymer solution. The structure-properties relationships as well as the physical principles beyond the observed phenomena were critically correlated and explained.

Acknowledgements

Financial support from the Czech Grant Foundation (grant # 18-07983S, P. Štěpánek), from the Ministry of Education, Youth and Sports of the Czech Republic (grant # LM2015064, L. Loukotová) and from the Ministry of Health of the Czech Republic (grant # 15-25781a, M. Hrubý) is gratefully appreciated. The authors also acknowledge the Charles University in Prague for the opportunity for doctoral studies for L. Loukotová.

Supplementary Material is available for the manuscript.

Literature

Bao, H., Li, L., Leong, W. C., & Gan, L. H. (2010). Thermo-responsive association of chitosan-graft-poly (N-isopropylacrylamide) in aqueous solutions. *The Journal of Physical Chemistry B*, *114*(32), 10666–10673.

Campo, V. L., Kawano, D. F., da Silva, D. B., & Carvalho, I. (2009). Carrageenans: Biological properties, chemical modifications and structural analysis–A review. *Carbohydrate Polymers*, *77*(2), 167–180.

Chen, W., Meng, F., Li, F., Ji, S.-J., & Zhong, Z. (2009). pH-responsive biodegradable micelles based on acid-labile polycarbonate hydrophobe: synthesis and triggered drug release. *Biomacromolecules*, *10*(7), 1727–1735.

Fujishige, S., Kubota, K., & Ando, I. (1989). Phase transition of aqueous solutions of poly (N-isopropylacrylamide) and poly (N-isopropylmethacrylamide). *The Journal of Physical Chemistry*, *93*(8), 3311–3313.

Funami, T., Hiroe, M., Noda, S., Asai, I., Ikeda, S., & Nishinari, K. (2007). Influence of molecular structure imaged with atomic force microscopy on the rheological behavior of carrageenan aqueous systems in the presence or absence of cations. *Food Hydrocolloids*, *21*(4), 617–629.

Gulrez, S. K. H., Al-Assaf, S., & Phillips, G. O. (2011). Hydrogels: methods of preparation, characterisation and applications. In *Progress in molecular and environmental bioengineering-from analysis and modeling to technology applications*. InTech.

Hatakeyama, H., Kikuchi, A., Yamato, M., & Okano, T. (2007). Patterned biofunctional designs of thermoresponsive surfaces for spatiotemporally controlled cell adhesion, growth, and thermally induced detachment. *Biomaterials*, *28*(25), 3632–3643.

Hermansson, A.-M., Eriksson, E., & Jordansson, E. (1991). Effects of potassium, sodium and calcium on the microstructure and rheological behaviour of kappa-carrageenan gels. *Carbohydrate Polymers*, *16*(3), 297–320.

Hoogenboom, R., & Schlaad, H. (2011). Bioinspired poly (2-oxazoline) s. *PolymersBioinspired Poly (2-Oxazoline) S*, *3*(1), 467–488.

Hoogenboom, R., Thijs, H. M. L., Jochems, M. J. H. C., van Lankvelt, B. M., Fijten, M. W. M., & Schubert, U. S. (2008). Tuning the LCST of poly (2-oxazoline) s by varying composition and molecular weight: alternatives to poly (N-isopropylacrylamide)? *Chemical Communications*, (44), 5758–5760.

Hruby, M., Filippov, S. K., Panek, J., Novakova, M., Mackova, H., Kucka, J., … Ulbrich, K. (2010). Polyoxazoline Thermoresponsive Micelles as Radionuclide Delivery Systems a, 916–924. http://doi.org/10.1002/mabi.201000034

Hrubý, M., Šubr, V., Kučka, J., Kozempel, J., Lebeda, O., & Sikora, A. (2005). Thermoresponsive polymers as promising new materials for local radiotherapy. *Applied Radiation and Isotopes*, *63*(4), 423–431.

Konefał, R., Spěváček, J., & Černoch, P. (2018). Thermoresponsive poly (2-oxazoline) homopolymers and copolymers in aqueous solutions studied by NMR spectroscopy and dynamic light scattering. *European Polymer Journal*, *100*, 241–252.

Ma, M., Guo, L., Anderson, D. G., & Langer, R. (2013). Bio-inspired polymer composite actuator and generator driven by water gradients. *Science*, *339*(6116), 186–189.

Meng, F., Zhong, Z., & Feijen, J. (2009). Stimuli-responsive polymersomes for programmed drug delivery. *Biomacromolecules*, *10*(2), 197–209.

Morris, C. J. (2003). Carrageenan-induced paw edema in the rat and mouse. *Inflammation Protocols*, 115–121.

Priest, J. H., Murray, S. L., Nelson, R. J., & Hoffman, A. S. (1987). Lower critical solution temperatures of aqueous copolymers of N-isopropylacrylamide and other N-substituted acrylamides. ACS Publications.

Schefer, L., Adamcik, J., Diener, M., & Mezzenga, R. (2015). Supramolecular chiral self-assembly and supercoiling behavior of carrageenans at varying salt conditions. *Nanoscale*, *7*(39), 16182–16188.

Sedláček, O., Černoch, P., Kučka, J., Konefal, R., Štěpánek, P., Vetrík, M., … Hrubý, M. (2016). Thermoresponsive polymers for nuclear medicine: which polymer is the best? *Langmuir*, *32*(24), 6115–6122.

Seo, Y., Schulz, A., Han, Y., He, Z., Bludau, H., Wan, X., … Kabanov, A. V. (2015). Poly (2-oxazoline) block copolymer based formulations of taxanes : effect of copolymer and drug structure , concentration , and environmental factors §¶, (April). http://doi.org/10.1002/pat.3556

Shamim, N., Hong, L., Hidajat, K., & Uddin, M. S. (2007). Thermosensitive polymer coated nanomagnetic particles for separation of bio-molecules. *Separation and Purification Technology*, *53*(2), 164–170.

Stuart, M. A. C., Huck, W. T. S., Genzer, J., Müller, M., Ober, C., Stamm, M., … Urban, M. (2010). Emerging applications of stimuli-responsive polymer materials. *Nature Materials*, *9*(2), 101–113.

Turquois, T., Acquistapace, S., Vera, F. A., & Welti, D. H. (1996). Composition of carrageenan blends inferred from 13C-NMR and infrared spectroscopic analysis. *Carbohydrate Polymers*, *31*(4), 269–278.

Van de Velde, F., Knutsen, S. H., Usov, A. I., Rollema, H. S., & Cerezo, A. S. (2002). 1H and 13C high resolution NMR spectroscopy of carrageenans: application in research and industry. *Trends in Food Science & Technology*, *13*(3), 73–92.

Yuan, H., Song, J., Li, X., Li, N., & Liu, S. (2011). Enhanced immunostimulatory and antitumor activity of different derivatives of κ-carrageenan oligosaccharides from Kappaphycus striatum. *Journal of Applied Phycology*, *23*(1), 59–65.

Zhang, Y., Furyk, S., Bergbreiter, D. E., & Cremer, P. S. (2005). Specific ion effects on the water solubility of macromolecules: PNIPAM and the Hofmeister series. *Journal of the American Chemical Society*, *127*(41), 14505–14510.

Appendix 4

Loukotová, L.; Hrubý, M. Polysacharidy jako stavební bloky hybridních kopolymerů, *Chem. Listy* **112**, 497 – 507 (2018). IF = 0.260.

Chem. Listy *112*, 498−507 (2018) Referát

POLYSACHARIDY JAKO STAVEBNÍ BLOKY HYBRIDNÍCH KOPOLYMERŮ

LENKA LOUKOTOVÁ a MARTIN HRUBÝ

Ústav makromolekulární chemie AV ČR, v.v.i., Heyrovského nám. 2, 162 06 Praha 6
mhruby@centrum.cz

Došlo 11.4.18, přijato 21.5.18.

Klíčová slova: polysacharidy, hybridní polymery, glykokonjugáty, cílený transport léčiv

Obsah

1. Úvod

Syntetické polymery a polymery vyskytující se v přírodě byly dříve zkoumány v poměrně oddělených oblastech výzkumu. Takové rozlišení je opodstatněné, protože obě skupiny polymerů se liší v mnoha základních aspektech. Biopolymery (proteiny, nukleové kyseliny a polysacharidy) mají velmi často dobře definovanou strukturu, optimalizovanou miliardami let evoluce. Jedná se především o jejich přesné chemické složení, pořadí jednotlivých sekvencí, nadmolekulární strukturu a také o přesně daný počet zabudovaných monomerních jednotek v jednom řetězci, v důsledku čehož je většina biopolymerů uniformní. Naproti tomu většina syntetických polymerů má mnohem jednodušší a náhodnější strukturu, avšak chemicky mnohem pestřejší. Před několika desetiletími se však tyto oblasti výzkumu částečně protly a vytvořily nové výzkumné odvětví hybridních makromolekul složených jak z přírodních, tak ze syntetických polymerů. Tyto kopolymery, označované v literatuře nejčastěji jako polymerní biokonjugáty, byly nejprve hojně studovány a posléze využívány ve farmacii[1,2]. Nicméně rychlý rozvoj v oblasti nanotechnologií a biotechnologií v nedávné době přispěl k tomu, že využití polymerních biokonjugátů výrazně překračuje farmaceutické pole a zahrnuje různorodá odvětví jako např. biosenzory, umělé enzymy, biometrii, fotoniku či nanoelektroniku[3–6]. Díky tomuto širokému využití se studium hybridních polymerů stalo důležitou oblastí polymerní chemie.

Cílem tohoto přehledu je poskytnout komplexní popis jedné specifické skupiny polymerních biokonjugátů – glykokonjugátů, tedy hybridních polymerů na bázi polysacharidů, které jsou nejčastěji využívány pro cílený transport léčiv či v tkáňovém inženýrství[7]. Tento úkol není jednoduchý, neboť obě kategorie (polysacharidy i syntetické polymery) mají extrémně různorodé vlastnosti. Polysacharidy se liší od ostatních biopolymerů tím, že mohou být vysoce rozvětvené a jejich monomerní jednotky mohou být navzájem spojeny mnoha různými typy vazeb. Typ spojující glykosidové vazby má přitom zásadní vliv na vlastnosti výsledného polysacharidu i na jeho nadmolekulární strukturu. Úlohou polysacharidů v organismech je především skladovat a transportovat energii (např. škrob, glykogen) či chránit proti mechanickému poškození (chitin), avšak mohou zastávat i poměrně složité biologické funkce[8]. Tento přehled nejprve ukazuje možné postupy příprav těchto polymerních glykokonjugátů a dále se věnuje jednotlivým příkladům, které jsou uspořádáné dle jednotlivých druhů polysacharidů.

2. Příprava polymerních glykokonjugátů

2.1. Zdroje polysacharidů

Je s podivem, že i když je studium polymerních glykokonjugátů důležitou oblastí současného výzkumu, tak syntéza/příprava samotných polysacharidů je poměrně složitá. Tento fakt je dán především tím, že zatím, narozdíl od proteinů a nukleových kyselin, neexistuje jednoduchý automatizovaný systém pro syntézu oligosacharidů, a to i přesto, že se výzkumu této tématiky věnovalo nemalé úsilí (viz tab. I). Vysvětlení prozatímního neúspěchu tkví ve struktuře samotných polysacharidů. Zatímco chemická syntéza oligopeptidu zahrnuje opakující se tvorbu peptidové vazby např. mezi jednou aktivovanou karboxylovou skupinu a volným aminem, chemická syntéza oligosacharidů vyžaduje několik hydroxylových skupin podobné reaktivity vhodně diferencovaných tak, aby se získal požadovaný produkt s příslušnou regio- a stereoselektivitou, odpovídající požadované trojdimenzionální struktuře. Tato syntéza tedy často zahrnuje namáhavé manipulace s chránícími skupinami a extrémně dlouhé syntetické cesty. V živých organismech existuje centrální dogma mole-

Tabulka I
Obecné metody využívané k získání biopolymerů

Biopolymery	Metody k získání
Proteiny	extrakce z biologického materiálu, automatizovaná peptidová syntéza, nativní ligace peptidů, nadměrná exprese genů vložených do produkčního organismu, katalýza proteasou
Nukleové kyseliny	extrakce z biologického materiálu, automatizovaná syntéza nukleových kyselin, polymerasová řetězová reakce
Oligo/ polysacharidy	extrakce z biologického materiálu, chemická syntéza, enzymatická syntéza

kulární biologie (DNA → RNA → proteiny), které bohužel neplatí pro glykokonjugáty. Ty totiž nejsou syntetizovány templátovou reakcí, ale spíše posttranslačním procesem, přičemž jejich výsledná struktura je ovlivněna mnoha faktory – kompeticí enzymů pro jeden substrát, substrátovou specifitou enzymu a také dostupností substrátu. Z tohoto důvodu jsou glykokonjugáty včetně glykoproteinů typicky polydisperzní[10].

Polysacharidy používané k přípravě polymerních glykokonjugátů jsou dostupné pomocí extrakce z biomateriálu, chemickou syntézou či enzymatickou syntézou (viz tab. I).

Relativně nejjednodušší a nejvíce prostudovaný způsob je zmiňovaná extrakce polysacharidů, avšak tyto metody často neprodukují dostatečné množství materiálu v potřebné kvalitě. Polysacharidy, získávané extrakcí, jsou obsaženy nejčastěji jako strukturní komponenty v buněčných stěnách, především hub, bakterií a řas. Výběr extrakční metody je závislý na struktuře dané buněčné stěny, např. buněčné stěny hub obsahují dva typy polysacharidů: fibrilární chitin (nebo celulosu) a vodorozpustné β-glukany, α-glukany a glykoproteiny[11]. Většina extrakčních metod zahrnuje nejprve odstranění nízkomolekulárních látek pomocí 80% ethanolu. Dále mohou následovat 3 postupné extrakce: vodou (100 °C, 3 h), 2% roztokem štavelanu amonného (100 °C, 6 h) a 5% roztokem hydroxidu sodného (80 °C, 6 h)[12]. Extrakce horkou vodou vedou obecně k polysacharidům rozpustným ve vodě, které se vyskytují na vnější vrstvě buněčné stěny (exopolysacharidy) a chrání ji před externím mechanickým poškozením. Extrakce alkalickými roztoky vedou naproti tomu spíše k polysacharidům ve vodě nerozpustným, které tvoří vnitřní vrstvu buněčné stěny (endopolysacharidy). Přesná metoda extrakce daného polysacharidu se může lišit od výše popsaného obecného postupu v závislosti na jeho struktuře a rozpustnosti ve vodě, avšak vždy je nutné narušit strukturu buněčné stěny pomocí vhodně zvolených extrakčních podmínek (pH a teplota). Nakonec mohou být extrahované polysacharidy přečištěny přesrážením v ethanolu. Často se také využívá iontová chromatografie na diethylaminoethyl (DEAE) celulosové koloně, separující neutrální a nabité polysacharidy, přičemž nejprve jsou eluovány neutrální polysacharidy vhodným pufrem a poté je eluován nabitý polysacharid pufrem o vysoké iontové síle[11]. Neutrální polysacharidy mohou být dále separovány na α- a β-glukany pomocí afinitní chromatografie, která využívá specifické reakce α-glukanů s imobilizovaným ligandem uvnitř kolony. Po přidání směsi α- a β-glukanů k takovémuto ligandu se na něj vážou jen α-glukany, které s ním tvoří silné vazby, a zbytek směsi protéká kolonou beze změny. Navázaný α-glukan se následně eluuje pomocí vysoce koncentrovaného roztoku solí (např. chloridu vápenatého, chloridu sodného či chloridu draselného). Jako ligandy se specifickou reakcí na α-glukany se většinou využívají lektiny.

Jak již bylo diskutováno výše, další způsobem získávání oligo/polysacharidů je chemická syntéza, která je však velmi náročná, což vyplývá ze struktury těchto látek. Vznik glykosidové vazby chemickou syntézou je uskutečněn nukleofilem („glykosidový akceptor“), který napadá aktivované anomerní centrum („glykosidový donor“), přičemž všechny hydroxylové a aminové skupiny musí být maskovány chránícími skupinami tak, aby pouze požadovaná hydroxylová skupina či skupiny byly glykosidovány (obr. 1). Velikost, elektronické vlastnosti a konformace chránících skupin mají obrovský vliv na finální reaktivitu a stereoselektivitu glykosidace, stejně jako použité rozpouštědlo, teplota a aktivátor. Vzhledem ke komplexitě

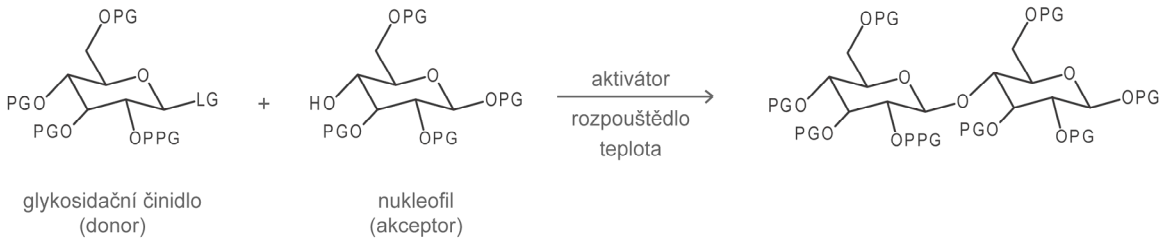

Obr. 1. **Obecné schéma vzniku glykosidové vazby pomocí chemické syntézy** (PG – chránící skupina, LG – odstupující skupina, PPG – „účastnící se“ chránící skupina). Stereochemie výsledného produktu závisí na povaze chránící skupiny, odstupující skupiny, aktivátoru, rozpoustědle a teplotě. Zde uvedeno pro přípravu PG-chráněného disacharidu D-glukosa-β(1→4)-D-glukosa

těchto reakcí vznikl specializovaný obor organické syntézy, pro nějž je charakteristická strategická jednoduchost, provozní složitost a nepředvídatelnost glykosidačních reakcí. V průběhu mnoha let byla vyvinuta řada odstupujících anomerních skupin, např. glykosylhalogenidy, avšak v poslední době byly nahrazeny především glykosylimidáty[13], thioglykosidy[14] nebo glykosylfosfáty[15]. K tomu navíc nové znalosti reaktivit glykosidačních činidel přinesly pokrok v sekvenční „one-pot“ syntéze, kdy je nutná správná kombinace jednotlivých stavebních bloků, které mohou sloužit jednak jako glykosidační činidla stejně jako nukleofily[16]. Touto metodou byly připraveny až hexasacharidy[17]. Rozdíly reaktivit jednotlivých glykosidačních činidel obecně komplikují syntézu glykanů, protože různé stavební bloky vyžadují různé reakční teploty a čas. Vcelku spolehlivá stereoselektivita je v případě vzniku *trans*-glykosidické vazby, kdy se chránící skupina (nejčastěji estery nebo amidy) v místě C-2 účastní vzniku oxoniového meziproduktu a blokuje tak jednu jeho stranu, a tudíž nukleofil má možnost přistoupit pouze z druhé strany. Přítomnost chránicích skupin v jakékoliv jiné poloze glykosidačního činidla může potenciálně ovlivnit stereochemický výsledek glykosidace[18]. Opačná situace je v případě vzniku *cis*-glykosidické vazby, kdy nelze využít tyto „účastnící se“ chránící skupiny (estery, amidy), ale využívají se tzv. „neúčastnící se“ skupiny v pozici C-2, např. benzyl ethery či azidy. Zde se bez vlivu „účastnící se“ skupiny vytváří termodynamicky stabilnější produkt – α-glykosid díky anomernímu efektu. Tento fakt naznačuje, že reakce vedoucí k *cis*-β-glykosidické vazbě, přítomné např. v β-mannosidech, jsou vcelku náročné, neboť nelze použít „účastnící se“ chránící skupiny a musí se zároveň eliminovat anomerní efekt pomocí tzv. „konformačního uzamknutí“[19]. Nejnovější výzkum pak přinesl koncept automatického oligosacharidového syntetizátoru na pevné fázi, Glyconeer 2.1, se kterým je možné syntetizovat různé oligosacharidy obsahující až 30 jednotek v řetězci[20].

Další možností přípravy oligosacharidů je enzymatická syntéza, která využívá glykosyltransferasy a glykosidasy jako cenné regio- a stereoselektivní katalyzátory vzniku glykosidové vazby. Glykosyltransyltransferasy jsou zodpovědné za syntézu většiny glykanů na povrchu savčích buněk, kde přenášejí daný sacharid od odpovídajícího donorového substrátu (nukleotid sacharidu) ke specifické hydroxylové skupině akceptujícího sacharidu (obr. 2a)[21]. Velké množství eukaryotických glykosyltransferas bylo již úspěšně klonováno, přičemž bylo zjištěno, že vykazují obecně vynikající vazebnou a substrátovou specifitu

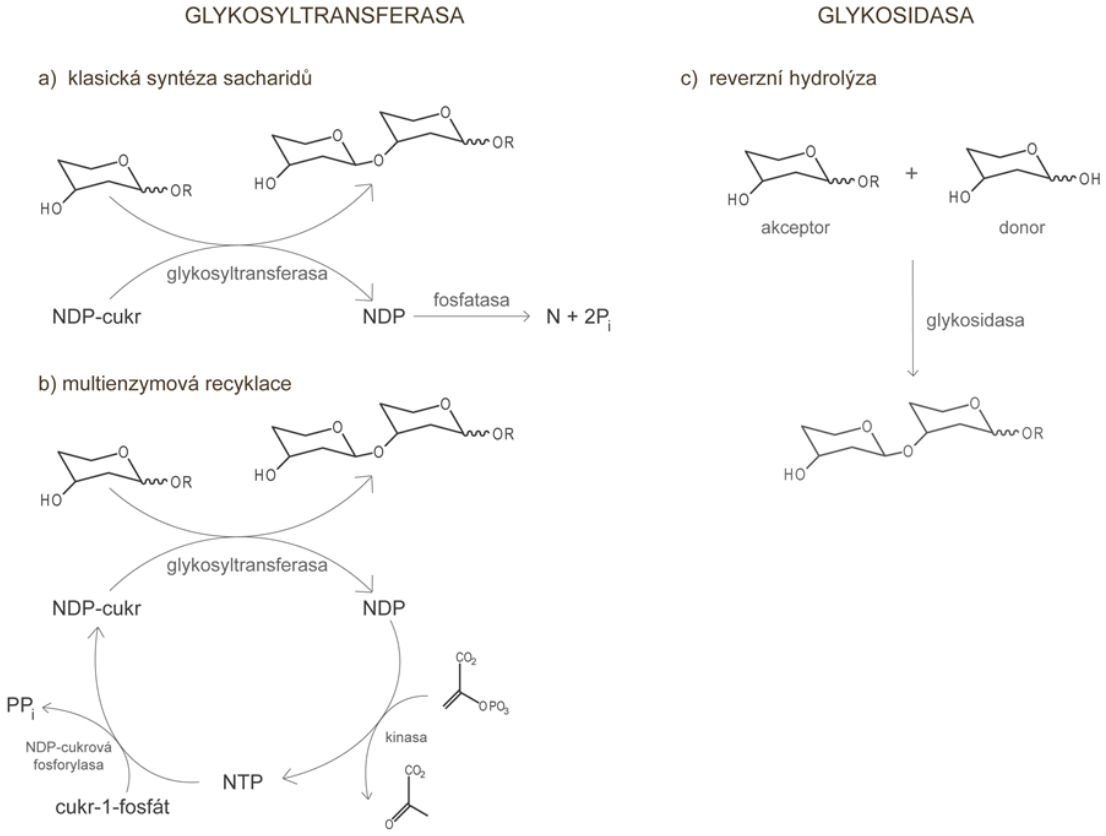

Obr. 2. **Obecné schéma enzymatické syntézy sacharidů pomocí a) klasické glykosyltransferasy; b) multienzymové recyklace s glykosyltransferasou[22] a c) reverzní hydrolýzy glykosidasou** (N – nukleosid, NDP – nukleosid-difosfát, NTP – nukleosid-trifosfát)

a zároveň velmi dobré výtěžky. Bohužel však i tyto syntézy mají i určité nevýhody. Mezi ně patří např. fakt, že nukleosid-difosfáty (NDP) generované během reakce jsou vcelku účinné inhibitory glykosyltransferasy a navíc při syntéze ve velkém měřítku se finanční náklady na výrobu nukleotidu cukru mohou stát velkou přítěží. A tak byla vyvinuta metoda multienzymové recyklace[22], při které je NDP-cukru vyžadován pouze v katalytickém množství, protože se generuje *in situ* z levných výchozích materiálů (obr. 2b). Kromě toho se vznikající NDP recykluje na NDP-cukry, čímž se zabraňuje inhibici produktem. Poslední nevýhodou využití glykosyltransferasy pro syntézu oligosacharidů je její špatná dostupnost. I když v dnešní době je na trhu dostupných mnoho komerčních glykosyltransferas, přesto lze najít chybějící specifické enzymy pro vznik určitých požadovaných glykosidových vazeb. Jak bylo výše uvedeno, vedle glykosyltransferas bývají využívány také exo-glykosidasy a endo-glykosidasy. V živých organismech jsou glykosidasy zodpovědné nejčastěji za štěpení glykosidických vazeb, ovšem za kontrolovaných podmínek mohou být použity spíše pro syntézu glykosidických vazeb než pro jejich štěpení (obr. 2c), přičemž jako katalyzátory při syntéze oligosacharidů již byly úspěšně použity[23, 24]. Ve srovnání s glykosyltransferasami jsou glykosidasy nenákladné, stabilní a snadno dostupné a navíc vyžadují levné donorové substráty oproti neekonomickým nukleotidům sacharidu. Jediná jejich nevýhoda je obecně slabá regiospecifita, která může bohužel vést ke tvorbě více produktů.

2.2. Příprava roubovaných kopolymerů

Nejčastějším typem studovaných modifikovaných polysacharidů jsou jejich roubované kopolymery, které se mohou připravit pomocí tří syntetických strategií (obr. 3): roubováním „z“ (a), roubováním „na“ (b) nebo roubováním „skrz“ (c), přičemž první dva přístupy jsou nejčastěji používané[25]. Technika roubování „z“ je obecně používána v případě, kdy je potřeba vyšší hustota roubování. Při této technice jsou nejprve zavedeny skupiny iniciátoru na hlavní řetězec polysacharidu, přičemž vzniká tzv. makroiniciátor, a následně je zahájen růst roubovaných řetězců z povrchu polysacharidu za přítomnosti požadovaného monomeru. Naproti tomu při technice roubování „na“ jsou nejprve samostatně vytvořeny živé polymerní řetězce, které jsou následně terminovány funkčními skupinami nesenými hlavním polymerním řetězcem. Tato technika je výhodná zvláště díky tomu, že polymerizace vedlejšího řetězce probíhá odděleně od polysacharidu, a tudíž na něj nemá žádný degradační vliv. Další výhodou roubování „na“ je možnost snadno a detailně charakterizovat rouby, např. jejich molekulovou hmotnost (pro charakterizaci se část polymerizační směsi terminuje nízkomolekulárním činidlem). Avšak při roubování „na“ je obecně dosahováno nižší roubovací hustoty, především kvůli sterickému efektu[26]. Nejméně používanou technikou přípravy roubovaných polysacharidů je roubování „skrz“, při kterém je na jeden konec oligo/polysacharidového řetězce zavedena polymerizovatelná skupina (nejčastěji dvojná vazba), přičemž při polymerizaci vytváří monomerní jednotky této skupiny hlavní řetězec nesoucí oligo/polysacharidové rouby.

Technika roubování „z“ bývá často zkoumána ve spojení s radikálovou polymerizací, kdy jsou nejprve radikály generovány podél hlavního polysacharidového řetězce pomocí chemického iniciátoru nebo záření. Takto vytvořený makroiniciátor je následně možné radikálově polymerizovat v přítomnosti monomeru za vzniku požadované-

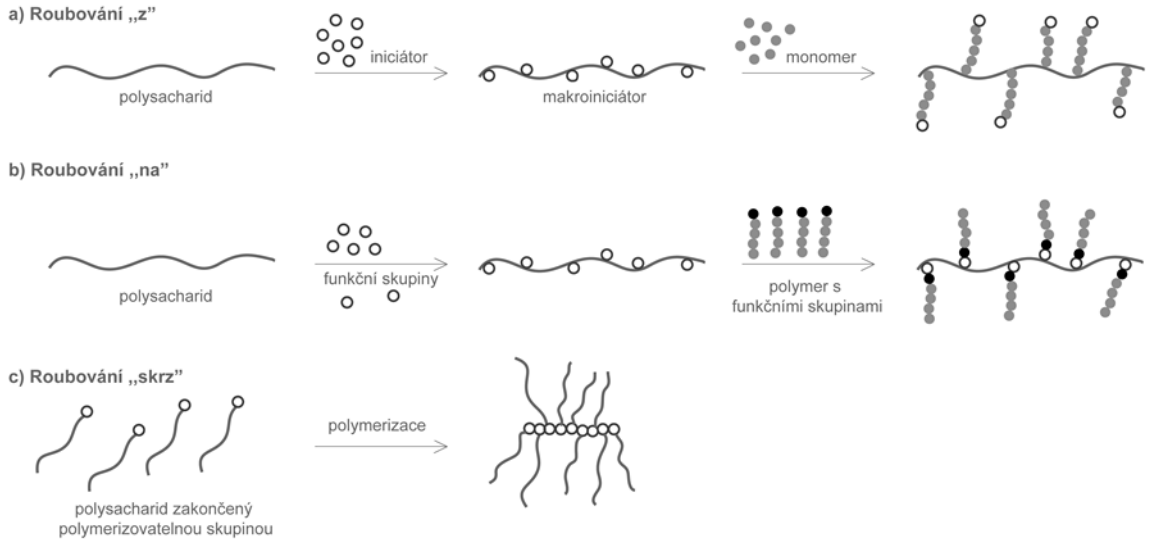

Obr. 3. **Syntetické strategie přípravy roubovaných polysacharidů: a) metodou roubování „z“; b) metodou roubování „na“ a c) metodou roubování „skrz“**

ho roubovaného glykokonjugátu. Nevýhodou této metody je však možná degradace polysacharidového řetězce a velmi omezená kontrola molekulové hmotnosti roubů stejně jako disperzity. Nové možnosti v kontrole délky syntetického roubu přinášejí speciální techniky řízené radikálové polymerizace – nitroxidem zprostředkovaná polymerizace (NMP)[27], radikálová polymerizace s přenosem atomu (ATRP)[28] a polymerizace s reverzibilním adičně-fragmentačním přenosem (RAFT)[29]. Tyto řízené polymerizace jsou více tolerantní vůči běžným nečistotám a vlhkosti a zároveň jsou kompatibilní s velkým množstvím funkčních skupin, a tak umožňují přesné přizpůsobení požadovaných vlastností polysacharidových hybridů. Principem této techniky je významné snížení koncentrace propagačních radikálových konců řetězce, čímž se výrazně minimalizuje také koncentrace ireverzibilních terminačních center, a jelikož rychlost rekombinace radikálových center je úměrná druhé mocnině koncentrace radikálů, zatímco rychlost propagace je pouze přímo úměrná této koncentraci radikálů, tak lze v systémech s velmi nízkou koncentrací radikálových center dosáhnout polymerů s úzkou distribucí molárních hmotností. Pro snížení koncentrace propagujících radikálových center se do systému přidávají látky, které zajišťují reverzibilní zachycení „aktivního“ radikálového centra a jeho přeměnu na „spící“ centrum. Například řízení techniky NMP spočívá v přídavku nitroxidu, vytvářející v reakční směsi relativně stabilní radikály, zatímco při ATRP se přidává komplex přechodného kovu jako katalyzátor a alkylhalogenid jako iniciátor. Při procesu RAFT je reverzibilní zachycení radikálu zajištěno přenosovými reakcemi pomocí např. dithioesterových sloučenin.

2.3. Příprava blokových kopolymerů

Naše literární rešerše překvapivě ukázala, že oproti roubovaným polysacharidovým kopolymerům se jen velmi málo publikací věnuje syntéze blokových kopolymerů oligosacharidů či polysacharidů. Jako první takovýto blokový kopolymer byl koncem 80. let připraven polyethylenoxid-*blok*-oligosacharid pomocí tzv. „couplingu“ koncových skupin[30]. Od té doby byly připraveny kopolymery obsahující syntetický blok spojený s polysacharidovým také pomocí radikálové[31] a enzymatické polymerizace[32]. V případě radikálové polymerizace je na konec polysacha-

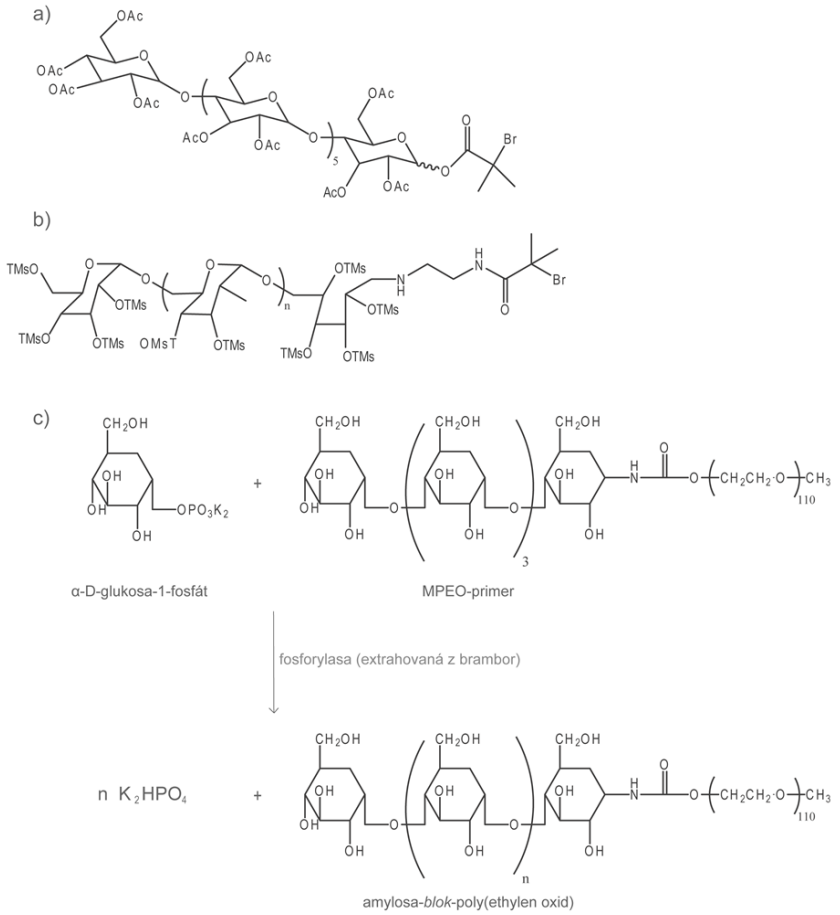

Obr. 4. **a), b) oligosacharidové prekurzory schopné iniciovat polymerizaci typu ATRP; c) schéma enzymaticke syntézy amylosa-*blok*-polyethylenoxid**

ridového řetězce zavedena skupina, která se následně účastní řízené polymerizace syntetického bloku. Například glykokonjugované adukty 2,2,6,6-tetramethylpiperidin-1--oxylu (TEMPO) byly připraveny z glukosy, maltooligosacharidů a β-cyklodextrinu[33], přičemž jejich následnou řízenou polymerizací typu NMP byly vytvořeny polymeru typu β-cyklodextrin-*blok*-polystyren (M_n = 5 až 37 kDa, $Đ$ < 1,5). Z komerčně dostupného β-cyklodextrinu byl také syntetizován acetylovaný oligosacharid schopný iniciovat polymerizaci typu ATRP (obr. 4a)[34], přičemž tento iniciátor umožnil řízenou polymerizaci řady monomerů, např. styrenu, methyl-methakrylátu a dalších funkčních hydrofilních methakrylátů. Získané oligosacharidové bloky byly následně kvantitativně deacetylovány methoxidem sodným ve směsi methanolu a chloroformu za získání blokových oligosacharidových polymerů. Navíc ATRP iniciátorová skupina byla také úspešně zavedena na reduktivní konec dextranu (M_n = 6,6 kDa) pomocí reduktivní aminace s α-terciárním bromidem, přičemž následně byly –OH skupiny dextranu chráněny silylací (obr. 4b). Poté byly řízenou polymerizací získány kopolymery dextran-*blok*-polystyren s nastavitelným složením jednotlivých bloků[35]. Jak již bylo výše zmíněno, blokové polysacharidové kopolymery byly také připraveny enzymatickou syntézou, přičemž nejdříve byl nasyntetizován první blok methoxypolyethylenoxid-*p*-nitrofenylkarbonát (M_w = 5,0 kDa), který následně reagoval s maltopentaozylaminem. Tento meziprodukt (MPEO-primer, obr. 4c) byl následně úspešně enzymaticky polymerizován fosforylázou extrahovanou z brambor využívající α-D-glukosa-1--fosfát jako substrát[36].

3. Využití polymerních glykokonjugátů v praxi

3.1. Kopolymery polysacharidů vyskytujících se v rostlinách

Celulosa je lineární ve vodě nerozpustný polysacharid obsahující jednotky 1,4-β-D-glukosy. Je hlavní stavební složkou rostlinných buněčných stěn, což ji staví do role nejrozšířenějšího biopolymeru na zemském povrchu (bylo odhadnuto, že ročně vzniká cca $1{,}5 \cdot 10^9$ tun celulosy[37]). Modifikovaná celulosa je již dlouhou dobu průmyslově využívána a tato historie sahá až do roku 1870, kdy byl poprvé vyroben polymerní materiál „celuloid“ (nitrát celulosy změkčený kafrem) ve firmě Hyatt Manufacturing Company[38], přičemž výroba nitrátu celulosy zahrnuje její esterifikaci kyselinou dusičnou v přítomnosti kyseliny sírové, fosforečné nebo octové. V současné době jsou dalšími obecně používanými estery celulosy acetát celulosy, propionát celulosy a butyrát celulosy. Dalším možným způsobem chemické modifikace celulosy jsou etherifikační reakce, kterými se dají získat důležité produkty, např. methylcelulosa, karboxymethylcelulosa a hydroxyalkylcelulosa. Tyto estery a ethery celulosy se využívají při výrobě nejrůznějších nátěrů, optických fólií, sorpčních medií, léčiv, potravin či kosmetiky. V roce 1943 se Ushakov pokoušel polymerizovat některé allyl estery a vinyl estery celulosy s estery kyseliny maleinové, přičemž získal nerozpustné produkty, což byly pravděpodobně první roubované kopolymery celulosy[39]. Od té doby bylo syntetizováno nepřeberné množství roubovaných kopolymerů celulosy. Například bylo provedeno kationtově iniciované roubování celulosového substrátu pomocí isobutylenu a α-methyl styrenu, přičemž iniciátor byl vytvořen reakcí fluoridu boritého (Lewisova kyselina) a hydroxylových skupin celulosy (Lewisova báze). Roubovaná celulosa polyakrylonitrilem, polymethakrylonitrilem a polymethylmethakrylátem byla připravena aniontovou polymerizací, využívající alkoholáty celulosy jako iniciátory. Velmi dobře řízené molekulové hmotnosti a úzké distribuce bylo dosaženo také při roubování celulosy pomocí poly(2--methyl-2-oxazolinu) a poly(isobutylvinyletheru)[40].

β-Glukany jsou polysacharidy obsahující β-D--glukosové jednotky, spojené většinou 1,3-β- nebo 1,6-β--glykosidovými vazbami. β-Glukany se v přírodě vyskytují v buněčných stěnách obilovin, bakterií a hub, přičemž vlastnosti jednotlivých β-glukanů se signifikantně liší v závislosti na jeho původu. β-Glukany se používají jako ztužovací činidla v nejrůznějších potravinářských a kosmetických výrobcích. Obecně je známo, že β-glukany mají velmi prospěšný vliv na lidské zdraví. Bylo prokázáno, že příjem nejméně 3 g ovesného β-glukanu denně sníží hladinu LDL cholesterolu a přispívá tak ke snížení rizika kardiovaskulárních chorob[41]. Velmi zajímavou skupinou β-glukanů, již v tradiční orientální medicíně využívaných, jsou β-glukany pocházející z buněčných stěn hub. V nedávných studiích byly popsány jejich imunoterapeutické vlastnosti, včetně zesílení protinádorové imunitní odpovědi[42], což je spojeno se stimulací imunitních receptorů (především Dektin-1 a Toll-like receptory), a tak se modifikované β-glukany v poslední době studují jako potenciální protinádorová immunoterapeutika. Kurdlan (β-1,3-glukan), vyrábějící se fermentací bakterií *Agrobacterium biobar*, byl roubován polyethylenglykolem, přičemž vzniklý kopolymer byl použit pro přípravu nanočástic nesoucích chemoterapeutickou látku doxorubicin. Připravené nanočástice tudíž kombinovaly dvě léčebné metody – chemoterapii a immunoterapii[43]. Na podobném konceptu byla také založena léčba immunoradioterapií, pro kterou byl β-glukan (pocházející z *Auricularia auricula-judae*) roubován poly(2-methyl-2-oxazolin-*co*-2-butyl-2--oxazolinem), který byl dále označen radioaktivním ^{90}Y. Takto označený polymer spojoval vhodné termoresponzivní vlastnosti pro tvorbu polymerního depa, terapeutickou lokální radioaktivitu a imunoterapeutické působení, což bylo úspešně prokázáno při *in vivo* testech na myších s lymfomem[44].

κ-Karagenan je polysacharid skládající se ze střídavě vázaných galaktosových a 3,6-anhydrogalaktosových jednotek, sulfátovaných i nesulfátovaných, přičemž tyto jednotky jsou propojeny α-1,3 a β-1,4 glykosidickými vazbami. κ-Karagenan se získává extrakcí z červených mořských řas, nejčastěji z *Chondrus crispus*. Graftováním κ-karagenanu pomocí polyvinylpyrrolidonu (M_n = 10 kDa)

vzniká materiál vytvářející ve vodném prostředí při pH ~ 7 hydrogely vykazující zvýšenou schopnost udržovat vodu i přes slabší gelovou pevnost než příslušné kontrolní polysacharidy[45]. Zajímavé pH-responzivní hydrogely κ-karagenan-*graft*-polymethakrylamid byly připraveny jako potenciální kandidáti pro řízený transport bioaktivních látek, přičemž fázový přechod byl pozorován při pH ~ 3 (cit.[46]). Později byla vytvořena interpenetrační pH-responzivní polymerní síť κ-karagenan-*graft*-polyakrylamidu a alginátu sodného, přičemž tento materiál byl úspěšně využit pro cílený transport ketoprofenu (nesteroidní protizánětlivé léčivo s analgetickými a antipyretickými účinky) do střev[47]. Podobné hydrogely, vykazující velmi výhodnou pH-responzivitu, byly připraveny roubováním polyakrylové kyseliny-*co*-poly-2-akrylamido-2-methylpropansulfonové kyseliny na κ-karagenan[48]. Pro použití k hojení ran, vyžadující od materiálu schopnost zadržovat vodu, absorbovat vlhkost a antimikrobiální aktivitu, byl κ-karagenan modifikován kyselinou chloroctovou. Vzniklý karboxymethyl-karagenan vykazoval všechny tyto potřebné vlastnosti, které byly silně závislé na jeho stupni substituce – čím byl větší stupeň substituce, tím lepší výsledky byly prokázány[49]. Tenké filmy pocházející z mořských porostů na bázi κ-karagenanu byly roubovány polymethylmethakrylátem s využitím peroxodisíranu draselného jako iniciátoru. Výsledné materiály vykazovaly vhodnou velikost pórů využitelnou pro membrány na separace plynů[50].

3.2. Kopolymery polysacharidů živočišného původu a vyskytujících se v houbách

Chitin je relativně hydrofobní lineární polysacharid tvořící primární komponentu buněčných stěn většiny hub a také se vyskytující v kutikule členovců, přičemž u některých z nich (např. u hmyzu, korýšů apod.) je kutikula zpevněna pomocí minerálních látek a přeměněna v pevný exoskelet. Chitin je složen z molekul *N*-acetyl-D-glukosaminu vzájemně propojených pomocí 1,4-β-glykosidické vazby. Je nerozpustný ve vodě při neutrálním pH, ale jeho modifikace pomocí *N*-deacetylace (→ chitosan obsahující jednotky *N*-acetyl-D-glukosaminu a D-glukosaminu) zvyšuje rozpustnost ve vodě a zároveň poskytuje podél řetězce reaktivní primární aminoskupiny, které je možné dále modifikovat. Chitosan rozpuštěný za kyselých podmínek společně v kombinaci s polyolovými solemi (např. glycerol- nebo glukosa-fosfátová sůl) vytváří termoresponzivní gel, který je při laboratorní teplotě v kapalném stavu a při 37 °C se přemění na gel, což je velmi užitečné pro enkapsulaci živých buněk či terapeutických proteinů. Tento systém byl úspěšně využit *in vivo* pro transport biologicky aktivních růstových faktorů a také pro enkapsulaci matric živých chondrocytů pro tkáňové inženýrství[51]. Dalším zajímavým příkladem využití chitosanu pro responzivní systémy je chitosan-*graft*-poly(2-dimethylamino)ethyl methakrylát, který je citlivý na změnu pH. Při pH ~ 4 vytváří polymer molekulární roztok, zatímco při pH 5–6 se začínají vytvářet „core-shell“ nanočástice, při pH ~ 7 se tyto nanočástice dále spojují a vytváří nanočástice typu dvouvrstvé koule a při pH ~ 8 nakonec dochází k jejich agregaci a vysrážení[52]. Dokonce byl připraven systém kombinující obojí výše zmíněné responzivní chování, chitosan-*graft*-poly-2-(*N*,*N*-dimethylamino)ethyl-methakrylát, který vykazuje jak pH- tak termoresponzivní chování[53]. Modifikovaný chitosan může být také využit pro selektivní adsorpci rtuťových iontů, přičemž za tímto účelem byl pomocí ATRP syntetizován chitosan-*graft*-polyakrylamid, který při následné studii vykazoval velmi dobrou maximální adsorpční kapacitu rtuti (až 322,6 mg Hg iontů/g polymeru)[54].

Kyselina hyaluronová (KH) je hydrofilní lineární glykosaminoglykan, obsahující kyselinu 1,4-β-D-glukuronovou a 1,3-β-*N*-acetylglukosamin. KH byla prvně objevena v dobytčím oku v roce 1934 (cit.[55]), avšak později bylo zjištěno, že KH je distribuováno v celém těle, zejména v extracelulární matrici a synoviálních tekutinách[56]. Přestože samotná KH může být pro aplikace izolována extrakcí z živých tkání, nejčastěji je produkována mikrobiální fermentací kvůli sníženému riziku infekcí, kontaminací a virů[57]. Bylo prokázáno, že KH podporuje angiogenezi a pomáhá při hojení ran[58], přičemž tato zjištění motivovala k masivnímu využití KH pro regeneraci poškozených hlasivek a léčbu jejich nedostatečné funkčnosti, pro výrobu protizánětlivých látek a také v kosmetickém a potravinářském průmyslu[59–64]. Dále také bylo zvažováno použití KH jako biomateriálu pro dlouhodobé implantáty, avšak využití nemodifikované KH bylo problematické kvůli její velmi rychlé enzymatické degradaci v těle (u lidí se syntetizuje a degraduje až 5 g KH denně, přičemž v průměrném člověku je celkem obsaženo přibližně 15 g KH)[65]. Pro snížení rychlosti degradace a také její kontrolu byla KH konjugována se syntetickými polymery, které navíc často i zvyšovaly mechanickou pevnost těchto materiálů. Prestwich a spol. studovali tvorbu hydrogelů tak, že nejříve KH převedli na derivát dihydrazidu adipové kyseliny, který potom zesíťovali s polyethylenglykol propiondialdehydem[66], ale nakonec se ukázalo, že pro polymerní sítě KH budou využitelnější spíše chemicky šetrnější postupy. Jako eventualita se ukázala možnost funkcionalizace KH volnými thioly a následné zesíťování pomocí Michaelovy adice s polyethylenglykol diakrylátem[67]. Takto připravené materiály mohou být použity pro kontrolované uvolňování protizánětlivých léků, zvýšení reepitelizace při hojení ran[68], stimulaci růstu vlásečnic pomocí uvolňování cytokinů[62] nebo jako náhražka tukové tkáně[69]. Na KH byla také roubována poly(mléčná-*co*-glykolová kyselina), přičemž výsledný kopolymer vytvářel nanočástice využitelné k cílenému transportu protinádorových léčiv[70]. Rovněž byla zkoumána konjugace methakrylátu KH s diakrylátem blokového kopolymeru Pluronic® F127 pomocí fotozesíťovacího efektu. Takto vzniklé hydrogely vykazovaly termoresponzivitu[71], tedy rychle ztrácely obsah vody ve své struktuře (odbotnaly) s rostoucí teplotou, což bylo následně využito v aplikaci kontrolovaného uvolňování lidských růstových faktorů a plazmidů DNA, indukujících transfekci *in vitro*. Podobné hydrogely byly vytvořeny roubováním methakrylátu KH

amino-funkcionalizovaným produktem Pluronic® F127 s následným fotozesíťováním s akrylátovými buněčně-adhezními doménami. Enkapsulace chondrocytů těmito hydrogelovými strukturami poté způsobila *in vitro* zvýšenou produkci proteinů extracelulární matrice, především kolagenu II (cit.[70]).

Chondroitin sulfát (CS) je lineární polysacharid obsahující 1,3-β-*N*-acetylgalaktosamin a 1,4-β-glukuronovou kyselinu. *N*-Acetylgalaktosamin je v řetězci sulfatován v poloze 4 nebo 6 (chondroitin-4-sulfát resp. chondroitin-6--sulfát). CS byl poprvé objeven v roce 1861 Fischerem[72], avšak jeho struktura byla objasněna až na začátku 20. století[73]. CS se nejvíce vyskytuje jako součást proteoglykanů v matricích pojivových tkání, plnící zde především strukturní úlohu, nebo na povrchu buněk a membrán, plnící úlohu receptorů[74]. Komerčně dostupný CS se získává extrakcí z mnoha přírodních zdrojů, např. chrupavky skotu, prasat či žraloka[75]. Důležitou roli hraje CS v kloubní chrupavce, kde mnoho řetězců CS je konjugováno na jeden řetězec proteinu, a vytváří tak gradient náboje, který zpevňuje chrupavku a zvyšuje tak její schopnost absorbovat zátěž[76]. Tato přirozená role CS nasměrovala jeho použití v tkáňovém inženýrství pro léčbu chrupavek[77]. Konkrétně pro tuto aplikaci byl CS nejdříve modifikován pomocí glycidyl-methakrylátu a následně fotozesíťován pomocí polyethylenglykol-diakrylátu. Modifikací CS aldehydem nebo sukcinimidyl-sukcinátem a následným zesíťováním poly(vinylalkohol-*co*-vinylaminem) vzniká materiál využitelný jako adhezivum při operacích rohovky, neboť tento materiál vykazuje minimální zánětlivé reakce a zároveň je odolný vůči poškození při velkých tlacích[78]. Tento materiál byl také studován při hojení ran, kdy hydrogelový film byl nanesen na povrchové zranění myším a také na vnitřní zranění čelistní sliznice králíků, přičemž v obou případech ukázala léčba pomocí těchto hydrogelů značné urychlení hojení oproti kontrolní skupině[78]. Dalším využívaným glykokonjugátem CS je CS-*graft*-polylaktid vytvářející ve vodných roztocích micely, které jsou vhodné pro enkapsulaci chondrocytů a pro cílený transport léčiv[79].

Heparin je lineární glukosamin s vysokým stupněm sulfatace a jeho struktura je složena z 1,4-α a také β-kyseliny uronové a α-D-glukosaminových zbytků, obsahujících směs funkčních skupin. Heparin byl poprvé objeven v roce 1916, přičemž od roku 1935 je klinicky používán jako antikoagulant[80]. Heparin je syntetizován jako proteoglykan obsažený v žírných buňkách (60–100 kDa) a poté je štěpen na menší fragmenty pomocí endoglykas (5 až 25 kDa)[81]. Komerčně se heparin vyrábí extrakcí z nejrůznějších tkání (např. prasečí či hovězí střevní sliznice) následovanou složitými purifikačními procesy. Vysoký negativní náboj heparinu vyvolává vznik mnoha iontových interakcí s řadou proteinů (růstové faktory, proteasy, chemokiny), což je předmětem intenzivního studia. Bylo např. prokázáno, že taková interakce může mít za následek stabilizaci, zejména proti denaturaci, řady růstových faktorů, např. bazálního fibroblastového růstového faktoru (bFGF) nebo vaskulárního endotelového růstového faktoru (VEGF), a zároveň způsobuje zvýšení afinity tohoto komplexu na buněčné receptory[82]. Pro zlepšení mechanických a chemických vlastností byl heparin konjugován nejprve s polystyrenem za vzniku specifických desek, jejichž povrch vykazoval zvýšenou aktivitu růstových faktorů VEGF a FGF-2. Heparin konjugovaný na hydrogely polyethylenglykolu byl také použit k prozkoumání diferenciace a fenotypové odpovědi mezenchymálních kmenových buněk a valvulárních intersticiálních buněk (VIC) tím, že zachytí růstové faktory a další proteiny vázající se na heparin[83]. V tomto případě bylo později zjištěno, že kovalentní konjugace heparinu s hydrogelovou sítí polyethylenoxidu k zachycení růstového faktoru FGF2 vyvolala expresi myofibroblastových fenotypových markerů, což naznačuje, že imobilizovaný heparin může modulovat buněčný osud přes vazbu růstových faktorů na rozhraní gel/buňky[84].

4. Závěr

Mnoho výše diskutovaných příkladů ukazuje širokou škálu využití polymerních glykokonjugátů, dostupných kombinací polysacharidů a syntetických polymerů. Tyto materiály jsou připravovány a používány z důvodu zlepšení vlastností samotných polysacharidů, neboť syntetické polymery mohou mít vliv na hydrofilitu, teplotní responzivitu a pH responzivitu, samouspořádání, citlivost k hydrolýze a také na umístění funkčních skupin ve výsledném hybridním materiálu. Pro jejich přípravu bývají obecně používány spíše šetrné konjugační techniky. Požadovaných vlastností syntetických polymerů se dá snadno docílit výběrem jejich struktury, a tudíž se dají snadno modifikovat i vlastnosti výsledného hybridního kopolymeru. Rozsáhlé využití polymerních glykokonjugátů je způsobeno kombinací jejich jedinečných vlastností a relativně nízké výrobní ceny. Polymerní glykokonjugáty využívající zvířecí polysacharidy se často používají k výrobě systémů vyžadujících nízkou imunogenicitu, zatímco glykokonjugáty z polysacharidů pocházejících z hub jsou potřebné pro imunologické aplikace, neboť jsou schopné vyvolávat specifické reakce receptorů. Nevýhodou všech polysacharidů pocházejících z přírodních zdrojů je jejich nečistota a obsah patogenů. Avšak tento problém odpadá při použití nových postupů výroby polysacharidů, tedy jejich chemickou nebo enzymatickou syntézou. Takto vytvořené polysacharidy mají dobře definovanou strukturu, ale ještě bohužel nebyly plně využity pro přípravu polymerních glykonjugátů. Vývoj polymerních glykokonjugátů umožnil výrobu velmi různorodých a funkčních materiálů s takovými biologickými odezvami a takovými chemickými a mechanickými vlastnostmi, aby lépe napodobovaly vlastnosti přirozených matric. Budoucnost konjugace polysacharidů a syntetických polymerů je především v pokračujícím trendu „přizpůsobování“ polysacharidů a jejich vlastností dle požadovaných potřeb.

Vypracováno s finanční podporou Ministerstva školství, mládeže a tělovýchovy České republiky v rámci Národního programu udržitelnosti I (NPU I), Projekt POLYMAT LO1507.

LITERATURA

1. Langer R., Tirrell D. A.: Nature *428*, 487 (2004).
2. Cobo I., Li M., Sumerlin B. S., Perrier S.: Nat. Mater. *14*, 143 (2015).
3. Niemeyer C. M., Mirkin C. A.: Nanobiotechnology: concepts, applications and perspectives *1* (2004).
4. Tu R. S., Tirrell M.: Adv. Drug. Del. Rev. *56*, 1537 (2004).
5. Canalle L. A., Löwik D., van Hest J.: Chem. Soc. Rev. *39*, 329 (2010).
6. Lutz J. F., Börner H. G.: Prog. Polym. Sci. *33*, 1 (2008).
7. Reis R. L., Neves N. M., Mano J. F., Gomes M. E., Marques A. P., Azevedo H. S.: Natural-Based Polymers for Biomedical Applications *1*, 1 (2008).
8. Dwek R. A.: Chem. Rev. *96*, 683 (1996).
9. Koeller K. M., Wong C. H.: Chem. Rev. *100*, 4465 (2000).
10. Jenkins R. A., Parekh R. B., James D. C.: Nat. Biotechnol. *14*, 975 (1996).
11. Zhang M., Cui P. S. W., Cheung C. K., Wang Q., Trends Food Sci. Technol. *18*, 4 (2007).
12. Mizuno T.: Int. J. Med. Mushrooms *1*, 9 (1999).
13. Schmidt R. R., Kinzy W.: Adv. Carbohydr. Chem. Biochem. *50*, 21 (1994).
14. Shiao T. C., Roy R.: Top. Curr. Chem. *301*, 69 (2011).
15. Palmacci E. R., Plante O. J., Seeberger P.: Eur. J. Org. Chem. *4*, 595 (2002).
16. Wu C. Y., Wong C. H.: Top. Curr. Chem. *301*, 223 (2011).
17. Miermont A., Zeng Y., Jing Y., Ye X. S., Huang X.: J. Org. Chem. *72*, 8958 (2007).
18. Baek J. Y., Lee B. Y., Jo M. G., Kim K.: J. Am. Chem. Soc. *131*, 17705 (2009).
19. Crich D., Sun S.: J. Org. Chem. *61*, 4506 (1996).
20. Hahm H. S., Schlegel M. K., Hurevich M., Eller S., Schuhmacher F., Hofmann J., Pagel K., Seeberger P. H.: Proc. Natl. Acad. Sci. U.S.A. *114*, 3385 (2017).
21. Leloir L. F.: Science *172*, 1299 (1971).
22. Ichikawa Y., Wang R., Wong C. H.: Methods Enzymol. *107*, 247 (1994).
23. Palcic M. M.: Curr. Opin. Biotechnol. *10*, 616 (1999).
24. Watt G. M., Lowden P. A. S., Flitsch S. L.: Curr. Opin. Struct. Biol. *7*, 652 (1997).
25. Singh V., Kumar P., Sanghi R.: Prog. Polym. Sci. *37*, 340 (2012).
26. Tizzotti M., Charlot A., Fleury E., Stenzel M., Bernard J.: Macromol. Rapid Commun. *31*, 1751 (2010).
27. Hawker C. J., Bosman A. W., Harth E.: Chem. Rev. *101*, 3661 (2001).
28. Matyjaszewski K., Xia J.: Chem. Rev. *101*, 2921 (2001).
29. Chiefari J., Chong Y. K., Ercole F., Krstina J., Jeffery J., Le T. P., Mayadunne R. T. A., Meijs G. F., Moad C. L., Moad G., Rizzardo E., Thang S. H.: Macromolecules *31*, 5559 (1998).
30. Ziegast G., Pfannemüller B.: Macromol. Chem. Rapid Commun. *5*, 373 (1984).
31. Schatz C., Louguet S., Le Meins J. F., Lecommandoux S.: Angew. Chem. *48*, 2572 (2009).
32. Akiyoshi K., Kohara M., Ito K., Kitamura S., Sunamoto J.: Macromol. Rapid Commun. *20*, 112 (1999).
33. Narumi A., Miura Y., Otsuka I., Yamane S., Kitajyo Y., Satoh T., Hirao A., Kaneko N., Kaga H., Kakuchi T.: J. Polym. Sci., Part A *44*, 4864 (2006).
34. Haddleton D. M., Ohno K.: Biomacromolecules *1*, 152 (2000).
35. Houga C., Le Mans J. F., Borsali R., Taton D., Gnanou Y.: Chem. Commun. *29*, 3063 (2007).
36. Akiyoshi K., Kohara M., Ito K., Kitamura S., Sunamoto J.: Macromol. Rapid Commun. *20*, 112 (1999).
37. Kim J., Yun S.: Macromolecules *39*, 4202 (2006).
38. Klemm D., Heublein B., Fink H. P., Bohn A.: Angew. Chem. *44*, 3358 (2005).
39. Tsubokawa N., Iida T., Takayama T.: J. Appl. Polym. Sci. *75*, 515 (2000).
40. Prasad K., Mehta G., Meena R., Siddhanta A. K.: J. Appl. Polym. Sci. *102*, 3654 (2006).
41. Ho H. V., Sievenpiper J. L., Zurbau A., Blanco Mejia S., Jovanovski E., Au-Yeung F., Jenkins A. L., Vuksan V.: Br. J. Nutr. *8*, 1369 (2016).
42. Zong A., Cao H., Wang F.: Carbohydr. Polym. *90*, 1395 (2012).
43. Lehtovaara B. C., Mohit S. V., Frank X. G.: J. Bioact. Compat. Polym. *27*, 3 (2012).
44. Loukotová L., Kučka J., Rabyk M., Höcherl A., Venclíková K., Janoušková O., Páral P., Kolářová V., Šefc L., Štěpánek P., Hrubý M.: J. Controlled Release *45*, 78 (2017).
45. Krassig H. A.: *Cellulose-Structure, Accessibility and Reactivity*. Gordon and Breach Science Publishing, Philadelphia 1993.
46. Pourjavadi A., Sadeghi M., Hosseinzadeh H.: Polym. Adv. Technol. *15*, 645 (2004).
47. Kulkarni R. V., Boppana R., Mohan G. K., Mutalik S., Kalyane N. V.: J. Colloid Interface Sci. *367*, 509 (2012).
48. Pourjavadi A., Barzegar S., Zeidabadi F.: React. Funct. Polym. *67*, 644 (2007).
49. Fan L., Wang L., Gao S., Wu P., Li M., Xie W.: Carbohydr. Polym. *86*, 1167 (2011).
50. Prasad K., Meena R., Siddhanta A. K.: J. Polym. Mater. *25*, 373 (2008).
51. Chenite A., Chaput C., Wang D., Combes C., Buschmann M. D., Hoemann C. D., Leroux J. C., Atkinson B. L., Binette F., Selmani A.: Biomaterials *21*, 2155 (2000).
52. Bao H., Hu J., Gan L. H., Li L.: J. Polym. Sci., Part A: Polym.Chem. *47*, 6682 (2009).
53. Yuan W., Zhao Z., Yuan J., Gu S., Zhang F., Xie X., Ren J.: Polym. Int. *60*, 194 (2011).
54. Li N., Bai R., Liu C.: Langmuir *21*, 11780 (2005).
55. Meyer K., Palmer J. W.: J. Biol. Chem. *107*, 629 (1934).
56. Lapcik L., De Smedt S., Demeester J., Chabrecek P.:

Chem. Rev. *98*, 2663 (1998).
57. Chong B. F., Blank L. M., McLaughlin R., Nielsen L. K.: Appl. Microbiol. Biotechnol. *66*, 341 (2005).
58. Chen W. Y. J., Abatangelo G.: Wound Repair and Regeneration *7*, 79 (1999).
59. Prestwich G. D., Marecak D. M., Marecek J. F., Vercruysse K. P., Ziebell M. R.: J. Controlled Release *53*, 93 (1998).
60. Sahiner N., Jha A. K., Nguyen D., Jia X.: J. Biomater. Sci. *19*, 223 (2008).
61. Luo Y., Kirker K. R., Prestwich G. D.: J. Controlled Release *69*, 169 (2000).
62. Peattie R. A., Nayate A. P., Firpo M. A., Shelby J., Fisher R. J., Prestwich G. D.: Biomaterials *25*, 2789 (2004).
63. Shu X. Z., Liu Y., Palumbo F. S., Luo Y., Prestwich G. D.: Biomaterials *25*, 1339 (2004).
64. Chun K. W., Lee J. B., Kim S. H., Park T. G.: Biomaterials *26*, 3319 (2005).
65. Stern R.: Eur. J. Cell Biol. *83*, 317 (2004).
66. Luo, Y., Kirker K. R., Prestwich G. D.: J. Controlled Release *69*, 169 (2000).
67. Zhang J., Skardal A., Prestwich G. D.: Biomaterials *29*, 4521 (2008).
68. Kirker K. R., Luo Y., Nielson J. H., Shelby J., Prestwich G. D.: Biomaterials *23*, 3661 (2002).
69. Flynn L., Prestwich G. D., Semple J. L., Woodhouse K. A.: Biomaterials *28*, 3834 (2007).
70. Lee H., Ahn C. H., Park T. G.: Macromol. Biosci. *9*, 336 (2009).
71. Kim M. R., Park T. G.: J. Controlled Release *80*, 69 (2002).
72. Fischer G., Boedeker C.: Ann. Chem. Pharm. *117*, 111 (1861).
73. Bray H. G., Gregory J. E., Stacey M.: Biochem. J. *38*, 142 (1944).
74. Silbert J. E., Sugumaran G.: IUBMB Life *54*, 177 (2002).
75. Volpi N.: *Chondroitin Sulfate: Structure, Role and Pharmacological Activity*. Elsevier, San Diego 2006.
76. Chahine N. O., Chen F. H., Hung C. T., Ateshian G. A.: Biophys. J. *89*, 1543 (2005).
77. Strehin I., Ambrose W. M., Schein O., Salahuddin A., Elisseeff J.: J. Cataract. Refract. Surg. *35*, 567 (2009).
78. Strehin I., Nahas Z., Arora K., Nguyen T., Elisseeff J.: Biomaterials *31*, 2788 (2010).
79. Lee C. T., Huang C. P., Lee Y. D.: Biomol. Eng. *24*, 131 (2007).
80. Capila I., Linhardt R. J.: Angew. Chem. *41*, 390 (2002).
81. Tipson R. S., Horton D.: *Advances in Carbohydrate Chemistry and Biochemistry*. Academic Press, San Diego 1985.
82. Neufeld G., Cohen T., Gengrinovitch S., Poltorak Z.: FASEB J. *13*, 9 (1999).
83. Benoit D. S., Collins S. D., Anseth K. S.: Adv. Funct. Mater. *17*, 2085 (2007).
84. Cushing M. C., Liao J. T., Jaeggli M. P., Anseth K. S.: Biomaterials *28*, 3378 (2007).

L. Loukotová and M. Hrubý *(Institute of Macromolecular Chemistry, Czech Academy of Sciences, Prague):*
Polysaccharides as Building Blocks of Hybrid Copolymers

Hybrid copolymers combine the biopolymer properties (biodegrability, biocompatibility, specific interactions) with the tunable properties of the synthetic polymers (hydrophility vs. hydrophobicity, external stimulus responsivity, ionic character). Therefore, these polymers can be used for the preparation of material with desired properties, while it is necessary to take into account the synthetic, physical, physico-chemical, economic and application aspects of the materials used. This review article shows the preparation procedures of polymeric glycoconjugates and also their use in technical and biomedical applications.

Keywords: polysaccharides, hybrid polymers, glycoconjugates, drug delivery